The design and evaluation of mRNA accessible siRNA to silence the Epidermal Growth Factor Receptor (EGFR)

Stephen Peter Fox

Doctor of Philosophy

Cardiff University

December 2007

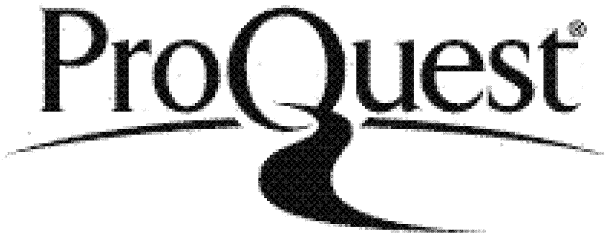

ProQuest LLC
789 East Eisenhower Parkway
P.O. Box 1346
Ann Arbor, MI 48106-1346

'It doesn't matter how beautiful the guess is, or how smart the guesser is, or how famous the guesser is; if the experiment disagrees with the guess, then the guess is wrong. That's all there is to it.'

Richard Feynman (Physicist)

Summary

Small interfering RNA (siRNA) promise to be highly effective molecules but susceptible to some of the limitations experienced with antisense oligonucleotide (ASO) technology: biological instability, design of target mRNA accessible sequences and efficient delivery to subcellular sites of action. This thesis has aim to address each of these limitations for siRNA.

The biological stability of 5'-end ^{32}P radiolabelled siRNA and ASO were tested in FBS, FBS-containing cell culture media and in A431 cell lysates. The biological degradation profiles of ASO and siRNA in serum were comparable (ASO $t_{1/2}$= 19 minutes and siRNA $t_{1/2}$= 19 minutes). The stability of siRNA was higher than ASO in A431 cell lysates (ASO $t_{1/2}$= 37 minutes and siRNA $t_{1/2}$= 43 minutes).

siRNA were designed using innovative scanning ASO array technologies to EGFR mRNA accessible sites. Initially seven siRNAs were designed against different mRNA accessible sites. Based on above a further five siRNAs were designed incorporating termini modifications to alter the thermodynamic stability of the siRNA duplex. These sequences were evaluated for biological activity following optimisation of a delivery strategy.

siRNA delivery to A431 cells was optimised using a FACs assay with Oligofectamine and fluorescently labelled siRNA. Oligofectamine delivery showed significant cell fluorescence associated with labelled siRNA compared with untreated controls ($P<0.05$). The activity, cell proliferation and EGFR protein and mRNA knockdown, of the designed siRNA was investigated in A431 and TamR cells. RT-PCR, Western blot and immunofluorescent microscopy showed inhibitory trends, but ultimately lacked sufficient resolution and reproducibility; A431 growth was not inhibited. A proprietary siRNA showed knockdown of EGFR mRNA in TamR cells, but all the custom designed siRNA produced highly variable effects, failing to show significant knockdown, even when various designed siRNA were pooled.

ASO and siRNA share common pharmaceutical developmental problems, although siRNAs can elicit the powerful innate RNAi mechanism. Further understanding of RNAi will allow siRNA to fulfill their enormous therapeutic potential.

Acknowledgements

I would like to dedicate my thesis to Mark Gumbleton, initially my deputy supervisor and then subsequent main supervisor. Mark's belief in me was unwavering and without his help and support I am certain I would not have completed this thesis.

The kindness and expertise I received from the Tenovus research group were essential for me to submit a complete body of work. My impatience and frustrations with my work were tolerated and dealt with humour, underlined their understanding and caring. I would like to thank in particular: Kathy Taylor, Denise Barrow, Carol Dutkowskil, Rhiannon Hendley, Huw Mottram, Richard McClelland, Julia Gee, Martin Giles, Iain Hutchinson, Bob Nicholson and Abdul Bensmail.

Muhammad Sohail of Oxford University taught me so much the brief time I spent with him. He generously provided the microarrays and without his help this work would not have been possible.

I recognise that my former group members deserve individual dedications to emphasize their contribution to this work but I will list them in no particular order under this proviso: Andrew Hollins, Claire Davis, Saly Al-Taei, Mustapha Benboubetra, Valerie Taylor and Yadollah Omidi. My fellow PhD students were: Ross Drayton, Sioned Griffiths, Siân Owens, Ian Gilmore and Maryam Afzal.

I would like to thank the Welsh School of Pharmacy for the help through the difficult times of my PhD.

Bronwen Evans for help with the PCR primers

Peter Estebeiro for his unlimited help and support with the ExpressOn arrays

Arwyn Jones for help with immunofluorescence and fluorescent microscopy

Finally, my friends and family, whose patience and support has remained for the 5 years it has taken to finish this thesis.

Table of contents

Table of figures

Table of tables

Abbreviations

°C degrees Celsius
µL microlitres
2'-O-Me 2'-O-Methyl
Å Angstrom ($1x10^{-10}$m)
A Adenosine
AGO Argonaute
ASO Antisense oligodeoxynucleotide
ATP Adenosine triphosphate
bp Base pairs
BPEI Branched polyethylene imine
BSA Bovine serum albumin
C Cytidine
CO_2 Carbon dioxide
cpm counts per minute
cps counts per second
D-MEM Dubecco's modified Eagle's media
DMSO Dimethyl sulphoxide
DNA Deoxyribonucleic acid
DNase Deoxyribonuclease
dT Deoxythymidine
dTdT Two deoxythymidine 3' siRNA overhangs
DTT Dithiothreitol
EDTA Ethylenediamine tetra-acetic acid
EGF Epidermal growth factor
EGFR Epidermal growth factor receptor
FBS Foetal bovine serum
G Guanosine
h hours
HCl Hydrochloric acid
kb Kilobases
kDa Kilo Daltons
LPEI Linear polyethylene imine
MEM Minimum essential media
mL millilitres
mRNA Messenger ribonucleic acid
miRNA MicroRNA
MW Molecular weight
N Any nucleotide (A,C,G, T or U)
nt Nucleotide
OF Oligofectamine
PAGE Polyacrylamide gel electrophoresis
PBS Phosphate buffered saline
PCR Polymerase chain reaction
Pi Free phosphate
PNK Polynucleotide kinase
RNase H Ribonuclease H
rpm Revolutions per minute
RNAi RNA interference
RNA Ribonucleic acid

RNase Ribonuclease
RISC RNA induced silencing complex
S Svedberg ($1x10^{-13}$ seconds)
SD Standard deviation
SDS Sodium dodecyl sulphate
SDS-PAGE Sodium dodecyl sulphate polyacrylamide gel electrophoresis
siRNA small interfering RNA
$t_{1/2}$ half life (hours)
T Thymidine
TBE Tris boric EDTA
TEMED N,N,N',N'-trimethylethylenediamine
Tris Tris(hydroxymethyl)amino methane
U Uridine
UTR Untranslated region
v/v volume *per* volume
w/v weight *per* volume
w/w weight *per* weight

Chapter 1
General Introduction

1.1 Small interfering RNA (siRNA)

Small interfering RNAs (siRNA) are the principle molecules in the biological process known as RNA interference (RNAi). RNAi is widely regarded as one of the most promising biological tools of recent years and since its discovery in 1998 there has been increasing interest in the targeted gene-silencing produced by siRNA molecules. In 2002, Science magazine named RNAi as its 'breakthrough of the year' (Couzin, 2002) and since then there has been an explosion of papers utilising siRNA to mediate gene-silencing in mammalian cells even in whole animals (Song et al., 2003). Now several siRNA therapeutics for ocular degradation and respiratory viruses have begun Phase 1 clinical trials (Corey, 2007).

In 1998, Andrew Fire and co-workers (Fire et al., 1998) discovered that nematodes (*Caenorhabditis elegans*) injected with complementary strands of RNA that annealed to form double stranded RNA produced long-term gene inactivation, which could last for several generations. These findings have also been observed in other organisms: plants (Matzke and Matzke, 1995), fruit flies (*Drosophila melanogaster*, Kennerdell and Carthew, 1998), frogs (Oelgeschlager et al., 2000), mammals such as mice (Lewis et al., 2002) and most importantly human cells (Chiu and Rana, 2002). Post-transcriptional gene silencing (PTGS) and Quelling are similar phenomena in plants and fungi (*Neurospora crassa*) respectively (Sharp, 2001), but in animals it is known as RNAi (Fire et al., 1998).

1.1.1 Structure of siRNA

A typical siRNA molecule consists of two 19-nucleotide strands of RNA that run anti-parallel to each other, 5' to 3' end (Figure 1.1). These two strands form a RNA duplex and at both 3' ends there are usually two DNA deoxythymidine overhangs (dTdT). These 21mer helices are deemed to be of optimal length (Elbashir et al., 2001c). The siRNA cleavage site is between 10 and 11 nucleotides downstream of the antisense strand (Elbashir et al., 2001a). The nucleotide sequences of the strands are not predetermined and are chosen as to be complementary to the intended target mRNA sequence. The choice of an mRNA target sequence within the mRNA of the target gene is one of the main issues of this work. The siRNA duplex is an A-form RNA helix that makes 1.7 complete helical turns (helical pitches) in its 19-mucleotides length (Figure 1.2).

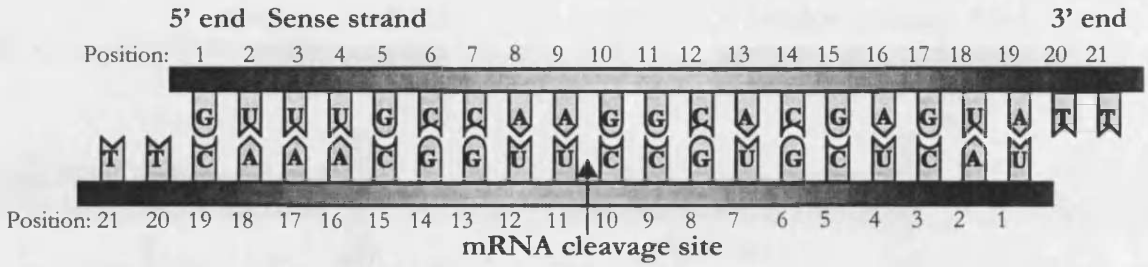

Figure 1.1: Schematic showing the sequence structure of a siRNA. Top strand represent sense strand and the bottom represents antisense strand. The two 3' deoxythymidine overhangs are shown on both strands. Sequence corresponds to HAR-1 siRNA

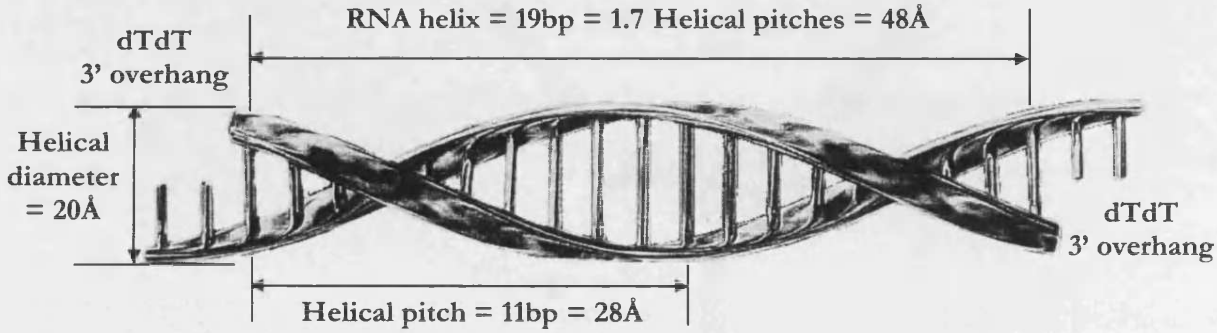

Figure 1.2: Helical three-dimensional representation of a siRNA duplex. A siRNA is an A-form RNA helix with 11bp per helical turn and a diameter of 20Å. One Angstrom (Å) is equivalent to $1x10^{-10}$m. Dimensions taken from (Rana, 2007).

1.1.2 Function (RNAi mechanism)

RNAi is the process of double-stranded RNA that leads to the down-regulation of complementary target mRNA. The down-regulation of target mRNA prevents the translation of the target protein and the gene is silenced. There are numerous molecules that act to trigger RNAi-like mechanisms within the cell, that include double stranded RNA and microRNA (miRNA), but the focus of this report will be on exogenously delivered siRNA.

Once inside cells exogenous siRNA are recognized by the RNA-induced silencing complex (RISC) present in the cytosol. The antisense RNA strand, often referred to as the guide strand, then directs this complex to its complementary sequence in target mRNA. The sense strand, also known as the passenger strand, does not enter RISC and is destroyed. This activated RISC complex leads to gene-silencing through either translational arrest or target mRNA cleavage. Although the mechanism of RNAi is still not fully understood (Rana, 2007), the key molecules in the RNAi pathways are discussed below (Figure 1.3).

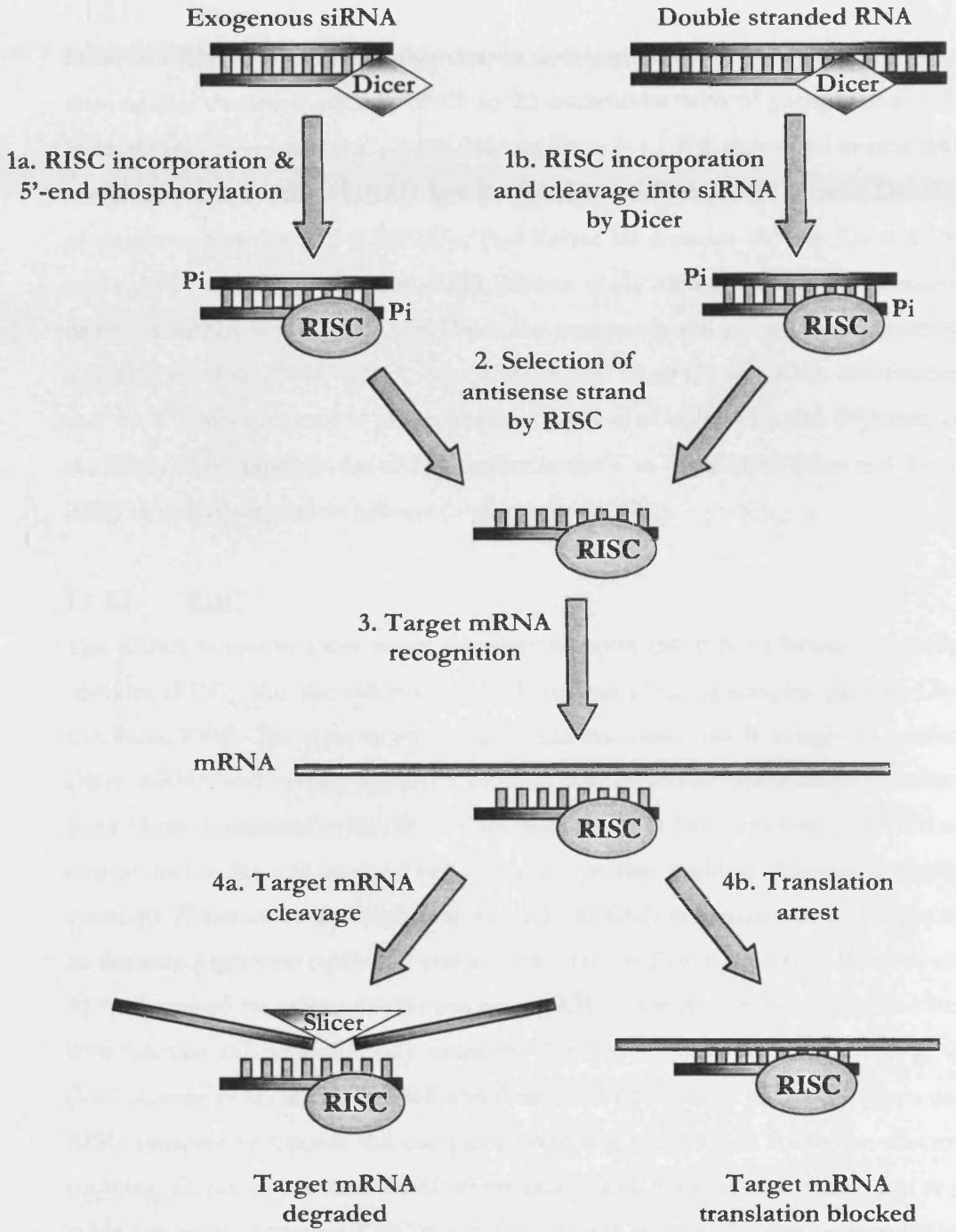

Figure 1.3: Mechanism of RNA interference (RNAi). Exogenously delivered siRNA has both its 5'-ends phosphorylated and is incorporated into the RNA-induced silencing complex (RISC). siRNA and are produced by Dicer cleavage from long double-stranded RNA. These exogenous siRNAs are further complexed into RISC and the active strand is unwound, depicted as the antisense strand, and taken to its mRNA target site were it mediates target mRNA cleavage or blocks mRNA translation. siRNA tends to cause cleavage utilising an endonuclease called 'Slicer' but can also mediate translation arrest. This active siRNA-RISC cleaving complex can be recycled to cleave additional copies of the same target mRNA. Adapted from (Rana, 2007).

1.1.2.1 Dicer

Dicer is a RNase III analogue that cleaves double-stranded RNA and pre-miRNAs into smaller duplexes, siRNA, of 21 to 23 nucleotides with 5' phosphate and 3' hydroxyl ends (Bernstein et al., 2001). Human Dicer is a 1,922 amino acid protein that contains several domains: DEAD box RNA-helicase domain, PAZ domain, Domain of unknown function 283 (DUF283), Two RNase III domains (RNase IIIa & IIIb) and a dsRNA-binding domain (dsRBD; Macrae et al., 2006). Although exogenously delivered siRNA is not cleaved by Dicer, the nuclease is still necessary for silencing activity (Doi et al., 2003). siRNA incorporation into Dicer initiates RNA interference and the 5' hydroxyl group is phosphorylated because of cellular kinases (Nykanen et al., 2001). Dicer unwinds the siRNA duplex in the 5' to 3' direction (Chiu and Rana, 2002) by a ATP-dependent helicase (Nykanen et al., 2001).

1.1.2.2 RISC

The siRNA bound to Dicer enters a protein complex called RNA induced silencing complex (RISC), this also called the siRNA-induced silencing complex (siRISC; Chu and Rana, 2006). The exact structure RISC remains unclear but is thought to involve Dicer, siRNA and several regulatory proteins and an endonuclease enzyme distinct from Dicer (Hammond et al., 2001). Argonaute proteins have also been identified as critical molecules and most eukaryotic cells contain multiple Argonaute family members (Okamura et al., 2004). Argonaute-2 (AGO-2) in human cells is thought to be the only Argonaute capable of endonuclease activity (Liu et al., 2004, Meister et al., 2004). Some of the other proteins composing RISC have also been characterized but their function still remains largely unknown: Tudor–SN, Fragile X, Vasa intronic gene (VIG; Caudy et al., 2002), Dmp68 and Gemin3 (Filipowicz et al., 2005). When the RISC complex recognises the complementary target mRNA, it forms an effector complex, known as activated RISC, where one strand, the antisense strand, acts as a guide for Slicer. Activated RISC is a multi-turnover enzyme that can be recycled to cleave addition target mRNAs (Hutvagner and Zamore, 2002).

1.1.2.3 'Slicer'

The putative RISC nuclease recruited by RISC to cleave the target mRNA was nicknamed 'Slicer' by Philip Zamore (Hutvagner and Zamore, 2002). Slicer uses the 5' end of the antisense or guide strand of the siRNA to determine the position of target

cleavage (Elbashir et al., 2001a). Cleavage of the mRNA occurs in the centre of the target region complementary to the 21-nucleotide guide strand of siRNA, between 10-11 nucleotides from the 5'-end of the antisense strand (Hammond et al., 2001). This cleavage site is interestingly one helical turn (one helical pitch) away from the site where Dicer would have cleaved the double stranded RNA (Elbashir et al., 2001a). AGO-2 is the most likely candidate for Slicer since it has an RNase H-like domain and mutations to it abrogate cleavage (Liu et al., 2004, Song et al., 2004). *In vitro* studies have shown the cleavage of target mRNA with just AGO-2 and siRNA (Rivas et al., 2005).

1.1.2.4 Cleaved mRNA degradation

Following Slicer cleavage, eukaryotic cells have two mechanisms for the degradation of bulk mRNA that may cause the further removal of 'sliced mRNA': deadenylation followed by either 3'-exonuclease digestion or decapping followed by 5'-exonuclease activity (Parker and Song, 2004).

1.1.2.5 Interferon response

In mammals, the use of strands of double stranded RNA longer than 30 nucleotides has been shown to cause a non-specific degradation of all mRNA (Stark et al., 1998). This non-specific pathway is thought to be a response to stress or viral infection (Bass, 2001). This response is through the activation of protein kinases (PKR) this phosphorylates a translational elongation initiation factor (eIF2a) leading to interferon activation and cell apoptosis. Also PKR activates 2',5'-oligoadenylate synthetase that triggers the non-specific RNase L (Elbashir et al., 2001b). The use of 21 nucleotide siRNAs overcomes this response and has led to a new method for gene knock down, although it has been reported that siRNA concentrations of 100nM and greater can cause an interferon response (Ui-Tei et al., 2004).

1.1.2.6 miRNA

Both miRNA and siRNA are short ~21nts RNA duplexes that trigger RNAi (Filipowicz et al., 2005, Rana, 2007, Tang, 2005). miRNA, unlike siRNA since they are endogenously produced, translated from non-coding RNA into hairpin RNAs, are key regulatory molecules for cytoplasmic control of mRNA translation and degradation (Valencia-Sanchez et al., 2006). miRNA inhibits translation by binding imperfectly to

the 3'-untranslated region (3'-UTR) of the target mRNA (Tang, 2005). miRNA have additional RNAi effects by enhancing mRNA degradation (Bagga et al., 2005) and causing heterochromatin methylation (Lippman and Martienssen, 2004). The composition and functions of siRISC and miRNA-induced silencing complex (miRISC) differ and are not yet fully understood (Chu and Rana, 2006). miRNA silencing occurs in cytoplasmic mRNA-protein foci, called processing (P) bodies, but this mechanism of silencing has not yet been elucidated (Dykxhoorn and Lieberman, 2006).

1.2 EGFR as a target

Epidermal growth factor (EGF) was the first identified growth factor (Cohen, 1962) and now its family of receptors are among the most studied cell signalling pathways (Schlessinger, 2000). The epidermal growth factor receptor (EGFR) is implicated in the immortalisation of several solid tumours and epidemiology studies have shown EGFR expression in numerous tumour cells (Table 1.1; Sebastian et al., 2006). A cell with an overactive EGFR displays the basic properties of cancer namely: increased proliferation, angiogenesis, metastasis and anti-apoptosis. The discovery that the avian erythroblastosis virus v-erb B oncogene (AEV) was homologous to cellular EGFR was the first evidence that EGFR is a proto-oncogene (Downward et al., 1984). Cells infected with avian blastosis virus, containing a v-erb oncogene that encodes for a truncated EGFR. When these were stimulated with EGF they undergo oncogenic transformation (Miller et al., 1992). So that, mutation, overexpression, structural changes and/or loss of it regulatory systems may lead to an oncogenic transformation of EGFR.

Table 1.1: Percentage of tumour cells expressing EGFR. Adapted from (Sebastian et al., 2006).

Tumour	Tumours expressing EGFR (%)
Head and neck	90-95
Breast	82-90
Renal	76-89
Cervix/uterus	90
Oesophageal	43-89
Pancreatic	30-89
Non-small cell lung	40-80
Prostate	40-80
Colon	25-77
Ovarian	35-70
Glioma	40-63
Bladder	31-48
Gastric	4-33

EGFR is one member of a family of four receptor tyrosine kinases (RTK): EFGR-1 (synonymous EGFR, HER-1 and erbB1), EGFR-2 (neu, HER-1 and erbB1), EGFR-3 (HER-3 and erbB3) and EGFR-4 (HER-4 and erbB4). In this thesis only the EGFR-1 to 4 notations will be used and whenever EGFR is written it will refer to EGFR-1. All the family members are membrane-spanning glycoproteins of approximately 170 kDa. They all have three main functional domains: an extracellular ligand binding domain, an intracellular tyrosine kinase domain and a transcellular hydrophobic domain. The structure of the EGFR receptor is shown in Figure 1.4. The several known ligands for EGFR shown in Table 1.2: Epidermal growth factor (EGF), Amphiregulin (AR), Epiregulin (EP), Betacellulin (BTC), Transforming growth factors (e.g. TFG-α) and Heparin-binding-EGF (HB-EGF). While the Neuregulins (NRG) regulate the functions of EGFR-3 and EGFR-4; there is no identified ligand for EGFR-2 (Arteaga, 2001).

Table 1.2: EGFR family receptors and their ligands

Receptor	Ligands
EGFR-1	EGF, TGF-α, AR, EP, BTC, HB-EGF
EGFR-2	None known
EGFR-3	NRG-1, NRG-2
EGFR-4	NRG-1, NRG-2, NRG-3, NRG-4, Tomoregulin, EP, BTC, HB-EGF

The binding of a ligand to EGFR starts a signalling cascade, shown in Figure 1.5, resulting in receptor activation by EGFR dimerisation where it binds to itself or one of its other family members, homodimerisation or heterodimerisation (Schlessinger, 2000). EGFR-2 has no known ligands but has a protruding dimerisation loop found in the CR1 subdomain (Figure 1.4), this gives it a higher capacity for heterodimerisation and the preferred partner for other activated EGFR family members (Graus-Porta et al., 1997). Receptor activation causes the phosphorylation of tyrosine residues (Figure 1.4). These act as docking sites for adapter proteins such as Shc (Normanno et al., 2006). The adaptor protein Grb2 will activate the directly the ras/raf/ERK/MAPK pathways or indirectly through activated Shc (Batzer et al., 1994). The JAK/STAT, PI3K/Akt and other key pathways are also activated (Figure 1.5).

The commonest mutation of EGFR is called EGFRvIII (synonymous ΔEGFR and de2-7 EGFR) and it causes the extra-cellular domain to be truncated (Wikstrand et al., 1998) and its structure is shown in Figure 1.4. This truncated EGFR molecule is not just seen in 60% of glioblastoma multiforme and 20% of anaplastic astrocytomas, but has been detected in cancers of the breast, lung, ovaries and prostate (Moscatello et al., 1995). EGFRvIII is constitutively active with adapter molecules, such as phosphorylated Grb and Shc, meaning it would be continuously activating downstream signalling molecules (Nagane et al., 2001). Nagane and co-workers also showed that in human glioma-derived cell line (U87MG) that expressed the truncated EGFR, tumorigenicity was increased due to the increased proliferation and reduced cell death. This would be expected with a continuously active tyrosine kinase EGFR molecule. Also, inhibition caused by AG1478, a small molecule inhibitor of EGFR with some selectivity for EGFRvIII (Han et al., 1996), in combination with a platinum-based chemotherapeutic agent (CDDP), induced apoptosis in these cells. This means EGFR can be targeted to not only to induce cell death but also to inhibit proliferation.

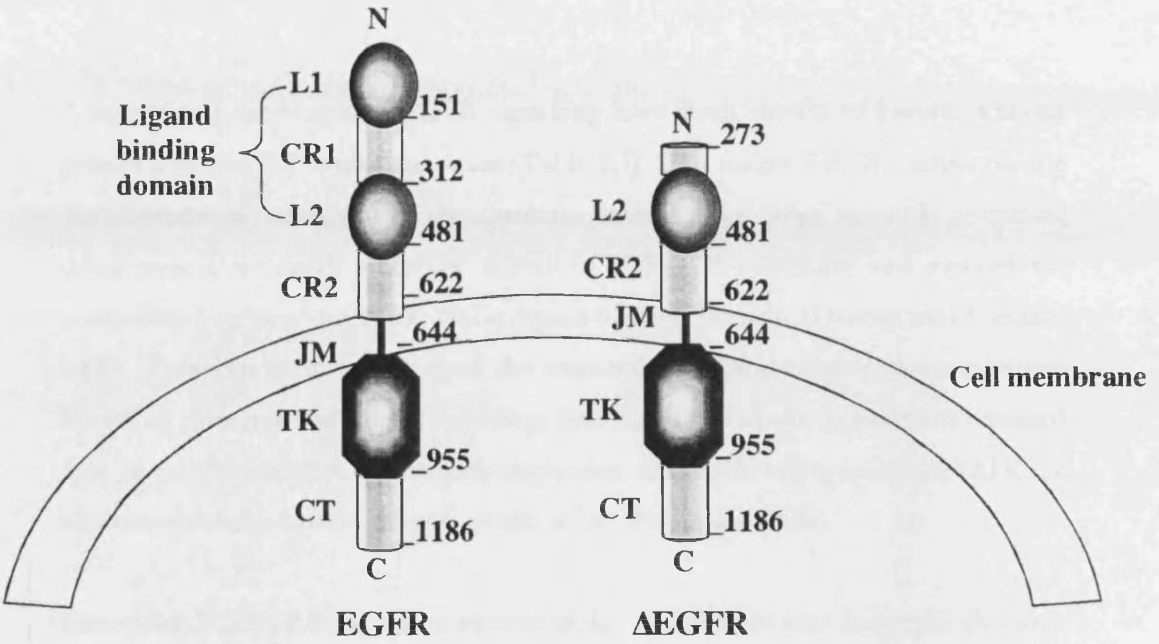

Figure 1.4: Structure of EGFR and truncated EGFR (ΔEGFR). The extracellular domain of the EGFR receptor contains; the N-terminus (N), two lysine rich domains (L1 & L2; residues 1-151 and 312-481) and two cytosine rich domains (CR1 & CR2; residues 151-312 and 481-622). These extracellular domains are also named domains I to IV, from the N-terminus, and domains I to III are thought constitute the ligand binding domain. A juxtamembrane domain (residues 622-644), also known as a transmembrane domain, links the extracellular domains to the intracellular. The intracellular domains contain a tyrosine kinase domain (TK; residues 644-955) and a carboxy-terminal terminus (CT; residues 955-1186) that ends in C-terminus (C). The truncated EGFR (ΔEGFR), also known as EGFRvIII, has residues 6-273 replaced by a single glycine. It therefore lacks a portion of the ligand binding domain and constitutively active tyrosine kinase. Figure produced from combining published figures (Sebastian et al., 2006, Ward et al., 2007).

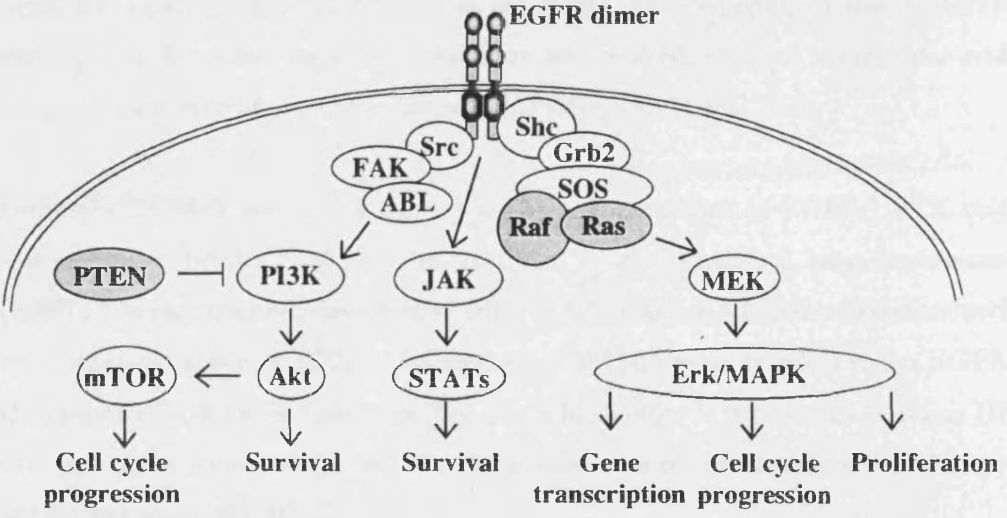

Figure 1.5: EGFR signalling pathway. Ligand binding to EGFR results in dimerisation with another EGFR family member leading to phosphorylation of tyrosine residues and kinase activation. The kinase recruits linker molecules and subsequent activation of Ras/Rak/Erk, PI3K/Akt and other signalling pathways. Modified from (Speake et al., 2005).

A number of inhibitors of EGFR signalling have been shown to prevent tumour growth and viability *in vitro* and *in vivo* (Table 1.3). This makes EFGR a target for the development of novel cancer therapeutics. Amongst the drugs currently in clinical development are small molecule inhibitors of EGFR activation and monoclonal antibodies targeting the extracellular ligand-binding domain (Dancey and Freidlin, 2003). Targeting antibodies versus the extracellular ligand-binding domain causes EGFR to dimerize and inhibit signalling, leading to cell death. It has been reported that an immune response, antibody-dependent cell-mediated cytotoxicity (ADCC), also contributes to the overall anti-cancer effect (Fan et al., 1993).

Cetuximab (C225, Erbitux) is an immunoglobin G antibody that competitively binds with EGFR this then prevents its receptor tyrosine kinase activation and also activates the complement system (Goldstein et al., 1995). Divgi and co-workers (Divgi et al., 1991) in a Phase I clinical trial showed that patients administered with EGFR mouse antibody demonstrated tumour-specific targeting, but unfortunately all the patients developed anti-mouse antibodies and the trial was stopped. A chimeric humanized antibody was developed to avoid this response.

Even small mutations in the EGFR receptor's tyrosine kinase ATP-binding site will affect enzyme function (Redemann et al., 1992). The targeting of this Mg-ATP binding site by small molecule inhibitors has proved, even in nanomolar and subnanomolar, to inhibit enzyme function (Al-Obeidi and Lam, 2000).

Gefitinib (ZD1839, Iressa) is a quinazoline selective inhibitor of EGFR-1 RTK that was approved by the FDA for the treatment of non-small cell lung carcinomas (NSCLC) in patients previously treated with, or intolerant to, platinium and docetaxel chemotherapy. Erlotinib (OSI-774, Tarceva) is 1,000 times more selective for EGFR than other EGFR family members (Dy and Adjei, 2002). It is currently in phase III clinical trials as monotherapy and in combination with conventionally chemotherapy for the treatment of NSCLC.

Trastuzumab (Herceptin) is a humanized monoclonal antibody that, although doesn't target EGFR, targets its family member EGFR-2 also called HER-2 and neu. It is

licensed for the treatment of breast cancers that overexpress the HER-2 receptor in combination and monotherapy.

Two large randomised placebo-control clinical trials showed that gefitinib when used in combination with tradition of chemotherapy provided no benefit in terms of survival, tumour response or disease progression (Giaccone et al., 2004, Herbst et al., 2004). It was argued that these results were due to patients being selected that were not known to have EGFR-expressing tumours (Dancey and Freidlin, 2003). This questions the role of EGFR in cancer cells and their use as a clinical marker. Maybe individual mutations in EGFR receptors and other proto-oncogenes will need to be detected, using immunohistochemical or gene-array technologies, and a patient/tumour-specific treatment provided.

Table 1.3: Selected EGFR agents in clinical trials as treatments for cancer. Modified from (Baselga, 2006).

Inhibitor	Type	Target	Tumour type	Stage
Gefitinib	Small molecule reversible inhibitor	EGFR-1	NSCLC	Restricted indications
Erlotinib		EGFR-1	NSCLC, pancreas	Market
Lapatinib		EGFR-1 EGFR-2	Breast EGFR-2 amplified	Phase III
BMS-599626		EGFR-1 EGFR-2	Colon, NSCLC	Phase II
AEE788		EGFR-1 EGFR-2 VEGR	-	Phase I
EKB-569	Small molecule irreversible inhibitor	EGFR-1	-	Phase I
Cetuximab	Chimeric monoclonal antibody	EGFR-1	Colon, head & neck	Market
			NSCLC, pancreas	Phase III
ABX-EGF	Human monoclonal antibody	EGFR-1	Colon, renal, head & neck	Phase III
EMD-72000	Humanised monoclonal antibody	EGFR-1	Head & neck, ovarian, colon, cervix	Phase II
h-R3		EGFR-1	Head & neck	Phase II
Pertuzumab		EGFR-2	Breast, ovarian, prostate, NSCLC	Phase III
Trastuzumab		EGFR-2	Breast advanced & adjuvant	Market

1.3 General issues with using ASOs as therapeutics

Antisense oligodeoxynucleotides (ASO) were the first gene-silencing tool. In 1978, Zamecnik and Stephenson showed that ASOs were able to inhibit Rous sarcoma replication and transformation in cell culture (Zamecnik and Stephenson, 1978). ASOs are short single strands of DNA of approximately 18 to 21 nucleotides that bind by Watson-Crick interactions to target mRNA to prevent translation. ASOs activate the endogenous nuclease RNase H to induce cleavage of the target mRNA (Figure 1.6). If the ASO does not cause enzyme induction it may inhibit translation by steric blockade of the ribosome, called translational arrest. Targeting the 5'-untranslated region (UTR) of the mRNA prevents the assembly of the translation machinery (Hughes et al., 2000).

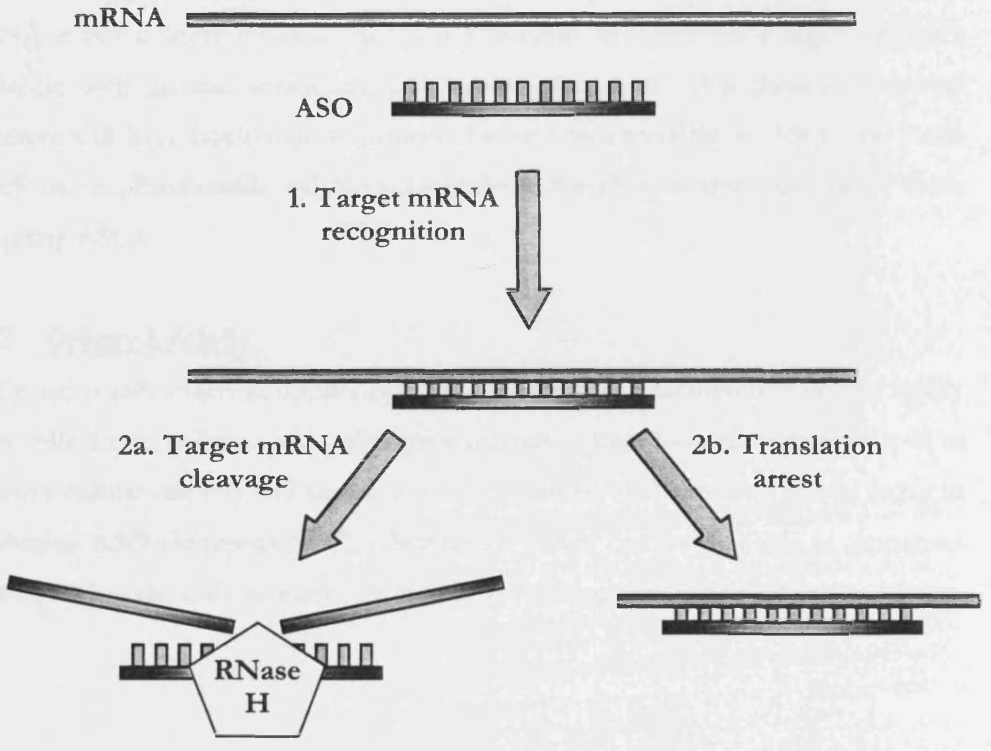

Figure 1.6: Mechanisms of action for antisense oligodeoxynucleotides (ASO). ASO binds with complementary target mRNA it can block translation by two key methods: recruitment of the endonuclease RNase H that cleaves the mRNA (2a) or the ASO bound to mRNA sterically inhibits ribosomes and other translation-associated proteins thus blocking target protein production.

Over the last three decades of ASO development there have been several key problems identified. These are briefly discussed below:

1.3.1 Biological stability

ASOs are rapidly degraded by nucleases found in biological media (Akhtar et al., 1991, Wickstrom, 1986). Unmodified ASOs are considered to have such poor biological stability that they are not used even in cell culture or *in vivo* experiments and chemical modifications that increase their stability are paramount in their activity (Crooke and Lebleu, 1993, Kurreck, 2003).

1.3.2 Design

The design of ASOs primarily relies on the selection of a sequence of nucleotides within the target mRNA to design a complementary ASO against (Crooke, 1998). mRNA is not a linear molecule nor is it a random structure but a highly complex molecule with distinct secondary and tertiary structures. This three-dimensional structure will have nucleotide sequences that will be accessible to ASOs and those which are not, inaccessible. mRNA accessibility is therefore an important factor when designing ASOs.

1.3.3 Delivery & Activity

ASOs are usually macromolecules of 6000-8000 Daltons and therefore do not readily enter cells. Lipid, polymer and polypeptide delivery system have all been developed to improve cellular delivery and targeting. Cellular delivery still remains a critical factor in producing ASO therapeutics. The delivery of ASOs can be detected in numerous techniques but the only definitive method is by showing that it is functionally active.

Aims & Objectives of thesis

The overall aim of this project was to design siRNA versus EGFR using the knowledge gained from conventional ASO technologies. mRNA accessibility has been shown to be important for active ASOs. Scanning ASO arrays are able to map mRNA accessibility and will provide ASO sequences that would be accessible to EGFR mRNA. Designing siRNA against these accessible ASO sites should produce active siRNA. The knockdown of EGFR in cancer cells inhibits their growth. This active siRNA could therefore be developed into a gene-specific treatment for cancer.

First results chapter's hypothesis: Biological stability

The biological stability of siRNA, like ASO, will be critical for activity. The stability in biological of siRNA can be expected to be no better than ASO, as siRNA is predominantly RNA readily degradable by nucleases present in media. Hence, the enhanced effects seen with siRNA are not expected to be attributed to their greater stability, but more likely to their improved gene-silencing mode of action. ASO require chemical modifications to improve their stability for them to be active in biological systems and therefore siRNA may need similar modifications.

Objectives

- Compare the stability of siRNA with ASOs in biological media used for cell culture transfections.

2nd results chapter's hypothesis: Design of active siRNA

The mRNA accessibility of the siRNA molecule will be critical to its activity. The reported large numbers of non-active siRNA molecules are due to them being inaccessible to there target mRNA, so that an inactive siRNA molecule is one that targets a cleavage site that is unreachable because of stearic hindrance. Scanning ASO arrays assess the map mRNA accessibility. Since it is the siRNA antisense strand that mediates cleavage of mRNA, siRNA will have the same mRNA accessibility constraints that apply to ASOs.

Objectives

- Design siRNA according to published design rules that have different mRNA accessibilities.

3rd results chapter's hypothesis: Delivery & Activity of siRNA

A reliable and reproducible assay will be necessary for determining siRNA activity. An active siRNA targeting EGFR, like EGFR targeting ASO, will inhibit growth of A431 cells and allow for easy comparison of siRNA molecules. Western blot and RT-PCR will confirm the gene-specific knockout with siRNA.

Objectives

- Determine the activity of the siRNA molecule by a cell growth assay.
- Develop a reliable *in vitro* delivery protocol for siRNA.
- Compare the activity of siRNA targeted to regions with varying levels of mRNA accessibility.
- Validate gene-silencing results with Western blot and RT-PCR methods.

Chapter 2
Materials & Methods

2.1 Materials & Methods for Chapter 3: 'Biological Stability of siRNA'

2.1.1 Production of radiolabelled nucleic acids

MATERIALS

The following materials were used in the radiolabelling nucleic acids: Adenosine 5'-[γ-^{32}P]-triphosphate triethylammonium salt, 9.25 MBq, 250 μCi, (GE Healthcare Cat.# PB10218-250UCI); Antisense oligodeoxynucleotide (ASO; for sequence see Appendix 2 Reverse 560 bp Primer; MWG Biotech); Microcentrifuge tubes 1.5ml (Elkay Cat.# 000-MICR-150); Nuclease-free water (Ambion Cat.# 9937); Single-stranded RNA Non-Specific Control VIII (Dharmacon Cat.# D-001206-08-05), siRNA HAR-1 (Qiagen; for sequence see Chapter 4); siRNA Suspension buffer (Qiagen Cat.# 1024183); T4 Polynucleotide kinase enzyme (AbGene Cat.# AB-0269).

METHODS

The lyophylised pellet of siRNA as supplied by the manufacturer was dissolved in siRNA suspension buffer to 20μM, reannealing was performed as recommended. This siRNA stock solution was further diluted with nuclease-free water to 0.2μM for radiolabelling reaction. The ASO was dissolved in nuclease-free water and the single strand siRNA was dissolved exactly as the doubled stranded. The nucleic acids either siRNA, single-stranded siRNA or ASO, were labelled by T4 polynucleotide kinase enzyme using a protocol developed from an established method for phosphorylation of 5' termini of oligonucleotides (Table 2.1; Sambrook et al., 2001). The 'cold' material were added first to a 1.5mL tube on ice before adding the 'hot' radiolabel and the mixture was incubated in a rotating hybridiser (Techne; Roller–Blot Rotating Hybridiser HB-3D) [Note: Rotating function not used], at 37°C for 60 minutes.

Table 2.1: T4 kinase reaction mixture

Reaction components	Volume
Nucleic acid (0.2μM)	2μL
γ-^{32}P-ATP	2μL
T4 Kinase (10 units)	1μL
Forward kinase buffer	5μL
Nuclease-free water	10μL
Total volume	20μL

2.1.2 Removal of free radiolabel by Sephadex column purification

MATERIALS

Microspin G-25 column (GE Healthcare Cat.# 27-5325-01) were used in the column purification of nucleic acids.

METHODS

A G-25 Sephadex column was briefly vortexed (Scientific Industries; Vortex-Genie 2 G-560E) then pre-spun in a bench top centrifuge (Eppendorf; Centrifuge 5415 D) at 600g for 1 minute. The labelled nucleotides were pooled (2x20μL) and then diluted by the addition of nuclease-free water (40μL). The diluted sample was added to the column and spun at 600g for 2 minutes, to remove free label. The free label is retained on the column while the nucleic acids are eluted. The samples were then passed through two columns to further remove free label.

2.1.3 Removal of free radiolabel by PAGE purification

MATERIALS

The following were used for the PAGE purification of nucleic acids: Autoradiography film blue sensitive (GRI Cat.# MXB 1824); Autoradiography sealed cassette (GE Healthcare Cat.# RPN 13642); Glycerol (Sigma Cat.# G2025); Liquid nitrogen (BOC).

METHODS

This method was developed from two established protocols (Ellington, 1998, Sambrook et al., 2001). The labelled samples were mixed with an equal amount of 5% glycerol in nuclease-free water v/v and loaded onto a polyacrylamide stability gel (Appendix 1) in a vertical gel electrophoresis system (Fisher; V20-CDC) with 1x TBE buffer (Appendix 1) as running buffer and run at 300 volts for 2 hours and 45 minutes. Autoradiography film was then was exposed to the gel in a sealed cassette. The developed film was replaced on top of the gel and the bands, corresponding to labelled nucleic acids, were excised. Another film was then placed over the gel to confirm the complete removal of the radioactive bands.

The excised bands were crushed and placed in three 1.5ml tubes each containing 0.5mL of nuclease-free water. The tubes were then immersed in liquid nitrogen to

crack open the gel using a modified protocol (Chen and Ruffner, 1996). The nucleic acids were eluted from the gel overnight on an orbital shaker (Stuart) set at the maximum revolutions. The centrifuge tubes were then briefly centrifuged and the water containing the eluted labelled nucleic acids was carefully removed. The 0.5mL of water was then replaced and the elution process was repeated twice, after 1-hour intervals, to increase nucleic acid recovery. The eluted nucleic acids were then dried for 4 hours in a speed vac (ThermoLife Science; DNA120) on the low temperature setting. The samples were then pooled and made up to a known amount with nuclease-free water.

2.1.4 Nucleic acid biological stability assay

MATERIALS

The following materials were used: A431 Cells (ECACC Cat.# 85090402) and Foetal Bovine Serum (FBS; Invitrogen Cat.# 10106-169).

METHODS

The stability assay was adapted from a protocol for measuring ASO stability (Akhtar et al., 1991). The nucleic acids were subjected to degradation by FBS of known protein concentrations and in A431 growth media (that contains supplements and 10% FBS as subsequently described; Table 2.12). A431 cell lysates and protein estimations were carried out as subsequently described for Western blots (Section 2.3.9).

Radiolabelled nucleic acids were incubated in 200µL of the respective biological media at 37°C. 10µL samples were taken at different time points, quenched with 10µL Loading stability buffer (Appendix 1), snap frozen in liquid nitrogen, to halt the degradation reaction, and stored at -80°C (Thermo Life Science; -86 Ultra Low Temperature Freezer) until needed.

A PAGE stability gel (Appendix 1) was prepared and the samples were thawed and added to the gel and TBE buffer (Appendix 1) was used as a running buffer. The gels were visualised using a phosphorimager, the image data was exported as a tagged image file form (.tif) into the ImageJ programme (Available as Freeware from http://rsb.info.nih.gov/ij/).

ImageJ was used to quantify the data by comparison of peak areas, as shown in an on-line tutorial (http://rsb.info.nih.gov/ij/docs/menus/analyze.html#gels). The data values were converted into percentages of the intact full-length nucleotide, this was deemed to be the largest, slowest moving, labelled fragment on the gels.

The half-lives of the nucleic acids in biological were calculated by plotting time against the natural log of 2 versus the percentage of full length oligonucleotide. The gradient of the linear regression is equal to the decay coefficient (k) and the half-life of the oligonucleotide can be calculated by the natural logarithm of 2 divided by the decay coefficient (0.693/k).

2.2 MATERIALS & METHODS FOR CHAPTER 4: 'Design of siRNA'

2.2.1 Determination of mRNA accessibility using a gene-specific ASO microarray

2.2.1.1 Construction of antisense oligonucleotide scanning arrays

An antisense oligonucleotide-scanning array consists of various lengths of antisense oligonucleotides, attached to fixed support, that act as complements to target mRNA.

Mohammad Sohail, University of Oxford, made two polypropylene scanning arrays with antisense sequences complementary to EGFR mRNA. Array 3 scans a region from 301 to 450 nucleotides downstream from the start codon (AUG). Array 4 scans a region 431 to 580 nucleotides downstream from the start codon. Appendix 3 shows figure showing the regions of the EGFR gene scanned by the arrays.

The method of fabrication was as described previously (Elder et al., 1999) and (Sohail and Southern, 2001). Briefly, the polypropylene support (Beckman Instruments) was aminated by plasma discharge with anhydrous ammonia (Matson et al., 1994) to produce derivatised linkers, which permits nucleotides to be fixed to the support by their 3' ends. The nucleotides used were standard cyanoethyl (CE) phosphoramidites (Cruachem), positioned with a 25.5mm (diagonal width) diamond-shaped mask which were synthesized with an adapted DNA synthesizer (Applied Biosystems; ABI 394). The offset for the mask was chosen to be 1.417mm to produce oligonucleotides ranging from monomers to a maximum of 18mers. For an array scanning 150 nucleotides of mRNA 150 stages of DNA synthesis would be required producing 150 monomers and 143 18mers. The arrays were then deprotected, to remove the benzoyl and isobutyryl groups, in 30% ammonia solution (Beckman Instruments) for 16 hours at 55°C in a closed chamber.

2.2.1.2 Production of cDNA from a bacterial EGFR expressing plasmid

MATERIALS

The following materials were used: Ampicillin solution 100 mg/mL (Sigma Cat.# A5354); BamH1 restriction enzyme kit (Promega Cat.# R6021); Hind III restriction enzyme kit (Promega Cat.# R6041); LB Agar Tablets (Sigma Cat.# L-7025); LB-Medium (Q.BIOgene Cat.# 3002-021); SpinPrep filters (Novagen Cat.# 709573).

Glycerol stocks of frozen EGFR expressing plasmid were a gift from Andrew Charity. A pCMV-HER vector containing an ampicillin resistant gene (ampR) was transformed in to *E. coli* (JM 109. Glycerol (25% v/v) was added to the transformation competent cells and aliquots were frozen at -80°C.

METHODS

The thawed *E. coli* were streaked onto LB agar plates containing ampicillin 50μg/mL (made according to LB agar tablets manufacturer's instructions) incubated overnight at 37°C. Twelve well isolated colonies were each added to 10mL of LB medium (made according to LB medium's manufacturer's instructions), placed in a shaking water bath (Grant; OLS 200), at 37°C for 16 hours, at 300 rotations per minute. Then 30mL of LB medium was processed through four SpinPrep filters by following the manufacturer's protocol. The extracted plasmid was eluted into 50μL of SpinPrep Elute buffer C and a 5μL sample was taken and quantified with a spectrophotometer (GE Healthcare; UV Ultraspec 3100 Pro).

The identity of plasmid was confirmed by the use restriction enzymes (Hind III and BamH1) to cleave the plasmid into known lengths. The restriction digest mixtures were made up as in (Table 2.2) and were left at 37°C for 2 hours. A horizontal electrophoresis system (Fisher HU10) was used to separate 5μL of the digested products with 1μL loading PCR buffer (Appendix 1) and run on a 1% agarose gel (Appendix 1) at 120 volts, until adequate separation was visualised with the use of a gel documentary system (Biorad; Gel Doc 1000).

Table 2.2: Restriction enzyme mixtures

Reaction components	Volume
Nuclease-free water	14.3μL
10x Enzyme buffer	2μL
BSA (10μg/μL)	0.2μL
Plasmid DNA (0.5μg)	3μL
Hind III/BamH1 enzyme	0.5μL
Total volume	20μL

2.2.1.3 Amplification of cDNA EGFR fragments using polymerase chain reaction

MATERIALS

The following materials were used: dNTPs 100mM (Invitrogen Cat.# 10297-018); Magnesium chloride 25mM (Qiagen); PCR buffer (with 1.5mM $MgCl_2$; Qiagen); PCR tubes 0.2mL (Simport Cat.# T320-3N); Qiaquick PCR purification Kit (Qiagen Cat.# 28104); Taq polymerase (Cancer Research UK).

METHODS

The primers to amplify the EGFR cDNA were as previously published (Beale et al., 2003, Petch et al., 2003) and their sequences are provided in Appendix 2. The forward primer had a T7 promoter for the transcription of RNA, different reverse primers were used to create different length cDNA fragments and subsequently RNA fragments. PCR reagents were thawed on ice and PCR reaction mixtures were prepared (Table 2.3) in 0.2mL PCR tubes before being placed in a thermocycler (Techne; Flexigene or Touchgene Gradient). PCR cycling programs were performed for 560 and 1000 base pairs (Table 2.4) and 3,600 base pairs (Table 2.5). The cDNA fragment sizes were confirmed using a horizontal electrophoresis system by running 5μL of the PCR products on a 1% agarose gel (Appendix 1). The PCR cDNA products were pooled and added to 100μL Qiaquick column according to manufacturer's instructions and finally resuspended in 50μL of nuclease-free water.

Table 2.3: 560, 1000 and 3,600 base pair fragments PCR reaction mixtures

	cDNA fragment size (bp)		
Reaction components	**560**	**1,000**	**3,600**
Nuclease-free water	11.3µL	10.3µL	9.8µL
PCR buffer (10x)	2.5µL	2.5µL	2.5µL
Magnesium chloride (25mM)	1.0µL	2.0µL	2.5µL
dNTPs (5mM)	2.5µL	2.5µL	2.5µL
Plasmid cDNA	2.5µL	2.5µL	2.5µL
Forward primer (10µM)	2.5µL	2.5µL	2.5µL
Reverse primer (10µM)	2.5µL	2.5µL	2.5µL
Taq polymerase enzyme	0.2µL	0.2µL	0.2µL
Total volume	25µL	25µL	25µL

Table 2.4: 560 & 1000 base pair fragments PCR programme

Program	Temp	Time	
Initial denature	95°C	5 mins	
Denature	94°C	45 secs	30 Cycles
Annealing	60°C	1 min	
Extension	72°C	1.5 min	
Final extension	72°C	10 mins	

Table 2.5: 3,600 base pair fragment PCR programme

Program	Temp	Time	
Initial denature	94°C	5 mins	
Denature	94°C	45 secs	25 Cycles
Annealing	62°C	1.5 min	
Extension	72°C	3.5 mins	
Denature	94°C	45 secs	5 Cycles
Annealing	62°C	1 min	
Extension	72°C	5 mins	
Final extension	72°C	10 mins	

2.2.1.4 Production of radiolabelled RNA by transcription with a T7 polymerase

MATERIALS

The following materials were used: DEPC (Diethyl Pyrocarbonate; Sigma Cat.# D-5758); RNaseZap (Sigma Cat.# R-2020); T7 Maxiscript kit (Ambion Cat.# 1308-26); Uridine 5'-[α-^{33}P]-triphosphate, triethylammonium salt (GE Healthcare Cat.# AH9903).

METHODS

All work with RNA was conducted in an RNase-free workspace to prevent loss of RNA through the action of ribonucleases. Work surfaces were cleaned with an inhibitor of ribonuclease before work (RnaseZap) and sterile plastics with filter tips were used to avoid contamination. Glassware was also treated with an inhibitor and glassware was cleaned with 0.1% v/v DEPC in double-distilled water and left for 4 hours before autoclaving. RNase inhibitors, such as Rnasin, were use to protect RNA in reaction mixtures and RNA transcripts were stored in aliquots at -80°C.

The unlabelled run-off transcriptions were used as proof of principle and were performed using a T7 Maxiscript kit by following the manufacturer's instructions. Firstly, the reagents were thawed, then briefly centrifuged. The 10x buffer was added after the water and cDNA, to prevent the spermidine present in the buffer co-precipitating the cDNA. The reagents were added (Table 2.6) and the reaction mixture was left at room temperature for 90 minutes.

The labelled (isotopic) run-off transcriptions were performed, as before, for the 1000 base pair EGFR fragment. The reagents were mixed but with the radiolabel being added last, to minimise operator exposure to radiation (Table 2.6). The reaction mixture was left at room temperature for 2 hours.

Table 2.6: T7 Transcription reaction mixtures

Components	Unlabelled	Labelled
DTT (100mM)	2μL	2μL
cDNA (1μg)	0.81μL	0.81μL
5x buffer	4μL	4μL
ATP (10mM)	1.5μL	1.5μL
CTP (10mM)	1.5μL	1.5μL
GTP (10mM)	1.5μL	1.5μL
UTP (10mM)	1.5μL	-
UTP (250μM)	-	1.5μL
Labelled UTP	-	3μL
T7 polymerase	2μL	2μL
Total volume	~20μL	~20μL

2.2.1.5 Determination of mRNA accessibility by hybridisation of radiolabelled RNA with scanning antisense oligonucleotide arrays

MATERIALS

The following materials were used: Absolute ethanol (Fisher Cat.# E/0650DF/17); Chromatography Paper (Whatman Cat.# 3030-931); Microspin G-25 column (GE Healthcare Cat.# 27-5325-01); PhotoMount Spray Adhesive (3M); RNasin (Promega Cat.# N211A).

METHODS

A G-25 Sephadex column was placed in a clean 1.5mL tube containing 2μL of RNAsin in 300μL of hybridisation buffer (Appendix 1). The transcription reaction mixture produced in 2.2.2.5 was added on top of a G-25 Sephadex column. The tube was then spun for two minutes in a bench top centrifuge at 800g to elute the radiolabeled RNA into the hybridisation buffer. The eluted product was further diluted with 30ml of hybridisation buffer. Both scanning arrays (Array 3 and 4) were firmly attached with PhotoMount adhesive to hybridisation tubes of the rotating hybridiser (Techne; Roller–Blot Rotating Hybridiser HB-3D). The arrays where left to hybridise with the labelled mRNA in hybridising buffer for 3 to 4 hours at 37°C at 3 to 4 rotations per minute.

The arrays were then washed for a few minutes with new hybridisation buffer to remove any unbound label and then dried with chromatography paper. The arrays were then exposed overnight to a storage phosphor screen. The screen was then scanned using a phosphorimager (Molecular Dynamics; Storm 860).

Any remaining radioactive mRNA was removed from the arrays using a microarray stripping solution (Appendix 1) heated to 90-95°C in a microwave. The arrays were immersed in this solution for 2 to 3 minutes. The arrays were then washed in DEPC-treated water, then DEPC-water containing 70% absolute ethanol, then absolute ethanol. The arrays were then tested for residual radioactivity by using Geiger-Müller Counter (Mini-Instruments; Series 900) then by exposure to a storage phosphor screen.

The image from each array was saved as a gel file and, along with its corresponding mRNA sequence, was imported into the *xvseq* analysis programme. *xvseq* is available by anonymous file transfer protocol (ftp://bioch.ox.ac.uk/pub/xvseq.tar.gz). The image was fitted with a template grid in the shape of the diamond-shaped mask, that was used to imprint the array in order to link the mRNA sequences to the array. The array grid was then integrated to produce histograms of hybridisation intensities corresponding to accessible mRNA sequences.

2.2.2 Validation of target mRNA accessibility by utilisation of a ribonuclease H assay

MATERIALS

The materials used were: Century Markers Template Plus (Ambion Cat.# 7782); Dithiothreitol 100mM (DTT; Invitrogen Cat.# Y00147); Microspin G-25 column (GE Healthcare Cat.# 27-5325-01); RNase H (Invitrogen Cat.# 18021-014); RNasin (Promega Cat.# N211A).

METHODS

Radiolabelled mRNA was produced as in 2.2.1.4. 1μL DNase was added to 20μL of reaction mixture and incubated at 37°C for 15 mins, then 1μL of EDTA Solution (Appendix 1) was added and the samples were transferred to a dry block heater (Techne; Dri-Block DB-3D) at 65°C for 10 min to denature the enzyme.

These RNA transcripts were purified using G-25 Sephadex columns by first prespinning the columns at 800g for 3 minutes. 80μL of nuclease-free water was added to the sample and was placed on the Sephadex column with 1μL RNasin in the collection tube, the columns were centrifuged at 800g for 4 mins.

RNase H reaction mixtures were prepared (Table 2.7) containing the radiolabelled transcripts along with each of the 18mer antisense oligonucleotides in Appendix 2. The abbreviations used for the primers correspond to the siRNA designed in chapter 4. The samples were incubated at 37°C for 15 minutes before adding the RNase H enzyme and incubating for a further hour.

A PAGE gel with 8M urea was cast and the wells were rinsed with 1x TBE buffer, which was also used as the running buffer. The samples were then added to 10μL

RNA loading buffer and 10μL RNA sample buffer and heated at 95°C for 3 mins. The samples were subsequently loaded onto the gel and were run at 250 volts for 2 to 3 hours. Details for producing the buffers and gels are found in Appendix 1.

Table 2.7: RNase H reaction mixture

Reaction components	Volume
RNase H buffer	1μL
DTT (100mM)	1μL
RNAsin	1μL
Transcript RNA	5μL
Primer (10μM)	1μL
RNase H (2U/μL)	1μL
Total volume	10μL

2.2.3 Determination of mRNA accessibility by using a non-gene-specific array

MATERIALS

The materials used were: ACCESSarray 4000 (ExpressOn Biosystems); Biotin-16-dUTP (Roche Cat.# 1093070); dATP, dCTP, dGTP (Invitrogen Cat.# 10297-018); ImProm-II Reverse Transcriptase (Promega Cat.# A3802); Milk Powder (Marvel); Qiaquick PCR purification Kit (Qiagen Cat.# 28104); RiboMAX T7 kit (Promega Cat.# P1300); RNase-free DNAse (RQ1; Promega Cat.# M6101); RNasin (Promega Cat.# N211A); Sigmacote (Sigma Cat.# SL2); Streptavidin-Cy5 (GE Healthcare Cat.# PA45001); Tween-20 (Polyethylenesorbitan monolaurate; Sigma Cat.# P5927).

METHODS

The manufacturer of ExpressOn arrays supplies two arrays as a starter kit, this allows the first array to be used to confirm that the user can accurately produce a mRNA accessibility map for a known gene sequence, the second array would then be used for the gene of interest, i.e. EGFR. The known gene sequence was a 200 base pair fragment of luciferase from a pGEM plasmid supplied by ExpressOn. The 20μg pellet of lyophilised plasmid template DNA was dissolved in 20μl of TE buffer (Appendix 1). 2μg of the resulting DNA solution was used in five separate 20μl Ribomax T7 transcription reactions according to the manufacturer's instructions (Table 2.8), apart from the reaction mixture was incubated overnight at room temperature, then the samples were then treated with deoxyribonuclease as directed in the kit. 2μg of cDNA

for the 1000 base pair EGFR fragment, as produced in cDNA amplification using PCR (Section 2.2.1.3.)

Table 2.8: T7 Polymerase reaction mixture to produce: 1kb EGFR fragment, ExpressOn positive array control and Promega positive transcription control.

Reaction components	Promega	ExpressOn	EGFR 1kb
T7 buffer (2x)	10μL	10μL	10μL
Promega pGEM cDNA (1μg)	1μL	-	-
ExpressOn luciferase cDNA (10μg)	-	2μL	-
EGFR 1k.b. cDNA (10μg)	-	-	1.6μL
Nuclease-free water	7μL	6μL	6.4μL
T7 Polymerase enzyme	2μL	2μL	2μL
Total volume	20μL	20μL	20μL

The ACCESSarray was removed from inner packaging and allowed to equilibrate at room temperature for a few minutes. All the washes were performed in a slide chamber (Fisher Cat.# MNK-825-A). The array was then washed for 30 minutes with gentle agitation in SSC buffer (Appendix 1) with 0.1% (v/v) Tween-20. An autoclaved empty pipette tip box, with the base filled with a reservoir of SSC buffer was prewarmed in the rotating hybridiser at 30°C

The ExpressOn Array reaction mix was prepared on ice (Table 2.9) into a 1.5mL tube then vortexed and centrifuged 16,100g for 5 seconds. The array was rinsed five times with nuclease-free water for 5 minutes and any excess water was removed from the array window. Coverslips (BDH Cat.# 406/0188/42) were siliconised using Sigmacote according to the manufacturer's instructions. The reaction mix was added onto the array window and a pre-siliconised coverslip was carefully placed, using tweezers, on top of the array window. The array was incubated on a dry block heater at 25°C for 15 minutes then transferred to the pre-warmed tip box and incubated for 90 minutes at 30°C.

Table 2.9: ExpressOn array reaction mixture

Reaction components	Volume
5x ImProm-II Reaction buffer	20μL
Magnesium chloride (25mM)	4μL
Tween 1% (v/v) in water	10μL
dATP, dCTP, dGTP (25mM)	10μL
Biotin-16-dUTP (1nmol/μL)	10μL
cRNA (100μg)	30μL
RNase-free water	11μL
Improm-II Reverse Transcriptase	2.5μL
RNasin (40U/μL)	2.5μL
Total volume	100μL

The coverslip was removed and the array was washed in SSC buffer for 10 minutes with gentle agitation and then rinsed with 10 changes of DEPC-treated water (Appendix 1) for a total of 5 minutes. The excess water was carefully removed from the array window. Streptavidin-Cy5 (1:500) was added to freshly prepared 1x TBS Tween buffer (Appendix 1) with 5% (w/v) milk powder. 500 μl of this solution was added to the array window and incubated in the dark at room temperature for 60 minutes.

The array was then washed in 1x TBS Tween with gentle agitation for 5 minutes, this repeated five times, then the array was rinsed with 10 changes of DEPC-treated water for a total of 5 minutes. Excess water was removed from the array window and the array was allowed to dry at room temperature for a few minutes.

The array was read in a microarray scanner (Affmetryx; Array Scanner 428) using the Cy5 channel. The scan was quantified using ImaGene software (BioDiscovery, Inc; Version 5) and scanner output was analysed with ACCESSmapper software (ExpressOn Biosystems; Version 1.0).

2.3 MATERIALS & METHODS FOR CHAPTER 5: 'Delivery & Activity of siRNA'

2.3.1 siRNA designs

MATERIALS

All siRNAs were two 19 nucleotides RNA strands with two DNA 3' overhangs that were complexed together to form an antiparallel duplex. The abbreviations that were given to the first siRNA sequences, designed according to target mRNA accessibility, were: HAR-1, A1, A2, A3, W1 and Z1 these were purchased from Qiagen. The abbreviations for subsequent siRNAs, designed with consideration to internal molecular thermodynamic stability profiles were: NS, HAR-1(+), HAR-1(-), A1(+), A2(+) and W1(+) were purchased from MWG for resource issues. They were all reconstituted to 20μM according to their respective manufacturer's instructions. In addition two more siRNAs were purchased from Dharmacon these were solely used with the TamR cells protocol and will be described in Section 2.3.10. Likewise fluorescently labelled siRNA details are given in the sections were they were used, Sections 2.3.5. and 2.3.6. Further details and discussion siRNA design including sequences is provided in Chapter 4.

2.3.2 A431 cell culture protocols

MATERIALS

The following materials were used: 6-well plates (Corning Cat.# 3506); 24-well plates (Corning Cat.# 3527); Centrifuge tube 50mL (Corning Cat.# 430829); CryoTube (NUNC Cat.# 377267); Culture flask 75cm^2 vented cap (Corning Cat.# 337); Dimethyl sulphoxide (DMSO; Sigma Cat.# D4540); Dulbecco's modified eagle medium (D-MEM; Invitrogen Cat.# 21969-035); Foetal bovine serum (FBS; Invitrogen Cat.# 10106-169); L-Glutamine 200mM (Invitrogen Cat.# 25030-024); Penicillin-Streptomycin in 0.85% saline (Invitrogen Cat.# 15070-063); Trypan Blue Solution 0.4% (Sigma Cat.# T8154); Trypsin-EDTA solution (Invitrogen Cat.# 25300-062).

METHODS

A431 cells are an adherent human cell line, derived from an epidermal carcinoma that are noted for their high expression of EGFR (Giard et al., 1973). A431 cells were purchased from the European Collection of Cell Cultures (ECACC number 85090402). Cells were cultured in 75cm^2 tissue culture flasks containing 20ml of A431

growth media (Table 2.10) solution in a humidified cell incubator (Kendro Laboratories; HeraCell) at 37°C maintained with a mix of 95% air and 5% carbon dioxide. All cell culture reagents were warmed to 37°C in a heated waterbath (Fisher; DMU-12) before being placed on cells.

Table 2.10: A431 growth media

Media components	Volume
D-MEM	500mL
Foetal bovine serum (FBS)	57.5mL
L-Glutamine 200mM	5.75mL
Penicillin-Streptomycin	11.5mL
Total volume	~575mL

Cells were subcultured in a Class II laminar flow cabinet (Kendro Laboratories; HeraSafe). Firstly, the complete removal of growth media was followed by three washes with 10ml of PBS buffer (Appendix 1). The complete removal of buffer was followed by 2.5mL of Trypsin-EDTA and removed after 1 minute and the flask was incubated at 37°C for 10 minutes. 10ml of fresh growth media was added and the cells were agitated with a pipette to resuspend the cells. Then the 10mL of cell suspension was transferred to a clean 50mL centrifuge tube and mixed thoroughly. A small aliquot (~200µl) was taken for cell counts.

Cells were visualised by an inverted light microscope (Nikon; Eclipse TS100) and were counted using a Neubauer dual chamber haemocytometer (Marienfield). Usually, 200µL of cell suspension was mixed with 50µL Trypan blue solution, then the solution was passed three times through a 25-gauge needle and 10µL was passed into each counting chamber. Normally, one well was counted in one chamber, all nine quadrants of the haemocytometer were counted and the mean value was used.

The cell suspension was centrifuged (Kendro Laboratories; Multifuge 3 S-R), at 200g for 10 minutes at 4°C. The resulting supernatant was removed and the cell pellet was resuspended in a known volume of culture media to give 1 million cells per mL. 3 million cells (3mL) were seeded per culture flask and cells were grown to 70-80% confluency (approximately 72 hours) before being passaged.

Transfections for cell proliferation assays (Section 2.3.4) were performed in 24-well plates where each well was seeded with 50,000 cells in 0.5mL of growth media. RT-PCR (Section 2.3.8) and Western blot (Section 2.3.9) transfections were both performed in a 6-well plate where each well was seeded with 250,000 cells in 2.5mL of growth media.

To maintain cell stocks, cell aliquots were stored in liquid nitrogen. The cells were trypsinised as above but were resuspended in cryopreservation media (Table 2.11). 1mL aliquots, containing 1 million cells, were placed in 1.8mL cryopreservation tubes. These aliquots were placed in a lagged box and placed at -80°C for at least 24 hours before transferring cells to a cryogenic cell storage system (Thermo Life Sciences; Cryoplus 1 LN2 Storage System).

Table 2.11: Cryopreservation media

Media components	Volume
Dimethyl sulphoxide	3.75mL
Foetal bovine serum	2.5mL
D-MEM	43.75mL
Total volume	50mL

2.3.3 Cell transfection protocol

MATERIALS

The lipid-based transfection reagents used were: Oligofectamine; Lipofectin; Lipofectamine; Lipofectamine 2000 (all Invitrogen); RNAifect (Qiagen); Metafectene (Biontex); Transit-TKO (Mirus). The cationic dendrimers transfection reagents used were Superfect and Polyfect (both Qiagen). Also polymeric delivery systems were used: Branched 25kDa polyethylenimine (BPEI; Aldrich Cat.# 408727) and Linear 25kDa polyethylenimine (LPEI; Polysciences Cat.# 23966). Transfection media were usually: Dulbecco's modified eagle medium (D-MEM; Invitrogen Cat.# 21969-035) without further supplements or Opti-Mem (Invitrogen Cat.# 22600-134).

METHODS

Transfections were performed under laminar flow and transfection reagents were prewarmed to 37°C. For cell proliferation assays (Section 2.3.4.), cells were seeded in 24-well plates. Oligofectamine was usually used and 1.5μL was determined to be

optimal for 50,000 cells per well. Thus 1.5μL of Oligofectamine was added to 50μL of D-MEM and siRNA enough to produce a final concentration of 100nM (equivalent to 1μL of a 20μM) in 50μL of D-MEM. These two solutions were mixed together and were left for 20 minutes at room temperature for complexation to occur. While complexation was happening, growth media was removed from the cells and washed once with 0.5mL of fresh D-MEM, this media was subsequently removed and replaced with 100μL of D-MEM. After 20 minutes the transfection media was evenly applied to the 100μL of D-MEM on the cells. The cells were then incubated at 37°C, usually for 4 hours, then the transfection solution was completely removed and replaced with fresh growth media.

For RT-PCR and Western blots 6-well plates were used because a greater number of cells were required to extract sufficient RNA and protein respectively. The experiment was scaled up by a factor of five to retain same number of cells per square centimetre. Hence each well of a 6-well plate was seeded with 250,000 cells in 2.5mL of A431 culture media, and 100nM siRNA (equivalent to 5μL) was transfected with 7.5μL Oligofectamine both were in transfections volumes of 250μL.

2.3.4 Cell proliferation assay utilizing haemocytometer counting

Materials

The materials used were: AG1478 hydrochloride (Trocris Cat.# 1276); Dimethyl sulphoxide (DMSO; Sigma Cat.# D4540); Trypan blue solution 0.4% (Sigma Cat.# T8154).

Methods

The activity of EGFR gene-silencing nucleic acids was assessed by their ability to reduce the growth of cells over 48 to 72 hours. Cells were transfected as described in Section 2.3.3. and usually took place 24-hours after seeding. 24 hours later the cells were trypsinised and counted as in Section 2.3.2.

AG1478 is a highly specific small molecule inhibitor of EGFR. AG1478 treatments, of different concentrations, were dissolved in DMSO before being added directly to A431 growth media to produce final solutions of 0.1% DMSO in media.

2.3.5 Assessment of cell association of fluorescent labelled siRNA by flow cytometry

MATERIALS

The materials used were: FACs tubes (Fahrenheit); siRNA labelled with Alexa Fluor 488 and 555 (Qiagen Cat.# 1022563 & 1027099).

METHODS

A flow cytometer (BD Biosciences; FACSCalibar) was used to determine the extent of cellular association of fluorescently labelled siRNA. Transfections were performed as in Section 2.3.3. Immediately after the transfection, usually 4 hours, the cells were washed three times with ice-cold (at 4°C) PBS buffer before the addition of Trypsin/EDTA. Cells were incubated with the trypsin on ice until most cells became detached usually less than 30 minutes. Then ice-cold growth media was then added, and the cells transferred to FACS tubes, and were analysed immediately. Cell associated fluorescence distributions were obtained from 10,000 events per cell sample through a bandpass filter (FL1) using a FACSCalibar flow cytometer. The fluorescence of gated cell populations was analysed using validated analysis software, WinMDI 2.8 software (freeware; http://facs.scripps.edu). Analysis performed on the raw (median fluorescence intensity) data.

2.3.6 Assessment of cell association of fluorescent labelled siRNA and EGFR expression by fluorescent microscopy

MATERIALS

The materials used were: Alexa Fluor 594 goat anti-mouse IgM (Invitrogen Cat.# A21044); Ammonium chloride 50mM in PBS buffer; Blocking buffer [2% F.B.S; 2% BSA fraction V (Biomol Cat.# 01400) in PBS buffer]; EGFR primary antibody Ab-10 (Stratech Scientific Ltd Cat.# MS-378); Glass bottomed culture dishes 35mm (MatTek Cat. P35G-1.5-10-C); Hoechst stain solution (Sigma Cat.# H6024); Mounting oil (Dako Cat.# S3020); Negative control siRNA Alexa Fluor 488 and 555 (Qiagen Cat.# 1022563 & 1027099); Paraformaldehyde 3% (PFA) in PBS buffer; Triton X-100 (Sigma Cat.# T8787).

METHODS

The cells were grown in glass-bottom culture dishes and transfected with siRNA (as in 2.3.3 as for 6-well plates). 24 hours later the cell culture media was removed and cells

washed three times in 1mL PBS. The cells were incubated at room temperature in 1mL 3% PFA in PBS for 15 minutes before again being washed in PBS three times. Then 50mM ammonium chloride was added for 10 minutes before being washed as before. 0.2% Triton in PBS buffer was added for 5 minutes before being washed again. Primary antibody in blocking buffer (1:50) was added and left for 30 minutes before washing three times in 0.2% Triton PBS, with an addition wash with ordinary PBS buffer. Secondary antibody in blocking buffer (1:400) was added and then 40μL Hoescht stain and left for 30 minutes. The cells were washed exactly as before for the primary antibody, this was followed by an additional wash with distilled water. All water was completely removed before the addition of 15-20μl drops of Dako mounting oil and finally coverslip was gently placed on top of the cells. The slide was left for 30 minutes before visualisation with a fluorescent (Leica; DMIRB).

2.3.7 Assessment of cellular association of radiolabelled siRNA

MATERIALS

The materials used were: Cell scraper (Fisher Cat.# TKV-127-515L); Scintillant (PerkinElmer; Optiphase Hi-Safe 3); Scintillation vials 4mL (Fisher Cat.# VGA-210-010N).

METHODS

The uptake and cellular association of nucleic acids were also determined by utilising 5'-end radiolabelled nucleotides that had been gel purified Section 2.1. The radiolabelled oligonucleotides (~50 counts per second per well) were added to 100nM (per well) of 'cold' oligonucleotides before complexation and transfection, as normal. After transfection the cells were placed on ice and their media was removed. The cells were washed 3 times with ice-cold PBS buffer (Appendix 1), these washes were kept for later scintillation counting. 100μL of ice-cold lysis buffer (Appendix 1) was added to each well and left on ice for 20 minutes, the contents of the wells were removed using a cell scraper. The samples were placed in 4mL scintillation vials containing 1.5mL of scintillant and analysis was performed using a scintillation analyzer (Packard; Tricarb 2900 TR).

2.3.8 Estimation of cellular EGFR mRNA levels by reverse transcription PCR

2.3.8.1 RNA extraction by Tri-reagent

MATERIALS

The materials used were: Absolute ethanol (Fisher Cat.# E/0650DF/17); Chloroform (Fisher Cat.# BPE1145-1); Isopropanol (Fisher Cat.# P/7490/17); TRI reagent (Sigma Cat.# T9424).

METHODS

0.3ml of TRI reagent was added to each well of a 6-well plate and the homogenous lysate was scraped into a clean 1.5mL tube. These samples could now be stored at -80°C for up to a month. The samples were left for 5 minutes to ensure complete dissociation of nucleoprotein complexes. 0.24ml of chloroform was added to each sample and briefly vortexed. The samples were allowed to stand for 10 minutes and centrifuged at 15,300g at 4°C in a refrigerated bench top centrifuge (Eppendorf; Centrifuge 5417R) for 15 minutes. This centrifugation separated the mixture into three layers: RNA, DNA and protein (from top to bottom).

The upper aqueous RNA layer was carefully transferred to 1.5mL. 0.6ml of isopropanol was added to the sample and was briefly vortexed and left to stand 10 minutes. Again, the samples were centrifuged at 15,300g at 4°C for 10 minutes. The RNA should precipitate and a small pellet should be seen at the bottom of the tube.

The supernatant was removed and the pellet was washed twice by the addition 1.2ml of 75% ethanol in nuclease-free water then solution was briefly vortexed and centrifuged at 15,300g at 4°C for 5 minute. The ethanol solution was carefully removed and the RNA pellet was briefly dried for 5 to 10 minutes by air-drying. 50µl of nuclease-free water was added to dissolve the pellet.

2.3.8.2 RNA extraction by RNeasy columns

MATERIALS

The materials used were: 2-Mercaptoethanol (Sigma Cat.# M3148); RNeasy Mini kit (Qiagen Cat.# 74104).

METHODS

Extractions were performed by following the manufacturer's instructions. 10μL of 2-mercaptoethanol was added per 1mL RLT buffer (provided in the kit). After completely removing the media, 350μL of this solution was added to each well of a 6-well plate. The cells were scraped with a pipette tip and were transferred to a clean 1.5mL tube. Cells were the homogenised by passing the cell suspension fives times through a 25-gauge needle. To this homogenized solution was added an equal volume of 70% ethanol (350μL) and mixed well by pipetting. This sample was added to RNeasy column and centrifuge at 16,100g for 30 seconds and the flow-through was discarded. 700μL RW1 buffer (provided in the kit) was added to the column that was then centrifuged at full speed for 30 seconds, the flow-through and collection tube were then discarded. 500μL RPE buffer (provided in the kit) was added to the column and centrifuged at full speed for 30 seconds, and then the flow-through was discarded. The last step was repeated but instead centrifuged for 2 minutes. RNeasy column was placed in new 1.5mL tube and centrifuged at full speed for 1 minute to elute the RNA.

2.3.8.3 Reverse transcription PCR Step (RT-PCR)

MATERIALS

The materials used were: DNA Ladder 1 kb (Sigma Cat. D-7058); dNTPs 100mM (Invitrogen Cat.# 10297-018); Ethidium Bromide Solution (Promega Cat.# H5041); Gel documentary system (Biorad; Gel Doc 1000); Magnesium Chloride (25mM $MgCl_2$; Qiagen); M-MLV Reverse Transcriptase 200 units/μL (Invitrogen Cat.# 28025-013); PCR buffer 10x (Qiagen; with 1.5mM $MgCl_2$); Random Hexamers ($pd(N)_6$ GE Healthcare Cat.# 27-2166-01); RNasin (Promega Cat.# N211A); Taq polymerase (Cancer Research UK).

METHODS

The extracted total RNA was added to the reverse transcription reaction mixture (Table 2.12) and incubated in the thermocycler at 95°C for 5 minutes. 0.5μl of RNAsin, 1μL M-MLV was added to each reaction mixture they were then incubated at 25°C for 5 minutes followed by 42°C for 42 minutes.

Table 2.12: Reverse transcription reaction mixture

Reaction components	Volume
Nuclease-free water	8.5-xμL
RNA (1μg)	XμL
First strand (5x) buffer	4μL
dNTPs (10mM)	2μL
DTT (100mM)	2μL
Random hexamers (50ng/μL)	2μL
RNAsin	0.5μL
M-MLV enzyme	1μL
Total volume	20μL

Where x equals the volume occupied by 1μg of RNA

The specific amplification of EGFR cDNA was performed using primers previously designed to target the EGFR gene (Thomas, 2004) with the ß-Actin primers being published earlier (O'Bryan et al., 1991; Appendix 2). Primers specific to the housekeeping gene ß-Actin were used as a control to ensure equal loading of cDNA (Appendix 2). Equal amounts of cDNA from all the different treatments were added to individual PCR mixtures containing primers specific to EGFR. This was repeated for all the treatments but using primers specific for ß-Actin. The mixtures were initially denatured at 94°C for 5 minutes, followed by 30 cycles of: 94°C for 30 seconds, 60°C for 45 seconds 72°C for 42 seconds, with a final extension at 72°C for 10 minutes.

Table 2.13: PCR reaction mixture

Reaction components	Volume
Nuclease-free water	16.8-xμL
Taq buffer	2.5μL
Magnesium chloride (25mM)	1μL
dNTPs (10mM)	0.5μL
cDNA (0.2μg)	xμL
Forward primer (1μM)	2μL
Reverse primer (1μM)	2μL
Taq enzyme	0.2μL
Total volume	25μL

Where x equals the volume occupied by 0.2μg of cDNA

5μL of EGFR and ß-Actin cDNA for all the treatment were run on a 1% agarose gel for 40 minutes. The bands were visualised and densitometry was performed.

2.3.9 Determination of cellular EGFR protein levels by Western blot

MATERIALS

The materials used were: Anti-actin antibody produced in mouse (Sigma Cat.# A5441); Anti-EGFR antibody produced in rabbit (Cell Signaling Cat.# 2232); Anti-mouse Ig-HRP-linked whole antibody (Amersham NA931V); Anti-rabbit Ig-HRP-linked whole antibody (GE Healthcare Cat.# NA934V); Autoradiography film blue sensitive (GRI Cat.# MXB 1824); Autoradiography sealed cassette (GE Healthcare Cat.# RPN 13642); Bovine Serum Albumin (BSA; Sigma Cat.# A7906); Cell scraper (Fisher Cat.# TKV-127-515L); Chemiluminescent supersignal West Dura substrate (Pierce Cat.# 34076); Chromatography Paper (Whatman Cat.# 3030-931); Coomassie blue (Sigma Cat.# B-0770); DC Bio-Rad protein assay kit (Bio-Rad Cat. 500-0116); Milk Powder (Marvel); Ponceau S Solution (Sigma Cat.# P7170); Protan 0.2μm nitrocellulose paper (Schleicher and Schuell Cat.# N401396); Rainbow molecular weight markers (GE Healthcare Cat.# RPN 800); RG Developer and Fixer (Photon-Imaging).

METHODS

The cells were harvested from 6-well plates on ice, first the culture media was removed and the cells were washed 3 times with ice-cold PBS buffer (Appendix 1). 100μl of ice-cold lysis buffer with the recent addition of protease inhibitors (Appendix 1) was added to each well and left on ice for 15 minutes. Cells were scraped and transferred to 1.5mL tubes and left for on ice for a further 15 minutes. Then the samples were centrifuged at 15,300g for 15 minutes at 4°C. Then the supernatant was removed and frozen at -20°C. The protein content of cell lysates were estimated using a DC Protein assay kit that is based on the principles of the Lowry assay (Lowry et al., 1951). Assays were carried out according to the manufacturer's instructions. First a standard curve was set-up using BSA in duplicate in cuvettes. The samples were diluted with lysis buffer (Appendix 1; the BSA was diluted with nuclease-free water), by a known amount to 50mL, so they have a colour in the range of the standard curve. 250mL of mixed Reagent A (20mL of Reagent S in 1mL Reagent A) and 2mL Reagent B were added to all the cuvettes. The cuvettes were mixed and then left for 15 to 30 minutes. The standard curve was then measured and the protein levels of the samples were estimated with a UV spectrophotometer at 750nm.

An electrophoresis system (Bio-Rad; Mini-Protean II) was used to run the SDS polyacrylamide gel by following the manufacturers instructions. A volume equal to 20μg of lysate, determined from protein estimation, was taken for each sample and mixed with 2x sample loading buffer (Appendix 1). This mixture was then heated to 95°C, to denature the proteins in to their primary structure, for 10 minutes using a dry block heater. The acrylamide was gel prepared so there was a stacking gel on top of a resolving gel. The samples and rainbow proteins were loaded onto the gel and run at 150 volts for 2 hours using 1x Western blot running buffer (Appendix 1).

Once the gel electrophoresis was completed, the gel was removed and soaked in protein transfer buffer (Appendix 1). The protein transfer system was set up, according to manufacturers instructions, using chromatography paper and nitrocellulose paper. The system was then run at 100 volts for 2 hours. Once the transfer was completed, the gel was removed from the nitrocellulose membrane. The well locations and the position of the rainbow protein on the membrane were marked with a pencil. To confirm protein transfer had occurred the nitrocellulose membrane and gel were stained with Ponceau S solution and Coomassie blue stain respectively. The nitrocellulose membrane was washed for 10 minutes with TBS Tween buffer, and repeated twice. To block all the non-specific binding sites on the nitrocellulose membrane it was placed in 1g of milk powder in 20ml TBS Tween buffer (Appendix 1) and incubated overnight at 4°C. The nitrocellulose strip was then washed with TBS Tween buffer (Appendix 1) three times for 10 minutes each. The nitrocellulose was probed with primary antibody by incubating with 20μl of rabbit anti-EGFR antibody in 20mL of TBS Tween containing 1g of milk powder for 1.5 hours at room temperature. Then the membrane was washed with TBS Tween 3 times for 10 minutes each to remove any excess primary antibodies. 20μl of secondary antibody in 20ml of TBS Tween containing 1g of milk powder was incubated with the membrane for 1.5 hours at room temperature. Then any excess secondary antibodies were removed from the membrane by the washing it three times with TBS Tween for 10 minutes each. The nitrocellulose membrane was placed in a clean autoradiography cassette. 0.5ml of Western Duro substrate was mixed with 0.5ml of Luminal/Enhancer solution and was added evenly onto the surface of the nitrocellulose membrane. After five minutes, the membrane was exposed in the dark to autoradiograph film for 5 seconds.

To ensure the removal of both primary and secondary antibodies the membrane was washed with 10x TBS buffer (Appendix 1) for 15 minutes and 1x TBS Tween buffer for a further 15 minutes. All the blotting procedures were the same as above but the primary antibody used was 20µl mouse anti-ß-actin and the secondary antibody was 10µL of stabilized goat anti-mouse HRP-conjugate. ß-Actin was used a loading control and was to used to normalise EGFR protein level from the densitometry values

2.3.10 TamR cell protocols

2.3.10.1 TamR cell culture

MATERIALS

The materials used were: 4-Hydroxytamoxifen (Sigma Cat.# H7904); Amphotericin B 250µg/mL (Fungizone; Invitrogen Cat.# 15290-026); Charcoal stripped foetal bovine serum (FBS stripped in Tenovus; Invitrogen Cat.# 10106-169); RPMI 1640 media without phenol red and L-glutamine (Invitrogen Cat.# 32404); L-Glutamine 200mM (Invitrogen Cat.# 25030-024); MCF-7 TamR cells (were generous gifts from Tenovus Centre for Cancer Research; Cardiff); Penicillin-Streptomycin in 0.85% saline (Invitrogen Cat.# 15070-063).

METHODS

Cells were seeded at 2.5 million cells per 6-well plate and grown in MCF-7 TamR growth media (Table 2.14). The 4-Hydroxytamoxifen was dissolved in absolute ethanol and made up to a solution of 1x 10^{-3}M.

Table 2.14: MCF-7 TamR growth media

Media components	Volume
RPMI medium	459mL
Stripped foetal bovine serum	25mL
L-Glutamine 200mM	10mL
Penicillin-Streptomycin	1mL
Amphotericin B 250µg/mL	5mL
4-Hydroxytamoxifen (10^{-3}M)	0.05mL
Total volume	500mL

2.3.11 TamR cell transfection protocol

MATERIALS

The materials used were: DharmaFECT 1 (Dharmacon Cat.# T-2001-01); Oligofectamine; siCONTROL Non-targeting siRNA (Dharmacon Cat.# D-001210-01-05); siGENOME SmartPool (Dharmacon Cat.# M-003144-01).

METHODS

The MCF-7 TamR cells were grown until 70% confluent. The growth media was removed and replaced with 2mL of fresh growth media, without antibiotics or amphotericin B. 12.5μL of siRNA and DharmaFECT were both diluted separately in 250μL of growth media (without serum and antibiotics and amphotericin) in two separate 1.5mL tubes. The two solutions, containing siRNA and lipid, were then mixed together and left for 20 minutes at room temperature for complexation before adding this solution on top of 2mL of fresh media on the cells. Leave for 48 hours before extraction using RNeasy columns as in Section 2.3.8.2.

2.3.11.1 TamR RT-PCR protocol

MATERIALS

The materials used were: Dithiothreitol 100mM (DTT; Invitrogen Cat.# Y00147); dNTPs 100mM (Invitrogen Cat.# 10297-018); M-MLV Reverse Transcriptase 200 units/μL (Invitrogen Cat.# 28025-013); Random Hexamers ($pd(N)_6$ GE Healthcare Cat. 27-2166-01); RNasin (Promega Cat.# N211A); Taq Polymerase 500units/100mL (Cancer Research UK).

METHODS

The RNA was extracted using the RNeasy protocol as above. The reverse transcription reaction mixture was prepared (Table 2.15) using PCR buffer from Tenovus (Appendix 1). This mixture was incubated at 95°C and then place immediately on ice for 5 minutes. Afterwards the tubes were briefly centrifuged and 0.5μL RNAsin and 1μL M-MLV were added followed by incubation at 22°C for 10 minutes, 42°C for 40 minutes then 95°C for 5 minutes.

Table 2.15: TamR reverse transcription reaction mixture

Reaction components	Volume
dNTPs (2.5mM)	5μL
Random hexamers (100μM)	2μL
DTT (100mM)	2μL
PCR buffer (Tenovus)	2μL
Nuclease-free water	7.5-xμL
RNA sample (0.1μg)	xμL
RNasin	0.5μL
M-MLV enzyme	1μL
Total volume	20μL

Where x equals the volume occupied by 0.1μg of RNA

Primers were designed using the Primer3 (http://frodo.wi.mit.edu/) online program to produce shorter length amplicons (Appendix 2). PCR reactions mixtures were prepared using PCR buffer Tenovus (Appendix 1) and placed in 0.2μL PCR tubes (Table 2.16). The mixtures were initially denatured at 94°C for 5 minutes, followed by 32 cycles for EGFR and 26 for ß-Actin: 94°C for 30 seconds, 61°C for 45 seconds 72°C for 45 seconds, with a final extension at 72°C for 10 minutes. Add 1μL cDNA for EGFR and 0.1 μL Actin. 4μL loading buffer PCR Tenovus (Appendix 1) was added to 12.5μL of each sample. A horizontal electrophoresis gel system was used to run 2% agarose gel (Appendix 1) in 1x TAE buffer (Appendix 1), at 100v for as least 15 minutes.

Table 2.16: TamR PCR reaction mixture

Reaction components	EGFR	Actin
Nuclease-free water	2.55μL	3.05μL
PCR buffer Tenovus	1.25μL	1.25μL
dNTP (2.5mM)	1μL	1μL
Reverse primer (3μM)	3.3μL	3.3μL
Forward primer (3μM)	3.3μL	3.3μL
cDNA	1μL	0.5μL
Taq enzyme	0.1μL	0.1μL
Total volume	12.5μL	12.5μL

Chapter 3
Biological stability of siRNA

3.1 Introduction

The biological stability of siRNA can be primarily defined as the resistance of the molecule to nucleases present in biological media although other issues such as conformational stability may also be defined as such, however this thesis is concerned with nuclease stability. Biological media, such as serum-containing cell culture media contain nucleases that hydrolyse the phosphodiester bonds found in oligonucleotides.

In 2002, when my thesis work began, the activity of oligonucleotides, such as siRNA and antisense oligodeoxynucleotides (ASO), were deemed to be highly dependent on their biological stability (Bertrand et al., 2002). A pertinent question at the time was whether siRNA was more active than ASO and whether this was due to its enhanced biological stability. This question was the basis of the work described in the chapter.

3.1.1 The involvement of nucleases in the biological stability of oligonucleotides

Nucleases have been classified by the Nomenclature Committee of the International Union of Biochemistry and Molecular Biology (NC-IUBMB), whose guidelines are available online (http://www.chem.qmul.ac.uk/iubmb/enzyme/), as hydrolases that act on ester bonds (EC 3.1). Examples of nuclease classification are summarised in Table 3.1; the table was adapted from one previously published (Roberts and Linn, 1982). This table classifies nucleases based on three criteria: a) RNA/DNA substrate specificity, b) preference for an open terminus (exo/endonuclease), c) position of the cleaved phosphate on the nucleolytic product (3'/5'-phosphomonoester). The EC number provides the NC-IUBMB classification and examples are included of the main types of nucleases.

a) Nucleases were historically classified into ribonucleases (RNases) or deoxyribonucleases (DNases), based on their specificity for their respective nucleic acid substrate (Kunitz, 1940). In addition, a third class of sugar-non-specific nucleases was needed for nucleases that act on both nucleic acid substrates, such as snake venom phosphodiesterase and micrococcal nuclease (Laskowski Sr, 1985).

b) Exonucleases were classified initially as only capable of removing mononucleotides from a terminus. But exonuclease is now considered to have a preference to act on nucleotide termini as an 'exophilic nuclease' (Mishra, 2002).

Table 3.1: Classification of nucleases based on the guidance by the Nomenclature Committee of the International Union of Biochemistry and Molecular Biology (NC-IUBMB)

Substrate	Nuclease	Nucleolytic product	Class	Examples
DNA	Exo-	5'-phosphomonoester	EC 3.1.11	Exodeoxyribonuclease I Exodeoxyribonuclease III Exodeoxyribonuclease (lambda-induced) Exodeoxyribonuclease (phage SP3-induced) Exodeoxyribonuclease V Exodeoxyribonuclease VII
	Endo-	5'-phosphomonoester	EC 3.1.21	Deoxyribonuclease I Deoxyribonuclease IV (phage-T4-induced) Type I site-specific deoxyribonuclease Type II site-specific deoxyribonuclease Type III site-specific deoxyribonuclease CC-preferring endodeoxyribonuclease Deoxyribonuclease V
		3'-phosphomonoester	EC 3.1.22	Deoxyribonuclease II *Aspergillus* deoxyribonuclease K1 Crossover junction endodeoxyribonuclease Deoxyribonuclease X
RNA	Exo-	5'-phosphomonoester	EC 3.1.13	Exoribonuclease II Exoribonuclease H (RNase H) Oligonucleotidase Poly(A)-specific ribonuclease Ribonuclease D
		3'-phosphomonoester	EC 3.1.14	Yeast ribonuclease
	Endo-	5'-phosphomonoester	EC 3.1.26	*Physarum polycephalum* ribonuclease Ribonuclease alpha Ribonuclease III Calf thymus ribonuclease H (RNase H) Ribonuclease P Ribonuclease IV Ribonuclease P4 Ribonuclease M5 Ribonuclease [poly-(U)-specific] Ribonuclease IX tRNase Z
		3'-phosphomonoester	EC 3.1.27	Ribonuclease T2 *Bacillus subtilis* ribonuclease Ribonuclease T1 Ribonuclease U2 Pancreatic ribonuclease (RNase A) *Enterobacter* ribonuclease Ribonuclease F Ribonuclease V tRNA-intron endonuclease rRNA endonuclease
Non-specific	Exo-	5'-phosphomonoester	EC 3.1.15	Snake venom exonuclease
		3'-phosphomonoester	EC 3.1.16	Spleen exonuclease
	Endo-	5'-phosphomonoester	EC 3.1.30	*Aspergillus* nuclease S1 *Serratia marcescens* nuclease
		3'-phosphomonoester	EC 3.1.31	Micrococcal nuclease

c) The nuclease products are always, without exception, exclusively either 3'- or 5'-phosphomonoesters. This is therefore the only absolute classification criterion (Mishra, 2002). Since this criterion cannot be applied to damage-specific nucleases, recombinases and topoisomerases were excluded from Table 3.1, also it is unlikely that they would be involved in nucleic acid degradation.

Glenn Hoke from ISIS Pharmaceuticals tested sera for nuclease activity (unpublished data) and of three kinds of biological media tested (FBS, mouse and human serum) FBS had the most nuclease activity and human serum the least (cited as a personal communication in Crooke and Lebleu, 1993). The predominate nuclease for ASO degradation in FBS is a 3'- exonuclease (Tidd and Warenius, 1989) and there are significant variations in nuclease activity between batches of sera (Crooke and Lebleu, 1993). ASO degradation in other sera is also due to a 3' exonuclease (Hoke et al., 1991, Shaw et al., 1991) while both exo- and endonucleases are thought to be responsible for degradation in cells (Crooke and Lebleu, 1993, Monia et al., 1996). So the stability of ASO in sera is not a good predictor of intracellular biological stability (Crooke and Lebleu, 1993).

siRNA are either completely RNA, or predominantly RNA, so ribonucleases would be thought to cause its degradation but investigators must be aware of the numerous classification exceptions. One notably exception is a pancreatic DNase that can digest a stand composed of a mixture of ribo- and deoxyribonucleotides (Pruch and Laskowski M, 1980).

Ribonucleases in the human serum can be separated into secretory or non-secretory (Sierakowska and Shugar, 1977): Secretory are pancreatic-type, with a high optimal pH (~8.5) and preference for Poly(C) chains. Non-secretory are liver-type, with a low optimal pH (6.5-7.0) and preference for Poly(U) chains (Mishra, 2002).

Akagi and co-workers (Akagi et al., 1976) fractionated human serum and determined that the majority of serum ribonuclease activity is of the pancreatic-type. Weickmann and Glitz using a radioimmunoassay determined that Human Pancreatic RNase (HP-RNase) to account for 60-80% of ribonuclease activity in human serum (Weickmann and Glitz, 1982). HP-RNase has a similar structure and function to Bovine RNase A

(E.C. 3.1.27.5) (Sorrentino and Libonati, 1997). RNase A is the most studied nuclease (Mishra, 2002) and was the first protein whose amino sequence was completely elucidated (Smyth et al., 1963) and it functions to cleave single-stranded RNA, shown in Figure 3.1. RNase A cleaves the pyrimidine-nucleotide bonds, i.e. UpN and CpN. Double-stranded RNA, such as siRNA, still can be cleaved by RNase A because thermal fluctuations can cause the two strands to temporarily separate allowing sporadic cleavage (Libonati and Gotte, 2004).

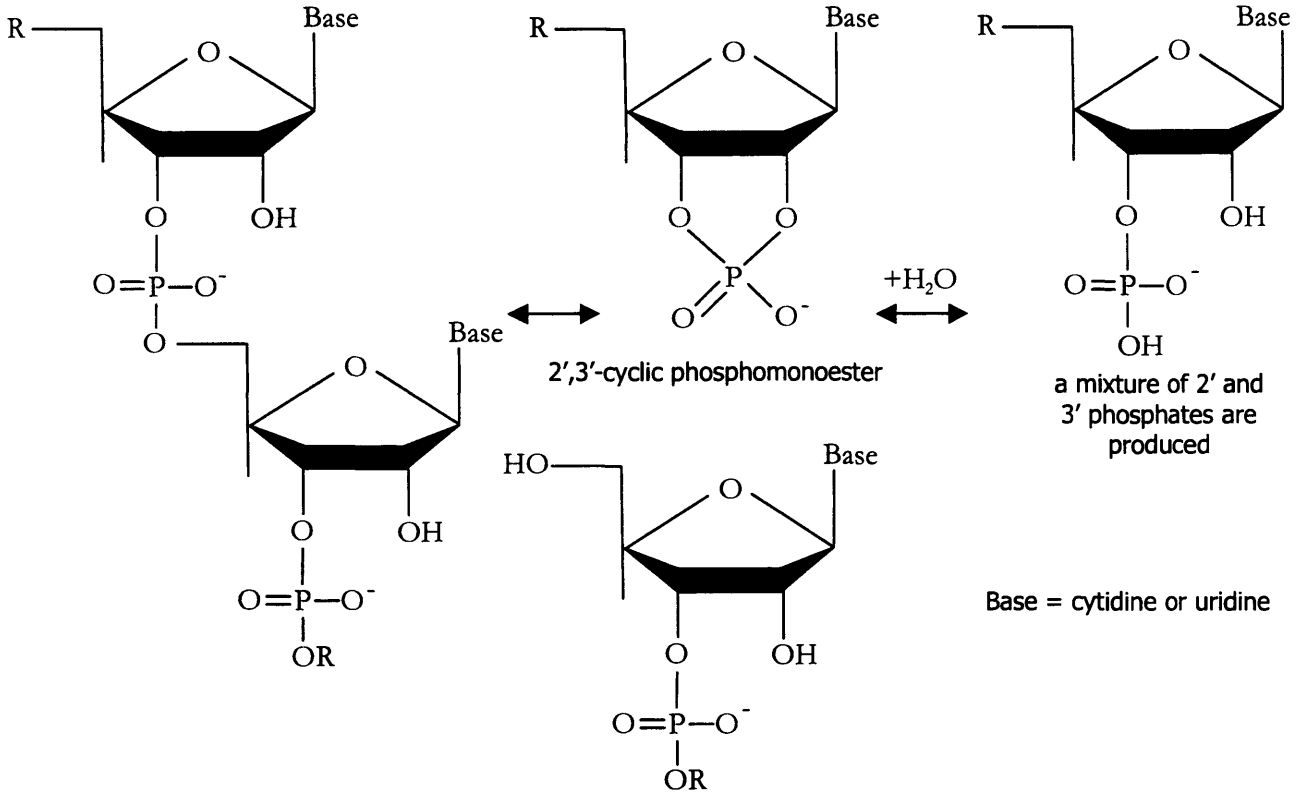

Figure 3.1: The hydrolysis of ribonucleic acid (RNA) by Ribonuclease A is a two-step mechanism. The first stage is a transesterification resulting in an intermediate 2',3'-cyclic phosphate ester and the cleavage of the RNA chain. The second step is the enzyme hydrolyses the cyclic phosphate ester to produce 3'-phosphomonoesters ending in cytidine or uridine 3'-phosphate. The major enzyme catalytic sites are the imidazole rings of Histidine-12, Histidine-119 and Lysine-41. The Histidine-12 deprotonates the 2'-hydroxyl group of the ribose and the acid imidazolium of Histidine-119 protonates the oxygen of the leaving nucleotide hydroxyl group.

3.1.2 Studies into the biological stabilities of antisense oligodeoxynucleotides (ASO)

There has been a considerable amount of published data on the biological stabilities of ASOs. Wickstrom first reported the biological stability half-life of unmodified ASO in FBS to be less than 15 minutes (Wickstrom, 1986). Kurreck & co-workers (Kurreck et al., 2002) reported the half-life of a radiolabelled 18mer ASO in human serum to be 1.5 hours. This disputed other previous data that placed the plasma half-life of ASO at less than one hour (Agrawal and Zhao, 1998b, Agrawal and Zhao, 1998a, Akhtar et al., 1991, Glover et al., 1997, Wickstrom, 1986).

The problem with absolute determination of half-lives is the discrepancies between the values reported by different laboratories. These inconsistencies could be due to the biological media including commercial media. Also the oligonucleotides vary in length, sequence, and may also form secondary structures that are resistant to nuclease activity. The methods of the stability assay and detection of oligonucleotides and analysis vary between groups (Crooke and Lebleu, 1993).

ASO chemical modifications that have been developed to improve biological stability can be generally split into three main classes: backbone modifications, modified sugars especially at 2'-OH of the ribose, and unnatural bases (Kurreck, 2003). Determination of intracellular biological stability is important since chemical modifications that improve serum stability do not accurately predict intracellular stability (Crooke and Lebleu, 1993). Intracellular degradation of ASOs results in a characteristic 'ladder' pattern on PAGE gels because of processive exonuclease activity but there may also be endonucleases present (Crooke, 1998).

3.1.3 Comparative studies of the biological stabilities of ASO and siRNA

As discussed earlier, the major issues with antisense biological stability studies is the discrepancy between absolute results, such as biological half-life, because of the inter-laboratory variations. Table 3.1 shows the majority of siRNA biological stability papers that were published when this work was started.

Bertrand and co-workers (Bertrand et al., 2002) reported that siRNA was more biologically stable than ASO. They stated, without showing the data, that siRNA has a half-life of 24 hours in FBS whereas intact ASO survived only for a few minutes.

They hypothesized that the second strand could hinder the action of nucleases and therefore gave siRNA additional stability benefits over single stranded ASO molecules.

Kurreck and co-workers (Grunweller et al., 2003) also reported that siRNA was more biologically stable than ASO in 10% FBS. The half-life of siRNA being over 2 hours while ASO was about half an hour. This ASO half-life was shorter than they previously reported (Kurreck et al., 2002), but may reflect the method used i.e. their first paper utilised a 5'-end radiolabelled stability assay and their following paper had an assay that detected oligonucleotides with ethidium bromide. This half-life of 2-hours for siRNA was much shorter than the 24-hours reported by Bertrand and co-workers in full FBS (Bertrand et al., 2002).

An intra-laboratory comparison of the biological stabilities of ASO and siRNA in the same media and under the same conditions would determine the more stable oligonucleotide. If siRNA molecules are not more biologically stable than ASOs they would therefore necessitate chemical modifications to improve their biological stabilities.

Table 3.2: Comparison of some published siRNA stability results. For completeness, the articles that compare siRNA stability to chemically modified siRNA or other oligonucleotides, those results are included as well.

Reference	Oligonucleotide	Chemistry	Media	Visualisation technique	Results
(Bertrand et al., 2002)	siRNA	22mer with 3' RNA overhangs	HeLa cell lysates and full FBS	100nM 5'-^{32}P radiolabelled nucleotides run on 20% 7M Urea PAGE	Half life of 24h in FBS
	ASO	18mer ASO			Lasts a few minutes in FBS
(Braasch et al., 2003)	ssRNA	PO 3'-dTdT	5% FBS	20μM siRNA run 15% 7M Urea PAGE. Gel stained with SYBE Green II	Modified and unmodified siRNA lasted >72h ssRNA <30s
		PS-modified			
(Braasch et al., 2004)	siRNA	PO 3'-dTdT	50% mouse serum (v/v)		50% loss in 24h
		PS-modified			
(Grunweller et al., 2003)	siRNA	PO 3'-dTdT	10% FBS	20pmol siRNA run on 20% 7M Urea. Gel stained with ethidium bromide	$t_{1/2}$=2.1h
	ASO	PO-unmodified			$t_{1/2}$=0.33h
		PS-modified			$t_{1/2}$=>>48h
		LNA			$t_{1/2}$=41h
		2'-O-Me			$t_{1/2}$=5.2h
(Czauderna et al., 2003)	siRNA	Unmodified 21mer	10% FBS	2.5μM siRNA 10% PAGE. Gel stained with ethidium bromide	No loss in 2h
		PO 3'-dTdT			>50% loss in 2h
		3'-iB			
		3'-NH_2			
		2'-O-Me			<50% in 2h*
(Layzer et al., 2004)	siRNA	PO 3'-dTdT	Human plasma	10pmol 5'-^{32}P radiolabelled siRNA on 15%PAGE	>50% loss in 1min, almost all lost in 4h
		2'-F			<50% loss after 24h

2'-F= 2'-Fluoro pyrimidine backbone, 2'-O-Me= 2' O-Methyl, dTdT= deoxythymidine-deoxythymidine 3'-overhangs, FBS= Foetal Bovine Serum, iB = inverted deoxy abasic ends, LNA= Locked Nucleic Acid, NH_2= 3' Amino-C6 linker end protection, ASO= Antisense oligodeoxynucleotides, PAGE= Polyacrylamide Gel Electrophoresis, PO-Phosphodiester linkages, PS=Phosphorothioate, $t_{1/2}$= Biological half life
*Depends on position and number of modifications

3.1.4 Studies into the biological stability of siRNA

Results with other RNA-based therapeutics ribozymes, reveals that unmodified RNA are extremely labile and require chemical modifications to improve their biological stability in order for it to be active in cellular and *in vivo* environments (Beigelman et al., 1995, Hudson et al., 1996). Tuschl & co-workers (Elbashir et al., 2002, Elbashir et al., 2001c) report that siRNA with two deoxythymidine (3'-TT) overhangs at each 3' end are more resistant to exonucleases present in media and cell lysates. In other published results (Table 3.2) there seemed to be conflicting results regarding the stability of siRNA. Published results seem to disagree on how quickly siRNA is degraded in serum-containing media varying from minutes (Layzer et al., 2004) to a few days (Bertrand et al., 2002, Braasch et al., 2003).

Chapter Aim

The aim of this chapter is to address the stability of siRNA in biological media and secondly, whether chemical modifications as used in ASOs, are necessary for siRNA activity.

Chapter Objectives

- To develop intra-laboratory assays for the direct comparison of the biological stabilites of ASO and siRNA.
- To determine whether siRNA is more biologically stable than ASO in serum-containing media. Could this responsible for its improved activity?
- What patterns of siRNA degradation are observed? Are they consistent with as endo- or exonucleases for ASO or RNase A?
- From the patterns of degradation assess what chemical modifications are required to improve siRNA stability?
- What are the intracellular stabilities of siRNA and ASO? Does this reflect sera degradation?

3.2 Methods

All methods have been described previously in Chapter 2 (see specific section below)

The siRNA used in stability assay was the HAR-1 siRNA, a 21mer duplex with two 3'-TT overhangs as designed in Chapter 4 (Table 4.6). The ASO was a 21mer DNA primer used in the PCR reactions in Materials and Methods (Section 2.1.1). The

single-stranded RNA was one strand, the antisense strand, of HAR-1 siRNA a 21mer that terminates with 3'-TT. All oligonucleotides were 5'-end radiolabelled (2.1.1) and purified by PAGE purification (2.1.3) unless otherwise stated.

The stability assay was performed in vitro with four biological media: 10% FBS-containing D-MEM, 100% FBS, A431 cells lysates and in 10% FBS-containing D-MEM in a cell culture well with A431 cells. Radiolabelled oligonucleotides were incubated in the media at 37°C, aliquots were taken at predetermined time intervals, mixed with loading buffer and immediately frozen to stop degradation. Samples were run on 20% PAGE gels to separate degradation fragments and were visualised using a phosphorimager.

3.3 Results & Discussion

3.3.1 Purification of radiolabelled oligonucleotides

The T4 polynucleotide kinase enzyme was used to label the 5'-hydroxy terminus of oligonucleotides by catalysing the transfer of a radiolabelled gamma phosphate (^{32}P) from ATP. ^{32}P is a synthetic isotope of phosphorous that is an emitter of high-energy beta particles. This reaction is used routinely in molecular biology to produce probes for RNA and DNA (Sambrook et al., 2001).

Gel filtration chromatography columns (also known as size exclusion chromatography columns) retain small molecules while allowing large molecules to pass through. Sephadex G-25 microspin columns have exclusion limit of molecules with a relative molecular mass of over 5000, so they have been used in the removal of unreacted label leftover from the radiolabelling of oligonucleotides. Therefore, these spin columns will retain free ATP molecules while allowing radiolabelled or unlabelled oligonucleotides to be eluted.

Figure 3.2 shows a phosphorimage of a PAGE gel used to separate and visualise elutions of product from a siRNA T4 kinase radiolabelling reaction through successive Sephadex columns. The siRNA labelling reaction contains a mixture of products that are inferred to be from largest fragment to smallest: labelled siRNA, free ATP label and free radioactive phosphate. In Figure 3.2A, two successive columns were needed to remove the free label, although elution through three

columns resulted in significant loss of labelled product the band was still visible. In Figure 3.2B, elution through two successive columns resulted in such a significant loss of labelled product, the band was no longer visible. This variation in results could be due to the manufacturer not recommending the G-25 Sephadex columns for the purification of RNA because they have small amounts of RNase activity, according to the Frequently Asked Questions (FAQ) section found on the GE Healthcare website. This RNase activity present on the columns could remove the trace amounts of labelled siRNA, although these columns were used successfully in our laboratory for purifications of oligonucleotides.

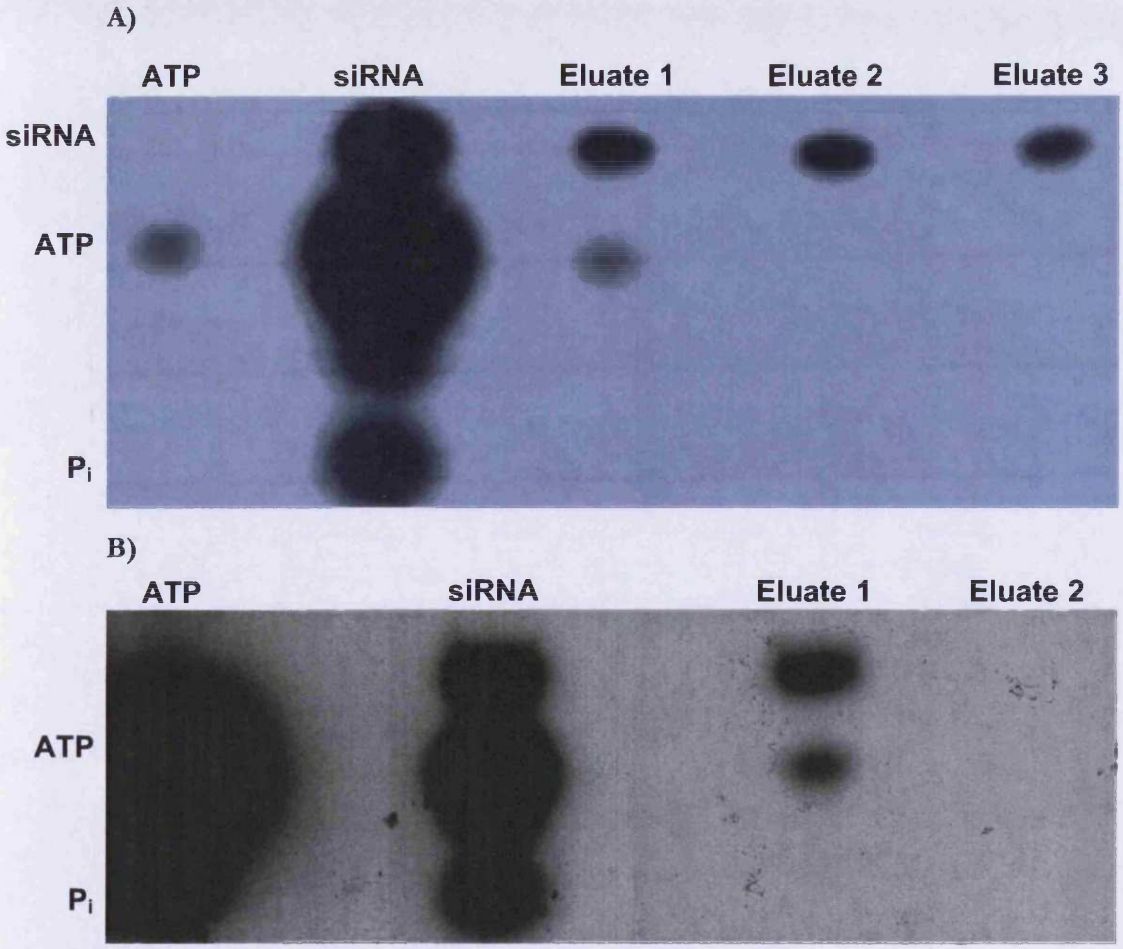

Figure 3.2: The removal of free radiolabel from a radiolabelling siRNA reaction by G25 Sephadex column purification. siRNA was labelled by the T4 kinase enzymatic addition of a radioactive phosphate atom. Free ATP label was run on a 20% PAGE gel alongside siRNA from a radiolabelling reaction and successive eluates passed through Sephadex columns. The PAGE gels were visualised by a phosphorimager. **A)** Shows an example image of a PAGE gel, the elution through one column (Eluate 1) reduces the amount of free ATP, subsequent elutions reduce this further but along with the amount of labelled siRNA **B)** Shows another representative image of column purifications, although free label is removed there is a corresponding and significant amount of loss of radiolabelled siRNA.

The purification of oligonucleotides using Sephadex columns proved too irreproducible and another method using PAGE purification was attempted. The radiolabelled oligonucleotides: radiolabelled antisense oligodeoxynucleotides (ASO), duplex HAR-1 siRNA (siRNA) and single stranded RNA (ssRNA) that is the sense strand of HAR-1 siRNA were purified using a 20% PAGE gel. The bands corresponding to labelled oligonucleotides (A1, S1, S2, S3, R1) were excised and eluted in water (Figure 3.3).

The multiple bands seen in the siRNA (Figure 3.3; S1, S2 and S3) and ASO (Figure 3.3; A1 and non-designated bands underneath) lanes could be degradation products caused by the labelling reaction or gel purification, or due to the labelling of impurities present in oligonucleotides. S1 is thought to be the intact siRNA duplex as it would have the largest molecular weight. S2 could be thought to be a single stand of siRNAs as it migrates at a similar rate as R1 (Figure 3.3).

The purification gel (Figure 3.3) had three labelled products of different molecular weights for siRNA (S1, S2 and S3). I proposed that the largest molecular weight product (S1) is the full-length undegraded siRNA duplex. The other two main bands could be due to the siRNA duplex separating into the individual strands. Several attempts were made using several different reannealing protocols to reanneal S2 and to reanneal denatured siRNA to produce the duplex (S1), shown in Figure 3.4.

Figure 3.4 shows how the denaturing protocol produces a band of a size between ATP and siRNA that could be the single strand. Although this single-strand could not be reannealed by the reannealing protocol, it actually appeared that the single-strand was degraded further.

Figure 3.3: Removal of free radiolabel from ASO, siRNA and ssRNA radiolabelling reactions by PAGE purification. The gel purification of radiolabelled antisense oligodeoxynucleotides (ASO), duplex HAR-1 siRNA (siRNA) and single stranded RNA (ssRNA) that is the sense strand of HAR-1 siRNA. The 20% PAGE purification gel shows the separation of the labelled oligonucleotides and the black borders represent the area of band excision: A1=ASO, S1=siRNA duplex, S2= siRNA first degradation product, S3=siRNA second degradation product, R1=single strand siRNA. Please note a light band corresponding to R1 was visible at different resolutions but this may appear as being absent from the printed image.

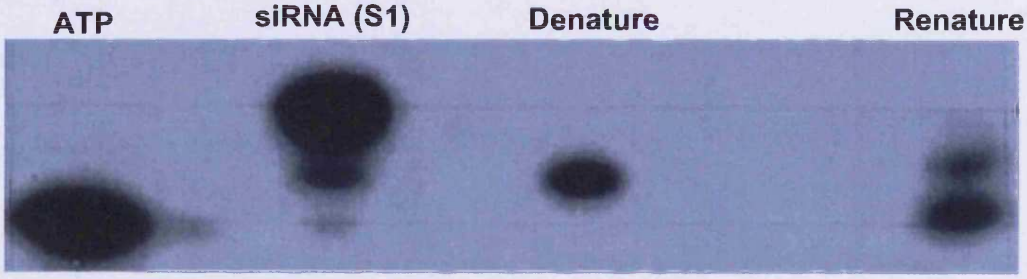

Figure 3.4: Radiolabelled siRNA purification products subjected to a denaturation followed by renaturation protocol. A 20% PAGE gel visualised by a phosphorimager shows the result of denaturing and renaturing protocols. The siRNA duplex was denatured by mixing with 7M urea and heating to 95°C for 1 minute, this was then diluted and passed through a Sephadex column. Renatured siRNA was heated to 95°C then ramped cooled to 25°C over 25 minutes.

3.3.2 Stability assay

3.3.2.1 Stability of ASO and siRNA in FBS-containing biological media

The stability of the different radiolabelled siRNA bands from the purification gel (Figure 3.3) were assessed in 10% serum-containing media and then run on a 20% PAGE gel (Figure 3.5). The first observation is that multiple bands exist for siRNA even in the control, i.e. siRNA that had not been exposed to FBS-containing media. This suggests that either the siRNA had been unpure from the manufacturer or degraded during radiolabelling or PAGE. The possibility of PAGE degradation is backed-up since bands from S1 (Figure 3.5) appear to match some in S2 and S3. The S1 and S2 bands (Figure 3.5) have more similar degradation profiles with full-length oligonucleotides still being visible after 2-hours compared with S3, were the full-length is lost before the first time point (t=1). Another point is that shadows above the full length S3 appear to match those seen in S2. Another observation is the presence of free-label within all samples suggesting the PAGE purification is not complete.

Single-stranded siRNA (ssRNA in Figure 3.6) is degraded quickly, within the time it takes to produce the first time point (t=1). This is similar to the S3 degradation profile as seen in Figure 3.2. This conflicts with the data that shows S2 runs at the same rate as R1 (Figure 3.3). The stability of single-strand siRNA is directly compared to ASO in 10% serum-containing media (Figures 3.3). ASO seems to last much longer in the media than single-strand siRNA (RNA) with a band still being visible after 2-hours. ASO degradation showed very little phosphatase activity or intermediatory degradation products.

siRNA degradation in 10% FBS-containing media (Figure 3.7) suggested significant phosphatase activity, shown by the presence of large bands beneath the level of ATP control in all time points, that would correspond to cleavage of a phosphate group.

A densitometer was used to quantify the loss of full-length oligonucleotide. Three PAGE gels for each oligonucleotide were used to produce Figure 3.8. This seems to show that siRNA is degraded at a faster rate than ASO, but this could be simply due to the loss of radiolabel by phosphatases.

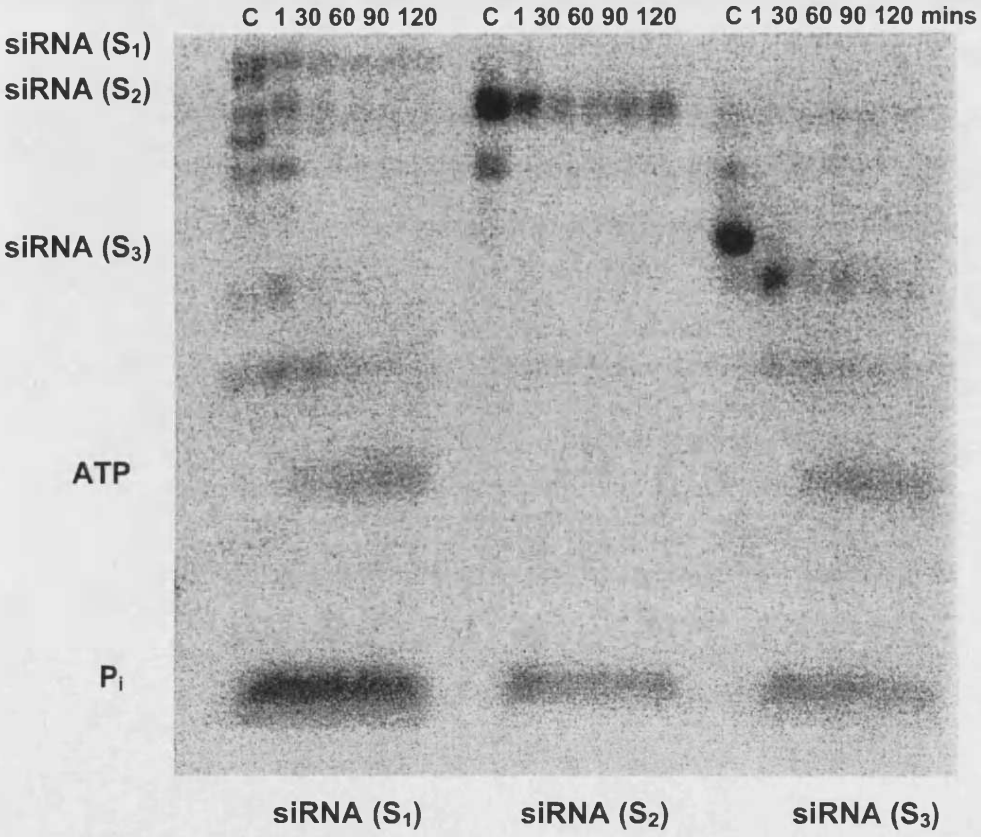

Figure 3.5: Stability assay in 10% FBS-containing media of radiolabelled duplex siRNA and possible gel purification degradation products. A 20% PAGE gel visualised by a phosphorimager shows a stability assay on the different radiolabelled siRNA bands shown in Figure 3.3; S1 had the largest molecular weight followed by S2 then S3. ATP refers to free label gamma ^{32}P ATP run as a control. P_i is the suspected band for free phosphate. C= control siRNA, not exposed to degrading media that is equivalent in radioactivity to the other samples. The numbers on top refer to the time exposed to the media in minutes.

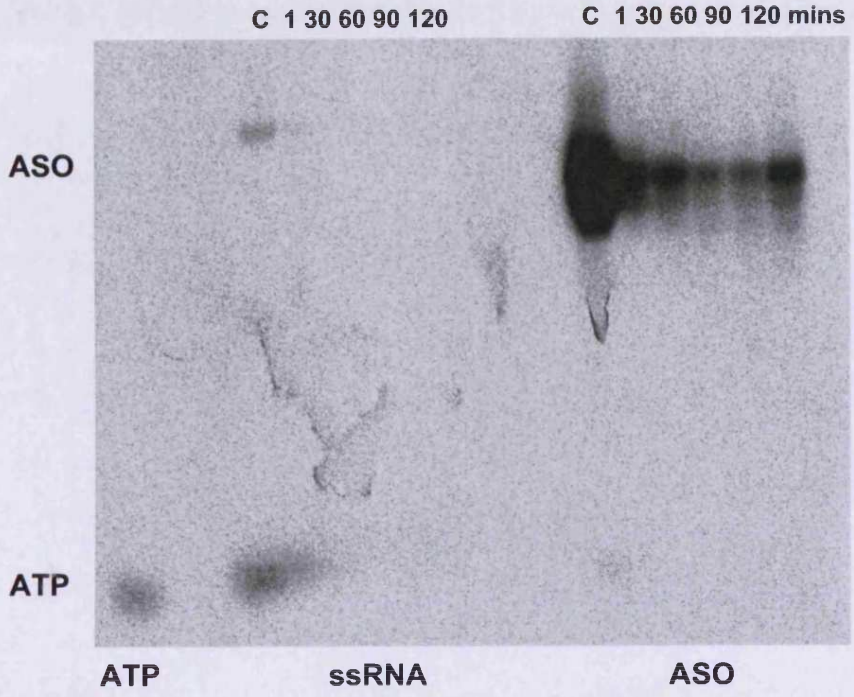

Figure 3.6: Stability assay in 10% FBS-containing media of radiolabelled single stranded siRNA (ssRNA) and antisense oligodeoxynucleotide (ASO). A 20% PAGE gel visualised by a phosphorimager shows a stability assay on ssRNA and ASO in 10% FBS-containing D-MEM over 2 hours. ATP refers to free label gamma ^{32}P ATP run as a control. C= control siRNA, not exposed to degrading media that is equivalent in radioactivity to the other samples. The numbers on top refer to the time exposed to the media in minutes.

Figure 3.7: Stability assay in 10% FBS-containing media of radiolabelled siRNA. A 20% PAGE gel visualised by a phosphorimager shows a stability assay on siRNA in 10% FBS-containing D-MEM over 72 hours. ATP refers to free label gamma ^{32}P ATP run as a control. P_i is the suspected band for free phosphate. C= control siRNA, not exposed to degrading media that is equivalent in radioactivity to the other samples. The numbers on top refer to the time exposed to the media in hours.

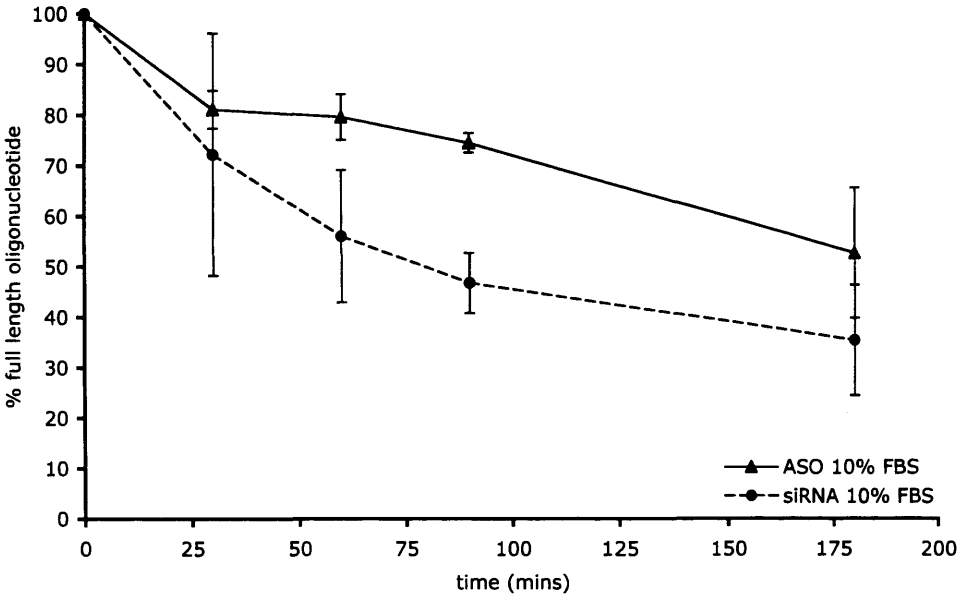

Figure 3.8: A plot of combined densitometry values for stability assays of radiolabelled siRNA and antisense oligodeoxynucleotide (ASO) in 10% FBS-containing media. Plot derived from densitometry performed on phosphorimages of PAGE gels of radiolabelled siRNA and ASO exposed to 10% FBS-containing media (n=3). Percentage full length was determined to be the density of the largest molecular weight product seen on the PAGE gel over the density of the unexposed control (C). The error bars are ± 1 standard deviation.

3.3.2.2 Stability of ASO and siRNA in full Foetal Bovine Serum (FBS)

Figure 3.9 and Figure 3.10 show examples of phosphorimages of stability PAGE gels for ASO and siRNA in full FBS. Figure 3.9 shows the degradation of ASO in full FBS, it also shows a large amount of ATP free label is still present in the purified sample; seen as a band across all the time periods. Secondly dephosphorylation is prevailed with a free phosphate band increasing in size with time. ASO degradation products are seen at as bands in-between the ATP band and the full-length bands.

Figure 3.10 compares the stability ASO with siRNA in full bovine serum, ASO seems last for over an hour while the siRNA band is much reduced after the first time point (t=1) and has completely disappeared after 30 minutes. Free phosphate was missing from this gel because it had ran off the bottom of the gel.

Densitometry was performed on the phosphorimages of 3 separate stability assays comparing ASO with siRNA, in full FBS these results were combined and plotted in Figure 3.11. These show siRNA and ASO degrade quickly and at similar rates in full FBS but dephosphorylation and loss of label is significant.

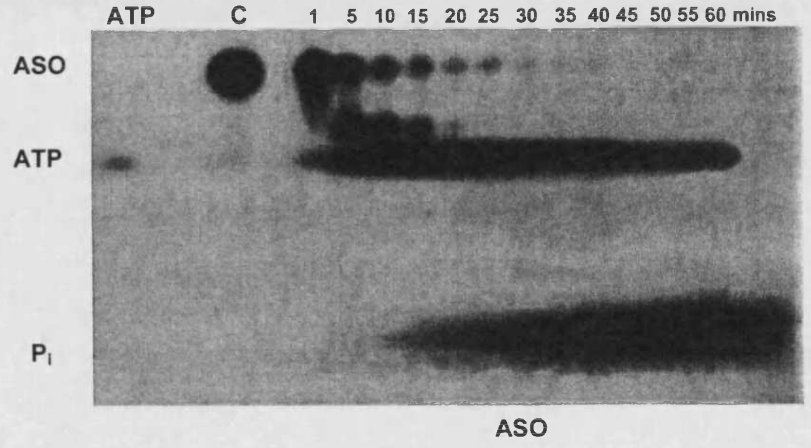

Figure 3.9: Stability assay in full FBS of radiolabelled antisense oligodeoxynucleotide (ASO). A 20% PAGE gel visualised by a phosphorimager shows a stability assay on ASO in full FBS over 1 hour. ATP refers to free label gamma ^{32}P ATP run as a control. P_i is the suspected band for free phosphate. C= control siRNA, not exposed to degrading media that is equivalent in radioactivity to the other samples. The numbers on top refer to the time exposed to the media in minutes. The protein content of the FBS was estimated to be 68.5mg/ml.

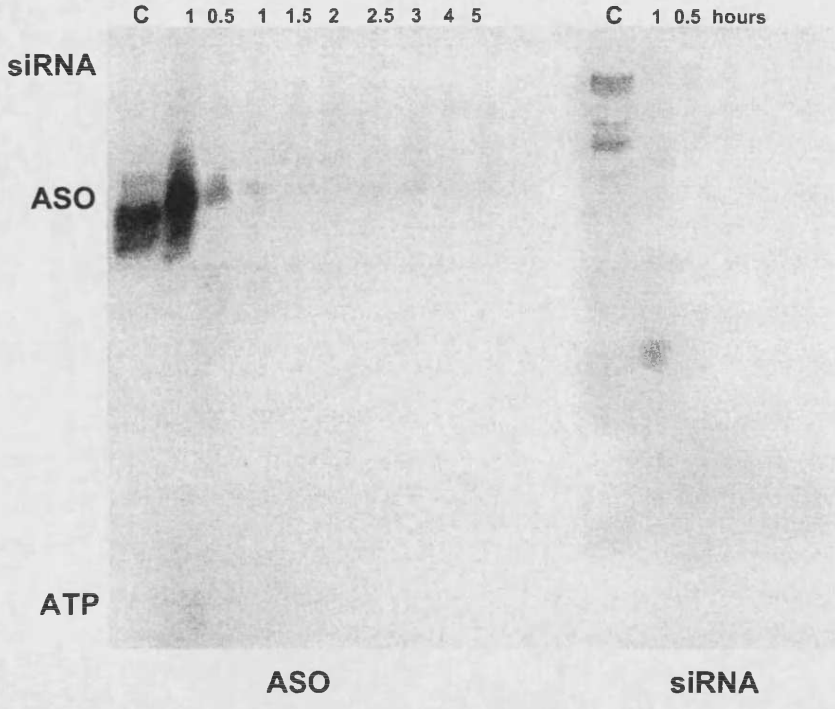

Figure 3.10: Stability assay in full FBS of radiolabelled antisense oligodeoxynucleotide (ASO) and siRNA. A 20% PAGE gel visualised by a phosphorimager shows a stability assay on ASO in full FBS over 5 hours. ATP refers to free label gamma ^{32}P ATP run as a control. P_i is the suspected band for free phosphate. C= control siRNA, not exposed to degrading media that is equivalent in radioactivity to the other samples. The numbers on top refer to the time exposed to the media in minutes. The protein content of the FBS was estimated to be 68.5mg/ml.

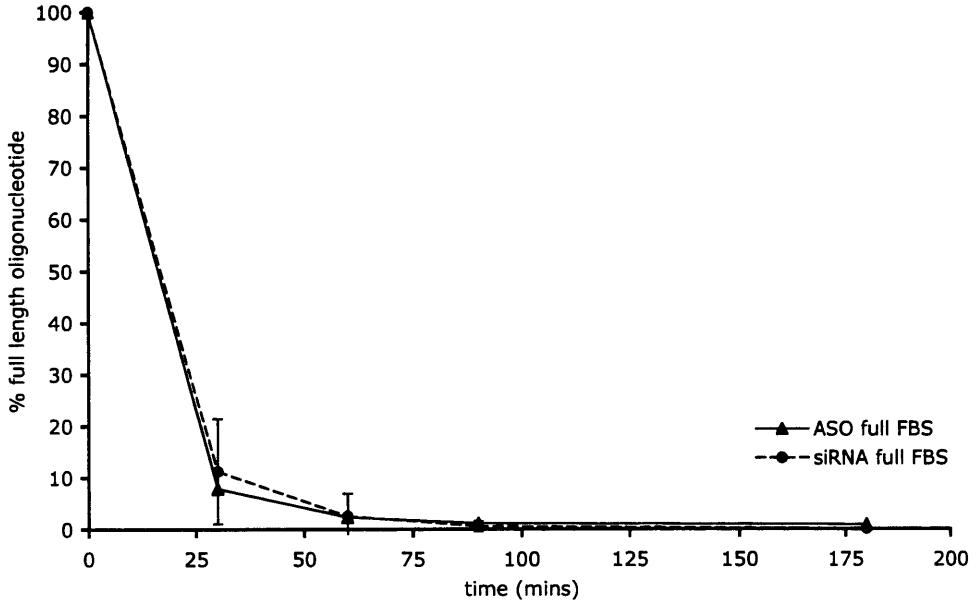

Figure 3.11: A plot of combined densitometry values for stability assays of radiolabelled siRNA and antisense oligodeoxynucleotide (ASO) in full FBS. Plot derived from densitometry performed on phosphorimages of PAGE gels of radiolabelled siRNA and ASO exposed to full FBS (n=3). Percentage full length was determined to be the density of the largest molecular weight product seen on the PAGE gel over the density of the unexposed control (C). The error bars are ± 1 standard deviation. The protein content of the FBS was estimated to be 68.5mg/ml.

3.3.2.3 Stability of ASO and siRNA in cell lysates & normalised FBS

The stability of the oligonucleotides was tested in A431 cell lysates of known protein concentrations (Figure 3.12). Both ASO and siRNA produce 'ladder' degradation patterns that are indicative of processive exonuclease activity. Another observation is that both full length ASO and siRNA degraded steadily over time. Also both PAGE purified oligonucleotides still have multiple bands in the unexposed controls. The stability of siRNA was higher than ASO in cell lysates (Figure 3.13).

Stability assays were also consecutively run for the oligonucleotides in serum-containing D-MEM diluted to an equivalent protein level as in the cell lysates, normalised serum (Figure 3.14).

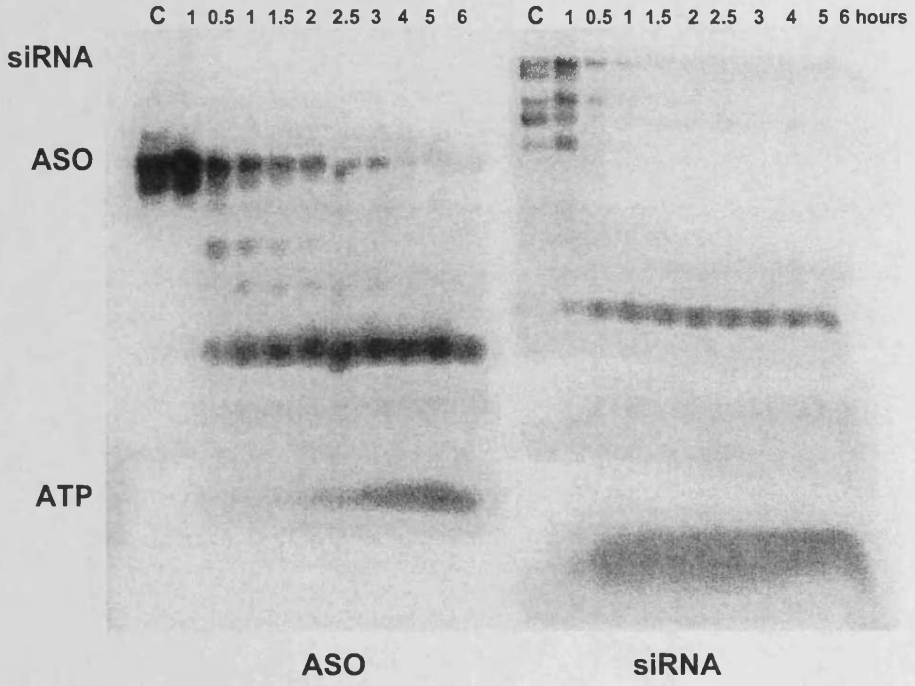

Figure 3.12: Stability assay in A431 cell lysates of radiolabelled antisense oligodeoxynucleotide (ASO) and siRNA. A 20% PAGE gel visualised by a phosphorimager shows a stability assay on ASO and siRNA in A431 cell lysates over 6 hours. ATP refers to free label gamma ^{32}P ATP run as a control. C= control siRNA, not exposed to degrading media that is equivalent in radioactivity to the other samples. The numbers on top refer to the time exposed to the media in hours. The protein content of the cell lysates was estimated to be 4.2mg/ml

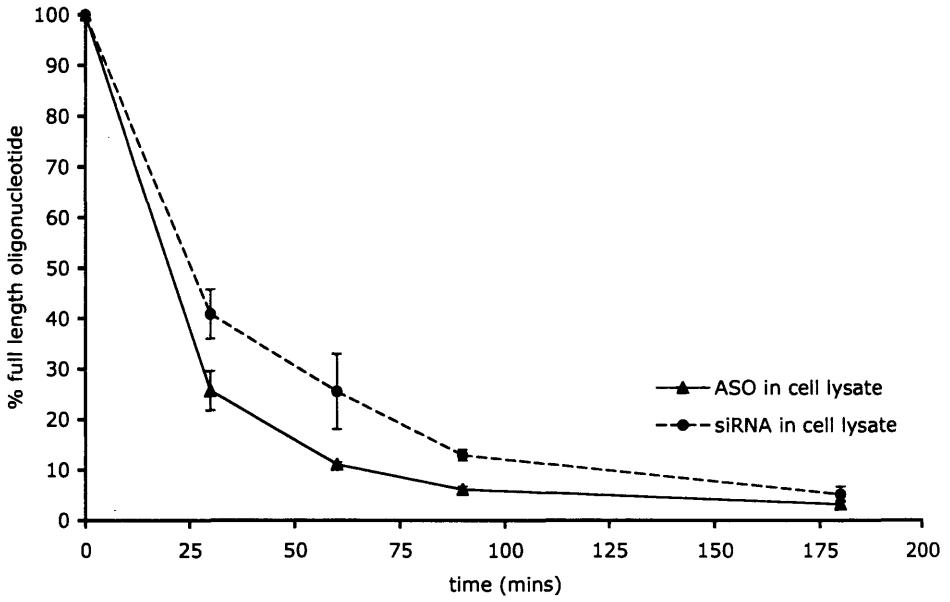

Figure 3.13: A plot of combined densitometry values for stability assays of radiolabelled siRNA and antisense oligodeoxynucleotide (ASO) in A431 cell lysates. Plot derived from densitometry performed on phosphorimages of PAGE gels of radiolabelled siRNA and ASO exposed to A431 cell lysates (n=3). Percentage full length was determined to be the density of the largest molecular weight product seen on the PAGE gel over the density of the unexposed control (C). The error bars are ± 1 standard deviation. The protein content of the cell lysates was estimated to be 4.2mg/ml.

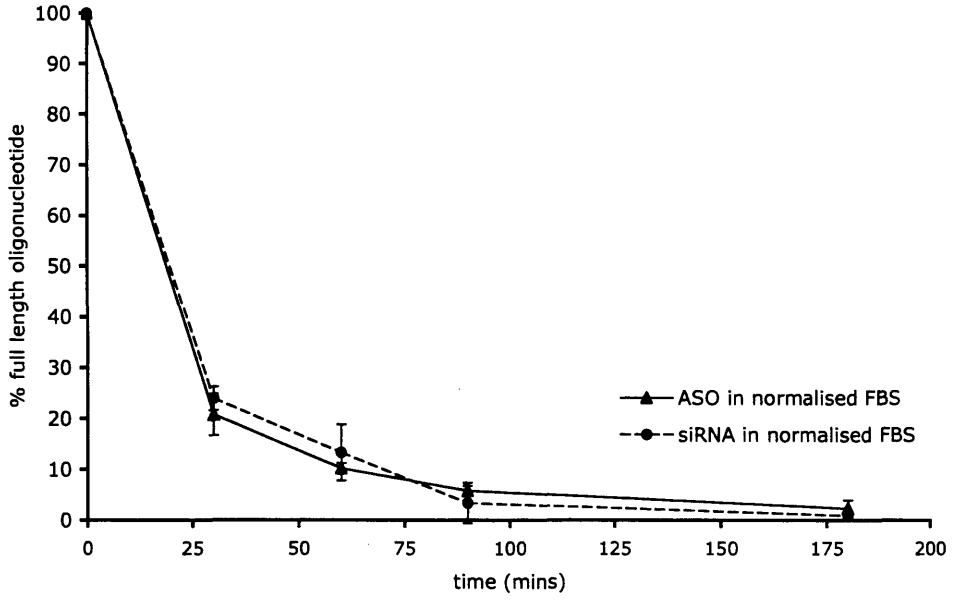

Figure 3.14: A plot of combined densitometry values for stability assays of radiolabelled siRNA and antisense oligodeoxynucleotide (ASO) in FBS normalised to the same protein concentration as the A431 cell lysates. Plot derived from densitometry performed on phosphorimages of PAGE gels of radiolabelled siRNA and ASO exposed to normalised FBS (n=3). The error bars are ± 1 standard deviation. The protein content of the cell lysates was estimated to be 4.2mg/ml and the FBS was diluted in media to produce a solution of equivalent concentration.

3.3.2.4 Biological stability half-lives

The half-lives of oligonucleotides were then calculated (2.1.4) and are shown in Table 3.3. The stabilities of ASO were more stable than siRNA in all serum containing media but the greatest differences were seen at the lowest serum concentrations ($t_{1/2}$= 204 compared with 124 minutes). The half-life of siRNA ($t_{1/2}$= 43 minutes) was slightly greater than ASO ($t_{1/2}$= 37 minutes) in A431 cell lysates. The oligonucleotides have slightly longer half-life in lysates than in normalised serum that contains equivalent level of protein to the lysates.

Table 3.3: Biological stability half-lives for radiolabelled oligonucleotides

Biological media	Oligonucleotide	Half-life (minutes)	Regression coefficient (R^2)
10% FBS-containing media	ASO	204	0.96
	siRNA	124	0.91
A431 cell lysates	ASO	37	0.86
	siRNA	43	0.95
Normalised serum	ASO	34	0.90
	siRNA	30	0.93
Full FBS	ASO	19	0.97
	siRNA	16	0.92

In this chapter I set out to establish assays to investigate and compare the biological stability of ASO and siRNA. These assays to be used to examine the degradation patterns of siRNA with the view that this may provide information about the design of more stable chemically modified analogues.

One of the major limitations of the work was the issue experienced with end-radiolabelled oligonucleotide purification, precisely the identification of the full-length radiolabelled species. The radiolabelled full-length oligonucleotide was never properly identified or characterised, it was assumed that the largest molecular weight species visualised on a purification PAGE gel (as shown in Figure 3.3) was the intact and labelled oligonucleotide.

The oligonucleotides were radiolabelled so that they could be detected at low concentrations, this is important in stability assays in order to detect small quantities of degraded products. Radiolabelling allowed small amounts of costly siRNA to be used in stability experiments. This was initially important since only recently have

siRNA manufacturer costs fallen. Compared with other detection techniques such as ethidium bromide the radiolabelling technique uses 1000 times less siRNA and it was decided that it would be more cost effective to use a radiolabelled detection technique for my studies.

A study by Kurreck and co-workers (Kurreck et al., 2002) reported that 300 picomoles ^{32}P end-labelled radiolabelled ASOs could be visualised on PAGE gels. In a subsequent publication, from the same group, it was reported that 100 picomoles ASO or 20 picomoles siRNA could be visualised on PAGE gels with staining for 20 minutes using ethidium bromide (Grunweller et al., 2003). Although this latter report that radiolabelling is more sensitive, the radiolabelling assay in my studies detected quantities by PAGE analysis as low as 400 femtomoles of oligonucleotides; Table 3.2 shows some other published quantities of the amounts of siRNAs used in stability assays, generally radiolabelling uses less oligonucleotide material.

A clear concern with ^{32}P end radiolabelling is that phosphatases may remove the radiolabel from the oligonucleotides and prevent their visualisation on the PAGE gels or indeed provide for incorrect assignment of signal to intact oligonucleotide. The potential loss of the radiolabelled phosphate by phosphatases means any biological stability results should be substantiated either with a gel stain such as ethidium bromide or SYBR green, or by using a radiolabel internalised within the nucleic acid strand as (Bertrand et al., 2002).

The use of radiolabelled oligonucleotides requires a purification step to remove the large amounts of unincorporated ^{32}P free-label used in the labelling reaction. If unremoved large amounts of highly radioactive free-label would obscure images taken from PAGE gels. The purification of oligonucleotides using Sephadex columns was not very reproducible with different numbers of columns needed to remove the free label ^{32}P- ATP. The purification using the columns was not efficient at removing the free-label and also resulted in considerable loss of intact radiolabelled oligonucleotide. Sephadex columns have been previously reported to successfully purify radiolabelled siRNA (Braasch et al., 2004), although columns in that study were washed five times with DEPC-treated water before use. In my studies I did not wash columns, to ensure consistency with the manufacturer's recommendations. These recommendations were

that the columns were free of RNases washing the columns was not necessary, even if even if washing prevented loss and degradation of radiolabelled oligonucleotides but it would not help in improving the effectiveness and reproducibility of free-label removal. The Sephadex columns were expensive and using two to three columns per purification was not economically viable. These issues should be considered in my subsequent interpretation of the data.

PAGE purification was considered in my laboratory to be the better alternative to column purification allowing the user to remove defined bands containing the specific radiolabel product. As such my studies involved purification ^{32}P end-labelled oligonucleotides by PAGE. The labelling of siRNA resulted in several different labelled products (Figure 3.3), as evidenced by the number of bands in my PAGE gels, which remain as I stated above to be fully identified. Further comparisons of the different siRNA labelled bands with standard RNA species may identify the single stranded product by distinguishing the double and single stranded full-length products. Suitable standards could be non-radiolabelled siRNA that have been stained by ethidium bromide that were ran on the same PAGE gel as radiolabelled siRNA and the positions of the bands could be compared. My attempts to determine the presence of a single stranded species within the multiple siRNA bands (Figure 3.3; S1, S2 and S3) involved reannealing experiments. These experiments aimed reanneal S2 or S3 to produce S1, the proposed full-length siRNA. It was attempted to denature the S1 product then to reanneal it using standard siRNA protocols but this was unsuccessful, as the denatured product could not be reannealed (Figure 3.4). Another concern is that process of running siRNA on PAGE gels may affect the stability of the molecules.

The radiolabelling and PAGE purification techniques were labour intensive over 12 hours and did not always successfully produce labelled oligonucleotides. The cost of the radiolabel coupled with the costs of safety equipment, PAGE gels and equipment meant an alternative non-radiolabelled detection system would have been much more cost effective. Safety concerns prevented easy analysis of the composition of radiolabelled oligonucleotides for example, the spectrophotometer in the laboratory was not to be used for ^{32}P radiation work and this prevented the quantification of purified oligonucleotides.

My initial biological studies involved the stability in FBS of my proposed full-length product (Figure 3.3; S1). The band associated with the migration of the full-length intact product for both ASO and siRNA was diminished by 90% within the first 30 minutes (Figure 3.11), with their estimated half-lives both being between 10 and 20 minutes (Table 3.3). In 10% FBS-containing media, the half-lives of ASO and siRNA were estimated to be about 2 and 3.5 hours respectively (Table 3.3; Figure 3.8). This clearly shows degradation to be dependent upon elements in FBS acting in a concentration-dependent manner. This rate of degradation in 10% FBS it may be unsuitable to use ASO and siRNA in 4-hour cell culture transfections in FBS-containing media, as the estimated levels of intact siRNA and ASO would be about 24% and 43% respectively at 4 hours. Bertrand and co-workers (Bertrand et al., 2002) report that siRNA ($t_{1/2}$= 24 hours) is more stable than ASO ($t_{1/2}$= a few minutes) in full FBS, although they do not publish the PAGE gels. Kurreck and co-workers (Grunweller et al., 2003) report the half-life of ASO to be 20 minutes in 10% FBS-containing media. It seems clear that published results are equivocal on how quickly siRNA is degraded in FBS-containing media (some literature is summarised in Table 3.2) varying from minutes (Layzer et al., 2004) to days (Bertrand et al., 2002, Braasch et al., 2003). This variation in time of degradation could simply be explained by the different techniques and practises employed by the different research groups but also by the wide range of different degradation media used, not just in its serum concentration but its source, protein concentration and nuclease activity. Serum from different species has also been shown to give different degradations rates, for example human serum was found to be more degrading than mouse but this aspect has so far received very little attention (Haupenthal et al., 2006). Further, a major problem with comparing different studies is that laboratories use different sequences, which can have different degradation rates (Haupenthal et al., 2006). The nucleotide sequences of a siRNA duplex will determine its thermodynamic stability profile, so that a siRNA with a low thermal stability will unwind readily and expose the individual strands to nuclease degradation (Braasch et al., 2003, Braasch et al., 2004). Further study into the biological stability of siRNA duplexes with different thermodynamic stabilities may explain the equivocal biological stabilities publications. Although siRNA with thermodynamic stability profiles reported to be theoretically beneficial for activity,

such as groups of AU bonds towards the 5' end of the antisense strand, may in fact be less active because they have poorer biological stabilities (Turner et al., 2007).

Moving from serum based degradation studies I sought to examine ASO and siRNA degradation in cell lysates. I chose A431 cells from to prepare lysates, as this was to be cell type in which much of my subsequent work was to be undertaken. In A431 cell lysates, the half-life of siRNA was slightly greater than ASO (Figure 3.10), with half-lives of ASO and siRNA being 37 and 43 minutes respectively. Bertrand & co-workers (Bertrand et al., 2002) report of the stability of siRNA to be greater than ASO in HeLa cell lysates. In my work siRNA oligonucleotides have slightly longer half-life in lysates than in normalised serum that contains equivalent level of protein to the lysates. One interpretion of my results is that the additional intracellular stability of siRNA is due to the protective effect of the RNA-induced silencing complex (RISC). The intracellular proteins that recognise and bind siRNA for RNAi may also protect the siRNA from degradative enzymes. But the levels of nucleases in serum and cell lysates are unknown and further *in vitro* analysis of extracted RISC and other subcellular fragments are needed to confirm this. Further, one must acknowledge that studying degradation in cell lysates is likely to bear little resemblance to that in the live cell. In the latter the degradative enzymes will be compartmentalised (e.g. in lysosomes) and may have only limited exposure to ASO and siRNA molecules. Raemdonck and co-workers (Raemdonck et al., 2006) investigated the intracellular degradation of siRNA in live cells. They reported that the double stranded siRNA was stable for 2 hours and that chemical modifications to improve stability did not increase duration of action and intracellular siRNA stability was therefore not critical for successful delivery. They however did not comment on the subcellular localisation of the siRNA in their studies.

The duplex nature of siRNA required that I use native PAGE not only for my purification but also for my stability analysis. PAGE analysis of oligonucleotides is problematic as it only separates nucleotides of different mobilities and native gels have additional charge complications. The major limitations of PAGE analysis are that very little can be inferred about the patterns or locations of cleavage (Turner et al., 2007). Other techniques have been used to assess stability of siRNA, and may be recommended to other researchers in this field and include: MALDI-TOF mass

spectrometry (Turner et al., 2007), capillary gel electrophoresis (Allerson et al., 2005) and electrospray ionization mass spectrometry (Beverly et al., 2006, Rose et al., 2005). These techniques have affectively allowed the identification of siRNA degradation products and have increased the knowledge on RNases that act to degrade siRNA (Haupenthal et al., 2006). In 2004, it was suggested that a 3'-exonuclease was mainly responsible for siRNA degradation in serum (Soutschek et al., 2004). One group claimed that endonucleases are the main enzymes that cause siRNA degradation in serum (Czauderna et al., 2003). The serum contains RNase A–like enzymes that have been shown to cause siRNA degradation (Haupenthal et al., 2006). Their workers used RNase A inhibitors and immunoprecipitation techniques to remove RNase A from serum, in order to show its importance in siRNA degradation. A hypothesized intermediate in the mechanism of RNAse A degradation (Figure 3.1), a 3'-fragment with a terminal 2',3'-cyclic phosphate was identified by MALDI-TOF mass spectrometry (Turner et al., 2007).

The considered chemical modification of an ASO can lead to an analogue with enhanced biological stability and subsequent activity. Chemical modifications to improve siRNA stability have been attempted within either the sense or antisense strand to increase the cellular gene silencing activity, some of the published results are shown in Table 3.2. Kurreck in his review of ASO identified three main chemical modifications, phosphate backbone modifications, modified sugars (especially with 2' ribose substitutions) and unnatural bases (Kurreck, 2003):

- Phosphorothioate (PS) is a backbone modification where the oxygen from the phosphodiester bond is replaced by a sulphur, this increases the half-life to 9-10 hours. Unfortunately, phosphorothioates have cytotoxic non-specific reactions that restrict their use (Levin, 1999). The substitution of the phosphodiester backbone with phosphorothioate linkages has been shown to increase ASO biological stability as the bond is more resistant to nucleases, this substitution however also increases serum protein binding and has been considered important in reducing the rates of ASO clearance and improving bioavailability (Geary et al., 2001). Extensive phosphorothioate substitutions to siRNA duplexes lead to increased cytotoxicity (Amarzguioui et al., 2003)

and even an alternate phosphate/phosphorothioate backbone still had significant toxic effects (Harborth et al., 2003).

- The most common 2'-O-methyl (2'-O-Me) have been reported to provide prolonged activity with no apparent toxicity (Amarzguioui et al., 2003). A sense strand consisting of a complete 2'-O-Me backbone has been shown to be active (Czauderna et al., 2003). Free unmodified 2'-OHs are not required for RNAi, therefore chemical modifications will not affect its incorporation into RISC and therefore not reduce activity (Chiu and Rana, 2003).

- Several unnatural base chemical modifications have been effectively used to improve ASO, Locked nucleic acids (LNA) and Morpholino oligonucleotides (MF), these are reviewed in detail (Kurreck, 2003). All these modifications have the potential to be used to increase the biological stability of siRNA. A number of groups have reported that nuclease resistance did not always provide longer lasting RNAi effects (Layzer et al., 2004; Raemdonck et al., 2006).

Table 3.2 showed that a few research groups chemically modified siRNA to improve its biological stability: Czauderna & co-workers utilised 3'-end modifications and 2' O-methyl ones. Fluorinated pyrimidines have also been reported to protect the siRNA from RNase A by (Capodici et al., 2002), the study showed fluorine modified siRNAs had equivalent activity to unmodified but could be delivered in the presence of serum and without a transfection reagent. (Layzer et al., 2004), recently showed that 2'-Fluorinated pyrimidines siRNA had greater in vitro stability in than unmodified, but this extra stability resulting in no increase in potency or duration of action in cells or *in vivo*. 2'-OH modified sugars include 2'-*O*-Methyl (OMe) and 2'-*O*-methoxyethyl (MOE) are less toxic than phosporothioates, but do not activate RNase H, and can only act to block mRNA translation.

In summary there are a number of technical limitations that impact upon my interpretation of data in this section. However my data showing siRNA and ASO have similar degradation profiles in serum and serum-containing media is not inconsistent with some aspects of the literature in this area because both had

equivocal results. The use of radiolabelled oligonucleotides and PAGE analysis for stability assays are fraught with problems. 5'-end radiolabelled oligonucleotides can readily have the label removed with phosphatases that are present in biological media. Phosphatase activity was present in the stability assays and was likely to underestimate the biological half-lives of oligonucleotides. PAGE analysis of biological stability degradation products does not provide their identities only their gel mobilities. Techniques such as HPLC and gel capillary electrophoresis would provide detailed information regarding nuclease activity and could help identify intramolecular sites suitable for chemical modification.

Table 3.4: Summary of stability results

Media	ASO	siRNA
Full FBS	*	*
10% FBS-containing media	*****	****
A431 cell lysates	**	***

The biological stabilities of siRNA and ASO have similar profiles in sera, therefore chemical modifications would probably be required for activity. Chemical modifications do improve stability but many compromise activity. Since individual sequences have shown to have different stabilities each individual molecule needs to be assessed what chemical modifications would be needed. Since chemical modification are expensive and several different species would need to be created it would be beyond the expectation of the work in this thesis.

Since siRNA are shown to be active in cell culture and can be used to assay function, emphasis in this thesis will be placed on improvements limited to sequence of siRNA.

Chapter 4
Design of siRNA

4.1 Introduction

It was reported that unlike antisense oligodeoxynucleotides (ASO), siRNA technology does not need to be designed to an optimal sequence of the target mRNA (Stein, 2001). For a target mRNA gene sequence of n nucleotides theoretically n-20 siRNA can be designed, where n is greater than 20 (Ui-Tei et al., 2006). Studies in *Drosophila melanogaster* show that almost all siRNAs (>90%) were highly active (>80% knockdown) while those performed in mammalian cells only very few siRNA (<20%) would be highly functional (Holen et al., 2002, Ui-Tei et al., 2004). These highly potent siRNAs are now considered to be as difficult to identify as effective ASO (Gilmore et al., 2004). Some genes are considered to have less siRNA target sites than others and this might be explained by the secondary structures of the target; those mRNAs with stronger or more complex intra-molecular structures may offer fewer target sites (Kurreck, 2006). The high initial cost of siRNA synthesis compared to ASO means that there is a commercial need to understand the rules governing the design of active siRNA.

4.1.1 Selection of mRNA accessible ASO

The theory the behind design of active ASO is simple, to design an ASO strand with a sequence complementary to the known target mRNA. However, in reality mRNA does not exist as a long open single-stranded structure that is readily accessible to ASO, rather it folds in on itself forming complex secondary and tertiary structures. These secondary and tertiary structures impede ASO accessibility to some mRNA target sites, therefore some ASOs are unable to reach their mRNA cleavage site and are inactive. Since the antisense strand of the siRNA molecule guides the cleavage components in RISC to the mRNA target site, it is thought active siRNA must also target mRNA accessible regions. A number of strategies exist to analyze the target mRNA for accessible sites in order to produce active ASOs. The four most widely used strategies are 'gene walking', RNAse H mapping, computational analysis and scanning ASO arrays, for review see (Smith et al., 2000, Sohail and Southern, 2000).

4.1.1.1 'Walk the gene'

In this strategy, several sequences along the target mRNA are selected randomly and about 50 corresponding and complementary ASOs are examined. These ASO molecules are compared *in vivo* for the most active molecule and from this is inferred

information about mRNA accessibility. This is laborious, expensive, time consuming and also requires good fortune to find an active ASO molecule.

4.1.1.2 RNase H assays

RNase H is an enzyme that cleaves DNA-RNA hybrids such as those formed by ASO binding to target mRNA. This assay is performed by hybridising target mRNA to a library of known ASOs, then adding RNase H to cleave the hybrids. These resulting fragments can be separated and identified by PAGE electrophoresis. Unfortunately this will not accurately locate the active site as the determined size of the fragments is imprecise. RNase H assays have been used to select active siRNA molecules (Vickers et al., 2003, Xu et al., 2003).

4.1.1.3 Computer-based RNA folding programs

The rational design of specific ASO may also utilise RNA folding programs (e.g. mFold). These programs work on the basis that the secondary structure will try to conform itself to its minimum global free energy. Ho and co-workers (Ho et al., 1998) reported that computer RNA folding programs show no obvious structural differences between accessible and non-accessible sites. Large, complex RNA structures never actually reach their minimum global free energy *in vivo* and the consensus is that currently these structures are too complex to be modelled by computer programs (Sohail et al., 1999). Although a group has reported an active siRNA against ICAM-1 from a target selected by the mFold programme (Kretschmer-Kazemi Far and Sczakiel, 2003).

4.1.1.4 Scanning ASO array

This technique identifies mRNA accessible sites for a specific gene (e.g. EGFR) by synthesizing an array of all ASO sequences up to a fixed length (e.g. 18mer) for a section of mRNA (e.g. 150 nucleotides). This array is then hybridized with radiolabelled target mRNA (e.g. EGFR mRNA), and ASO that result in strong mRNA binding are identified. Milner & co-workers (Milner et al., 1997) recommend RNase mapping followed by scanning ASO arrays for the selection of active ASO. Two groups have used scanning ASO arrays data to produce active siRNA (Beale et al., 2003, Bohula et al., 2003). Figure 4.1 shows illustration of a scanning ASO array describing its fabrication. The arrays are produced by the subsequent position of

diamond shape templates that imprint ASO on the base substrate. These arrays are produced against a known mRNA target.

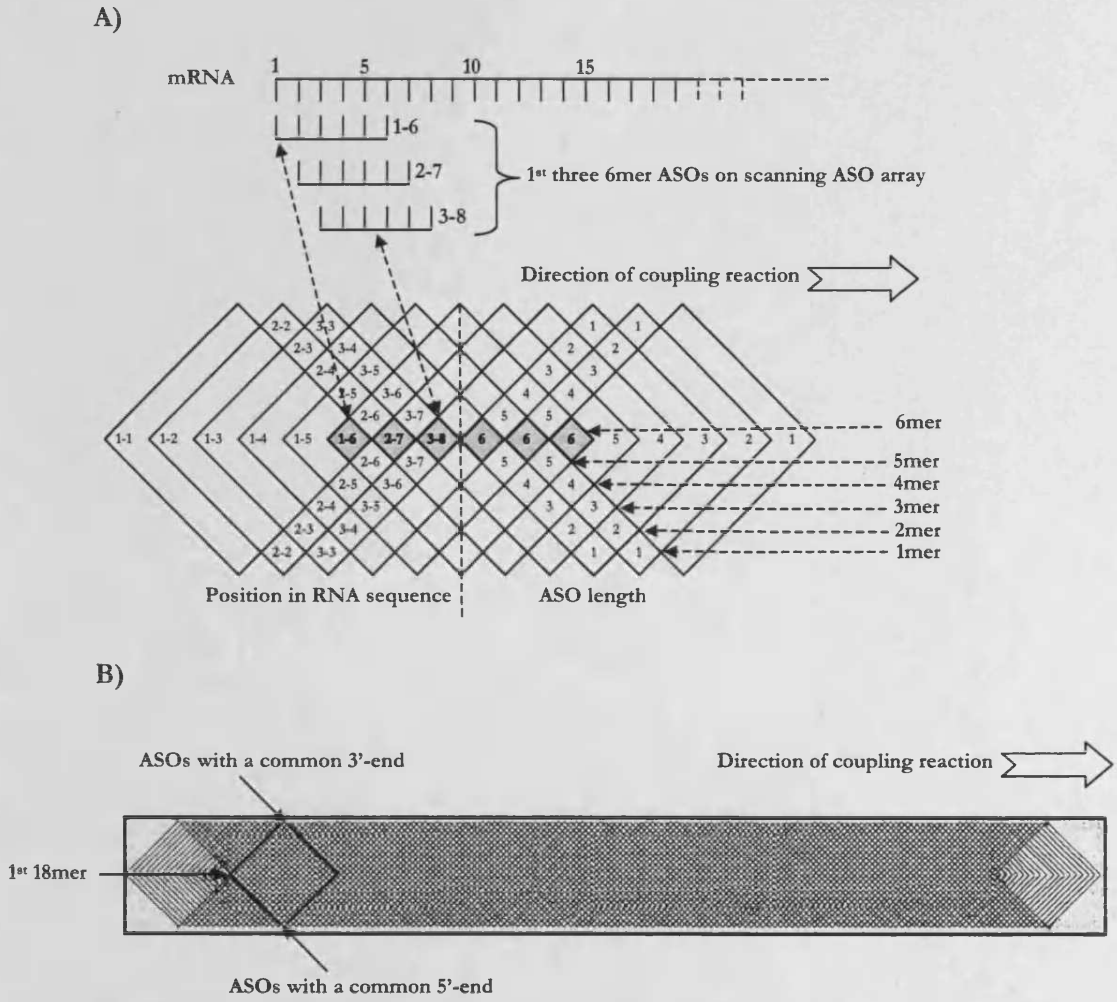

Figure 4.1: An illustration of the organization of a scanning ASO array. **A:** The template of a diamond-shaped mask produces footprints of overlapping diamonds used to make the scanning ASO array. After each coupling reaction step, the mask is moved along the substrate by a predetermined size of step (offset). At each step, the length of the ASO is the number of bases that have been coupled at the point where the back of the mask passes the front. The first longest ASO on the array is when the number of coupling steps that equal the length diagonal of the mask or step size (1-6). **B:** The template of overlapping diamonds produced by the computer programme, xvseq, used to analyze the images obtained after hybridization. Adapted from (Sohail et al., 1999).

Although each analytical approach has its own individual merits, a combination of the different procedures provides a powerful strategy for the elucidation of mRNA accessible sites and secondary structure. At the present time the siRNA mRNA targets are, on the whole, selected seemingly at random by a 'gene walking'-like strategy which is very uneconomic especially considering the high price of siRNA synthesis. However, since the RISC enzyme complex has known helicase activity (Nykanen et al., 2001) it is therefore feasible that target mRNA sites, that although do not bind strongly to antisense, may be made readily accessible through the action of RISC to siRNA. Therefore, there exists a need for research into the effect on siRNA activity of mRNA structure and whether the strategies used for the design of ASO are applicable to siRNA.

4.1.2 Design of siRNA molecules

The chapter has already discussed the importance of understanding mRNA target structure for the design of ASO. This section will concentrate on the other published factors that are thought to be important in the design of active siRNA. A summary of some commonly used criteria for selecting siRNAs is given below. A number of on-line algorithms exist for the design of siRNA, many utilise the criteria described below however most do not account for the target mRNA structure.

4.1.2.1 Structural constraints

RNA duplexes longer than 30 nucleotides when introduced into mammalian cells have been shown to induce a non-specific response that causes degradation of all cellular mRNA (Bass, 2001, Caplen, 2002). Tuschl & co-workers (Elbashir et al., 2001c) recommend a duplex of 19 nucleotides, with a two-nucleotide overhang consisting of two thymidine nucleotides. They studied siRNA activity in *Drosophila* cells and showed there was need for 3' overhangs of 2 to 3 nucleotides, usually 3' dTdT (Elbashir et al., 2001c). Another group (Czauderna et al., 2003) claimed that overhangs provided no additional activity or stability in mammalian cells. Recently a group (Haupenthal et al., 2006) reported that siRNA containing overhangs were twice as potent in eliciting a knockdown as blunt-ended siRNA, even though the blunt-ended siRNA were more biologically stable.

Tuschl & co-workers (Elbashir et al., 2002, Elbashir et al., 2001c) reported that siRNA with 3'-TT overhangs are more resistant to exonucleases present in media and cell lysates. Symmetric overhangs such as 3'-TT on both strands ensure that siRNA ribonuclease complexes have equal loading of antisense and sense strands of siRNA, whether this is actually beneficial is not discussed. They also recommend that TT overhangs ensures that siRNA are manufactured in the correct 5' to 3' direction and DNA bases are cheaper. Their data shows that the sequence of the overhangs are not thought to significantly effect siRNA function and therefore the selection of overhangs is not critical (http://www.rockefeller.edu/labheads/tuschl/sirna.html).

Chiu & Rana investigated the requirement for a perfect RNA helix, an A-form helix, for eliciting RNA interference. They introduced two nucleotide bulges to the sense or antisense strand of the siRNA in order to distort the helical structure. These bulges in the sense strand were tolerated but those in the antisense or in both strands completely abolished RNAi activity. They concluded that siRNA-mediated RNAi requires a perfect A-form RNA helix between the antisense strand and target mRNA (Chiu and Rana, 2002).

4.1.2.2 Sequence constraints

Tuschl and co-workers (Elbashir et al., 2002) came up with several rules for the design of siRNA. These rules are summarised in Table 4.1:

- The mRNA target sequence should be within the coding region, and at least 50 nucleotides downstream of the start codon.
- GC content should be approximately 50% but can vary without major loss of activity.
- GC stretches of more than 3 nucleotides, palindromic sequences and tandem repeats should be avoided.
- Each strand should have a sequence motif of 5'-AA-(N_{19})-TT-3'.
- Avoid sequences that have more than 75% homology with non-target genes.

This group then later investigated base mismatches within the siRNA nucleotide sequence. A single nucleotide mismatch in central cleavage region of siRNA (nine nucleotides from the 5' end) duplex is enough to abolish RNAi activity but mutations in the flanks are tolerated but at risk of off-target effects (Martinez and Tuschl, 2004).

Table 4.1: Tuschl's 'rules' for the design of siRNA (Elbashir et al., 2002)

1.	Target 50-100 nucleotides downstream of start codon
2.	Avoid untranslated regions (UTR)
3.	5'-AA-(N_{19})-UU-3' target sequence motif
4.	5'-AA-(N_{21})-3' or 5'-NA-(N_{21})-3' target sequence
5.	G/C Content = About 50% range 32-79%
6.	2-nt deoxythymidine 5'-(N_{19})-TT 3' overhangs
7.	Blast search final sequences

4.1.2.3 Thermodynamic stabilities

The silencing complex RISC must select one strand from the duplex to mediate the cleavage of the target mRNA. A siRNA molecule is an asymmetric duplex where the two complementary nucleotide strands run antiparallel to each other, so it follows that both strands could potentially be incorporated into RISC. The thermodynamic stability profile of the duplex could determine the strand selection so that the strand with the lower 5' end thermodynamic stability is more likely to 'fray' and be selected by RISC. Two independent reports proposed that a major factor in siRNA activity was the thermodynamic stability profile of the duplex (Khvorova et al., 2003, Schwarz et al., 2003). An active siRNA had an antisense strand with a 5' end that was more likely to fray when compared to the 3' end; that is an antisense 5' end with a relatively lower thermodynamic stability.

The thermodynamic stability profile of a siRNA duplex could be improved by selecting target sequences that have more A/U base pairs (that have a lower thermodynamic stabilities than G/C) towards the 5' end of the antisense strand (Reynolds et al., 2004, Ui-Tei et al., 2004). Reynolds and co-workers (Reynolds et al., 2004) also suggested that the central region of the siRNA duplex should also have a low thermodynamic stability to facility strand unwinding and mRNA cleavage. They also came up with a set of eight criteria (Table 4.2); a siRNA with a score of 6 or more had a significant greater probability of being potent. Others groups suggested that the A/U content differential between the terminal three nucleotides of the antisense 5' ends compared to the sense strand is a better indicator of functionality (Amarzguioui and Prydz, 2004).

Table 4.2: Reynolds' scoring system for the design of siRNA; a siRNA with a score of 6 or more had a significant greater probability of being potent (Reynolds et al., 2004)

Criterion	Score
GC content between 30–52%	+1
A or U at positions 15–19	+1 for each
A at position 19	+1
A at position 3	+1
U at position 10	+1
G or C at position 19	-1
G at position 13	-1

4.1.2.4 On-line design tools

Numerous on-line design tools for the design of siRNA exist these are summarised in Table 4.3. These websites contain one or more algorithms based on the rules of Tuschl, Reynolds or thermodynamic stabilities by Khvorova (Elbashir et al., 2002, Khvorova et al., 2003, Ui-Tei et al., 2004). Not all the websites have published their algorithms making evaluation unreliable (Ui-Tei et al., 2006). These on-line algorithms do not guarantee to produce active siRNA; conversely there are numerous reports of active siRNAs that disobey the rules (Kurreck, 2006).

Chapter aim

To design active siRNA molecules using current design rules with additional mRNA accessibility parameters.

Chapter objectives

- Map EGFR mRNA accessibility using scanning ASO arrays that have been shown to select effective ASO sequences.
- Select mRNA target sites that have different mRNA accessibilities.
- Design siRNA using current design rules against mRNA target sites.
- Validate mRNA accessibility using RNase H assay.
- Investigate mRNA accessibilities using non-gene-specific accessibility ASO arrays.
- Investigate hybridising ASO with target mRNA, before addition to the ASO array in order produce a unique mRNA accessible site. This unique site could be targeted by co-operatively acting ASO and siRNA that could be more potent and specific than the individual technologies.

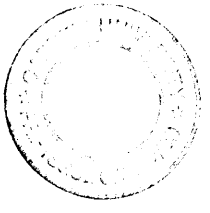

Table 4.3: A selection of online design tools

Program	Homepage	Parameters	Comments	Refs
Ambion	www.ambion.com	T, B, V		
Clontech	bioinfo.clontech.com	T, B, K, O, V, R	No ranking of siRNAs	
DEQOR	cluster-1.mpi-cbg.de	O		(Henschel et al., 2004)
Dharmacon	www.dharmacon.com	T, R, S		(Reynolds et al., 2004)
DsCheck	alps3.gi.k.u-tokyo.ac.jp	O	Not currently for mammals	(Naito et al., 2005)
EMBOSS	inn.weizmann.ac.il	T	No blast	
Eurogentec	www.eurogentec.com	E	Email sequence	
GenScript	www.genscript.com	T, R, U	ΔE parameter sequence specificity	(Wang and Mu, 2004)
IDT	www.idtdna.com	T, K, S	27mer design program	
Interagon	demo1.interagon.com	E, B	Mouse transcript only	(Saetrom, 2004)
Invitrogen	rnaidesigner.invitrogen.com	T, O, S, B	Rank no score	
Invivogen	www.sirnawizard.com	B	Gives top 10, mixed rules	
Jack Lin's	www.ic.sunysb.edu	T, B		
Molcula	www.molecula.com			
MWG	www.mwg-biotech.com	B		5
OligoEngine	www.oligoengine.com	V	Download free software	
OligoRetriever	katahdin.cshl.org	V	No score/rank	
OptiRNAi	bioit.dbi.udel.edu	T, S, B		(Cui et al., 2004)
Proligo	www.sigmaaldrich.com	E, B	SNP search, plus scrambled design	
Promega	www.promega.com	H, B		
Qiagen	www1.qiagen.com	T, O, S, B		
SFOLD	sfold.wadsworth.org	F, T, R		(Ding et al., 2004)
SiDE	side.bioinfo.ochoa.fib.es	B	Mixed rules	(Santoyo et al., 2005)
SiDirect	alps3.gi.k.u-tokyo.ac.jp	U, B		(Yamada and Morishita, 2005)
SDS	i.cs.hku.hk	T, F	Checks 11 different online programs	(Yiu et al., 2005)
SiSearch	sonnhammer.cgb.ki.se	B	Mixed rules, top 10	(Chalk et al., 2004)
TROD	www.unige.ch	B	T7 specific	(Dudek and Picard, 2004)
Whitehead	jura.wi.mit.edu	E, T, R, B, P, K		(Yuan et al., 2004)
Wistar	hydra1.wistar.upenn.edu	R, K, B		(Levenkova et al., 2004)

E= Email registration required, T= Tuschl rules, K= Khvorova rules, R= Reynolds rules, U= Ui-Tei rules, B= BLAST search, O= Other rules, S= siRNA Scored or Ranked, F= mRNA folding/Secondary structure, V= Plasmid expression vector design, P= Parameters adjustable, H= Hairpin design, 7= T7 Promoter design

4.2 Methods

All methods have been described previously in Chapter 2 (see specific sections given below)

4.2.1 Determination of mRNA accessibility using a gene-specific ASO microarray

Radiolabelled EGFR mRNA was produced from frozen EGFR plasmid stock that was amplified and transcribed in the presence of radiolabelled nucleotides (2.2.1). Two scanning EGFR ASO arrays were hybridised with radiolabelled target mRNA then analysed. The two gene-specific scanning ASO microarrays both span 150-nucleotide regions of the EGFR mRNA. Array 3 spanning the section 301 to 450 and Array 4 from 431 to 580 downstream of the start AUG codon (Figure 4.2). The two arrays were hybridised with a 1000 base pair fragment of radiolabelled EGFR. Two phosphorimages showing areas of bound labelled mRNA were analysed by the *xvseq* programme to identify regions of mRNA accessibility. siRNA were designed against these identified regions of mRNA accessibility on Arrays 1, 3 and 4. Also 18mers ASOs were produced for each of these regions for mRNA accessibility validation by a RNase H assay.

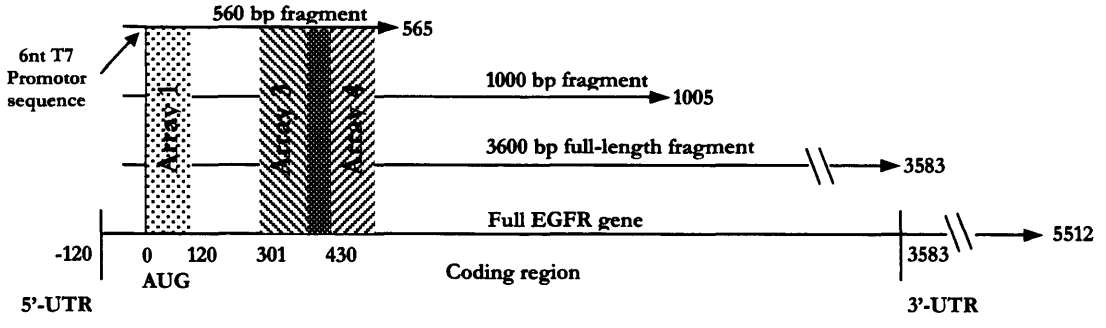

Figure 4.2: Illustration depicting the various lengths of EGFR mRNA fragments and the positioning of the three scanning ASO arrays. Transcriptions were performed under the control of a T7 promoter and all transcripts have the first 6nt from the T7 promoter sequence (5' ggg aga) and the final numbers are inclusive of those. There is a 20-nucleotide overlap between Arrays 3 and 4.

4.2.2 Validation of target mRNA accessibility by utilisation of a ribonuclease H assay

The 1000kb fragment of radiolabelled EGFR mRNA was used in an RNase H assay as described in Section 2.2.2. The assay involved the use of RNase H to cleave DNA-RNA hybrids formed from the complexation of the radiolabelled mRNA fragment with the ASOs produced in the previous section. This would result in mRNA cleavage with only accessible ASOs and these fragments were identified by PAGE analysis.

4.2.3 Determination of mRNA accessibility by using a non-gene-specific array

ExpressOn produce proprietary accessibility arrays that are not gene-specific unlike the scanning ASO arrays used previously. These arrays use non-radiolabelled mRNA and a non-labelled 1kb fragment of EGFR mRNA was complexed with an ExpressOn microarray (2.2.3). The arrays scanned into the ImaGene programme and were analysed using the manufacturer's ACCESSmapper software.

4.3 Results & Discussion

4.3.1 Determination of mRNA accessibility using a scanning ASO microarray

EGFR cDNA coupled with a T7 promoter was amplified from frozen *E. coli* stock and extracted and identified by restriction enzyme digestion. These restriction digests (designated New) were run on an agarose gel with previously made and frozen EGFR cDNA (designated Old; Figure 4.3). The newly produced plasmid was cut into the expected BamH1 (5988, 1059, 1031, 539bp) and HindIII (8617bp) fragments, and ran at the same rate as the previously produced frozen plasmid (Old). This shows that the *E. coli* are competent and will produce the unchanged pCMV-HER plasmid. The sequencing of these plasmids was not performed since they were previously used with an ASO array, Array 1 (Petch et al., 2003). In hindsight, sequencing of plasmids and the PCR products should have been performed to ensure the integrity of the data.

The EGFR cDNA from the plasmid was amplified further using two different PCR reactions; one producing the shorter 560 bp and 1kb EGFR fragments and the other producing the longer full-length 3.6 kb fragment (Figure 4.4). Both reactions were successful and produced the PCR products effectively and consistently, to make available quantities of EGFR cDNA needed to produce sufficient mRNA to be hybridized to the scanning arrays. The EGFR cDNA was then transcribed into the corresponding mRNA. This non-labelled mRNA was run on an agarose gel to validate the transcription protocol (Figure 4.5). The 560 bp and 1kb EGFR mRNA were both successfully produced along with the positive control of transcription supplied by the kit manufacturer that produces a pTRI-Actin 304 bp RNA fragment (Figure 4.5 and Figure 4.6).

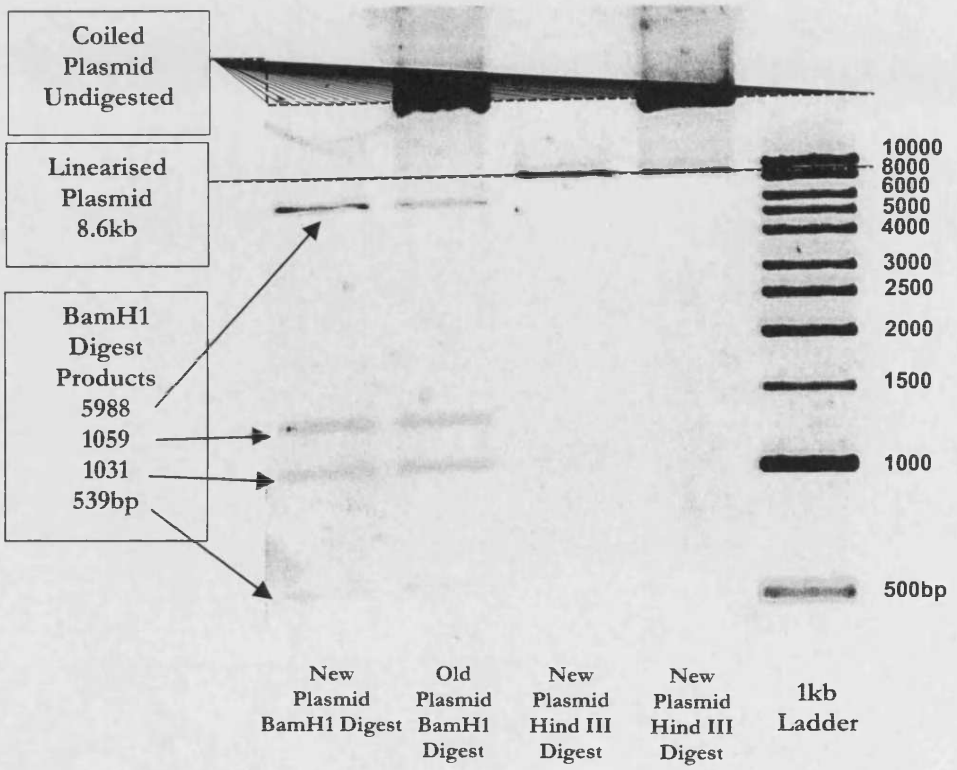

Figure 4.3: Restriction enzyme digestion of EGFR-expressing plasmid. A 1% agarose gel showing the restriction digests of plasmid (pCMV-HER) by BamH1 and HindIII. These restriction digests (designated New) were run with previously made and frozen EGFR cDNA (designated Old).

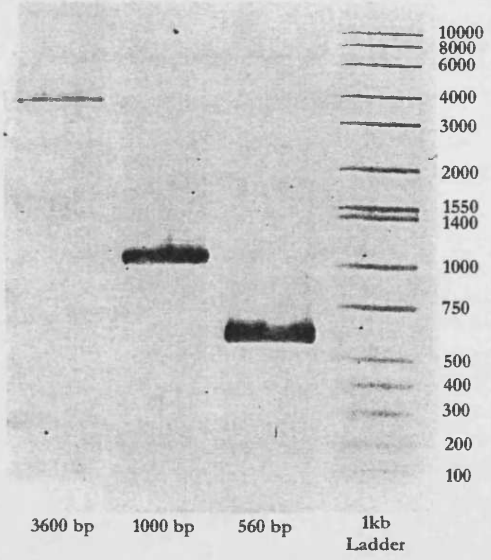

Figure 4.4: PCR on EGFR-expressing plasmid to produce EGFR cDNA fragments of different lengths that contain a T7 plasmid promoter. A 1% agarose gel shows cDNA EGFR fragments produced by PCR amplification. Three different length fragments, 560, 1000, 3600 base pairs, were made by using reverse primers at different sites along the plasmid's DNA.

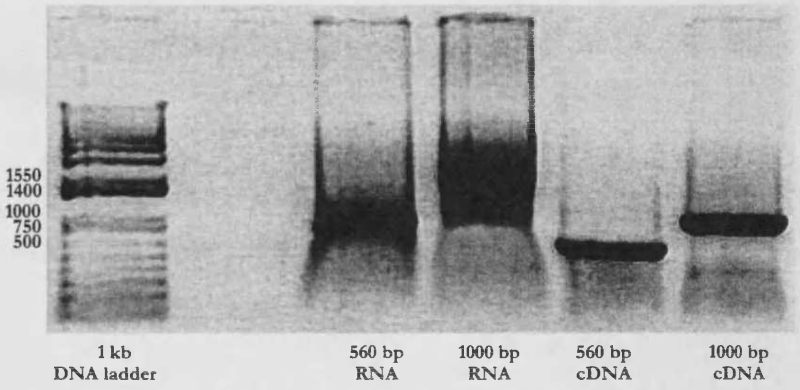

Figure 4.5: Runoff transcriptions of EGFR mRNA fragments produced from cDNA. 1% Agarose gel showing T7 RNA runoff transcripts for 560 and 1000 base pairs produced from their respective EGFR cDNA fragments.

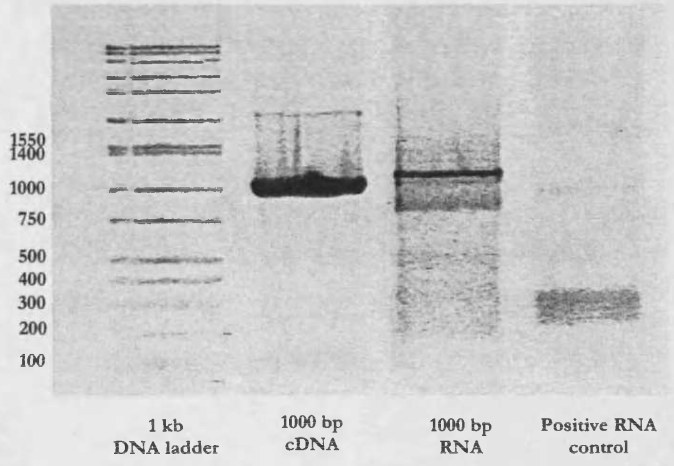

Figure 4.6: Runoff transcription of EGFR 1kb mRNA fragment including positive control. Agarose gel showing 1000bp EGFR cDNA fragment and its T7 RNA runoff and includes the Ambion transcription positive control that produces 304bp fragment of RNA.

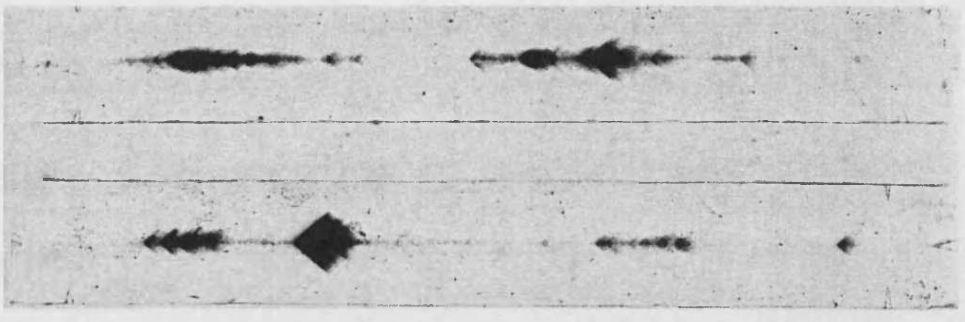

Figure 4.7: Phosphorimage of scanning ASO array 3 (top) and array 4 (bottom) hybridised with radiolabelled 1kb EGFR mRNA. The black chevrons indicate hybridised radiolabelled 1kb fragment of EGFR mRNA.

The radiolabelled 1kb EGFR mRNA fragment was hybridized with Array 3 (above; Figure 4.7) and Array 4 (below; Figure 4.7). The phosphorimage of the arrays shows dark chevrons that represent regions of radiolabelled mRNA hybridisation. The phosphorimages in Figure 4.7 were imported into the *xvseq* programme for analysis. The output from the programme for Array 3 and 4 are shown in Figure 4.8 and Figure 4.9 respectively. The programme produces histograms of hybridisation intensities that correspond to mRNA accessibilities. 18mer mRNA targets with a range of hybridisation intensities were selected and their sequences and individual hybridisation intensities were shown.

HAR-1 was my first siRNA design; its EGFR mRNA target sequence was chosen from previously published scanning ASO array data (Petch et al., 2003). The target sequence was selected to be similar to active 21mer ASO, designated AS2 in the Petch paper (Figure 4.10). The target was shifted one nucleotide upstream so it contained a 5'-AA-(N_{21})-3' motif that followed Tuschl's rules (Table 4.1). Two dTdT overhangs were also added to each strand according to Tuschl's recommendations (Elbashir et al., 2002).

Array 3 and 4 were fabricated to further span the EGFR mRNA (Figure 4.2). 18mer regions of varying hybridisation intensities were selected for both arrays (Figure 4.11 and Figure 4.12). Initially two regions were selected from Array 3 with a high and a medium hybridisation intensity (designated A2 and A1 respectively). Also two were selected from Array 4, one with a high and a zero hybridisation intensity (A3 and Z1). An on-line siRNA design algorithm provided by Whitehead Institute (http://jura.wi.mit.edu/), was used to design another siRNA (W1). This algorithm searches the imported mRNA sequences and selects AA-N19-UU motifs, which will produce siRNA with 3' TT overhangs. Two of these motifs were found on the sequence corresponding to Array 3 (none were present on Array 4), and the one with lowest hybridisation intensity was selected (W1), note the other was named W2. The 18mers were extrapolated to 21mers by adding one base to the 5' end and dTdT overhangs to the 3' ends. This located the siRNA cleavage site between antisense positions 10-11 at the highest hybridisation intensity.

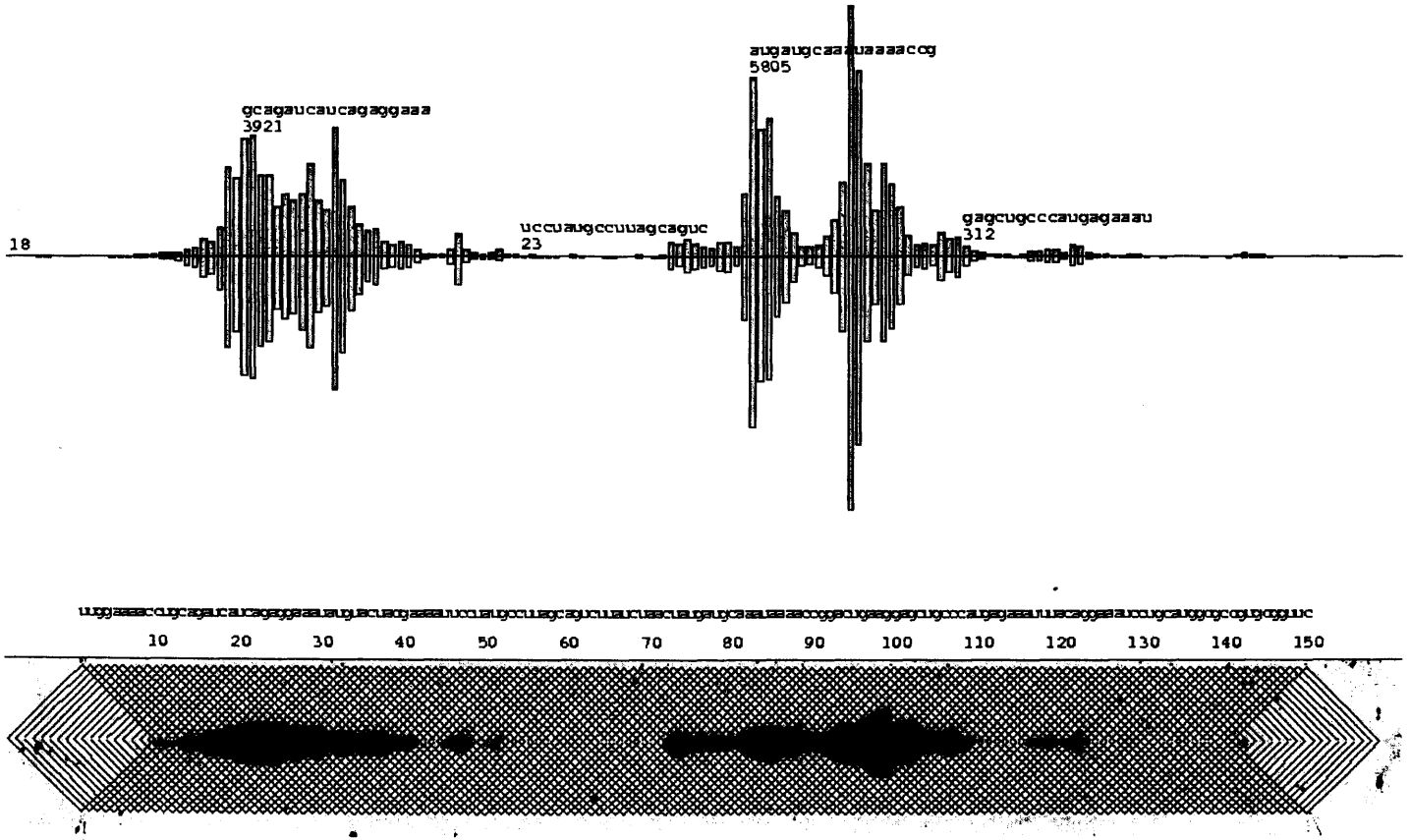

Figure 4.8: Output from xvseq programme from phosphorimage of the radiolabelled 1kb EGFR mRNA fragment hybridised to Array 3. Histogram of hybridisation intensity (top) with the sequence of the mRNA fragment (middle) and phosphorimage of the array with hybridised radiolabelled mRNA (bottom). The histogram of hybridisation intensities is annotated with selected 18mer mRNA targets; the numbers correspond to their respective hybridisation intensities.

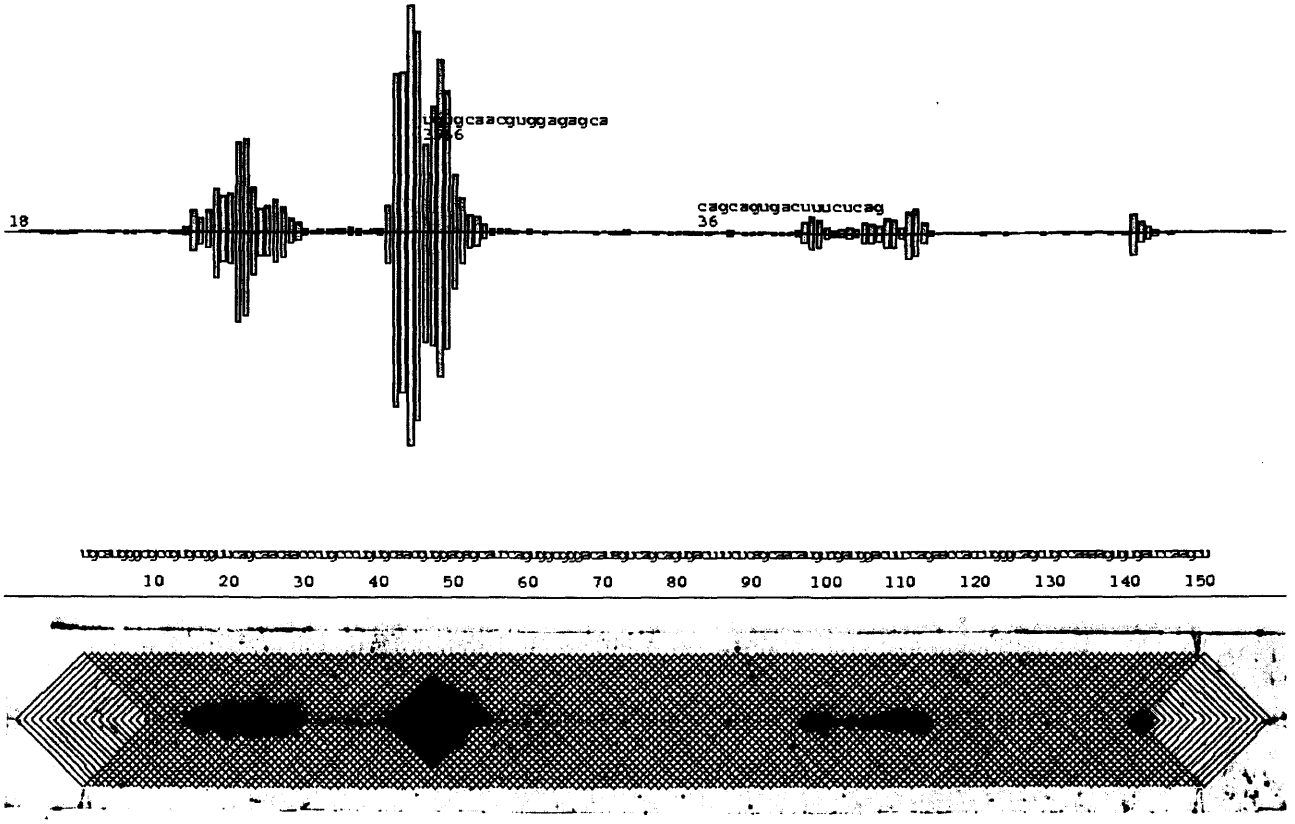

Figure 4.9: Output from xvseq programme from phosphorimage of the radiolabelled 1kb EGFR mRNA fragment hybridised to Array 4. Histogram of hybridisation intensity (top) with the sequence of the mRNA fragment (middle) and phosphorimage of the array with hybridised radiolabelled mRNA (bottom). The histogram of hybridisation intensities is annotated with selected 18mer mRNA targets; the numbers correspond to their respective hybridisation intensities.

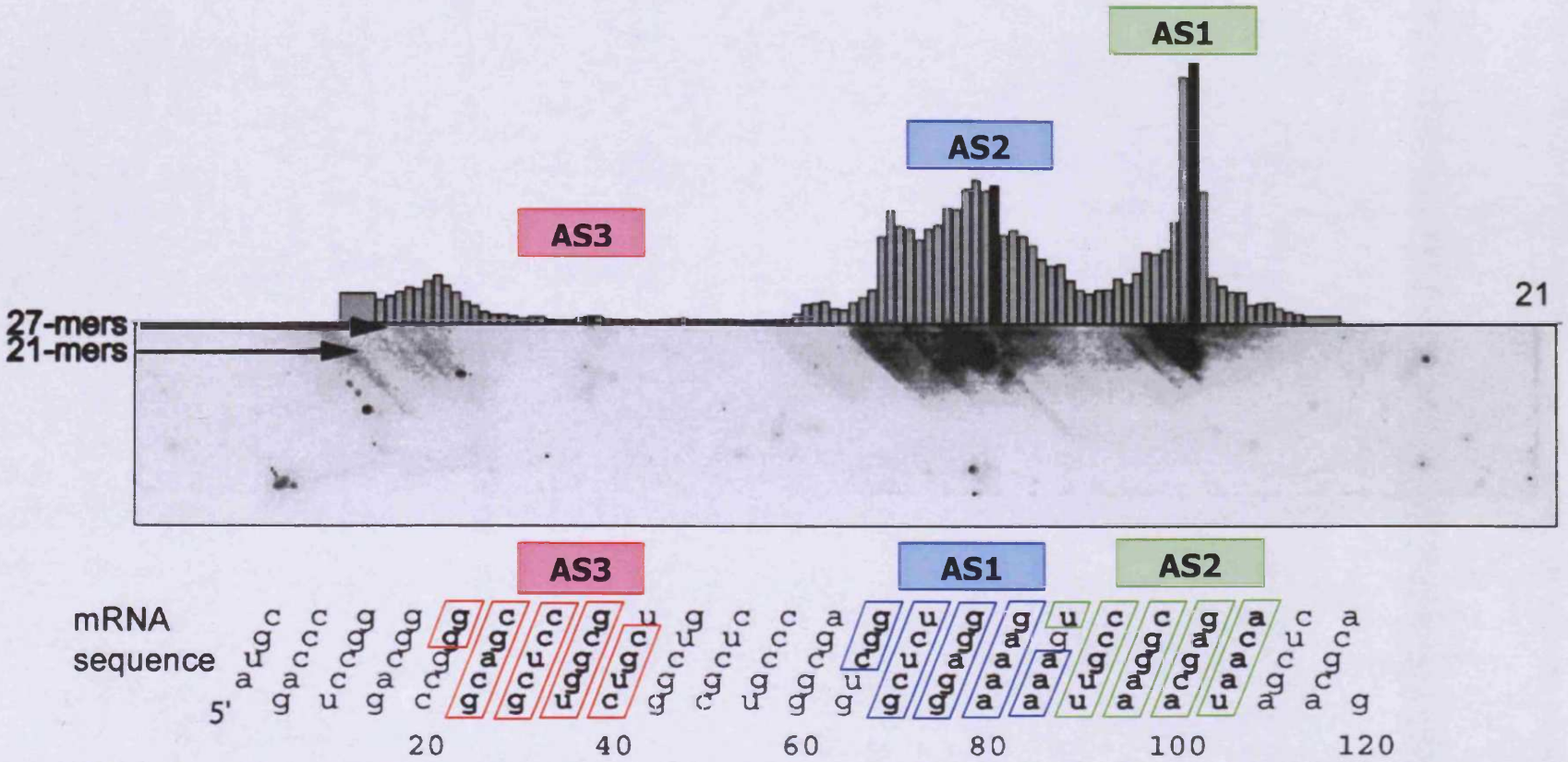

Figure 4.10: Amalgamated xvseq output image of a scanning ASO Array 1 maps the first 120 nucleotides downstream of the EGFR start (AUG) codon. The target sequence of three 21mer ASOs are shown; AS1 (blue), AS2 (green) and AS3 (red). xvseq histogram of Array 1 with the overlaid region of HAR-1 to show the region of HAR-1 designed siRNA. The position of HAR-1 siRNA overlies the region of AS1 and AS2; shifted 1 nucleotide upstream of AS2. The target sequence of HAR-1 is: GUU UGC CAA GGC ACG AGU AAC. Note that AA precedes the target sequence as specified in Tuschl's rules (Table 4.1). This figure was adapted from (Petch et al., 2003)

A)

B)

C)

D)

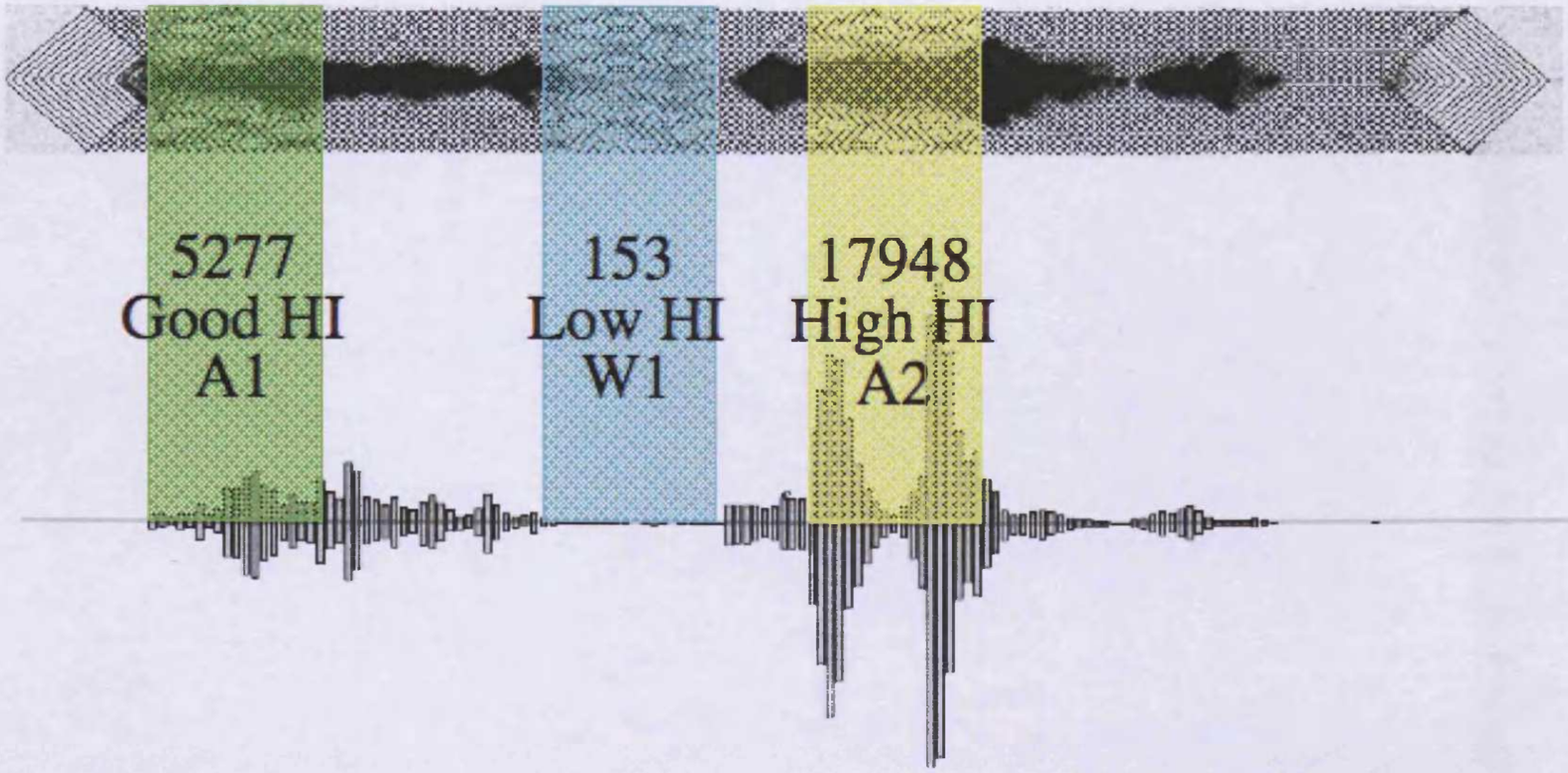

Array 3 Sequence (301-450)

uggaaaaccugcagaucaucagaggaaauauguacuacgaaaauuccuaugccuuagcagucuuaucuaacuaugaugcaaauaaaaccgg
acugaaggagcugcccaugagaaauuuacaggaaauccugcauggcgccgugcgguuc

Figure 4.11: xvseq histogram of Array 3 to show the region of A1, A2, W1 designed siRNA. **A)** Phosphorimage of scanning antisense oligonucleotide EGFR Array 3. **B)** The coloured bars correspond to 18mer regions selected for siRNA design, the hybridisation intensity (HI) is shown above the level of HI and on top of the given siRNA name. **C)** Histogram of hybridisation intensity. **D)** The sequence of EGFR mRNA on Array 3 the coloured regions correspond to the colour coordinated 18mer selected for siRNA design.

A)

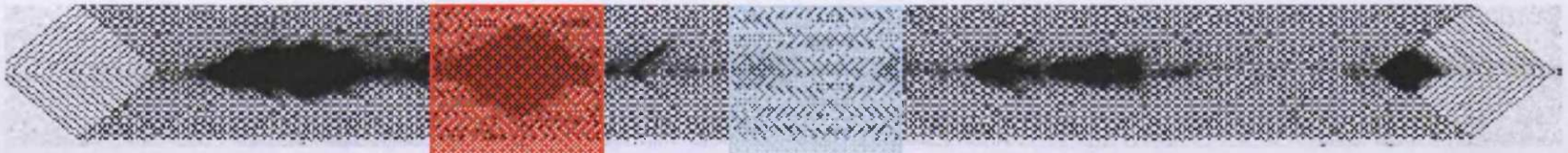

B)

C)

D)

Array 4 Sequence (431-580)

ugcaugggcgccgugcgguucagcaacaacccugcccugugcaacguggagagcauccaguggcgggacauagucagcagugacuuucuca
gcaacaugucgauggacuuccagaaccaccugggcagcugccaaaagugugauccaagcu

Figure 4.12: xvseq histogram of Array 4 to show the region of A3 and Z1 designed siRNA **A)** Phosphorimage of scanning antisense oligonucleotide EGFR Array 4. **B)** The coloured bars correspond to 18mer regions selected for siRNA design, the hybridisation intensity (HI) is shown above the level of HI and on top of the given siRNA name. **C)** Histogram of hybridisation intensity. **D)** The sequence of EGFR mRNA on Array 4 the coloured regions correspond to the colour coordinated 18mer selected for siRNA design.

4.3.2 RNase H Assay

RNAse H Assay allowed the validation of scanning ASO arrays, as it is another method for the determination of mRNA accessibility. ASOs that target the regions selected by the Array 3 and 4 (Figure 4.11 and Figure 4.12) were manufactured. The radiolabelled 1kb fragment was first incubated with the RNase reaction mixture, this resulted in complete cleavage of the full-length fragment for the selected accessible ASOs; A1, A2 and A3 but not for the inaccessible W1, W2 and Z1 (Figure 4.13). The predicted RNAse H cleavage fragments are shown in Tables 4.3 and 4.5 they seem to correlate well with the experimental values. The deemed inaccessible ASOs still mediate some cleavage of the full-length fragment (Figure 4.13). The shorter fragment of 560bp was used to improve resolution although the resolution of cleaved fragment was improved there was still incomplete cleavage of the full-length mRNA fragment (Figure 4.14).

4.3.3 ExpressOn arrays

The ExpressOn proprietary arrays require validation of array experimental technique by producing array results for a luciferase mRNA (provided by the manufacturer) and comparing them to those by the manufacturer. The manufacturer's results are shown in Figure 4.15 and my results are shown in Figure 4.16. There were 8 prominent peaks seen in both figures although the amplitude varied this was not thought to correlate with activity (personal communication with Peter Esterbeiro from ExpressOn).

After performing the results with EGFR 1kb fragments three figures were produced corresponding to the three Arrays: Array 1, 2 and 3 (Figure 4.17, Figure 4.18 and Figure 4.19). Array 1 showed good similarity between the ExpressOn and the scanning ASO arrays as two peaks A1 and A2 were clearly visible, even the peak upstream of A3 was seen (Figure 4.17 compared with Figure 4.10). The mRNA target regions of Array 3 and Array 4 on the ExpressON array did not show similar patterns to those seen in the scanning ASO arrays (Figure 4.18 and Figure 4.19 compared with Figure 4.11 and Figure 4.12).

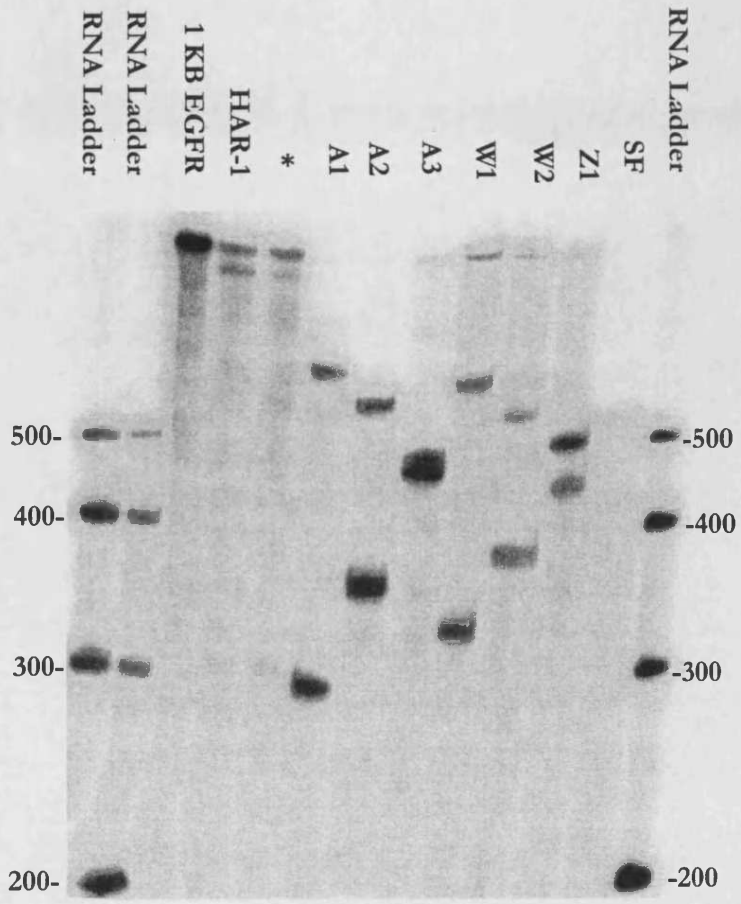

Figure 4.13: RNase H Assay on 1kb EGFR mRNA fragment. A 20% PAGE gel with RNase H assay products. RNA ladder was commercially available RNA ladder that was radiolabelled. SF was an additional target site on Array 4 that was not selected for siRNA design. *Represents a dendrimer that is not relevant to this thesis.

Table 4.4: Predicted sizes of 1kb EGFR mRNA RNase H cleavage fragments

mRNA target site	1st fragment	2nd fragment
HAR-1	102	903
A1	325	680
A2	387	618
A3	480	525
W1	359	646
W2	413	592
Z1	517	488
SF	542	463

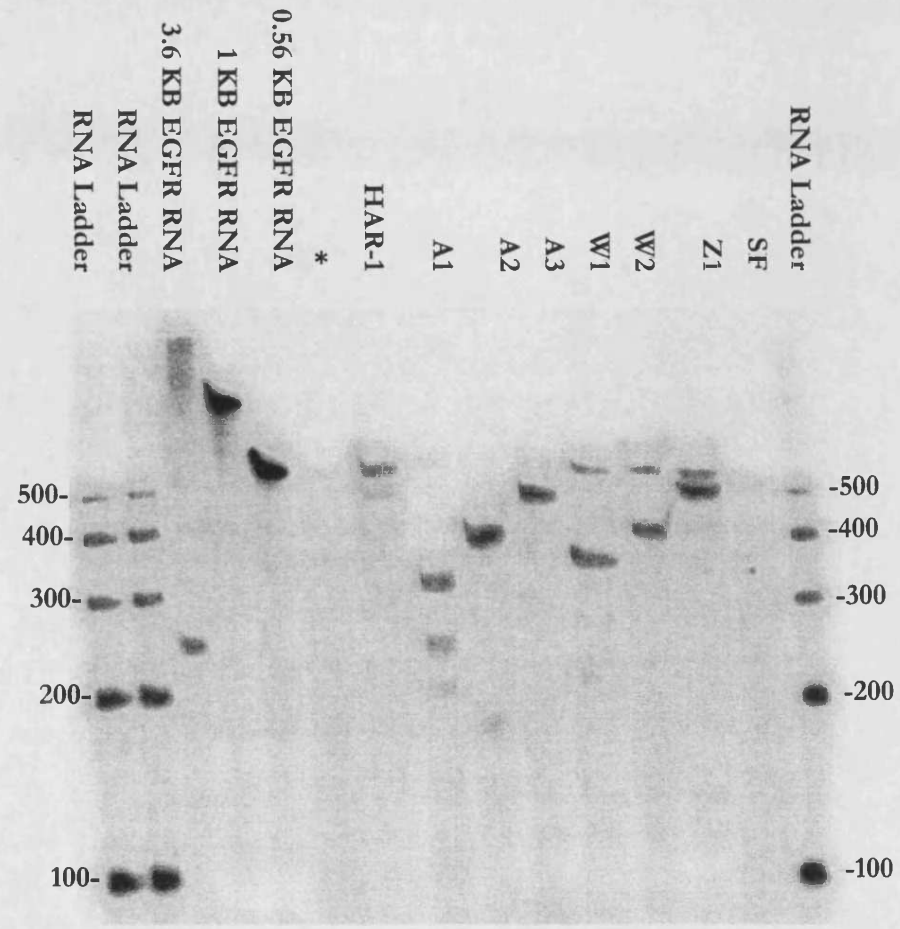

Figure 4.14: RNase H Assay on 560bp EGFR mRNA fragment. A 20% PAGE gel with RNase H assay products. RNA ladder was commercially available RNA ladder that was radiolabelled. SF was an additional target site on Array 4 that was not selected for siRNA design. *Represents a dendrimer that is not relevant to this thesis.

Table 4.5: Predicted sizes of 0.56kb EGFR mRNA RNase H cleavage fragments

mRNA target site	1st fragment	2nd fragment
HAR-1	102	463
A1	325	240
A2	387	178
A3	480	85
W1	359	206
W2	413	152
Z1	517	48
SF	542	23

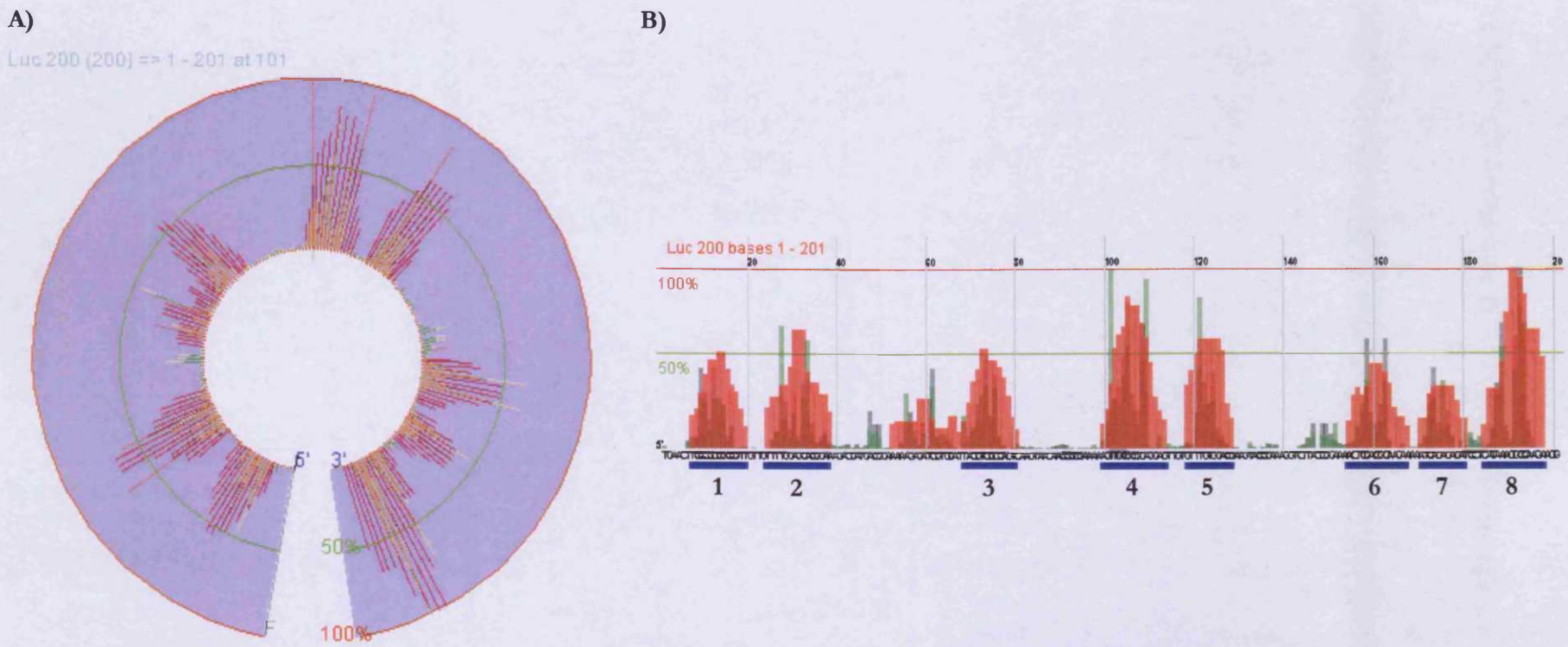

Figure 4.15: ACCESSmapper software output for the ExpressOn Luciferase control array, this data provided by ExpressOn. ExpressOn arrays are commercially available mRNA accessibility arrays and the Luciferase control pattern is copied from the manufacturers program. **A)** Horseshoe figure shows the full 200bp accessibility map of luciferase fragment **B)** Graph figure shows the accessibility map with the luciferase mRNA sequence beneath the prominent peaks were labelled 1 to 8.

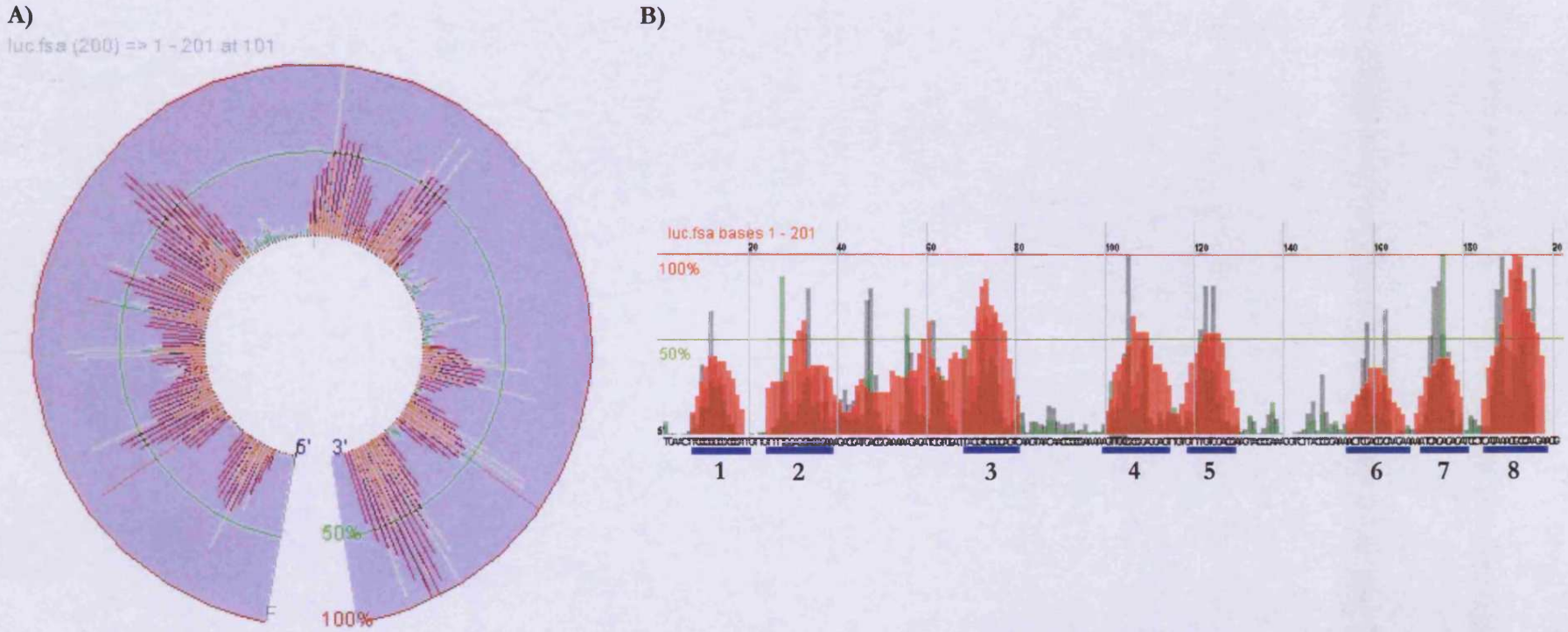

Figure 4.16: ACCESSmapper software output for the ExpressOn Luciferase control array, this data produced in laboratory. ExpressOn arrays are commercially available mRNA accessibility arrays and the Luciferase control pattern was produced from RNA transcript from cDNA supplied by the manufacturer. **A)** Horseshoe figure shows the full 200bp accessibility map of luciferase fragment **B)** Graph figure shows the accessibility map with the luciferase mRNA sequence beneath the prominent peaks were labelled 1 to 8.

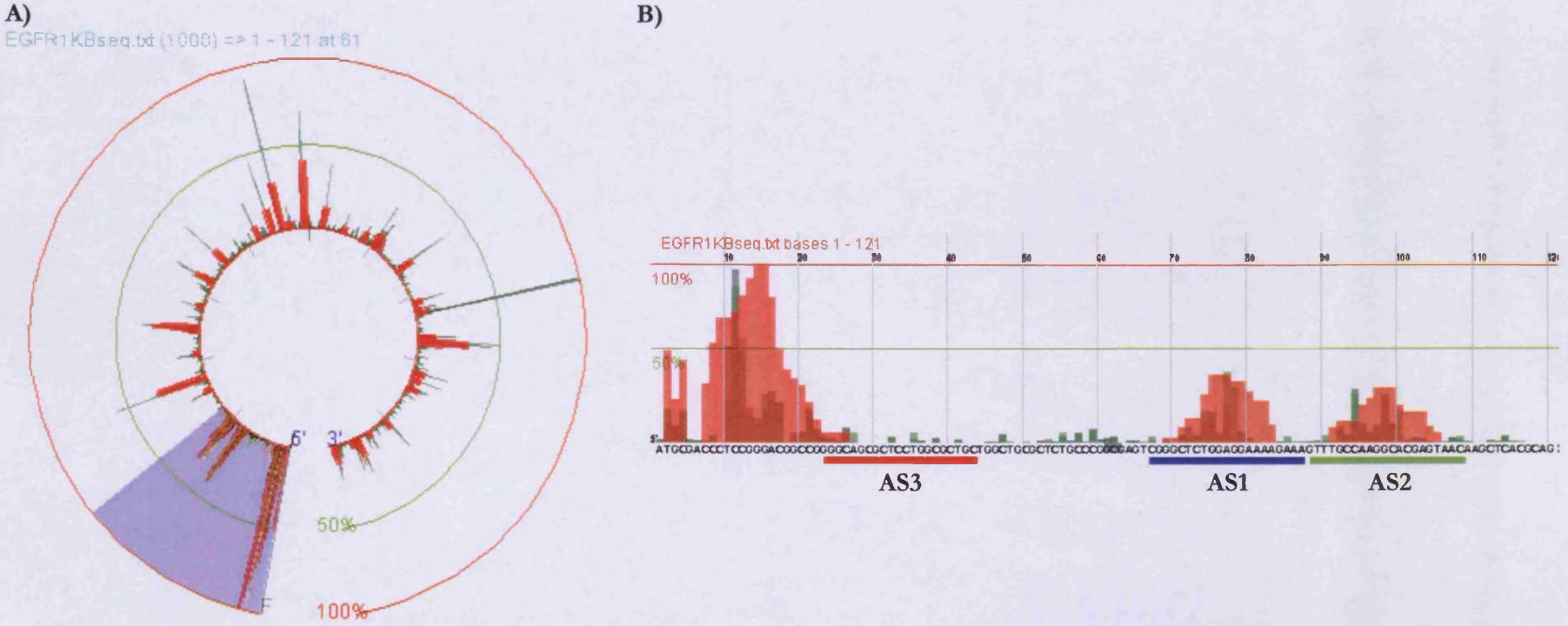

Figure 4.17: ACCESSmapper software output for the EGFR 1kb array, this data produced in laboratory, a region corresponding to Array 1 is selected. ExpressOn arrays are commercially available mRNA accessibility arrays and the Luciferase control pattern was produced from RNA transcript from cDNA supplied by the manufacturer. **A)** Horseshoe figure shows the full 1kb accessibility map of the EGFR fragment **B)** Graph figure shows the accessibility map with the 1kb EGFR mRNA sequence beneath, the selected region from Array 1 (AS1, AS2 and AS3) are highlighted.

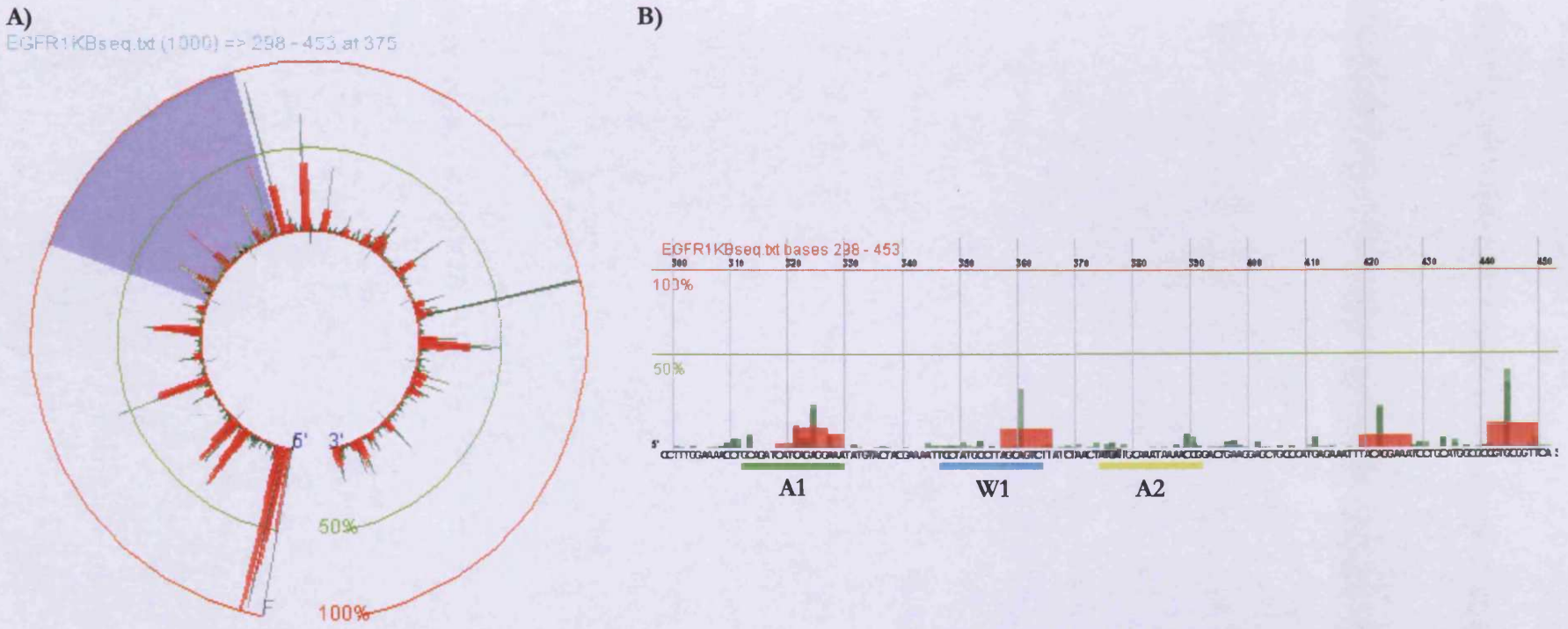

Figure 4.18: ACCESSmapper software output for the EGFR 1kb array, this data produced in laboratory, a region corresponding to Array 3 is selected. ExpressOn arrays are commercially available mRNA accessibility arrays and the Luciferase control pattern was produced from RNA transcript from cDNA supplied by the manufacturer. **A)** Horseshoe figure shows the full 1kb accessibility map of the EGFR fragment **B)** Graph figure shows the accessibility map with the 1kb EGFR mRNA sequence beneath, the selected region from Array 3 (A1, A2 and W1) are highlighted.

A)

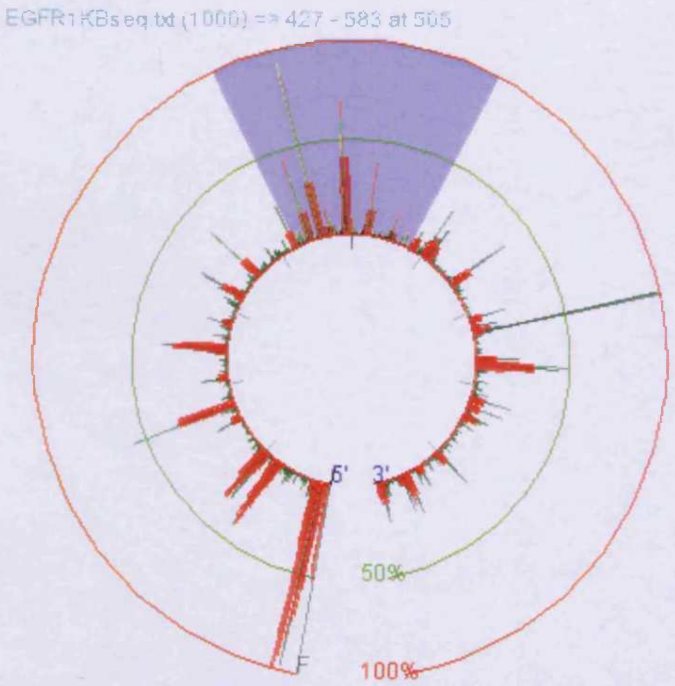

B)

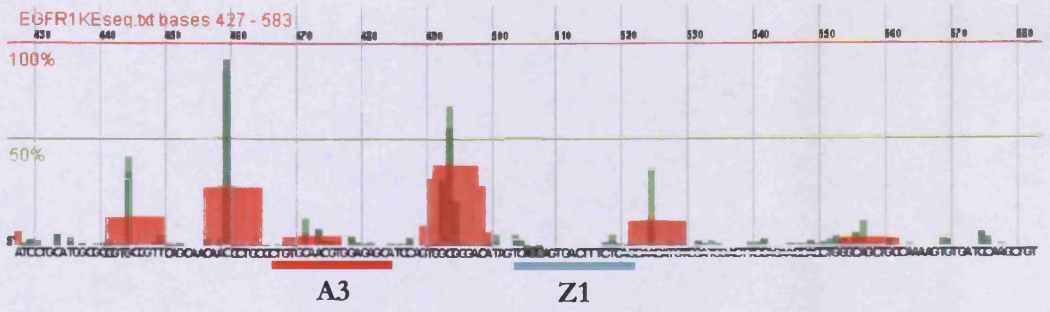

Figure 4.19: ACCESSmapper software output for the EGFR 1kb array, this data produced in laboratory, a region corresponding to Array 4 is selected. ExpressOn arrays are commercially available mRNA accessibility arrays and the Luciferase control pattern was produced from RNA transcript from cDNA supplied by the manufacturer. **A)** Horseshoe figure shows the full 1kb accessibility map of the EGFR fragment **B)** Graph figure shows the accessibility map with the 1kb EGFR mRNA sequence beneath, the selected region from Array 4 (A3 and Z1) are highlighted.

4.3.4 Co-operatively acting ASO & siRNA

Sohail & co-worker developed the idea of co-operatively-acting ASOs and siRNA (Sohail et al., 2005). First, a 2'-O-methyl backbone ASO targeting an accessible region of the EGFR mRNA is introduced into the cell, this will then bind strongly to the target mRNA thus altering its secondary structure, which may reveal a site that is not usually accessible. Targeting a siRNA molecule against this new site could provide a more specific and effective response. This specificity could be tested with gene expression microarrays.

An ASO versus region A3 (Figure 4.12) was hybridised with the radiolabelled 1kb EGFR mRNA before being hybridised onto the scanning ASO arrays. This seemed to only affect local mRNA accessibility since the hybridisation patterns of Array 3 were unchanged (Figure 4.20; top array), compared with Figure 4.7. The patterns of Array 4 seemed to change since the A3 chevron disappeared and a new region that was previously inaccessible became visible (Figure 4.20; designated with an asterisk). The xvseq analysis of Array 3 does not show significant differences (Figure 4.21) but note the values of hybridisation intensity are not the same this is because the values are dependent on numerous factors and cannot compared between arrays. Array 4, the peak upstream of A3 becomes broader and may be used to target a siRNA (Figure 4.22).

Two other research groups (Brown et al., 2005, Sohail, 2005) delivered a 2'-*O*-methyl ASO along with siRNA to provide improved cleavage of the target mRNA. Binding of the 2'-*O*-Methyl ASO did not cause mRNA cleavage but caused mRNA structural changes that resulting in accessible regions that could be targeted with siRNA producing enhanced effects. Sites for cooperatively acting ASO and siRNA for EGFR were elucidated (Figure 4.22) that could be tested for enhanced activity.

The co-delivery of ASO and siRNA was investigated in my thesis using fluorescently labelled oligonucleotides in the next chapter (Figure 5.20). Although the activity of co-operatively acting ASO and siRNA was not investigated in my work.

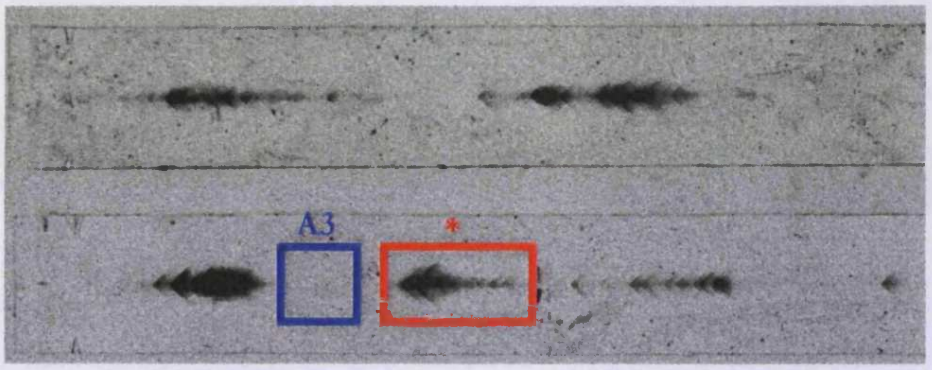

Figure 4.20: Phosphorimage of Array 3 (top) and Array 4 (bottom) co-hybridised with ASO targeting region A3 and radiolabelled 1kb EGFR mRNA. Array 3 is largely unaffected by the binding of antisense to A3 but Array 4 loses completely its A3 chevron (A3). A new mRNA region becomes accessible (designated with an asterisk) this could be a new target for a siRNA.

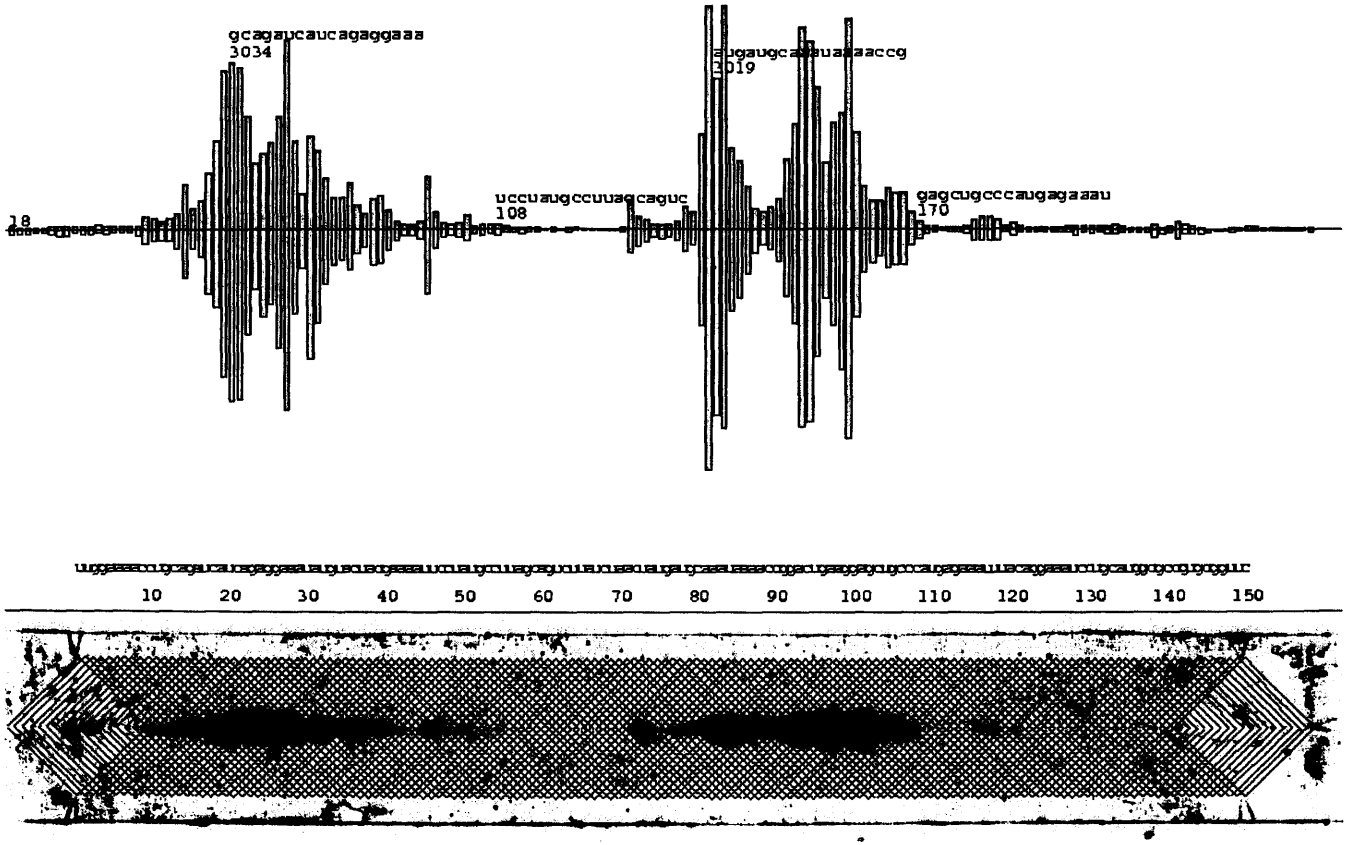

Figure 4.21: xvseq output of Array 3 co-hybridised with ASO versus region A3 and radiolabelled 1kb EGFR mRNA. xvseq figure created from Array 4 with histogram of hybridisation intensity (top) with mRNA sequence (middle) and phosphorimage of the array with hybridised radiolabelled mRNA (bottom). The histogram is annotated with selected 18mer mRNA targets; the numbers correspond to their respective hybridisation intensities.

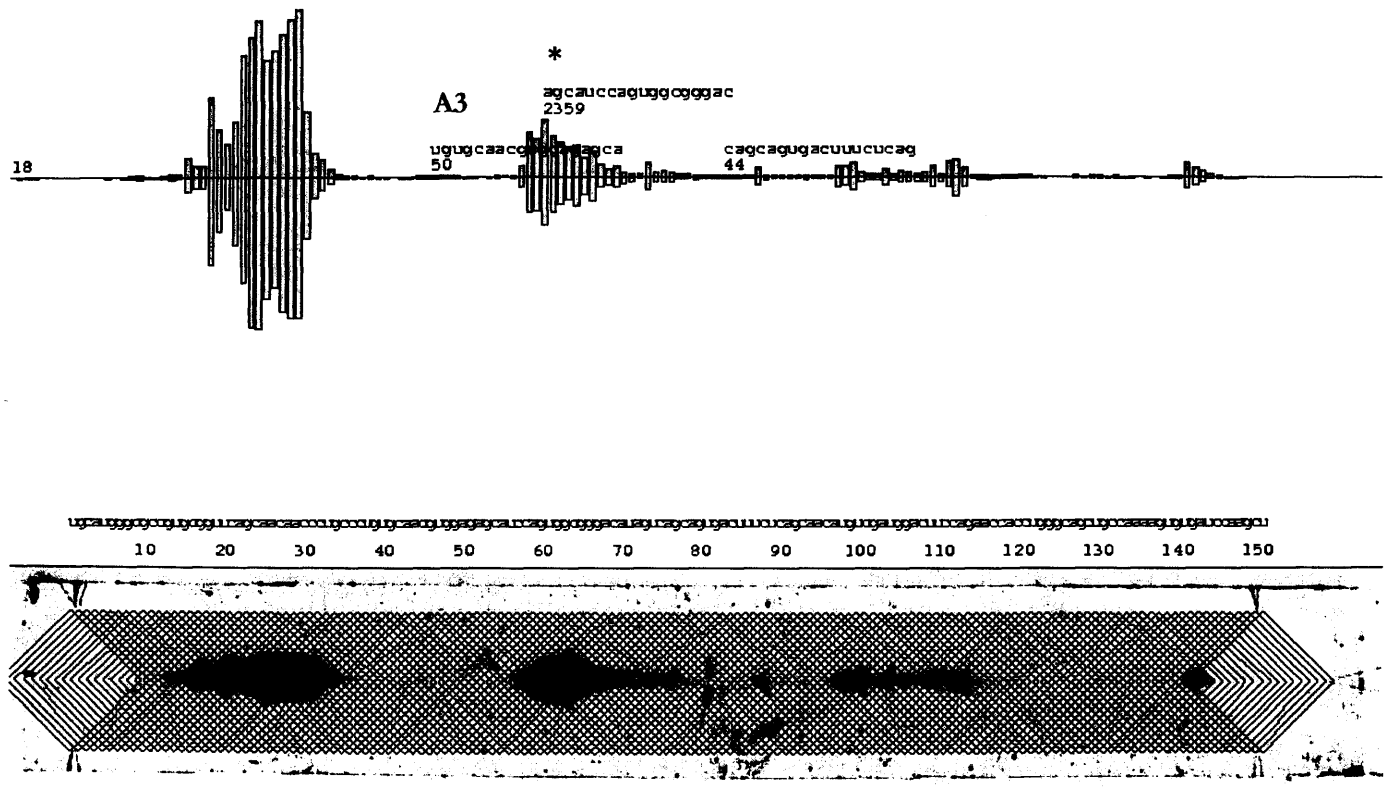

Figure 4.22: xvseq output of Array 4 co-hybridised with ASO versus region A3 and radiolabelled 1kb EGFR mRNA. xvseq figure created from Array 4 with histogram of hybridisation intensity (top) with mRNA sequence (middle) and phosphorimage of the array with hybridised radiolabelled mRNA (bottom). The histogram is annotated with selected 18mer mRNA targets; the numbers correspond to their respective hybridisation intensities.

In summary, an understanding of target mRNA structure was critical to the design of active ASO and is now considered as being a significant factor in the design of active siRNA. Although some initial reports proposed that mRNA accessibility determined siRNA activity (Bohula et al., 2003, Kretschmer-Kazemi Far and Sczakiel, 2003, Vickers et al., 2003) not until thermodynamic stability algorithms were shown not to guarantee success there has been a renewed interest in mapping mRNA structures for siRNA target sites (Kurreck, 2006). siRNA were produced against regions of varying mRNA accessibility against Arrays 1, 3 and 4 (Table 4.6). These siRNAs could determine the effect of mRNA accessibility on their activity; their hybridisation intensity (HI) is a measure of accessibility. Initial mFold investigations were explored but without the required intellectual support this element of the work was not progressed. This should be able to provide a greater understanding of the conformational structures of mRNA and could elucidate strategies to target them.

The thermodynamic stability of the siRNA duplexes is also critical to activity and four additional siRNAs were designed with improved thermodynamic stability characteristics (Table 4.6). The thermodynamic stability of the 5' end of the antisense strand was lowered by adding a base pair mismatch such as a U:G base pair wobble (HAR-1[+] and W1[+]), or by shifting the target sequences up or downstream to find a weaker bond pair such as A-U (A1[+]). One siRNA uses both strategies plus an additional 5' end wobble at position 2 (A2[+]). A further siRNA had U:C mismatch bond at the 5' end of the sense strand in order to impair the thermodynamic stability profile (HAR-1[-]). There are computer programmes that can be used to calculate the thermodynamic stability profiles for siRNA duplexes, e.g. Oligo 5.0 Primer Analysis Software (National Biosciences Inc., Plymouth, Minnesota, USA). These programmes along with other algorithms for assessing the thermodynamic of RNA, require intellectual support and these elements were not progressed in my work. The calculation of the individual thermodynamic stabilities for my designed siRNA would allow them to be ranked in order of most favourable thermodynamic stability profiles. This would mean the biological activity of the siRNA could be directly compared with thermodynamic stability and allow comparisons with other key factors including mRNA accessibility. The siRNA designs need to be assayed for activity which is the focus of the next chapter.

Table 4.6: Sequences of siRNA used in this thesis. Hybridisation intensities (HI)

Name	Sequence (top strand sense strand 5' to 3')	HI	Comments
HAR-1 (H1)	GUU UGC CAA GGC ACG AGU ATT TT CAA ACG GUU CCG UGC UCA U	+++	Array 1 designed siRNA
siHARscr	GUU UGC *ACG GAA CAG CGU* ATT TT CAA ACG *UGC CUU GUC UCA* U	-	HAR-1 sequence scrambled
NS	ACU CUA UCU GCA CGC UGA CUU UUUGA GAU AGA CGU GCG ACU G	-	Non-specific negative control
A1	UGC AGA UCA UCA GAG GAA ATT TT ACG UCU AGU AGU CUC CUU U	++	Array 3, Site 1 designed
A2	UAU GAU GCA AAU AAA ACC GTT TT AUA CUA CGU UUA UUU UGG C	+++	Array 3, Site 2 designed
A3	CUG UGC AAC GUG GAG AGC ATT TT GAC ACG UUG CAC CUC UCG U	+++	Array 4 designed
W1	UUC CUA UGC CUU AGC AGU CTT TT AAG GAU ACG GAA UCG UCA G	+	1st Whitehead designed (Array 3)
W2	GGA GCU GCC CAU GAG AAA UTT TT CCU CGA CGG GUA CUC UUU A	+	2nd Whitehead designed (Array 3)
Z1	UCA GCA GUG ACU UUC UCA GTT TT AGU CGU CAC UGA AAG AGU C	0	Zero hybridisation site (Array 4)
HAR-1 [+]	GUU UGC CAA GGC ACG AGU GTT TT CAA ACG GUU CCG UGC UCA U	+++	HAR-1 with improved TS
HAR-1 [-]	UUU UGC CAA GGC ACG AGU ATT TT CAA ACG GUU CCG UGC UCA U	+++	HAR-1 with worsened TS
A1 [+]	GCA GAU CAU CAG AGG AAA UTT TT CGU CUA GUA GUC UCC UUU A	++	A1 with improved TS
A2 [+]	CUA UGA UGC AAA UAA AAU UTT TT GAU ACU ACG UUU AUU UUG G	+++	A2 with improved TS
W1 [+]	UUC CUA UGC CUU AGC AGU UTT TT AAG GAU ACG GAA UCG UCA G	+	W1 with improved TS

Italics= scrambled bases; underline= mismatch base; •= mismatch bond;
bold= upstream or downstream shift

Chapter 5
Delivery & Activity of siRNA

5.1 Introduction

While the unique specificity of nucleic acid therapeutics is attractive, one of the major challenges beyond the design of the active molecules itself to enhance pharmacological target interaction, is actually the delivery of the oligonucleotide therapeutic efficiently to the site of activity within the cell.

In this chapter I have decided to combine both delivery and activity elements together to afford a more logical presentation and discussion of results. This is particularly pertinent if one considers that the delivery aspects of siRNA, even within *in vitro* systems, must be optimised and understood to some extent before interpretation of differing pharmacological effectiveness can be assessed.

The delivery of siRNA in my work was mainly determined by the cell fluorescence associated with fluorescently labelled siRNA as measured by FACs analysis, although fluorescent microscopy and radiolabelled siRNA assays were also utilised. The activity was defined as the ability of the siRNA molecule to cause gene silencing of the EGFR gene. Activity of the siRNA duplexes designed in Chapter 4 were primarily assayed by their ability to inhibit the growth of A431 cells, although RT-PCR and Western blot analysis was used to assess corresponding reductions in mRNA and protein expression.

The cellular delivery of ASO requires delivery systems not only to protect the nucleotides from degradation by biological fluids but also to efficiently mediate cellular uptake. Although a wide variety of delivery system have been developed the most commonly used delivery systems are charged lipids and lipoplexes that encapsulate or complex with nucleic acids (Kurreck, 2003). These lipoplexes are mainly taken up by endocytosis and ASOs once released from endosomes accummulate in the nucleus (Takle et al., 1997). The cytoplasm is the site of action for siRNA and the intracellular fate of siRNA could be critical for activity.

Chapter aim

To assay the designed siRNA for activity and assess two key parameters important for siRNA activity; thermodynamic stability and accessibility of the mRNA target site.

Chapter objectives

- Effectively deliver siRNA to cells in culture.
- Investigate the effects of the designed siRNA on the growth of cultured cells.
- Investigate the effects of the designed siRNA on EGFR expression.
- Investigate the delivery of co-operatively acting ASO and siRNA.

5.2 Methods

All methods have been described previously in Chapter 2 (See specific section given below)

The uptake of siRNA into A431 cells was investigated using fluorescent (2.3.5) and radiolabelled (2.3.7) siRNA in order to develop an optimised cell transfection protocol (2.3.3). The activities of my designed siRNA from Chapter 4 were assessed using a cell proliferation assay (2.3.4) and validated using semi-quantitative RT-PCR (2.3.8) and Western blot techniques (2.3.9). A fluorescent microscope technique utilising fluorescent labelled and active siRNA were used to determine cellular association of siRNA and EGFR expression, by an anti-EGFR antibody (2.3.6). MCF-7 tamoxifen resistant cells (TamR) were also transfected with siRNA and assessed for activity (2.3.10).

5.3 siRNA Delivery Results & Discussion

5.3.1 Delivery of siRNA to A431 cells

A431 cells were chosen for my studies as they over-express EGFR, approximately 2 million receptors per cell (Filmus et al., 1985), which is a 30-fold amplification when compared with normal human fibroblasts and other cell types (Merlino et al., 1984). In retrospect this may not have been the most appropriate choice as the overexpression enhances the challenges for siRNA-mediated knockdown of EGFR. However, Petch & co-workers (Petch et al., 2003) were able to show that ASO-targeting EGFR was effective in reducing the expression of EGFR at both RNA and protein levels and that these reductions led to the reduced growth of A431 cells. In my studies I did not investigate the effects of ASO targeting EGFR. Investigating the knockdown of EGFR in A431 with ASO could provide a comparator for my siRNA work.

Many groups in order to achieve gene knockout in cultured cells have used Oligofectamine to effectively deliver siRNA (Bai et al., 2001, Elbashir et al., 2001a). Oligofectamine is a lipid–based delivery system and has been utilised in my studies using the manufacturer's recommendations. A431 cells were transfected for 4 hours with 100nM of fluorescent-labelled siRNA that was complexed with Oligofectamine. Oligofectamine alone does not have an effect on cell auto-fluorescence (Figure 5.1). In the following sections fluorescence associated with the cell in the absence of fluorescently labelled siRNA will be termed 'auto-fluorescence'. At 37°C this siRNA-Oligofectamine associated cell fluorescence increased 3-fold ($P<0.05$) from the respective 4°C siRNA-Oligofectamine control (Figure 5.1D). In siRNA uptake studies a low temperature control (4°C) was used to prevent active transport mechanisms in the cell that may internalise the siRNA. At 4°C there was understandably no increase in cell fluorescence associated with the binding of siRNA-Oligofectamine complex to the cell membrane (Figure 5.1D).

Increasing the transfection time beyond 4 hours did not significantly increase cell fluorescence associated with labelled siRNA-Oligofectamine complex. The 4 hours transfection period was selected as the most appropriate transfection time (Figure 5.2).

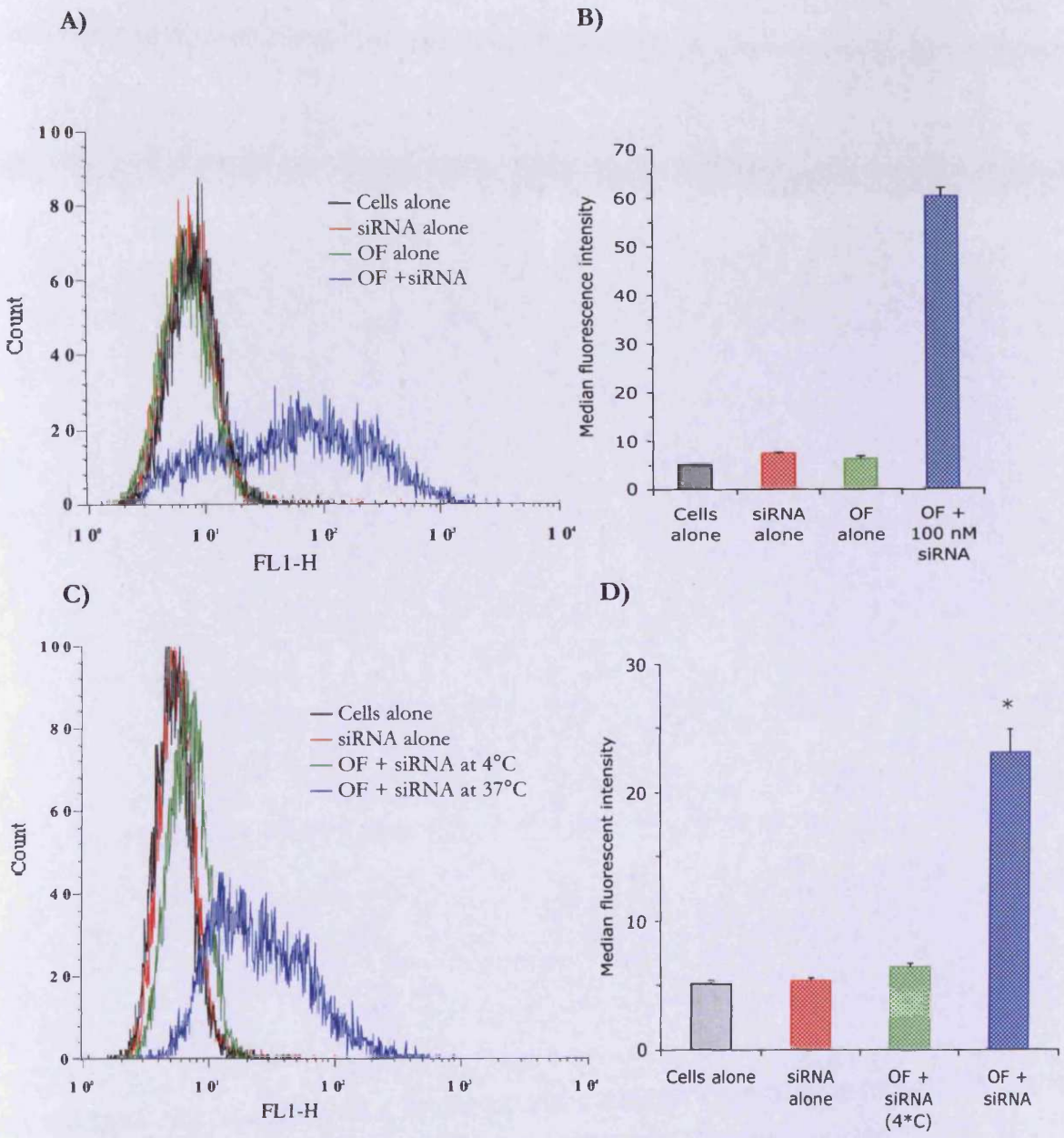

Figure 5.1: Vehicle and temperature control validation using FACs analysis of A431 cells transfected with fluorescently labelled siRNA complexed with Oligofectamine. The cells were left at 37°C for transfection to take place and cell-associated fluorescence was the measured using FACs, the data was analysed using WinMDI and FCSPress software. **A)** Histogram of cell associated green fluorescence (FL-1) for different treatments of siRNA on A431 cells. **B)** Bar chart representation of median fluorescent shown in the previous figure. **C)** Histogram of cell associated green fluorescence (FL-1) for different treatments of siRNA on A431 cells. D) Another bar chart representation of FACs histograms. *Represents a significant difference ($p<0.05$) compared to control (untreated cells). Statistics One-way ANOVA with Dunnetts *Post Hoc* test. Results mean ± standard deviation (n=3)

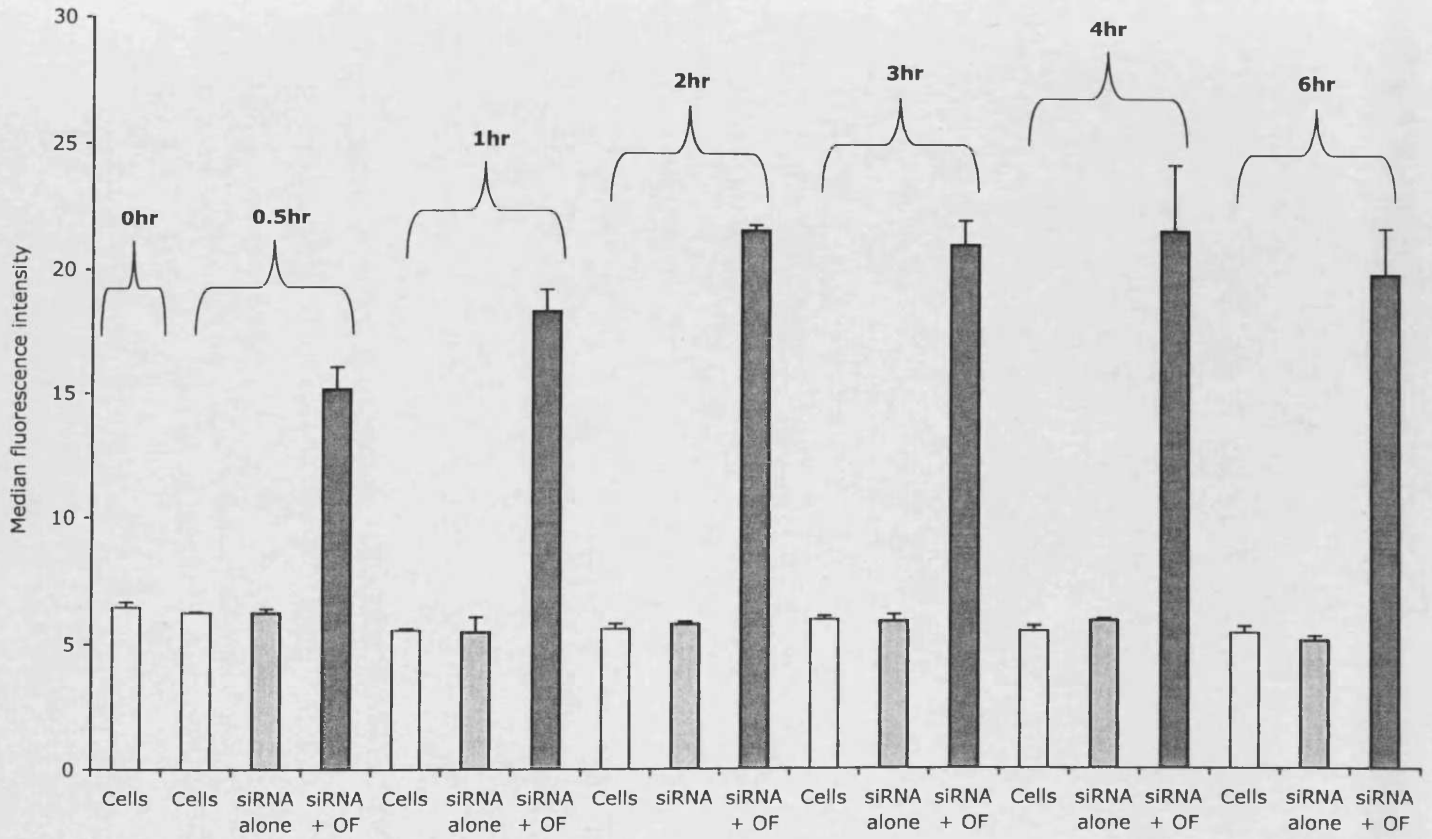

Figure 5.2: Determination of transfection duration using FACs analysis of A431 cells transfected with fluorescently labelled siRNA complexed with Oligofectamine. Fluorescently labelled siRNA was transfected for increasing periods of time up to the manufacturers maximum recommended transfection time. The A431 cells growth media were removed and replaced with serum-free media only (Cells), and media containing fluorescent siRNA alone (siRNA alone) and media containing fluorescent siRNA complex with Oligofectamine (siRNA + OF). After the designated time period, cells were washed 3 times with PBS and trypsinised, these cells were kept on ice until they were analysed by FACs. Results mean ± standard deviation (n=3)

The degree of cell confluency at transfection is another key parameter to be considered in optimising transfection. The growth of A431 cells was investigated and the degree of confluency at 24 hours after seeding (point of transfection) of the A431 cells was determined to be 25% (Figure 5.3). The manufacturers of Oligofectamine recommend for optimim transfection a degree of confluency of 30-50%. A higher degree of confluency at 36 hours after seeding (approximately 30%) showed a slightly lower level of cell fluorescence associated with labelled siRNA-Oligofectamine complexes compared to 24 hours, 25% confluency (Figure 5.4). Since slightly increasing the confluency at the time transfection did not improve the delivery of siRNA all subsequent cell transfections were performed 24 hours after seeding.

In the FACs analysis gated populations of cells were established based upon control cells i.e. not exposed to oligonucleotides. The majority of cells (>80%) transfected with siRNA-Oligofectamine complexes remain within the gated population, shown as a polygon (Figure 5.5). This could be interpreted as the majority of these cells remaining undamaged by the transfection protocol. However, biochemical toxicity studies should be ideally performed to determine the cellular damage caused by delivery systems. The manufacturer of Oligofectamine does not provide composition information and this prohibits the use of charge-ratios, such as Nitrogen to Phosphate (N:P) ratios, that would be the standard convention when discussing the lipid delivery of nucleic acids. The quantities of Oligofectamine were therefore given as a fluid volume and 1μL of Oligofectamine gave the highest cell fluorescence associated with 100nM of labelled siRNA (Figure 5.5).

Opti-MEM was the transfection media recommended by the manufacturer of Oligofectamine. There was no difference seen in the cell fluorescence associated with labelled siRNA-Oligofectamine when cells were transfected in Opti-MEM or the normal cell growth media, 10% serum-containing D-MEM (Figure 5.6A). Since serum contains nucleases that could degrade siRNA, serum-free D-MEM could be a more suitable transfection media. Serum-free D-MEM was then compared as a transfection media to 10% serum-containing D-MEM over 6-hours (Figure 5.6B), at four hours it provided comparable siRNA delivery.

A range of other delivery systems were trialed for the transfection of A431 cells and whether they provided good siRNA delivery. The delivery systems tested included: Cationic dendrimer Superfect and Polyfect (Figure 5.7); the branched polymer Polyethylene imine (BPEI; Figure 5.8) and Lipid systems: RNAifect (Figure 5.9), Metafectene (Figure 5.10), Transit-TKO (Figure 5.11) and Oligofectamine (Figure 5.12). A semi-quantitive scoring system of these agents is shown in Table 5.1 and Oligofectamine was selected as the delivery system for the rest of my studies as it seemed to leave the most undamaged A431 cells, 80% of cells were within the gated region, while maintaining acceptable siRNA delivery (Figure 5.12).

The toxicity of delivery systems was not further investigated in this thesis but one should appreciate that delivery systems can have significant effects on gene expression and signal transduction (Kabanov, 2006). Alterations in expression of EGFR and the genes involved in cell growth could have consequences on the results of my studies. A notable effect was that Oligofectamine treatment caused an upregulation of EGFR expression this has been reported for other delivery systems (Omidi et al., 2003). This upregulation of EGFR expression was subsequently seen with the Dharmafect delivery system in Chapter 5. Since this effect was not investigated it will not be further discussed but it does have implications over the selection of delivery for gene-silencing experiments.

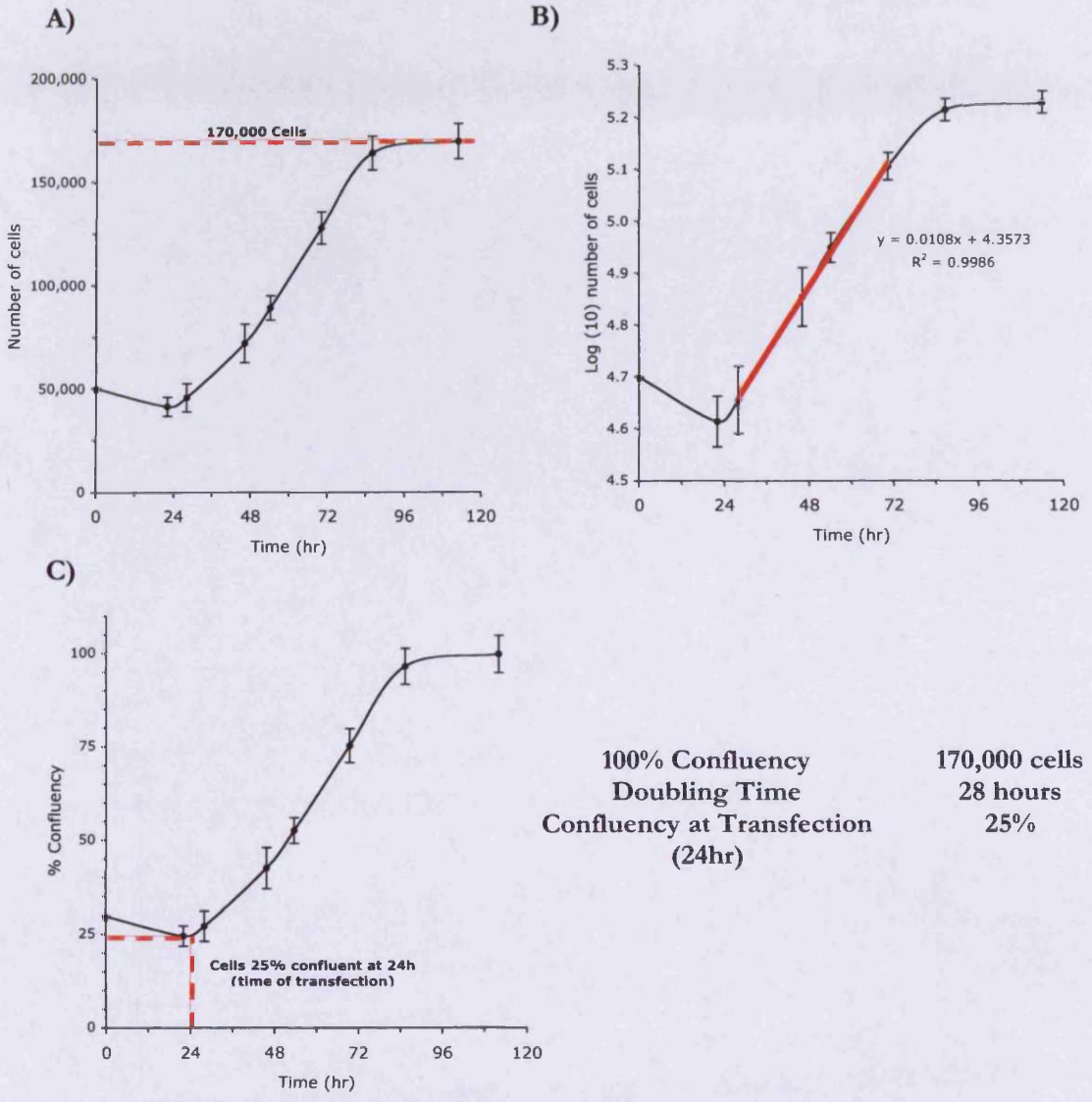

100% Confluency	170,000 cells
Doubling Time	28 hours
Confluency at Transfection (24hr)	25%

Figure 5.3: Growth curves of A431 cells to calculate: confluency, doubling time and transfection confluency. Growth curves for A431 cells, cells were incubated for up to 5 days with fresh media being applied after 48 hours. For each time point cells were wash and trypsinized and counted with a haemocytometer. **A)** Cell growth plateaued after 96 hours and confluence was determined to be 170,000 cells. **B)** The y-axis was logged so the logarithmic growth part of the curve was linearised and a straight line was plotted and the double time for the cells was calculated to be 28 hours. **C)** The y-axis was converted to percentage confluence and the confluency at time of transfection (24hrs) was estimated to be 25%. Error bars correspond to 1 standard deviation.

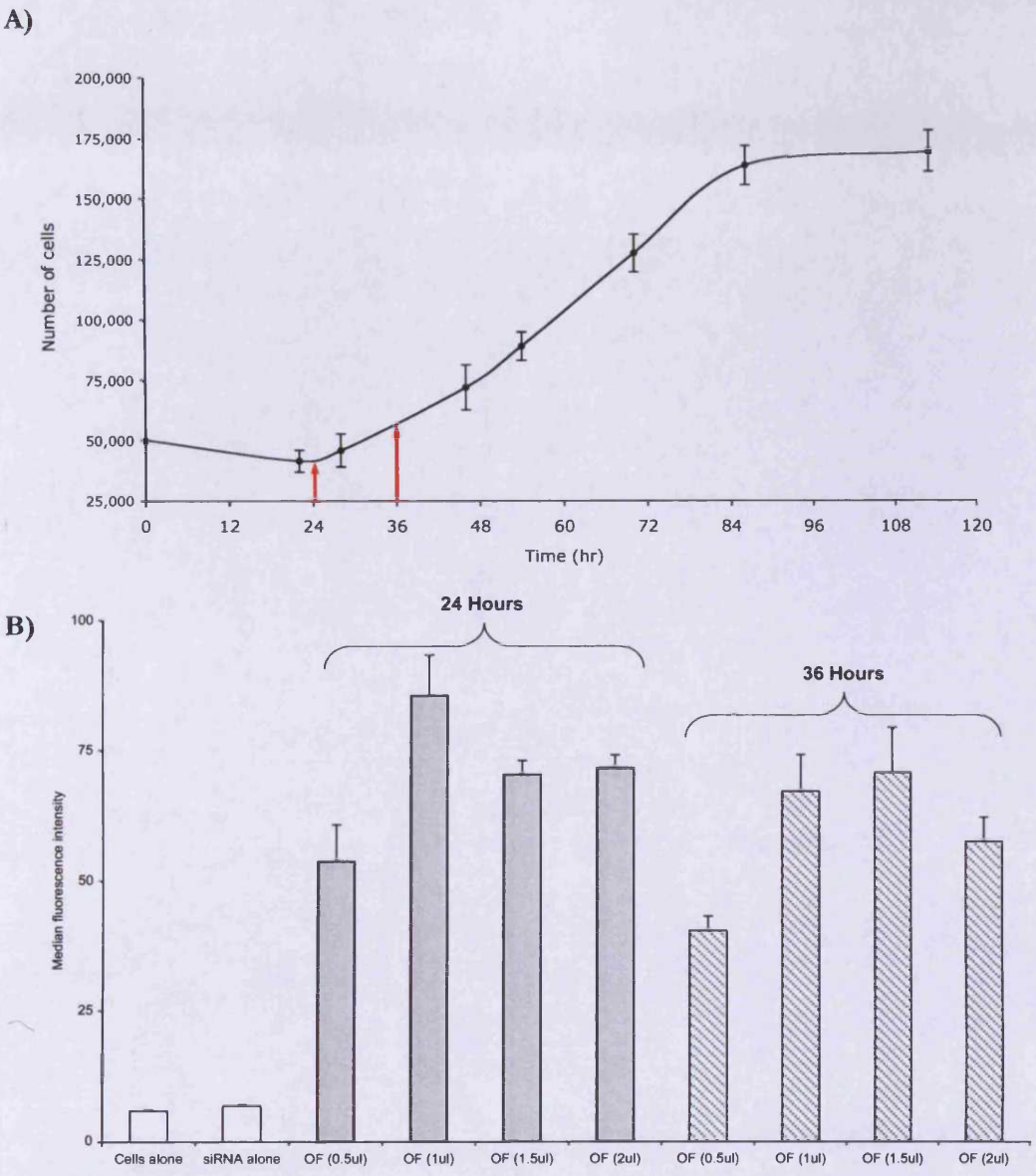

Figure 5.4: Determination of transfection time using FACs analysis of A431 cells transfected with fluorescently labelled siRNA complexed with Oligofectamine. Cells have previously been seeded and transfected 24 hours later. **A)** The growth curve replicated from the previous figure shows that 36 hours is definitely within the period of logarithmic growth and may be a better time to transfect cells. **B)** Bar charts of median fluorescence intensities, obtained from cell-associated fluorescent histograms, were produced for cells transfected 24 hours and 36 hours after seeding. 100nM fluorescent siRNA was complexed with a range of volumes of Oligofectamine (OF), from 0.5µL to 2µL, as specified by the manufacturer. Error bars correspond to 1 standard deviation.

A)

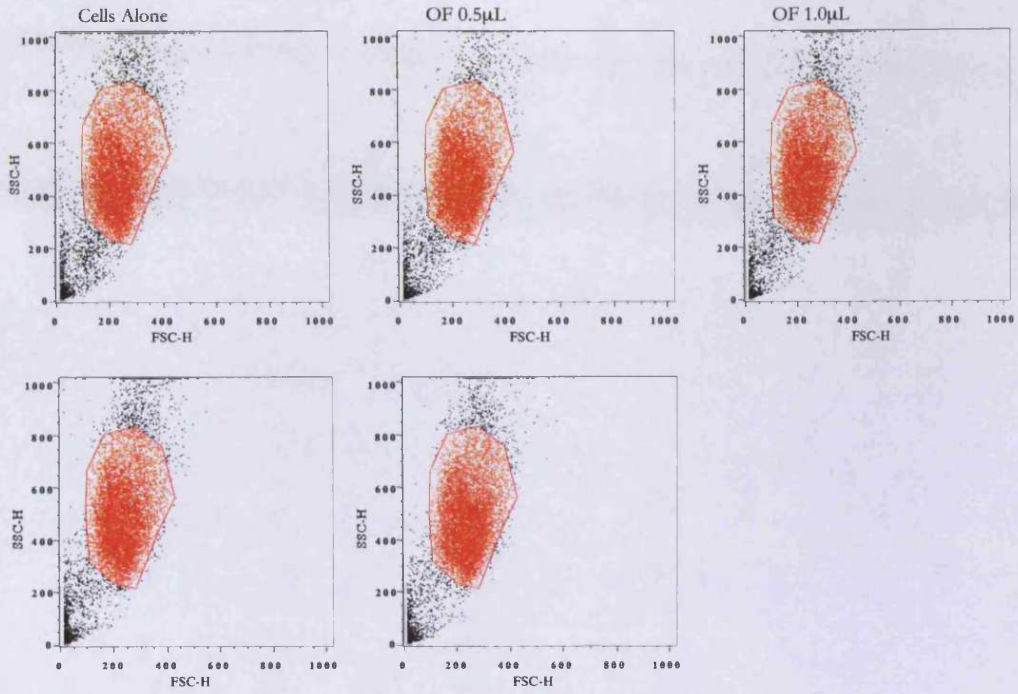

B)

Amount OF (µL)	Mean Gated Cells (%)	SD Gated Cells (%)
0	81.4	2.4
0.5	81.3	1.2
1.0	82.5	1.0
1.5	84.4	0.3
2.0	81.8	1.8

C)

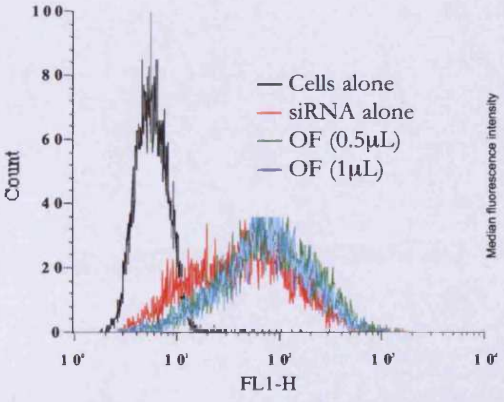

D)

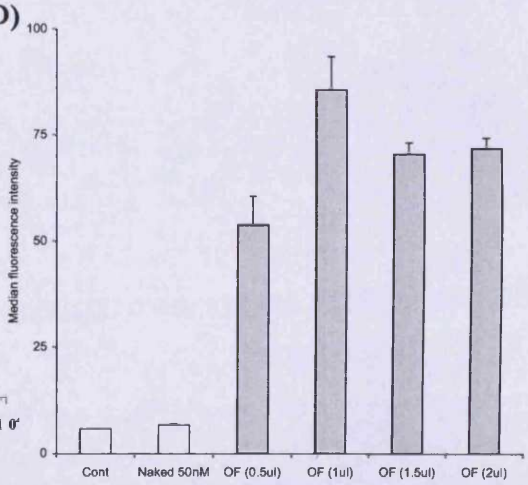

Figure 5.5: Optimisation of Oligofectamine volume using FACs analysis of A431 cells transfected with fluorescently labelled siRNA complexed with Oligofectamine. **A)** Dot plots produced from FACs data Forward Scatter (FSC) plotted against Side Scatter (SSC). The gated region was selected for the majority of cells of the population of untreated cells. There was little change in the number of cells in the gated region with increasing quantities of Oligofectamine. **B)** Tabulates the data represented in the previous figure with means (n=3). **C)** A histogram for the cell associated fluorescent of increasing amounts of Oligofectamine complexed with 100nM fluorescent siRNA. **D)** Bar Chart representation of the previous figure, where 1µL is optimal. Error bars correspond to 1 standard deviation.

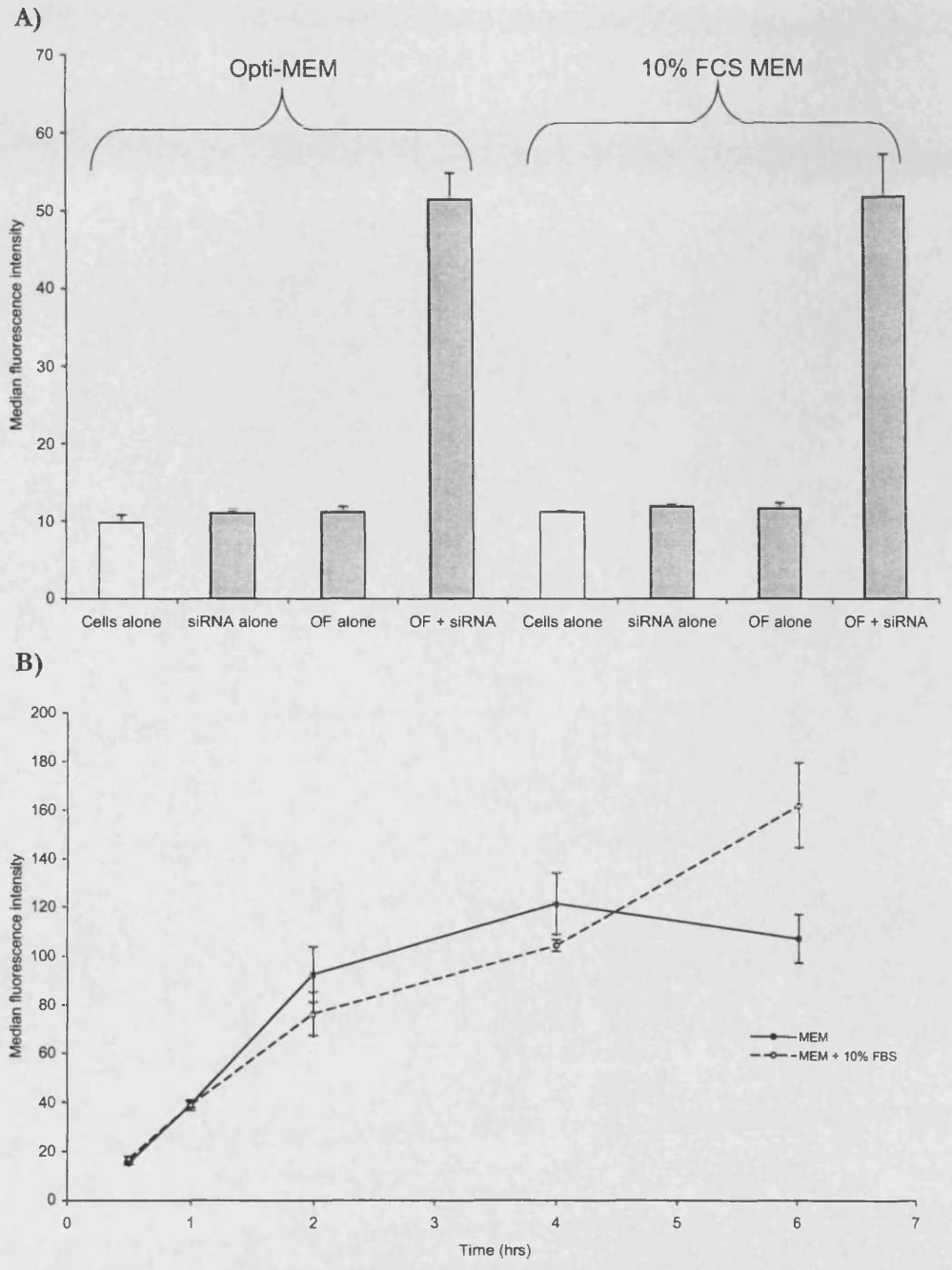

Figure 5.6: Determination of transfection media composition using FACs analysis of A431 cells transfected with fluorescently labelled siRNA complexed with Oligofectamine. **A)** Oligofectamine and fluorescent siRNA was complexed and transfected in Opti-MEM or ordinary MEM (Minimal Essential Media). There was little difference in the amounts of cell associated fluorescence with the two different transfection media so the cheaper MEM was chosen for all transfections **B)** MEM with serum was compared with serum-free MEM for a time course study with transfections up to the manufacturers recommended maximum tranfection time of 6 hours. Since the transfection time was selected previously as 4 hours (Figure 5.2), serum-free MEM was selected as the transfection media since it gave slightly higher cellular association and also negated possible biological stability issues. Error bars correspond to 1 standard deviation.

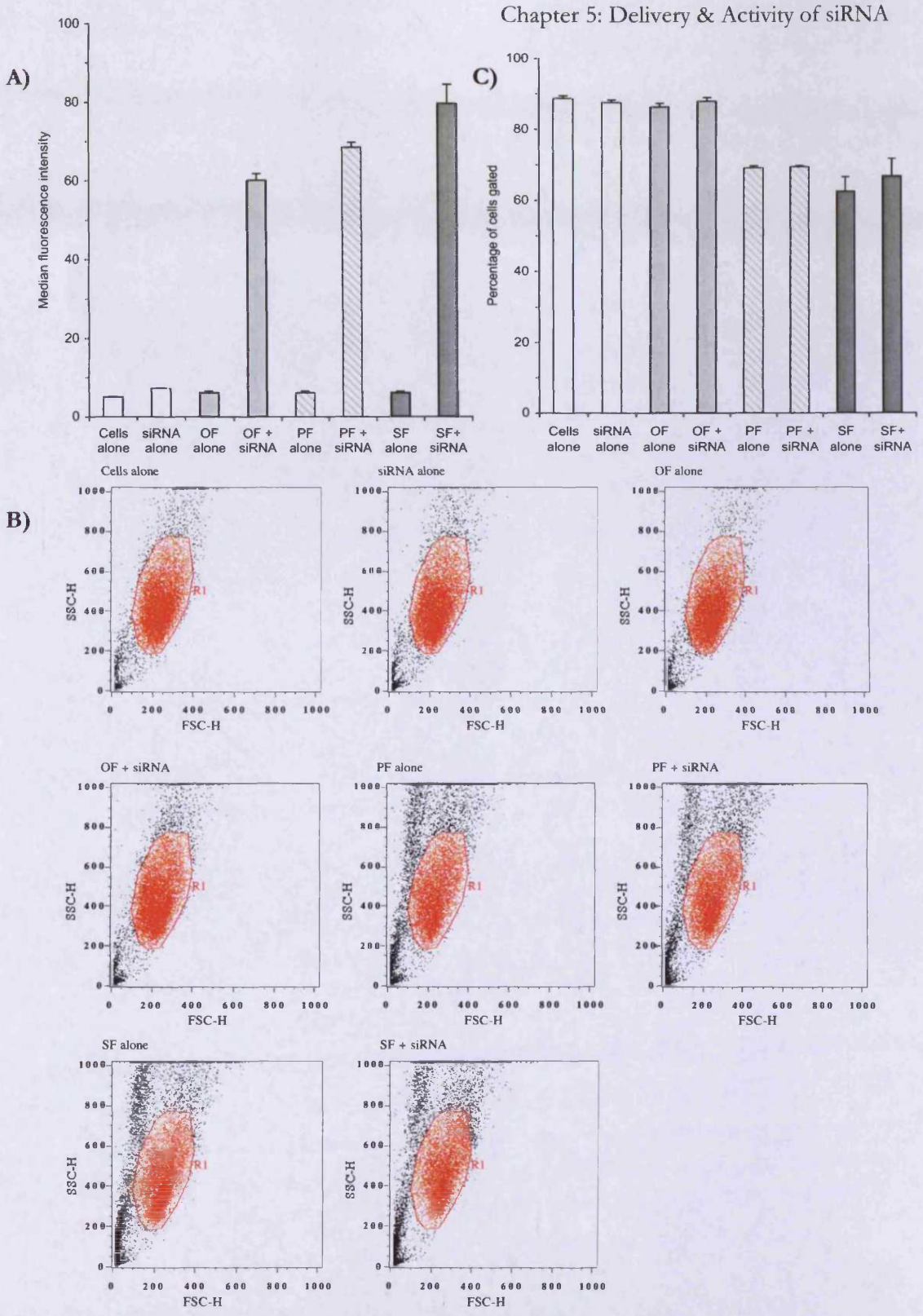

Figure 5.7: Investigation of optimised delivery systems using FACs analysis of A431 cells transfected with fluorescently labelled siRNA complexed with Oligofectamine or Polyfect or Superfect. **A)** Oligofectamine (OF), Polyfect (PF) and Superfect (SF) provide good cellular association **B)** A population of A431 cells were gated that showed similar side-scatter (FSC) and forward–scatter profiles (SSC). **C)** The number of gated cells for each treatment was represented as a bar chart. Error bars correspond to 1 standard deviation.

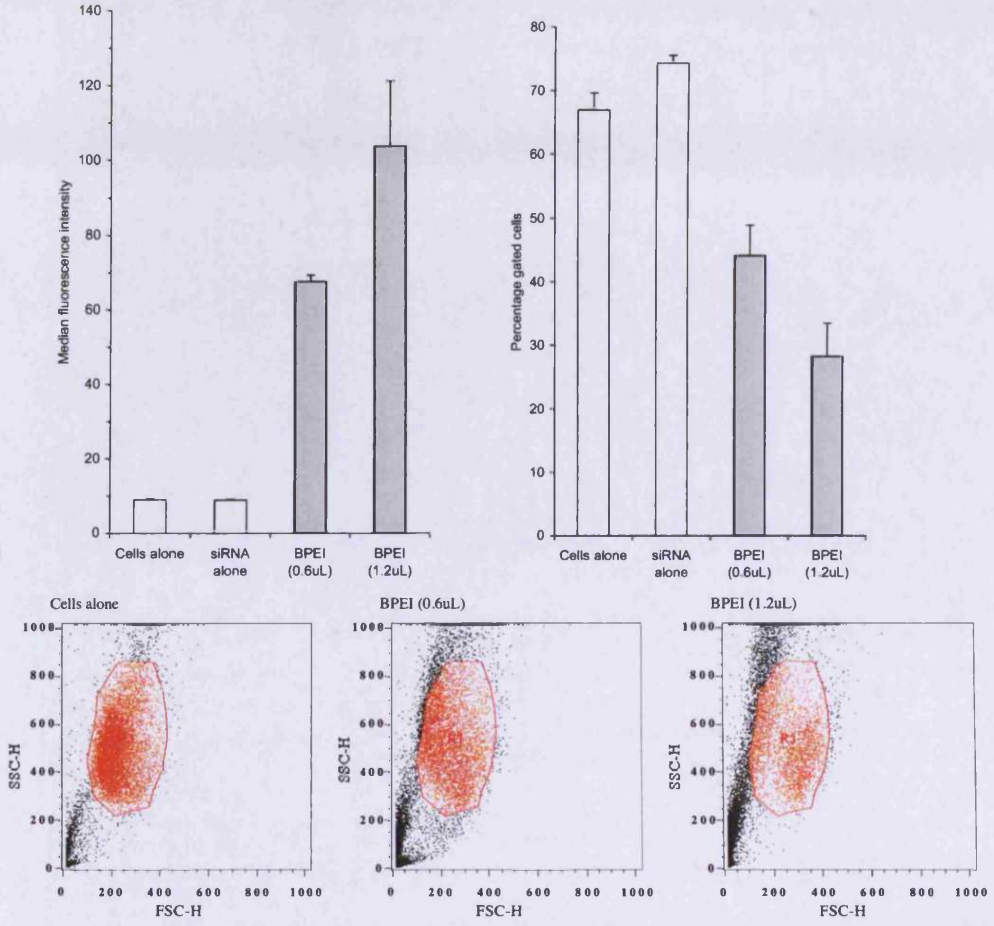

Figure 5.8: Investigation of a BPEI dendrimer delivery system using FACs analysis of A431 cells transfected with fluorescently labelled siRNA complexed with the dendrimer branched Polyethylene imine (BPEI). Error bars correspond to 1 standard deviation.

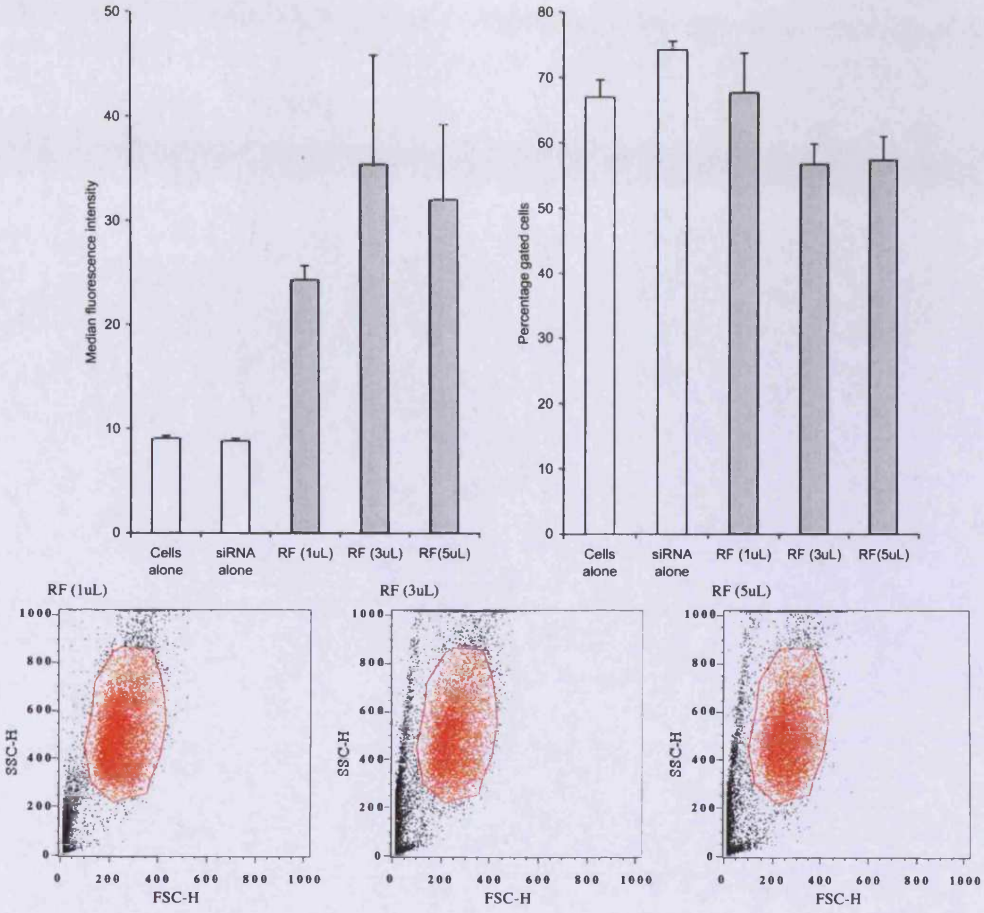

Figure 5.9: Investigation of RNAiFect a proprietary lipid delivery system using FACs analysis of A431 cells transfected with fluorescently labelled siRNA complexed with the RNAifect. Error bars correspond to 1 standard deviation.

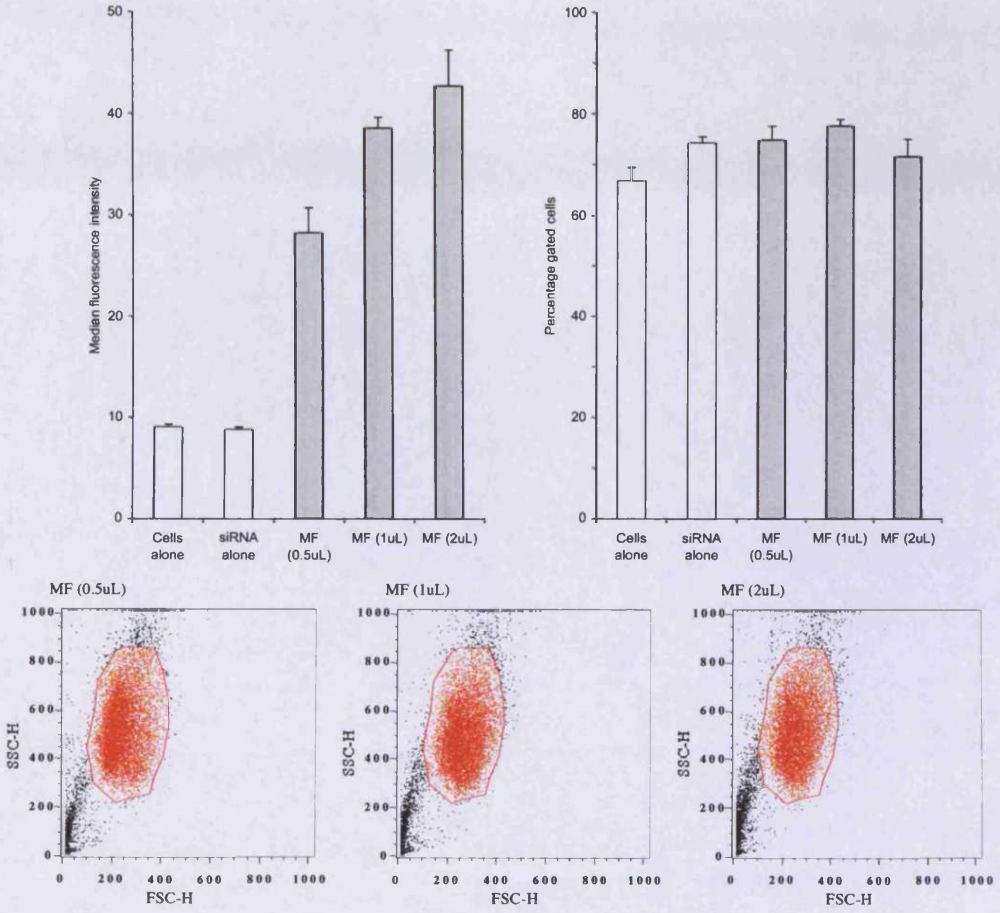

Figure 5.10: Investigation of Metafectene a proprietary lipid delivery system using FACs analysis of A431 cells transfected with fluorescently labelled siRNA complexed with the Metafectene. Error bars correspond to 1 standard deviation.

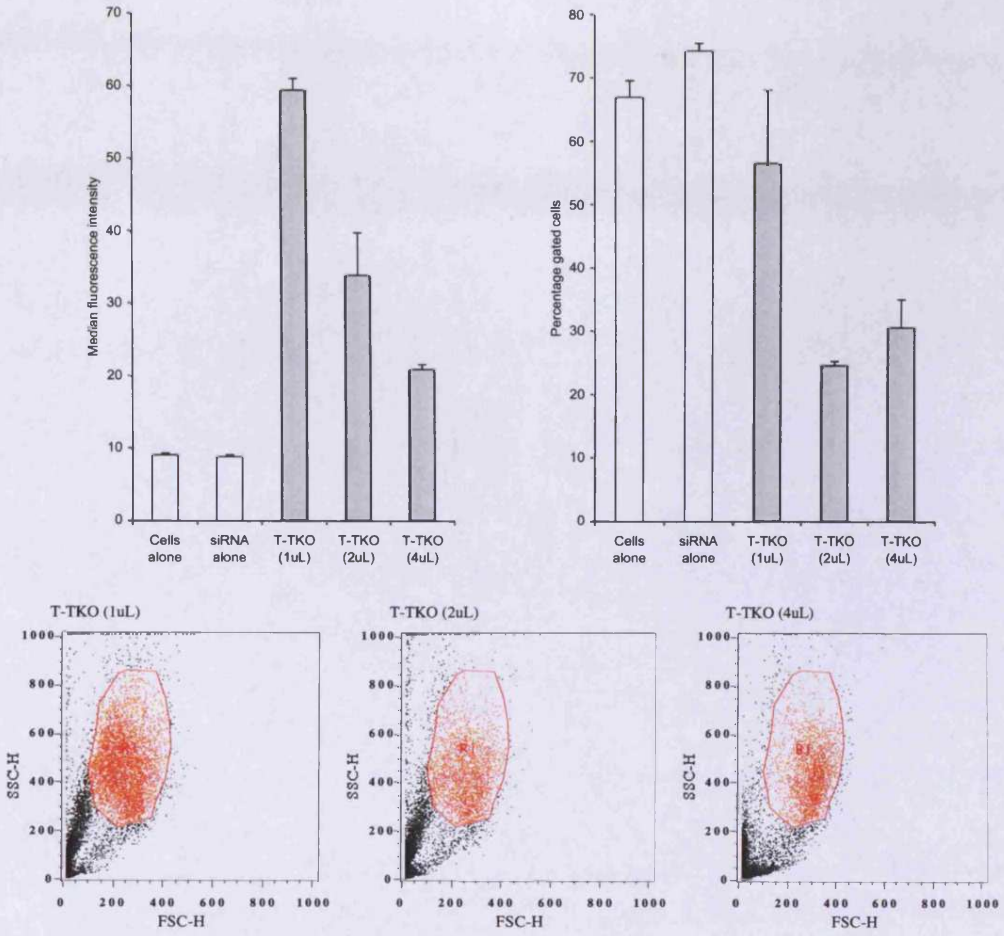

Figure 5.11: Investigation of Transit-TKO a proprietary lipid delivery system using FACs analysis of A431 cells transfected with fluorescently labelled siRNA complexed with the Transit-TKO. Error bars correspond to 1 standard deviation.

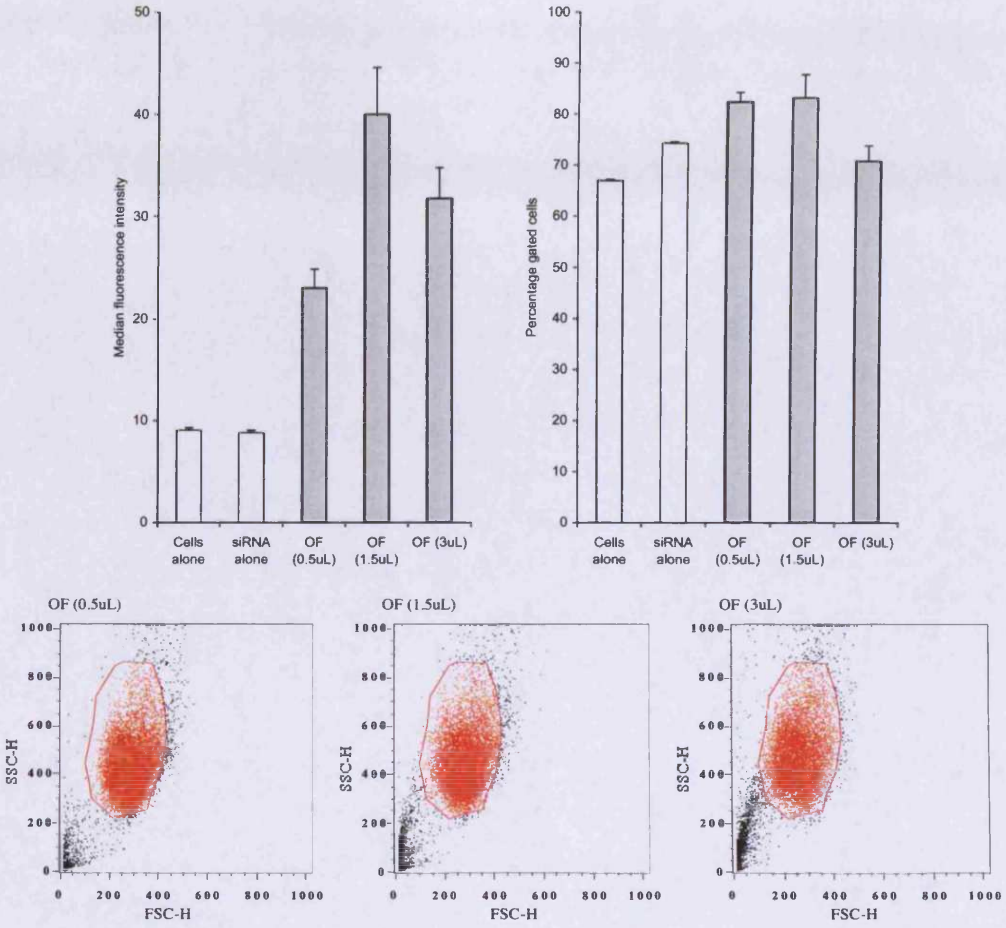

Figure 5.12: Further investigation of Oligofectamine a proprietary lipid delivery system using FACs analysis of A431 cells transfected with fluorescently labelled siRNA complexed with the Oligofectamine. Error bars correspond to 1 standard deviation.

Table 5.1: A semi-quantitative scoring system to summarise the delivery systems data shown in Figures 5.7 to 5.12

Delivery system	Proprietary name	Maximum median cell-associated fluorescence	Minimum percentage gated cells
Lipid	Oligofectamine	***	*****
	RNAifect	**	***
	Metafectene	**	****
	Transit-TKO	***	*
Dendrimer	Superfect	****	****
	Polyfect	****	****
Polymer	BPEI	*****	*

Following these studies, work was planned to investigate the effect of anti-EGFR siRNA-Oligofectamine complexes on the activity of A431 cells. This siRNA would knockdown EGFR leading to reduced growth factor signalling and thus preventing cell growth. Although preliminary results appeared promising that siRNA targeting EGFR inhibited the growth of A431 cells, this inhibition of growth was not reproducible. These abnormal effects were seen over a 12-month period and the thoughts and possible solutions to the problem centred around:

(i) FACs analysis showed a loss in cell fluorescence associated with labelled siRNA-Oligofectamine complexes (Figure 5.13A). The median fluorescence intensities were reduced from about 40-50 arbitrary units (Figure 5.12) to 12 units (Figure 5.13A). This loss of transfection efficiency was not seen with another delivery system, RNAifect (Figure 5.13B). At the time, it was thought that the new batch of Oligofectamine was faulty. A personal communication with the manufacturer seemed to confirm this, as there was a recent formulation change in Oligofectamine to enable air transportation.

(ii) As the A431 cells were subcultured there was subsequent loss in cell fluorescence associated with labelled siRNA-Oligofectamine complexes (Figure 5.14). This loss of transfection efficiency with Oligofectamine was also observed in two other cell lines A549 (Figure 5.15A) and ECV-304 (Figure 5.15B). At this time, it was thought that subculturing of A431 cells had an unexpected effect on the transfection efficiency of Oligofectamine.

(iii) The FACs machine was also suspected of causing the unusual effects. So an additional radiolabelled cell association assay (Section 2.3.7) was developed that utilised the radiolabelled siRNA used in the Biological Stability of siRNA chapter (Section 2.1.1.). The radiolabelled siRNA was PAGE purified as in Section 2.1.3. (Figure 5.16). There was an increase observed in cellular radioactivity associated with radiolabelled siRNA complexed with the branched polymer, polyethyleneimine (BPEI; Figure 5.17A). Again, this observed increase in siRNA delivery was not reproducible, as BPEI failed along with other delivery systems to provide adequate cellular association (Figure 5.17B). Since the unusual FACs results were also seen with the radiolabelled siRNA cellular association assay, it is unlikely that the FACs assay was wholly responsible.

(iv) Microscopy also revealed unusual cellular effects, the cells often had irregular growth patterns and required larger transfection volumes to avoid post-transfection cell death. The cells often detached from the surface of the centre and edges of 24-well plates. The media on top of cells in culture flasks discoloured quickly and 24-well plates showed an edging effect of discoloured media. These cellular effects were attributed to poor cell culture techniques or a contaminated batch of culture plastics.

These abnormal effects were seen over a 12-month period and not until some A431 cells from my laboratory were sent to an external laboratory, for reasons not relating to my work, did they test positive for a mycoplasma infection. Subsequent PCR-based mycoplasma tests were performed on my cell cultures showed them to be positive for mycoplasma infection (Figure 5.18A)

Mycoplasma are common contaminants of cell lines with up to 30% of cell cultures being infected (Uphoff and Drexler, 2002). The source of Mycoplasmal infections are usually from: bovine serum (*Mycoplasma arginini*, *M. hyorhinis*, *Acholeplasma laidlawii*), cell culture operators (*M. Orale*, *M. fermentans*) or from other contaminated cultures introduced from other laboratories (*M. hyorhinis*; Garner et al., 2000). Cell lines do not necessarily show obvious signs of infection since many mycoplasma species grow extremely slowly, and contamination can remain undetected for months (Rottem and Barile, 1993). Mycoplasma rapidly metabolise simple sugars to acidic products causing a shift in pH and this may be seen as a rapid colour change of the media (to yellow), this was observed in my cell lines and this media colour change is often regarded as the only noticeable effect of mycoplasma infection (Butler and Leach, 1964). The pH shift caused by the production of acidic metabolites can cause the monolayer to detach from the culture vessels (Rottem and Barile, 1993), this could explain some of the other effects seen by microscopy. These authors (Rottem and Barile, 1993) also state that the results produced from infected cells are unreliable and could be false.

Mycoplasma infection can also considerably reduce the potency of transfection reagents; these low transfection efficiencies may go undetected for some time due to the presence of these antibiotic resistant organisms (Xia et al., 1997). Mycoplasma infections also have an effect on the cell membrane; mycoplasma attachment to the

host membrane can disrupt its integrity making it 'leaky' (Rottem and Barile, 1993). This may explain the differential effects seen with RNAifect and Oligofectamine (Figures 5.13 and 5.15), especially since RNAifect is thought to punch holes in the cell membrane (from a personal communication with Bettina Haedrich from Qiagen).

All the cell lines that have tested positive including frozen stocks were disposed of along with any other possibly contaminated cell culture reagents. The cell culture facilities underwent a thorough decontamination and new cell lines were purchased. Stricter cell culture protocols have been drafted, with regular testing for mycoplasma, showed no signs of infection (Figures 5.18B).

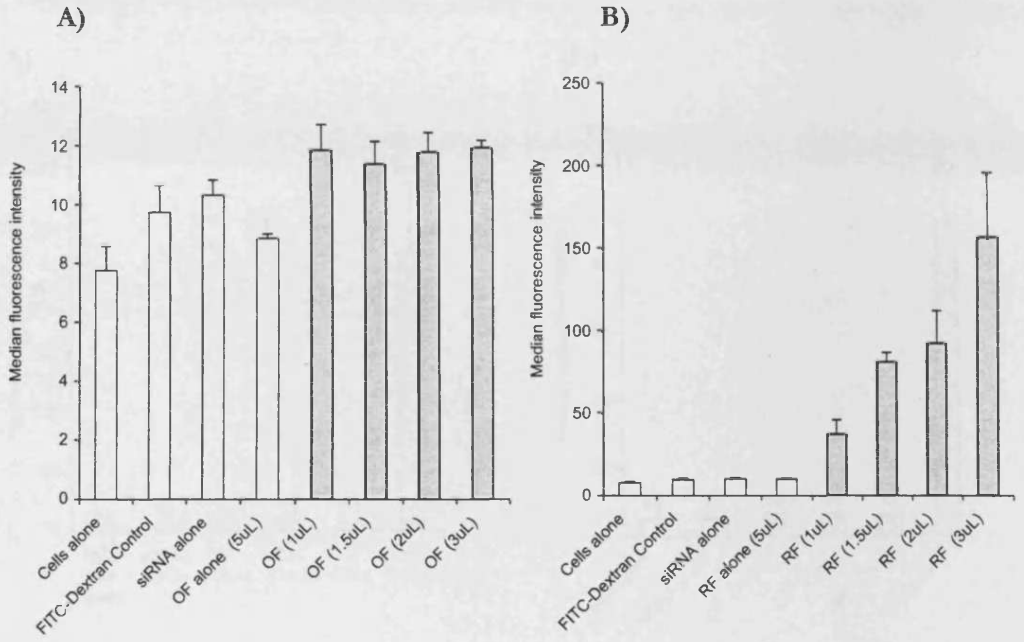

Figure 5.13: Loss of transfection efficiency with Oligofectamine but not with RNAifect proprietary lipid delivery systems measured using FACs analysis of A431 cells transfected with fluorescently labelled siRNA complexed with the Oligofectamine/RNAifect. **A)** Bar chart produced from median fluorescent from FACs data for A431 cells transfected with Oligofectamine or RNAifect and fluorescent siRNA. A reduction in A431 cell associated was seen with Oligofectamine (OF) delivered fluorescent siRNA **B)** RNAifect delivered siRNA was still able to provide good cell associated fluorescence

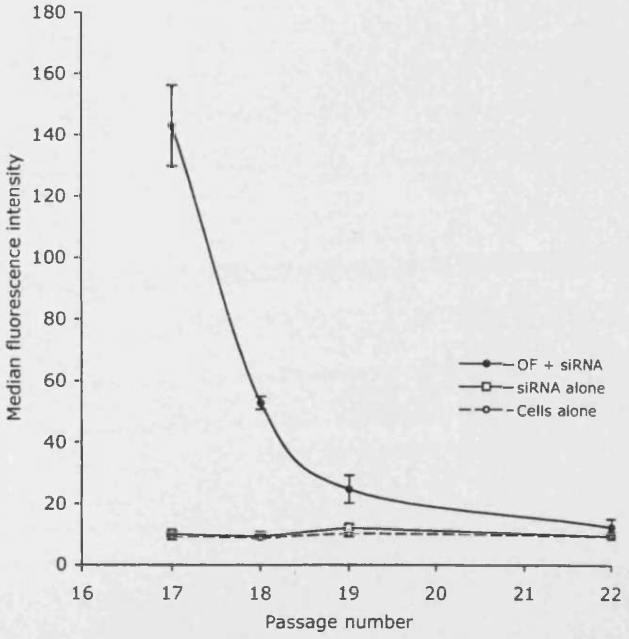

Figure 5.14: Loss of transfection efficiency with passage number measured using FACs analysis cells were transfected with fluorescently labelled siRNA complexed with the Oligofectamine. Error bars are standard deviations of results in triplicate.

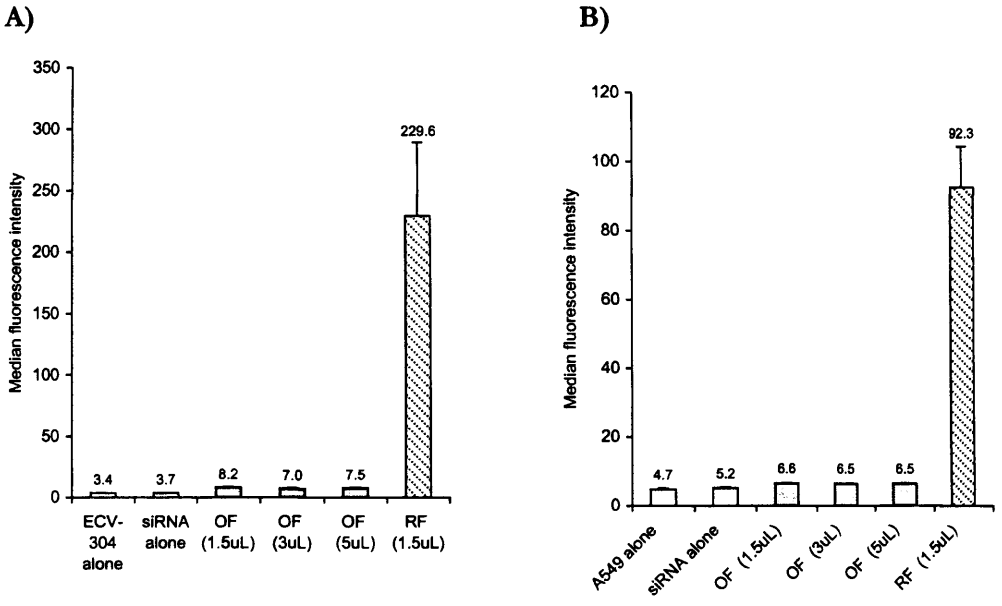

Figure 5.15: Loss of transfection efficiency with Oligofectamine in A549 and ECV-304 cells using FACs analysis of cells transfected with fluorescently labelled siRNA complexed with the Oligofectamine. In both cells lines A549 **(A)** and ECV-304 **(B)** fluorescent siRNA delivered with Oligofectamine (OF) results in relatively poor cell association but good association with RNAifect (RF).

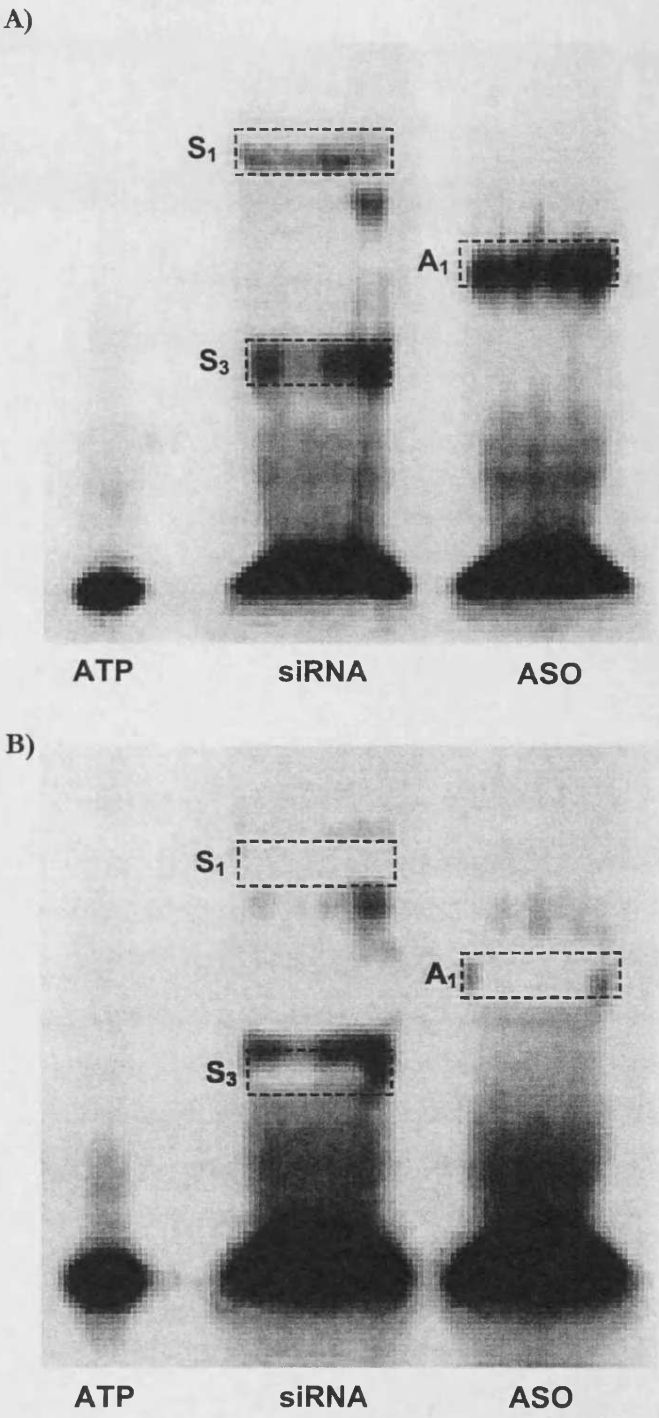

Figure 5.16: PAGE purification of both radiolabelled siRNA and ASO. Radiolabelled ASO and siRNA was run on a 20% PAGE gel with the free ^{32}P-ATP label. **A)** The radioactive oilgonucleotides were imaged using a phosphor screen and phosphorimager. Highlighted are the regions corresponding to labelled siRNA (S_1 and S_2) and ASO (A_1). **B)** These bands were then excised and the labelled oligonucleotides recovered, the gel was the re-exposed to the phosphor screen to ensure correct band removal. The S_1 band was excised and the extracted radiolabelled siRNA were used for the radiolabelled siRNA cell association assay (Figure 5.17)

A)

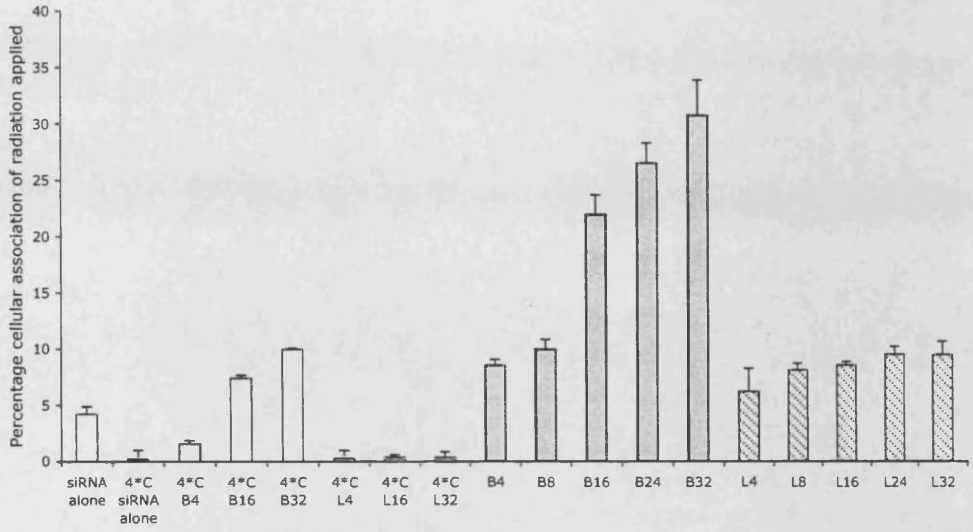

B)

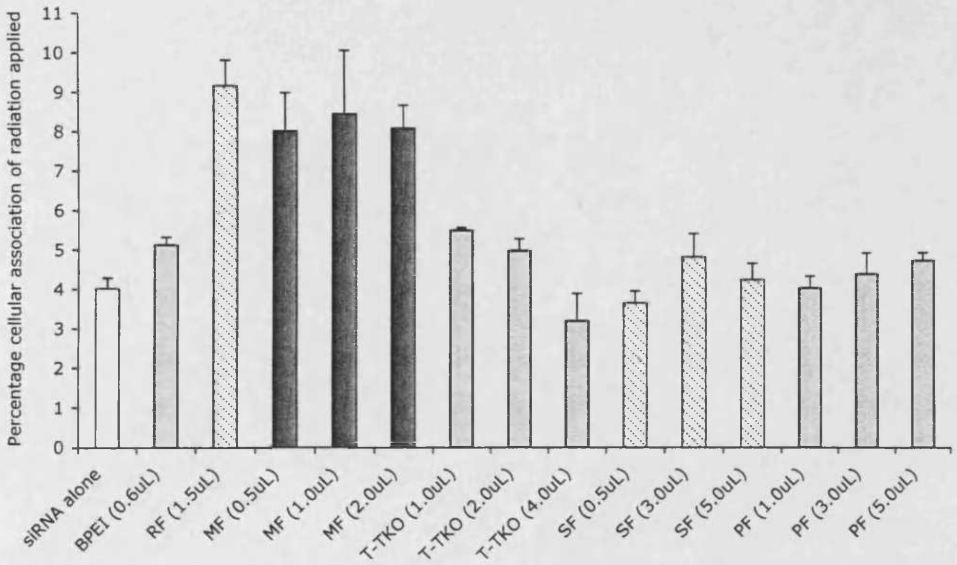

Figure 5.17: A431 cellular association of radiolabelled siRNA complexed with different delivery systems **A)** Radiolabelled siRNA was produced and complexed with branched (BPEI) and linear (LPEI) Polyethylene imine both had an approximate molecular weight of 25,000 Daltons and were made up in a solution pH 7.4 to 1mg/mL. BPEI was used in Nitrogen (PEI) to Phosphate (siRNA) ratios of 4:1 (B4) to 32:1 (B32). LPEI also was used in similar ratios but the notations were given the prefix L4 to L32. Radiolabelled siRNA was complexed with the PEI and placed on A431 cells. After the transfection period cells were washed 3 times with PBS and the cells were lysed using lysis buffer. The cell lysates were transferred to liquid scintillation vials and scintillant was added and the emitted radiation was counted. **B)** A range of previously tested delivery systems were then analysed by this method: RNAifect (RF) Metafectene (MF), Transit-TKO (T-TKO) Superfect (SF) and Polyfect (PF).

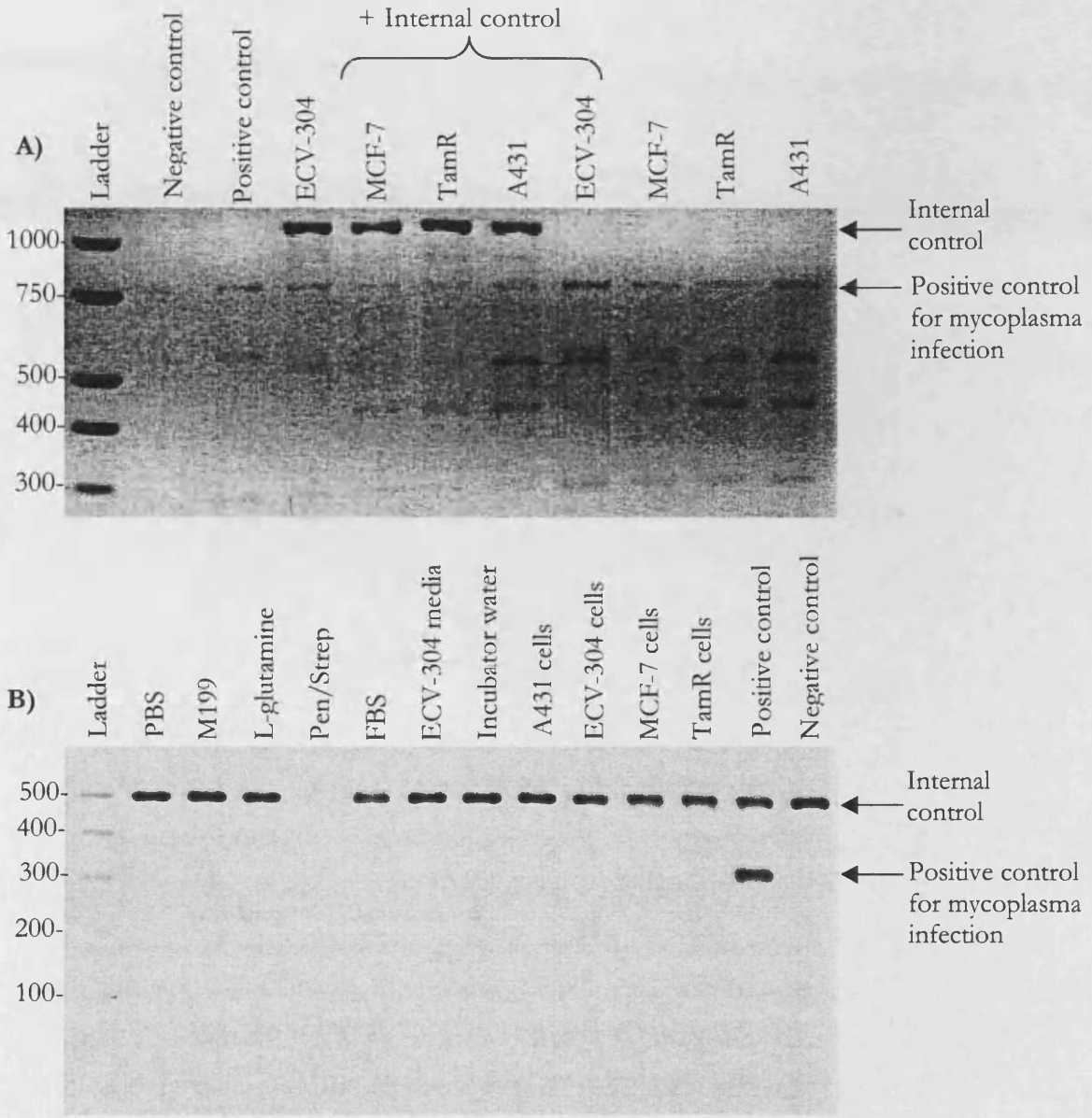

Figure 5.18: Detection, identification and eradication of a mycoplasma infection using a PCR-based mycoplasma detection kit. **A)** A mycoplasma test PCR test was performed and all the laboratory cell lines were found to be positive although the exact strain of the infection was not identified. **B)** Following new stricter cell culture procedures, the cells were along with other culture reagents were tested and found to be negative of mycoplasma.

Further FACs studies were performed in new mycoplasma-free A431 cells. The cells were confirmed to be clear of mycoplasma and the transfection efficiencies returned to those levels previously observed with successful transfections. Different doses of siRNA are required to be delivered to produce activity dose-response relationships. 1.5μL of Oligofectamine provided the optimal delivery over the three siRNA concentrations tested (25, 50 and 100nM; Figure 5.19A). A dose range of 1 to 500nM of siRNA was explored with fixed volume of Oligofectamine (1.5μL) and was able to provide significant increases in siRNA delivery up to the maximum tested, 500nM (Figure 5.19B and 5.19C). The ratio of Oligofectamine to siRNA did not seem to be pertinent to the delivery of siRNA and a fixed volume of Oligofectamine (1.5μL) was used for activity dose-response experiments.

The delivery of co-operatively acting ASO and siRNA (previously mentioned as a discussion point in Chapter 4, Section 4.3.4) was investigated by FACs analysis using oligonucleotides labelled with different fluorophores. When delivered to A431 cells separately either of the fluorescently labelled oligonucleotides (green ASO and red siRNA) could be clearly identified in their respective FL-1 or FL-2 channels; exemplified by the fluorescent plots in Figure 5.20. Examination of the fluorescence plots for the co-delivery of ASO and siRNA revealed that the A431 populations interact with both the ASO and siRNA complexes (Figure 5.20). This dual label FACs assay demonstrated its potential ability in the optimisation of the delivery co-operative acting oligonucleotides.

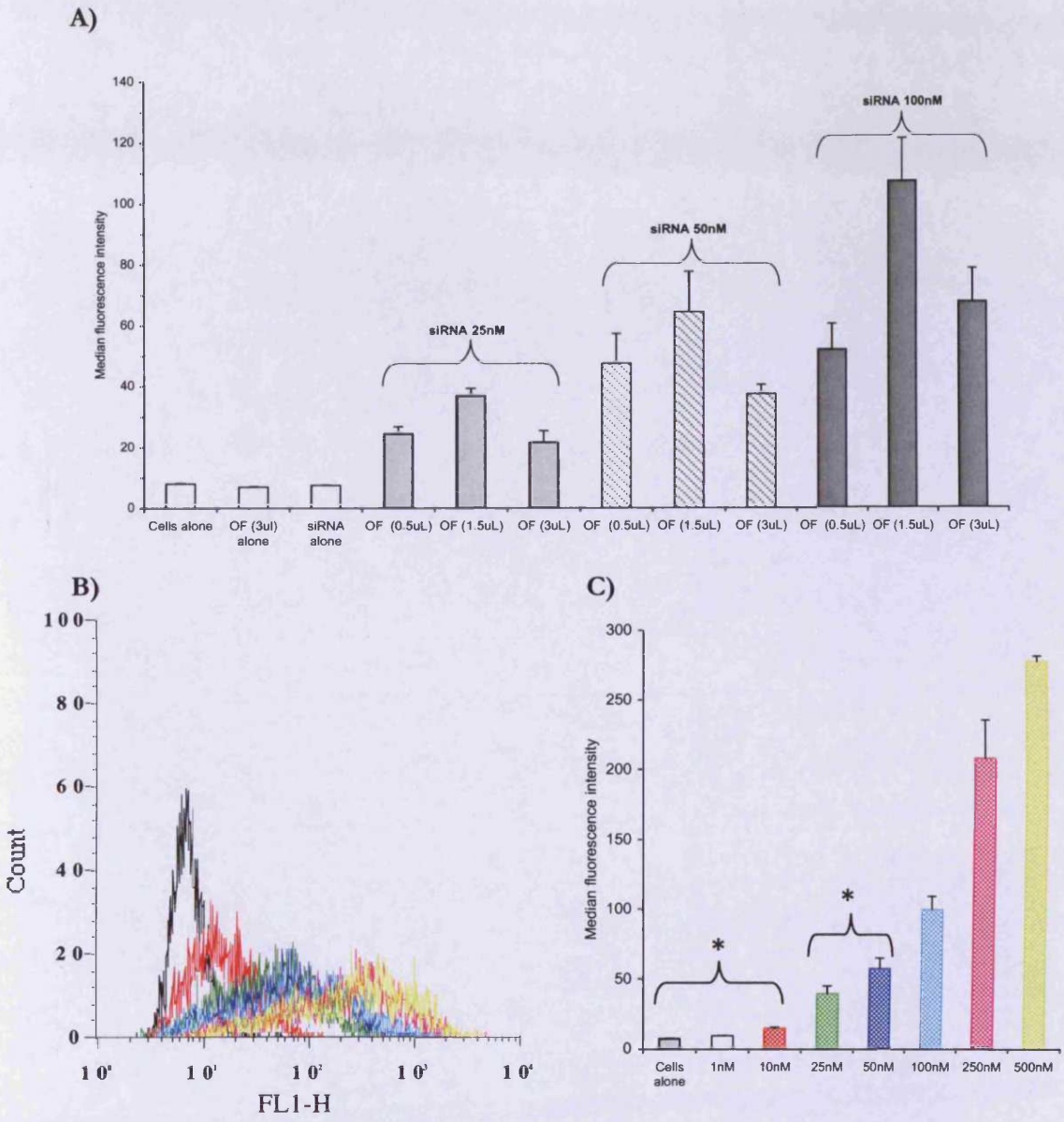

Figure 5.19: Optimisation of different doses of siRNA measured using FACs analysis cells were transfected with fluorescently labelled siRNA complexed with the Oligofectamine. **A)** Bar chart showing median fluorescent intensities for a range of siRNA doses and amounts of Oligofectamine. 1.5µL of Oligofectamine provided the optimal amount of cell-associated fluorescent for 25nM, 50nM and 100nM of fluorescent siRNA. **B)** FACs histograms of FL-1 versus frequency for increasing doses of fluorescent siRNA with a fixed amount, 1.5µL, of Oligofectamine (OF), note 1nM siRNA histogram was removed for clarity. **C)** Bar chart produced from the previous figure; median fluorescence intensities were plotted for increasing amounts of fluorescent siRNA with a fixed amount of Oligofectamine. 1.5µL of Oligofectamine was sufficient to produce increasing amounts of cell-associated fluorescent for the increasing dose of fluorescent siRNA. * Not significantly different ($p<0.05$) from each other, all other values are statistically different from each other. Statistics One-way ANOVA with Duncans *Post hoc* test. Results mean ± s.d. (n=3).

A)

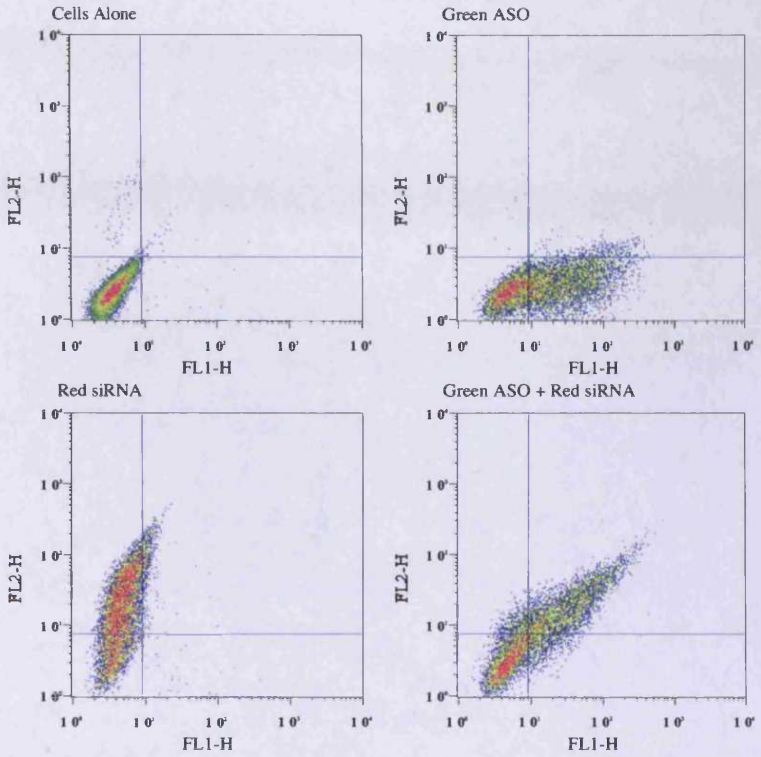

B)

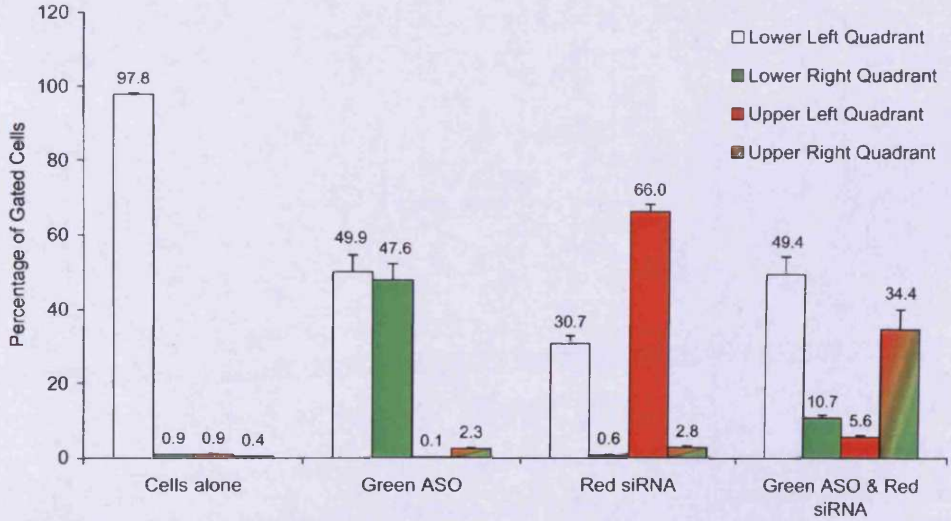

Figure 5.20: The cell-associated fluorescence of co-delivered green ASO and red siRNA. **A)** Dot plots of the FL-1 versus FL-2 channels for the different treatment of ASO and siRNA. Green ASO caused a shift in the green channel (FL-1), while red siRNA caused a shift in the red channel (FL-2), and mixture of the two resulted in a shift in both directions (FL-1 and FL-2) **B)** Bar chart representation of part A, the figure were split into quadrants and the percentages of cell in each quadrant were shown for each of the treatments.

5.3.2 Delivery of siRNA to TamR cells

Preliminary investigations were performed for the delivery of siRNA to a derived tamoxifen-resistant strain of MCF-7 cells (TamR). These experiments were conducted after the detection and eradiation of the mycoplasma infection. The purpose of these experiments was to optimise the delivery of siRNA-oligofectamine complexes to a second cell line that could substantiate the A431 results.

This preliminary data showed siRNA Oligofectamine complexes provided satisfactory cell fluorescence associated with labelled siRNA with minimal cell damage (Figure 5.21).

Note that the Tenovus research group previously optimised TamR Dharmafect-siRNA delivery and I followed their transfection protocols for the TamR transfections.

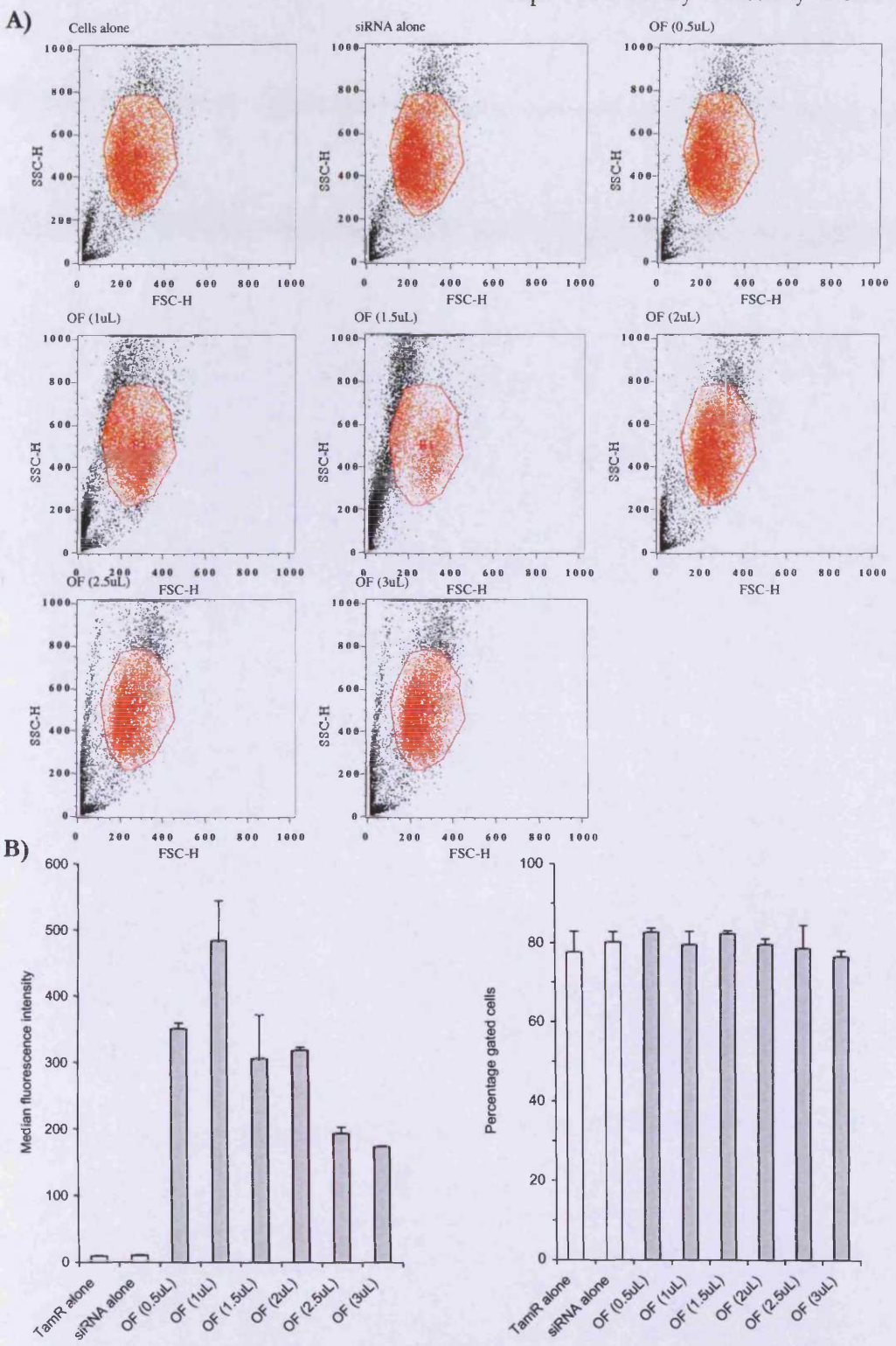

Figure 5.21: Investigation of TamR cells using FACs analysis transfected with fluorescently labelled siRNA complexed with Oligofectamine. **A)** Dot plots of side-scatter (SSC) versus forward scatter (FSC) for TamR cells treated with fluorescent siRNA and increasing amounts of Oligofectamine (OF). **B)** Bar chart representations of median fluorescence intensity and percentage of gated cells for TamR cells treated with Oligofectamine.

5.4 siRNA Activity Results & Discussion

5.4.1 Activity of siRNA in A431 cells

The A431 proliferation assay was followed on from previously published work (Beale et al., 2003, Petch et al., 2003). Petch and co-workers transfected cells in serum-free media for 48 hours however in my work the growth of cells was poor in serum-free media (Figure 5.22). Therefore it was decided to replace the serum-free transfection media with serum-containing media after the transfection. Growth curves for A431 cells were performed at different seeded densities. The optimal seeding density for growth was at 50,000 cells per 24-well in 10% serum-containing media (Figure 5.22).

The transfection of HAR-1 siRNA-Oligofectamine complexes failed to produce a significant effect on A431 proliferation (Figure 5.23). Nagy and co-workers (Nagy et al., 2003) investigated the inhibition of A431 growth using anti-EGFR siRNA-Oligofectamine complexes. The Nagy and co-workers' siRNA was designed to target a region of EGFR mRNA that actually appears on Array 1 used in my work (Figure 4.10). The target sequence for the Nagy and co-workers' siRNA overlies region AS1 (a 21mer mRNA target sequence: 5'-CUC UGG AGG AAA AGA AAG UUU-3'). This siRNA reduced A431 cell growth by around 80% while a non-EGFR-targeting siRNA caused an approximately 30% reduction in cell growth. Again in the Nagy and co-workers studies their cells were transfected according to the Oligofectamine manufacturer's instructions then serum-starved 12-hours after transfection for 24-hours, then placed in 10% serum-containing media for 48-hours before being counted by Coulter-counter. This transfection protocol could be used to elicit knockdown in A431 in my work but I feel the serum starvation does not reflect the physiological environment and could well have cytotoxic effects. In addition, A431 cells have a unique concentration-dependent epidermal growth factor (EGF) effect; 0.1ng/mL of EGF promotes cell growth but 1ng/mL induces cell cycle arrest (Cao et al., 2000).

A small molecule inhibitor of EGFR was thought to provide a good positive control for use in my A431 growth assays. AG1478 is highly potent and selective small molecule inhibitor of the EGFR receptor (Levitzki and Gazit, 1995). 48 hours after treatment, AG1478 inhibited A431 cell growth by 40% compared with untreated control in 10% (Figure 5.24). Dowlati and co-workers (Dowlati et al., 2004) reported that AG1478 alone did not completely inhibit A431 growth (36% after 72 hours) due

to activation of other pathways downstream of EGFR. They showed that complete block of proliferation was only possible with AG1478 and a specific inhibitor of Stat-3, AG490. This reported incomplete A431 growth inhibition is in contrast to other published data that report 80% reductions in A431 growth with anti-EGFR siRNA (Beale et al., 2003; Nagy et al., 2003). In my work I did not observe an 80% inhibition in A431 growth with anti-EGFR siRNA or with a small molecule inhibitor of EGFR (AG1478).

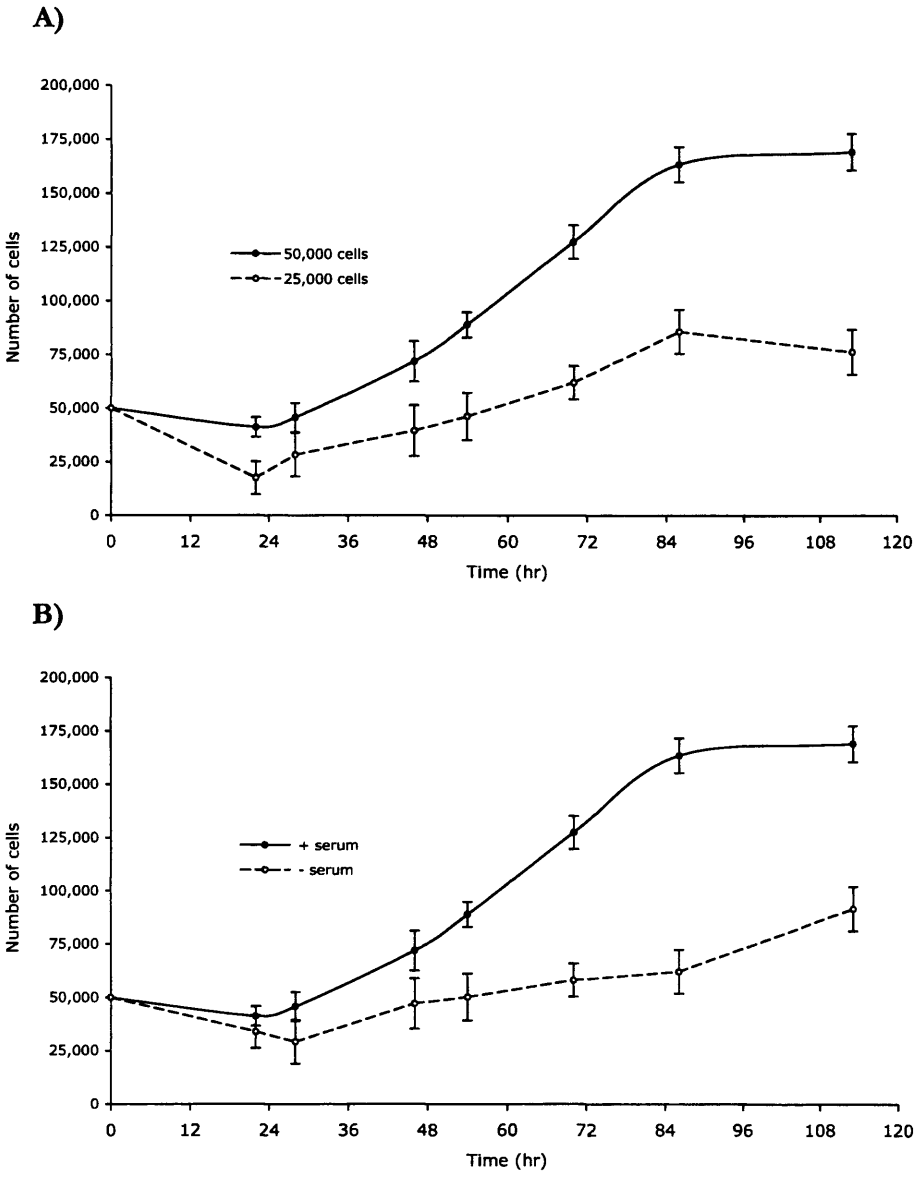

Figure 5.22: Growth of A431 cells at different seeding densities with and without serum, cells were counted using a haemocytometer. **A)** A431 cells were seeded at 25,000 and 50,000 cells per well and allowed to grow for 5 days in serum-containing media. **B)** A431 cells were grown in the presence and absence of serum.

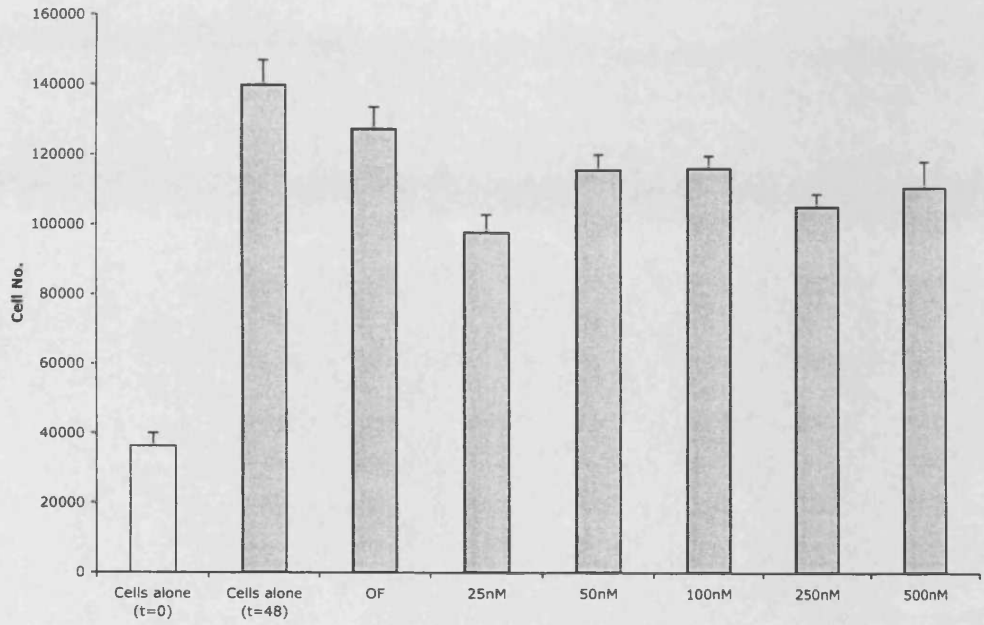

Figure 5.23: Proliferation assay of A431 cells transfected with HAR-1 siRNA. siRNA was complexed with Oligofectamine (OF) and transfected 24 hours after seeded. Cells were then counted with a haemocytometer 48 hours after transfection.

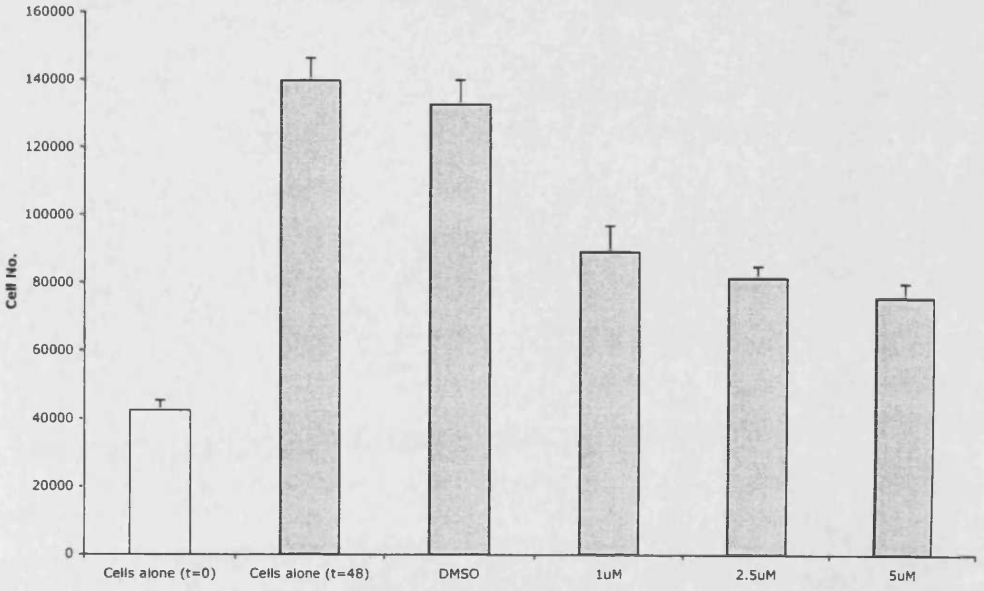

Figure 5.24: Proliferation assay A431 cells inhibited by AG1478. The small molecule inhibitor of EGFR was dissolved in 0.1% dimethyl sulfoxide (DMSO) then added to serum-containing media 24 hours after seeding (t=0), cells were then counted with a haemocytometer 48 hours later (t=48). The concentrations of AG1478 are given in micromolar.

A431 cells did not adequately show differential growth effects for the HAR-1 siRNA, so a Western blot technique was developed to provide a better functional assay. A431 cells were seeded and grown for 24-hours before being transfected with the siRNA designed in Chapter 4. The transfection media was replaced with serum-containing media and cells were left for 48 hours before being lysed. The siRNAs were tested over a concentration range (10, 25 and 50nM) and some of those tested seem to provide dose dependent knockdown of EGFR, such as HAR-1 (Figure 5.25). The Western blot assay was not a quantitative technique and it was difficult to detect differences in the expression levels of EGFR protein. Nagy and co-workers (Nagy et al., 2003) reported a 70% knockdown of EGFR protein in A431 cells when measured by a Western blot assay. Nagy and co-workers used a FACs assay to select the subpopulation of cells that were transfected with siRNA. Thus by measuring only transfected cells they reported a 90% knockdown in EGFR protein. They therefore recommend a single-cell measurement technique in cell populations where the fraction of transfected cells is low.

Semi-quantitative RT-PCR can compare the levels of mRNA transcripts in cell lysates and could lead to a more direct assay of siRNA function, since siRNA acts on target mRNA. HAR-1 siRNA (200nM) was unable to completely knockdown the EGFR mRNA (Figure 5.26).

As discussed above, Western blot and RT-PCR are techniques that assimilate the subpopulation of untransfected cells (that show no knockdown of the target) into the general cell population and hence reduce the overall observed knockdown. Fluorescent microscopy with a fluorescently labelled anti-EGFR antibody could allow the detection of EGFR protein expression on individual A431 cells. This technique could measure the knockdown of EGFR in only siRNA-transfected cells. Unfortunately, the green fluorescent-labelled siRNA could not be observed to be associated with the A431 cells (Figures 5.27D and E). The addition of the non-target fluorescent siRNA resulted in stimulation of EGFR of individual cells that appear brighter (Figures 5.27; D and E). HAR-1 siRNA caused several cells in the field of view to appear darker, this may be the result of successful transfection and knockdown (Figures 5.27; F, G and H). Optimisation and the use of confocal microscopy may lead to superior results.

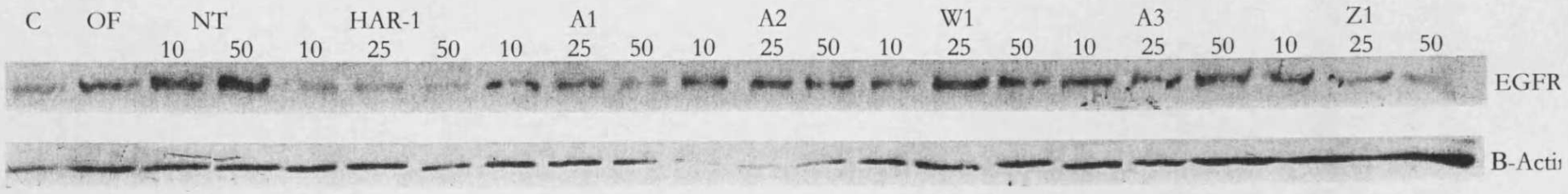

Figure 5.25: Western blot of A431 cells transfected with Oligofectamine and a screen of active siRNA. A431 cells were seeded 24 hours before transfection. Cells were left for 48 hours before being lysed and used in a western blot protocol. Cells alone (C) and Oligofectamine alone (OF) and non-targeted siRNA (NT) were used as controls. HAR-1 siRNA designed on Array 1. Two siRNAs targeted mRNA accessible regions on Array 3 (A1 and A2) and one against a poorly accessible region (W1). Another siRNA targeted an accessible region on Array 4 (A3) and a region that was determined to have a hybridisation intensity or mRNA accessibility that was effectively zero (Z1).

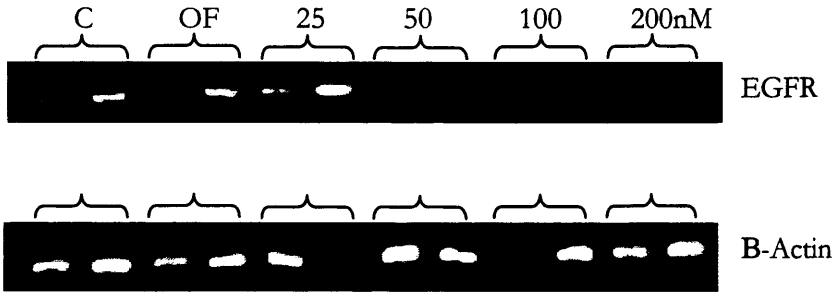

Figure 5.26: RT-PCR of A431 cells transfected with HAR-1 siRNA complexed with Oligofectamine. Cells were seeded 24 hours before transfection, 48 hours later cells were lysed and RNA extracted using a Tri-reagent protocol. Cells alone (C) and Oligofectamine alone (OF) transfection controls were used and 25, 50, 100 and 200 nanomoles of HAR-1 siRNA.

A) Control 1

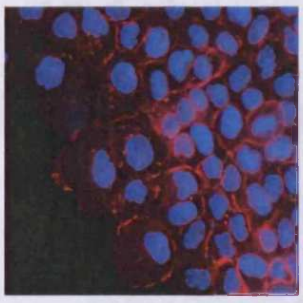

B) Control 2

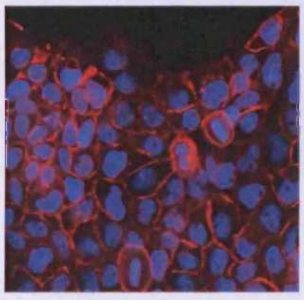

C) Control 3

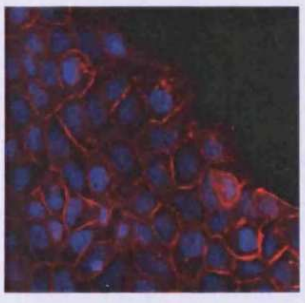

D) Fluorescent siRNA 1

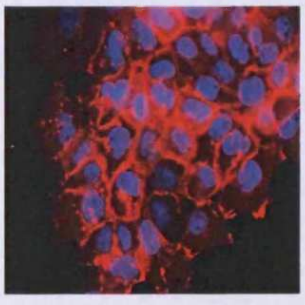

E) Fluorescent siRNA 2

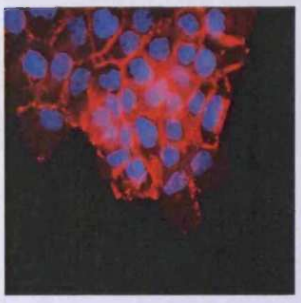

F) HAR-1 siRNA 1

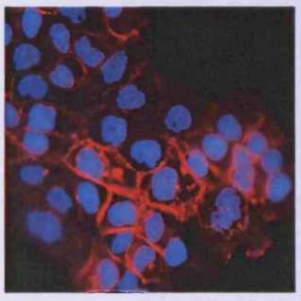

G) HAR-1 siRNA 2

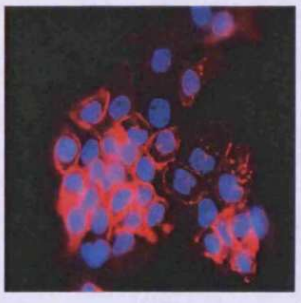

H) HAR-1 siRNA 3

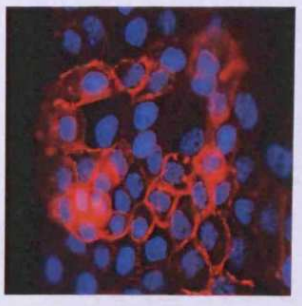

Figure 5.27: Fluorescent Microscopy of fluorescent siRNA and fixed A431 cells with a fluorescent tagged EGFR antibody. Cells were transfected 24 hours after seeding, 24 hours later the cells were fixed and incubated with anti-EGFR antibody. The secondary antibody has a red-fluorescent tag and the nuclei are stained blue. The fluorescent siRNA has a green tag and targets the luciferase gene. Green fluorescent siRNA was not visible in cells after transfection or 24 hours later.

An additional RT-PCR assay for was utilised based on the experience of the Tenovus research group that have been investigating EGFR knockdown in MCF-7 TamR cells as part of their research looking at the development of drug resistance in breast cancer. Tenovus use a pooled anti-EGFR siRNA delivered by a propriety lipid system (Dharmafect; Dharmacon) from Dharmacon to achieve knockdown. Despite technical support from Tenovus no combination of HAR-1 or Dharmacon siRNA delivered by Oligofectamine or even Dharmafect was able to elicit knockdown of EGFR in A431 cells (Figure 5.28A). The reasons for this remain unclear but the high expression of EGFR in A431 cells could make knockdown difficult.

ImageJ software converted the RT-PCR bands (Figure 5.28A) into peaks (Figure 5.28B) whose area could be calculated to produce a semi-quantitative analysis of mRNA levels. This software was used in all subsequent RT-PCR gels.

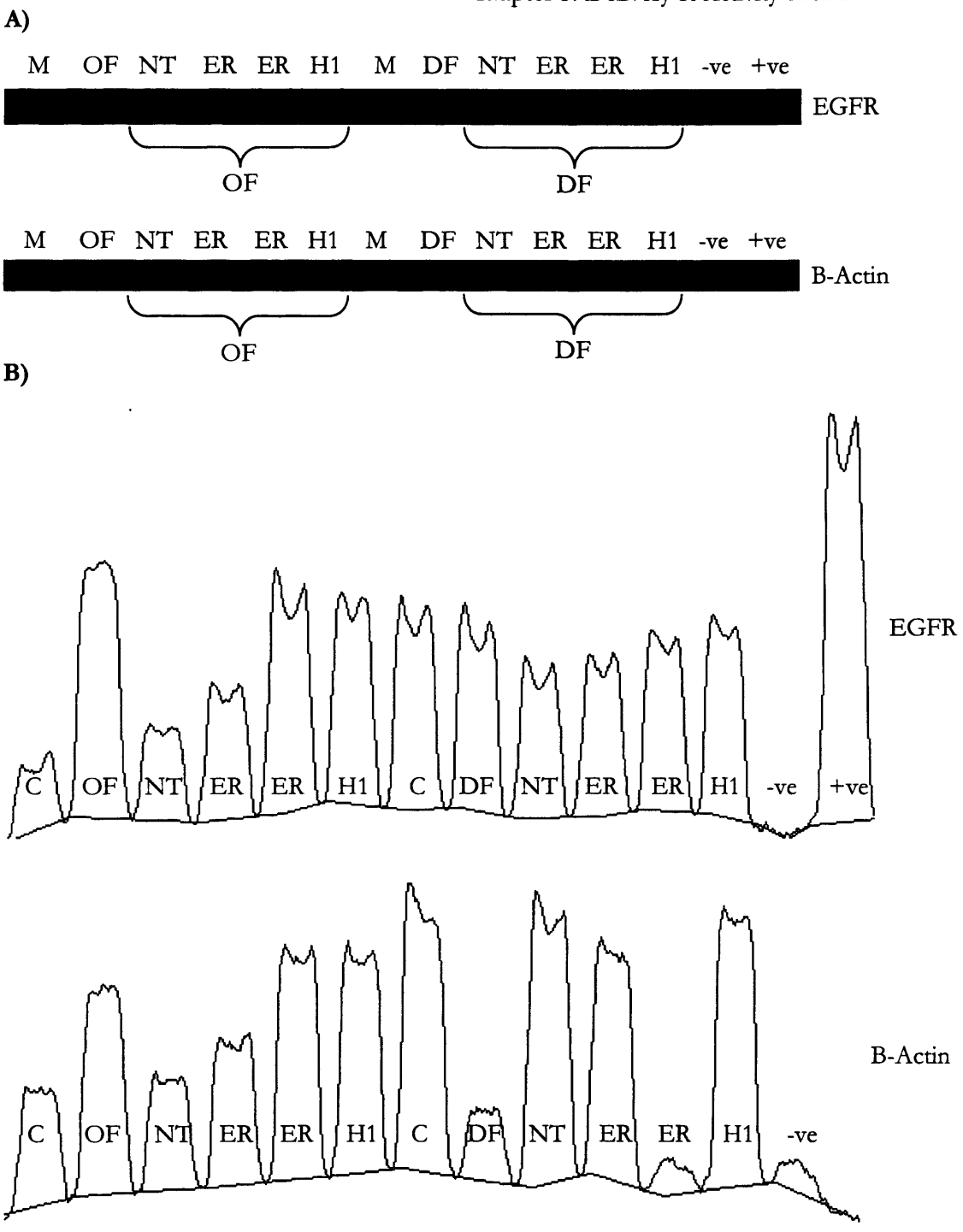

Figure 5.28: A431 cells transfected with Dharmafect (DF) or Oligofectamine (OF) complexed with siRNA. **A)** RT-PCR analysis: Dharmacon pooled EGFR targeted siRNA (ER) was used as a positive control. Dharmacon non-targeted control (NT) was used conversely as a negative control. HAR-1 siRNA (H1) was siRNA designed from Array 1. A negative blank control (-ve) that was a reaction mixture control without RNA and a PCR positive control (+ve) contains EGFR 3.6kb cDNA that was used to produce EGFR RNA in the previous array experiments. **B)** Densitometry plots of above gels produced using ImageJ whose volume was subsequently used to produce bar chart to compare expression levels.

5.4.2 Activity of siRNA in TamR cells

The anti-EGFR siRNA failed to show adequate activity in A431 cells. Since the Tenovus research group had obtained good success with TamR and anti-EGFR siRNA it was decided to use these cells and techniques to assay the siRNA designed in Chapter 4.

In TamR cells, the siRNA from Dharmacon (ER) resulted in knockdown with both Oligofectamine and Dharmafect (Figure 5.29A). The area of the bands was calculated using the ImageJ programme and bar charts normalised to non-targeted (NT) control siRNA (Figure 5.29B). A knockdown of about 50% of EGFR mRNA was observed with the Dharmacon siRNA (ER). Dharmacon pooled siRNA (100nM) is guaranteed (where delivery is optimised) to reduce the mRNA target by greater than 75% (when tested between 24 and 48 hours). A greater than 75% knockdown in EGFR mRNA was not observed although the transfection protocols I used were optimised in Tenovus further optimisation may be required. Dharmafect was selected for all subsequent transfections since Tenovus protocols use Dharmafect and it showed a slightly more consistent knockdown than Oligofectamine (Figure 5.29).

The siRNA designed in Chapter 4 (summarised in Table 5.2) were screened for activity using the protocols developed from Tenovus. The RT-PCR gels produced from three successive siRNA screens are shown in Figure 5.30. Only Dharmacon pooled siRNA produced reproducible knockdown of about 50% (Figure 5.31), although this is not a statistical difference. For a better comparison of the activity of Dharmacon siRNA and my siRNA designs the delivery of siRNA could even be bypassed by using a technique such as electroporation. There was a high variability in the knockdown achieved by the siRNA tested (Figure 5.31). Dharmacon proposes that poor to moderately active siRNAs show variability in silencing efficiency (http://www.dharmacon.com/tech/faq.aspx). It could therefore be easily concluded that my designs of siRNA were not very active.

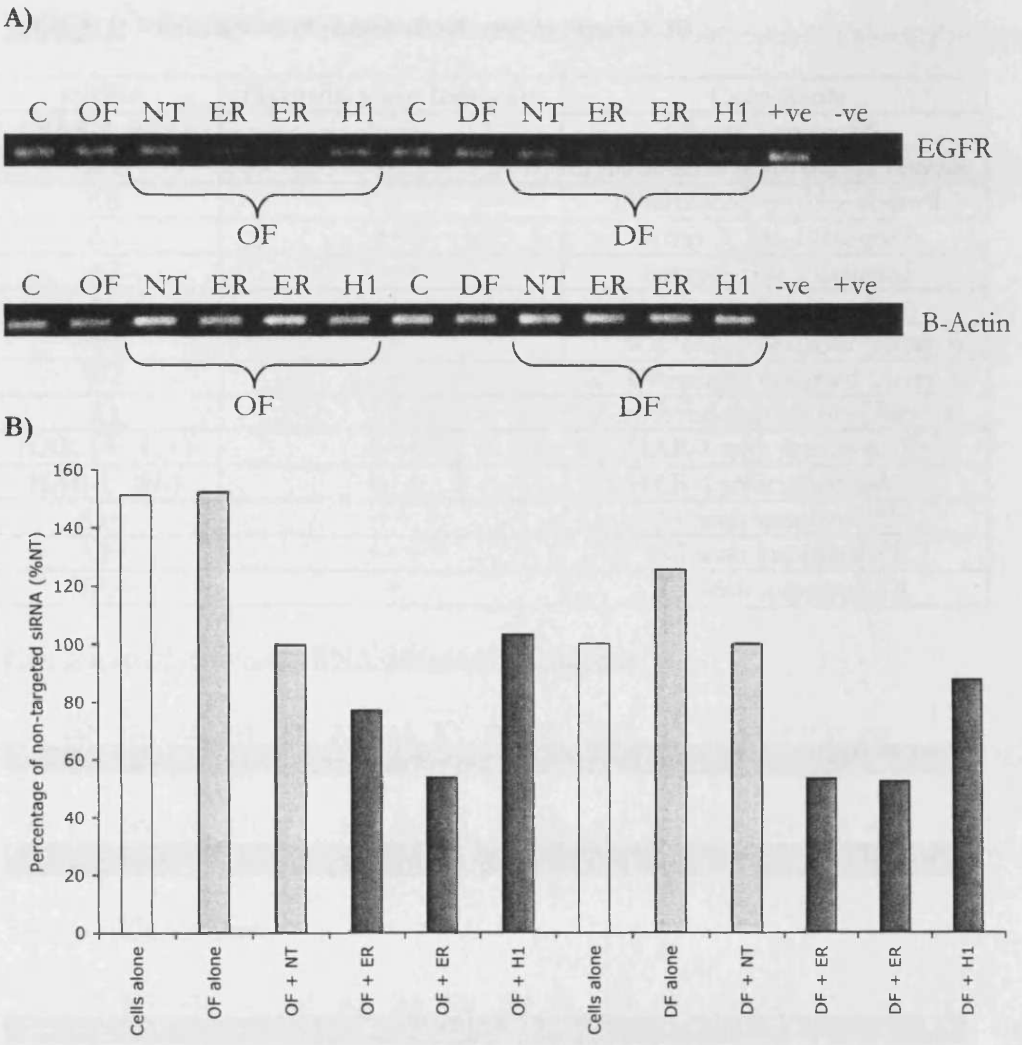

Figure 5.29: TamR cells transfected with Dharmafect (DF) or Oligofectamine (OF) complexed with siRNA. **A)** RT-PCR: Dharmacon pooled EGFR targeted siRNA (ER) was used as a positive control. Dharmacon non-targeted control (NT) was used conversely as a negative control. HAR-1 siRNA (H1) was the siRNA designed in Chapter 4. A negative blank control (-ve) that was a reaction mixture control without RNA and a PCR positive control (+ve) contains EGFR 3.6kb cDNA that was used to produce EGFR mRNA in the previous array experiments. **B)** Bar chart representation of above data.

Table 5.2: Abbreviations of pooled siRNA used in Figure 5.30

siRNA	Hybridisation Intensity	Comments
HAR-1 (H1)	+++	Array 1 designed
NT	-	Dharmacon non-targeted control
ER	-	Dharmacon positive control
A1	++	Array 3, Site 1 designed
A2	+++	Array 3, Site 2 designed
A3	+++	Array 4 designed
W1	+	1st Whitehead designed (Array 3)
W2	+	2nd Whitehead designed (Array 3)
Z1	0	Zero hybridisation site (Array 4)
HAR-1+ (H+)	+++	HAR-1 with improved TS
HAR-1- (H-)	+++	HAR-1 with worsened TS
A1+	++	A1 with improved TS
A2+	+++	A2 with improved TS
W1+	+	W1 with improved TS

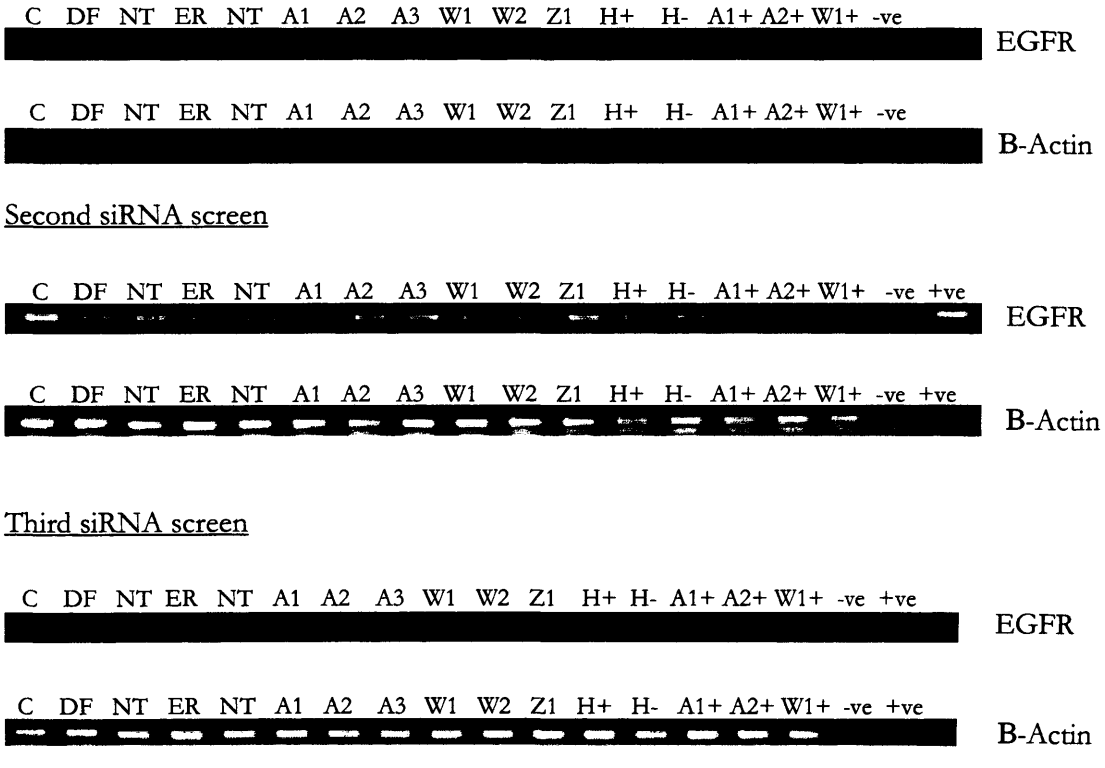

Figure 5.30: RT-PCR gels for TamR cells screened with the designed siRNA. Dharmafect (DF) was the delivery system and Dharmacon pooled EGFR targeted siRNA (ER) was used as a positive control. Dharmacon non-targeted control (NT) was used conversely as a negative control. HAR-1 siRNA (H1) was siRNA designed from Array 1. A negative blank control (-ve) that was a reaction mixture control without RNA and a PCR positive control (+ve) contains EGFR 3.6kb cDNA that was used to produce EGFR RNA in the previous array experiments. The designed siRNA's sequences are provided in Table 4.6.

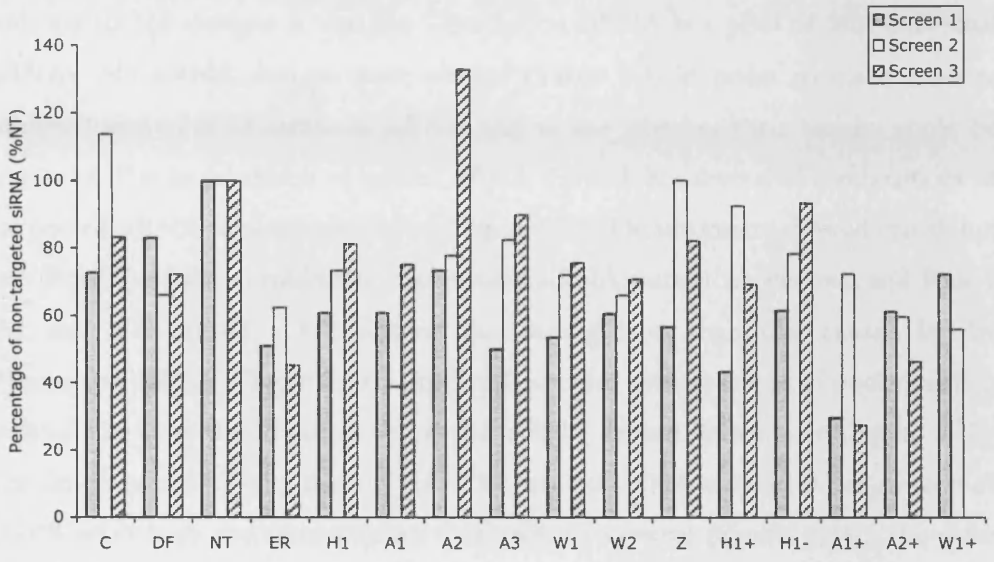

Figure 5.31: Bar charts produced by densitometry from RT-PCR gels for TamR cells screened with the designed siRNA. Dharmafect (DF) was the delivery system and Dharmacon pooled EGFR targeted siRNA (ER) was used as a positive control. Dharmacon non-targeted control (NT) was used conversely as a negative control. HAR-1 siRNA (H1) was siRNA designed from Array 1. A negative blank control (-ve) that was a reaction mixture control without RNA and a PCR positive control (+ve) contains EGFR 3.6kb cDNA that was used to produce EGFR RNA in the previous array experiments. The designed siRNA's sequences are provided in Table 4.6. The first screen's results were removed for clarity. There is no statistical difference ($p<0.05$) between any of the groups. Statistics one-way ANOVA with Duncans *Post Hoc* test.

One other factor to be aware of when comparing the activity of Dharmacon siRNA with my siRNA designs is that the Dharmacon siRNA is a pool of four individual siRNAs. My siRNA designs were pooled (Table 5.3) in order to make a better comparison to the Dharmacon siRNA and to see whether their activity could be improved. The initial screen of pooled siRNA showed that several of combinations of the pooled siRNA caused knockdown (Figure 5.32). Densitometry showed that all but one (Pool 7) of the combinations of pooled siRNA caused knockdown and Pool 1 (A1 and A3) caused a knockdown that was greater than that caused by the Dharmacon siRNA (Figure 5.34). Unfortunately, the second screen of pooled siRNA showed that only the Dharmacon pooled siRNA caused knockdown (Figure 5.32). The densitometry showed that only the Dharmacon siRNA reduced the expression of EGFR relative to the non-targeted (NT) siRNA control (Figure 5.34). The three designed siRNA that showed the most activity (A1, A3 and H1) were then pooled together in different combinations and ratios (Table 5.4) to hopefully elicit a synergistic effect. No activity was seen for any of the pooled siRNAs including the Dharmacon siRNA (Figure 5.33). During these pooling experiments I noticed that the growth of TamR cells was much slower than previously observed. These cells were later deemed to be clear of mycoplasma and it was not known what was the cause of this loss of activity.

The use of Dharmacon pooled siRNA although useful as a positive control to test for activity has several problems when used as a direct comparison for other siRNA. Firstly, there may be synergistic pooling effect and therefore activity of the siRNA comprising the pool must also be compared. Secondly, the Dharmacon siRNA have unknown chemical modifications thus it would be unfair to compare with unmodified siRNA. The PCR assay could also falsely report that pooled siRNA is more active than individual siRNA. To accurately report activity the selection of a PCR primer set should encompass the siRNA target sequence (Shepard et al., 2005). Pooled siRNA have multiple target sites and therefore have a greater chance of being included within a primer set. I did not know the sequences of the Dharmacon pooled siRNA so further comments cannot be made on the suitability of the primer sites. Future experiments would need to be performed to investigate the siRNA knockdown reported by different PCR primer sets along EGFR gene.

Multiple siRNA versus the same target reflects the natural function of Dicer, which produces many siRNA from a larger double stranded RNA. A 27mer duplex of RNA can act as Dicer substrate to produce a pool of similar siRNAs. These siRNA were 100-fold more active and had less off-target effects than 21mer siRNAs (Kim et al., 2005). The pooling of siRNA can improve activity and reduce off-target effects (Kurreck, 2006). However, there is still a lot of controversy over the use of pooling, such as whether it affects the occurrence of false results (Smith, 2006).

A recent study (Tschaharganeh et al., 2007), reported that cells transfected with non-targeted siRNA showed functional changes in proliferation and apoptosis that were interferon-independent. This report stresses the importance of using non-targeted control siRNA to ensure that functional cellular changes, especially anti-cancer effects, are only due to target-specific effects and not due to off-target effects.

Table 5.3: Abbreviations of pooled siRNA used in Figure 5.32

Abbreviation	Combinations of pooled siRNA
1	A1 (50%) + A3 (50%)
2	A3 (50%) + H1 (50%)
3	A1 (50%) + H1 (50%)
4	A1 (33%) + A3 (33%) + H1 (33%)
5	A1 (33%) + A3 (33%) + Z1 (33%)
6	A1 (25%) + A2 (25%) + A3 (25%) + H1 (25%)
7	A2 (25%) + A3 (25%) + H1 (25%) + W1 (25%)
8	A1(25%) + A2 (25%) + H1 (25%) + Z1 (25%)

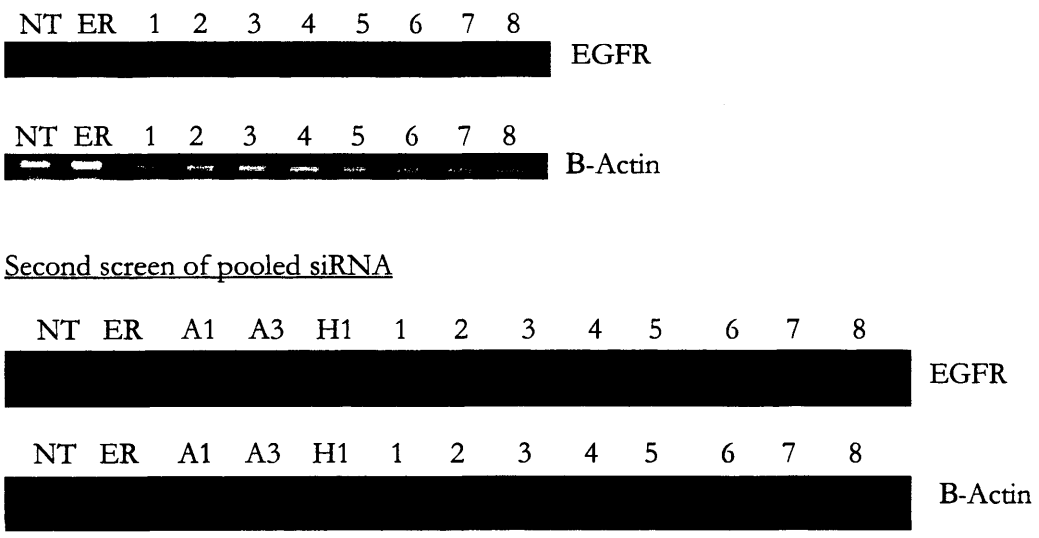

Figure 5.32: RT-PCR gels of TamR cells transfected with pooled siRNA. Dharmafect (DF) was the delivery system and Dharmacon pooled EGFR targeted siRNA (ER) was used as a positive control. Dharmacon non-targeted control (NT) was used conversely as a negative control. HAR-1 siRNA (H1) was siRNA designed from Array 1. The designed siRNA sequences are provided in Table 4.6. The combinations (1 to 8) of pooled siRNA are given in Table 5.3. Note the first two lanes (NT and ER) for EGFR and ß-Actin of the first screen of pooled siRNA for reader clarity were electronically cut and pasted to beginning of the gel, subsequent densitometry was not affected as results were processed from the uncut images. The absence of a band from Pool 6 was deemed to be a false result caused by a missed well.

Table 5.4: Abbreviations of pooled siRNA used in Figure 5.33

Abbreviation	Combinations of pooled siRNA
A	A1 (50%) + A3 (50%)
B	A1 (50%) + H1 (50%)
C	A3 (50%) + H1 (50%)
D	A1 (33%) + A3 (33%) + H1 (33%)
E	A1 (60%) + A3 (20%) + H1 (20%)
F	A1 (20%) + A3 (60%) + H1 (20%)
G	A1 (20%) + A3 (20%) + H1 (60%)

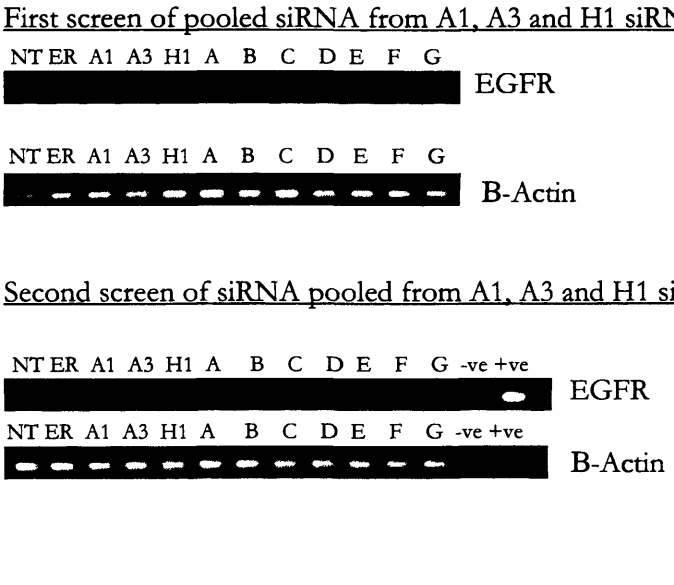

Figure 5.33: RT-PCR gels of TamR cells transfected with designed siRNA pooled from A1, A3 and H1. Dharmafect (DF) was the delivery system and Dharmacon pooled EGFR targeted siRNA (ER) was used as a positive control. Dharmacon non-targeted control (NT) was used conversely as a negative control. HAR-1 siRNA (H1) was siRNA designed from Array 1. The designed siRNA sequences are provided in Table 4.6. The combinations (A to G) of pooled siRNA are given in Table 5.4

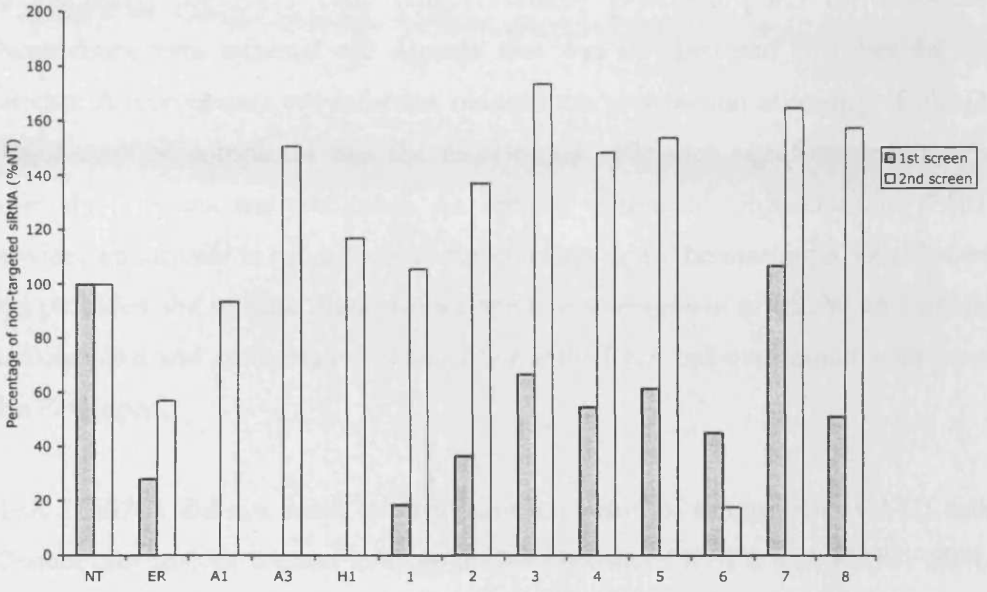

Figure 5.34: Bar charts produced by densitometry from RT-PCR gels of TamR cells transfected with pooled designed siRNA. Mean values were produced from the four gels from Figure 5.32 and error bars represent one standard deviation. Dharmafect (DF) was the delivery system and Dharmacon pooled EGFR targeted siRNA (ER) was used as a positive control. Dharmacon non-targeted control (NT) was used conversely as a negative control. HAR-1 siRNA (H1) was siRNA designed from Array 1. The designed siRNA's sequences are provided in Table 4.6. The combinations (1 to 8) of pooled siRNA are given in Table 5.3.

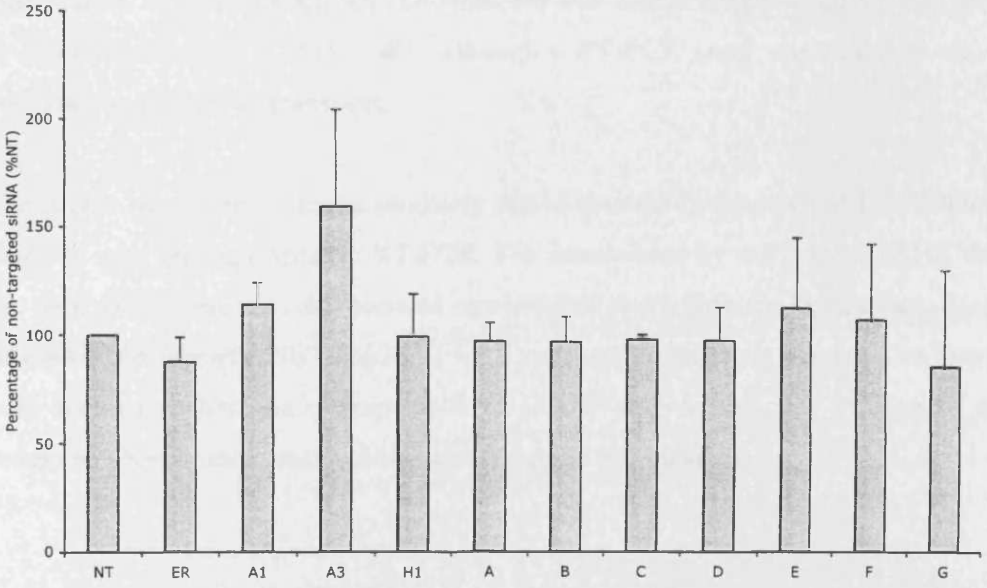

Figure 5.35: Bar charts produced by densitometry from RT-PCR gels of TamR cells transfected with pooled designed siRNA. Mean values were produced from the four gels from Figure 5.33 and error bars represent one standard deviation. Dharmafect (DF) was the delivery system and Dharmacon pooled EGFR targeted siRNA (ER) was used as a positive control. Dharmacon non-targeted control (NT) was used conversely as a negative control. HAR-1 siRNA (H1) was siRNA designed from Array 1. The designed siRNA's sequences are provided in Table 4.6. The combinations (A to G) of pooled siRNA are given in Table 5.4.

In summary, for A431 cells Oligofectamine provided good cell-associated fluorescence with minimal cell damage that was not bettered by other delivery systems. A mycoplasma cell infection reduced the transfection efficiency of siRNA-Oligofectamine complexes and the transfection efficiency significantly improved when the infection was eradicated. An optimal volume of Oligofectamine (1.5μL) provided an increase in cell-associated fluorescence up to the maximum 500nM tested and provided the optimal fluorescence for a dose-response of 25, 50 and 100nM. Radiolabelled and co-operative acting ASO and siRNA cell-association assays were also developed.

HAR-1 siRNA did not result in significant inhibition of the growth of A431 cells. Western blot analysis seemed to show the knockdown of EGFR with HAR-1 siRNA but it was difficult to detect differences in expression of EGFR from a cell line with such high expression levels. Both RT-PCR and Western blots deal with populations of cells and if the fraction of transfected cells is low an individual cell assay is required. A fluorescent microscope technique to investigate individual cell expression levels was developed but detecting differences in expression levels was again difficult and non-quantitative. A propriety siRNA (Dharmacon) that had guaranteed activity was used as a positive control in A431 cells, although a RT-PCR assay was unable to show knockdown in EGFR expression.

TamR cells transfected with the propriety siRNA showed knockdown of EGFR when detected with semi-quantitative RT-PCR. The knockdown by this pooled siRNA was the only siRNA screened that showed reproducible and consistent knockdown. Pools of the siRNA (designed in Chapter 4) were produced to improve activity. The TamR cells seemed to become unresponsive to all the siRNA, this was because of an unknown phenomenon that was thought not to be mycoplasma.

Chapter 6
General Discussion

In Chapter 3, I investigated the biological stability of siRNA by labelling ASO and siRNA with a 5'-end ^{32}P radiolabel. These radiolabelled oligonucleotides when ran on PAGE gels appear as several different molecular weight radiolabelled products. The highest molecular weight band from the labelled siRNA lane was thought to be the intact duplex. This could be established by the addition of appropriate controls, such as running unlabelled single-strand siRNA and duplex siRNA on PAGE gel then visualising them with an alternative staining method like ethidium bromide. The stability of ^{32}P radiolabelled siRNA was compared to 32P radiolabelled phosphodiester ASO in serum, serum-containing D-MEM and A431 cell lysates. The half-lives for both oligonucleotides in the different degradation media were then estimated. The half-lives were not significantly different in full serum, but in 10% serum-containing D-MEM ASO was more stable than siRNA (about 3.5 hours for ASO compared with 2 hours for siRNA). But in cell lysates siRNA was slightly more stable than ASO (43 for siRNA compared with 37 minutes for ASO). This increased siRNA lysate stability may explain the increased duration of siRNA action if intracellular molecules, possibly associated the RISC complex, that protect the siRNA from degradation. These stabilities assays need to be validated by another siRNA gel visualisation techniques to ensure the results are not solely due to 5'-end dephosphorylation by phosphatases present in serum. Since the determination of chemical modifications required to improve the biological stability are unfeasible for this work, the additional protection provided by the delivery system must be thought to be sufficient for cell culture transfections. A recent publication (Haupenthal et al., 2007), observed that pre-incubation of siRNA in human serum shortened the siRNA duplex, reduced silencing and anti-cancer activity. They were successful in using PAGE gels to investigate biological stability of siRNA by using appropriate double stranded RNA controls that were visualised by silver staining, however they did not calculate the biological stability half-lives of the siRNA.

In Chapter 4, siRNA were designed against regions in the EGFR mRNA corresponding to three scanning ASO arrays (Arrays 1, 3 and 4) that map the accessibility of ASOs targeting the first 500 nucleotides downstream of the start codon. The siRNA duplexes were designed according to rules published at the time and were targeted against ASO accessible regions (H1, A1, A2, A3). Another siRNA was designed following these rules but targeting a region that had poor mRNA

accessibility (i.e. zero hybridisation intensity; Z1). Finally, the EGFR mRNA sequence was entered into an online siRNA design algorithm from the Whitehead Institute (Yuan et al., 2004). Two of duplexes selected by the programme targeted regions spanned by Array 3 (W1 & W2). An additional set of siRNAs was designed to have altered thermodynamic stability profiles in order to establish whether these changes could alter its activity. Computer-based analysis into mRNA mapping for accessibility and thermodynamic stability calculations were initially explored, but without the necessary intellectual support, were not progressed. These should be a fruitful area research for investigators seeking to optimise the experimental therapeutic aspects of designed siRNA.

In the Delivery Section of Chapter 5, the delivery of siRNA was investigated prior to assay for siRNA activity. FACs analysis of cell association of fluorescent-labelled siRNA was used to optimise their delivery to A431 cells. The delivery of siRNA with Oligofectamine was optimised for A431 cells. A fixed dose of Oligofectamine (1.5μL) could be used for siRNA (25, 50 and 100nM) dose-activity relationships. An assay to investigate the delivery of co-operatively acting ASO and siRNA was successfully developed. The cell fluorescence associated with labelled siRNA does not however ensure that the cell has taken up the siRNA or that the siRNA has been delivered to its site of action, the cytoplasm. The successful delivery of siRNA to the target in the cytoplasm is ultimately best judged by gene knockdown. As a reporter gene Kinesin Eg5 knockdown resulting in rapid mitotic arrest, could be an easily detected biomarker of siRNA activity that has resulted from successful siRNA delivery (Weil et al., 2002).

In the Activity Section of Chapter 5, the activity of siRNA was addressed in A431 cells. Endpoints included RT-PCR and Western blots but the limitation of these techniques when applied to A431 cells are:

(i) Only semi-quantitative and therefore not truly quantitiative. Fusion constructs, consisting of an exogenously delivered gene fused to a reporter protein (e.g. Luciferase), have been successfully used to provide a quantitative assay for screening siRNA for activity (Elbashir et al., 2002). This assay would easily be adapted to screen the activity of my designed siRNA but it was decided that it was more relevant to

develop an assay targeting endogenous genes. A recent study provided quantitative information against targeted endogenous genes (Krueger et al., 2007), Real-time PCR was used to screen thousands of siRNA targeting various endogenous genes in a number of different cell lines. Real-time PCR would provide an ideal assay to screen siRNA design versus an endogenous gene target.

(ii) Are not applied to subpopulations of cells within harvested samples. The exception would be harvesting of subpopulations by cell sorting prior to RT-PCR or Western blot. A recent publication (Narz et al., 2007) reports that the background of untransfected cells can prevent analysis of gene-silencing especially in hard-to-transfect cell lines. They demonstrate two strategies for the enrichment of siRNA-transfected cells: Firstly, for cell suspensions the siRNA is co-transfected with heterologous surface and transfected cells are separated from untransfected by antibody-coated magnetic particles. Secondly, for adherent cells the siRNA is co-transfected with a plasmid that expresses a eukaryotic antibiotic resistance gene. The addition of puromycin 24 hours after transfection kills untransfected cells which can be washed off. However, both techniques are limited by the initial transfection rates.

(iii) A431 cells contain unusually large amounts of EGFR and therefore measuring difference in knockdown is difficult. A recent paper (Krueger et al., 2007) reported that the expression level of the target gene had no influence the level of its silencing. A431 cells are widely known to overexpress EGFR and Kruger and co-workers did not investigate the knockdown in cell lines that overexpress specific genes.

My results in A431 showed that a designed siRNA (HAR-1) did not result in significant inhibition of the growth of A431 cells. Preliminary Western blot analysis seemed to show the knockdown of EGFR with HAR-1 siRNA. The Tenovus research group based in the Welsh School of Pharmacy had previously showed by semi-quantitative RT-PCR the knockdown of EGFR in MCF-7 TamR cells by a proprietary siRNA (Dharmacon). This research group was unable to knockdown EGFR in A431 cells (from a personal communication with Rob Nicholson, Julia Gee and Denise Barrow). So the TamR cells were chosen to assay the activity of siRNA. The Dharmacon siRNA was used as a postive control and was compared for activity to the siRNA designed in Chapter 4 of this thesis. The Dharmacon siRNA was the

only siRNA screened to produce consistent knockdown of EGFR. The pooling of the designed siRNA showed promising preliminary results. The TamR cells became unexpectedly unresponsive to siRNA because of an unknown effect and as a result of this the increased potential activity of pooling of designed siRNA could not be investigated. Comparisons with my designed siRNA the Dharmacon siRNA may be unfair since the composition of the Dharmacon siRNA is not known. The Dharmacon siRNA consists of pool of four siRNAs where the sequences are not known and are potentially chemically modified. These chemical modifications may improve its delivery, especially when using a proprietary delivery system from the same manufacturer. So that, an individual proprietary siRNA, that is not a pool of siRNA, may be a better positive control although there still could be problems regarding the knowledge of its sequence and of any chemical modifications. The semi-quantitative RT-PCR assay may bias a pool of siRNA that has multiple targets over a single target siRNA. So an assay using cleavage site spanning primers may be more appropriate for a single target siRNA.

Tenovus optimised the delivery of siRNA to TamR cells for only the Dharmacon siRNA this may need to be optimised for the siRNA designed in Chapter 4. A recent study (Lavigne and Thierry, 2007), used fluorescent microscopy to investigate the subcellular localisation of rhodamine-labeled siRNA delivered by a lipid vector in MCF-7 cells, the cell line from which TamR cells are derived. They reported that siRNA were localised to the cytoplasm, specifically to perinuclear regions. The siRNA was co-transfected with an endosomal antigen (EEA1) that did not co-localise together and the authors concluded that the siRNA was trapped in endosomes. Confirming that fluorescent-labelled siRNA localised perinuclear regions of the cytoplasm in TamR cells would provide validation for my transfection protocol.

Unfortunately, I could not produce data that was able to determine the effects of mRNA accessibility and thermodynamic on the activity of siRNA. mRNA accessibility and thermodynamic stability have been successfully investigated by other research groups. Schubert and co-workers (Schubert et al., 2005), transfected COS-7 cells with plasmids that produce artificial constructs of mRNA target sites that could be either accessible or inaccessible because they form hairpin structures. They concluded that intrinsic thermodynamic stability of the siRNA determines the

selection of the active antisense strand of the siRNA for incorporation into RISC but the mRNA accessibility, the local free energy of base pairing, determines the efficacy of the siRNA. This strategy could be used to produce constructs against my siRNA target sites, in the EGFR mRNA, in order to investigate the *in vivo* folding of mRNA. Patzel and co-workers (Patzel et al., 2005) conversely proposed that neither thermodynamic stability nor mRNA accessibility were important factors in determining silencing potential. They report that the secondary structure of the antisense strand of the siRNA is the decisive factor, which is an antisense strand that does not form defined structures and that has available terminal nucleotides especially at the 3' end.

Small molecule inhibitors of EGFR have shown poor clinical activity, this is hypothesised to be because inhibition of EGFR alone does not affect the other multiple growth pathways present in cancer, especially those downstream of EGFR, that may remain active despite complete blockage of EGFR (Dowlati et al., 2004). Downstream EGFR pathways, such as Ras/Erk signalling, lead to increased proliferation and Akt/STATs are anti-apoptotic (Sordella et al., 2004). Wild-type EGFR stimulates downstream Ras/Erk, while mutant EGFR activates the anti-apoptotic pathways. This is thought to explain the response of patients to Gefitinib to those with the mutant EGFR (Willingham et al., 2004). A coupling of several targeted pathways individualised to the genetic variation of the patient would be the way forward for cancer therapeutics (Sharma et al., 2007). Therefore EGFR coupled with key downstream molecules must be targeted to inhibit proliferation or induce apoptosis. Pooled siRNA versus multiple cancer targets could provide a new strategy, including targeting EGFR and other downstream signalling molecules, that could induce apoptosis, such as Ras. Also the targeting of other EGFR heterodimerisation partners, such as EGFR-2 (HER-2), could have therapeutic potentials.

siRNA unlike ASO activates the RNA interference pathway. MicroRNA (miRNA) also act through this to cause gene-silencing. miRNA are thought to regulate post-transcriptionally the expression of about 30% of all mRNA (Esau and Monia, 2007). miRNA functions include the complex intracellular mechanisms such as epigenetics that when corrupted causes oncogenetic transformation (Waldman and Terzic, 2007). Many recent papers have highlighted the importance of miRNA in cancer pathology

(Bandres et al., 2007, Chuang and Jones, 2007, Esau and Monia, 2007, Negrini et al., 2007, Waldman and Terzic, 2007, Wiemer, 2007). ASOs are unlike siRNA since they seem not to have an evolved biological process for its intracellular recognition (Corey, 2007). siRNA were thought to be free from the painstaking design rules, delivery issues that plague ASOs. In fact, siRNA have more complex rules and mechanism that seem intimately linked to their therapeutic targets. Further investigation into these mechanisms could release their phenomenal therapeutic potentials.

In summary, it is clear that for an effective siRNA therapeutic one needs to consider all steps involved: from the design of siRNA accessible to target mRNA, the suitable stability of these molecules in biological media and the ways in which the delivery systems can be optimised to protect against degradation and also to promote efficient uptake into the cellular target. My first objective was to compare the stability of siRNA within biological media used for *in vitro* cell experimentation. Given the limitations with respect to the technical aspects of the radiolabelled methodology used, my conclusions from studies conducted in serum, cell culture media and mammalian cell lysates showed that ASO and siRNA stability were comparable and indeed, no clear evidence existed for siRNA as a less stable species compared to ASO.

My second objective related to the design of siRNA to target accessible regions within the EGFR mRNA. This was undertaken using innovative array technology. Through binding to antisense arrays a series of seven different siRNA accessible regions were identified and siRNA molecules designed. These seven siRNA were designed according to knowledge in 2002/03 and targeted different sites of EGFR mRNA accessibility. In addition, a further five siRNAs were designed, that the targeting sequences of which were the same as in the seven siRNAs above, where the termini differed, with the aim of altering the thermodynamic stability of the siRNA duplex.

My third objective was to examine the designed siRNA for activity. Prior to activity investigations there was a need to redress the efficiency of delivery in the *in vitro* models. FACs analysis using fluorescently labelled siRNA optimised the delivery of siRNA using Oligofectamine to A431 cells. Activity studies included assessment of cell proliferation and EGFR down-regulation in both A431 and TamR cell lines. TamR cells were preferred over A431 cells to measure the activity of the designed

siRNA. In screens of the designed siRNA, only the proprietary siRNA (Dharmacon) showed consistent knockdown of EGFR mRNA in TamR cells, although not statistically significant. The proprietary siRNA consisted of a pool of four siRNAs, so to mimic this pooling strategy and with the aim of enhancing knockdown, my designed siRNA were likewise pooled. These siRNA pools showed promising activity but before confirmatory experiments the TamR cells unexpectedly lost their silencing response to siRNA knockdown.

ASO and siRNA share common pharmaceutical problems with respect to their drug development such as their biological instability, design enabling mRNA accessibility and delivery to site subcellular activity. siRNA unlike ASO elicits RNA interference (RNAi), an innate mechanism that controls the expression of endogenous genes. Further understanding of these RNAi mechanisms will allow researchers to develop siRNA molecules that can therapeutically target genes.

Appendix

Appendix 1: buffers, solutions & gels

MATERIALS

The following materials were used to make the buffers solutions and gels that were used in Chapter 2: 'Material & Methods': Acrylamide (USB Corporation Cat.# 75820); Agarose (GE Healthcare Cat.# 17-0554-02); Ammonium persulfate (APS; Promega Cat.# V3131); Aprotinin (Sigma Cat.# A-1153); Bis-acrylamide (USB Corporation Cat.# 75821); Boric acid (Fisher Cat.# B/3750/60); Bromophenol blue (Sigma Cat.# B-5525); Diethyl Pyrocarbonate (DEPC; Sigma Cat.# D-5758); Disodium hydrogen orthophosphate anhydrous (Fisher Cat.# S/4520/53); Ethylenediaminetetraacetic acid (EDTA) disodium salt dihydrate (Sigma Cat.# E-5134); Ethylene glycol-bis(2-aminoethylether)-N;N;N';N'-tetraacetic acid (EGTA; Sigma Cat.# E-4378); Ethidium bromide Solution (Promega Cat.# H5041); Formaldehyde 37% solution (Sigma Cat.# F-8775); Formamide (Fisher Cat.# F/15551/PB08); Glacial acetic acid (Fisher A/0400/PB15); Glycine (Fisher Cat.# BPE381); Leupeptin (Sigma L-9783); Magnesium chloride (Sigma Cat.# M8266); Methanol (Fisher Cat.# M/39000/17); Minisart high flow PES 0.2 μm filters (Sartorius Cat.# 16532); MOPS (Sigma Cat.# M-5162); Nuclease-free water (Ambion Cat.# 9937); Phenylarsine (Sigma Cat.# P-3075) Phenylmethanesulfonyl fluoride (PMSF; Sigma Cat.# P-7626); Potassium chloride (Fisher Cat.# P/4280/53); Potassium phosphate monobasic (Fisher Cat.# P/4800/53); Sodium acetate (Sigma Cat.# S-2889); Sodium Bicarbonate (Fisher; S/4240/60) Sodium Carbonate (Fisher; S/2880/53); Sodium chloride (Fisher Cat.# S/3120/63); Sodium citrate (Sigma Cat.# S-4641); Sodium dodecyl sulfate (SDS; Fisher Cat.# BPE166); Sodium fluoride (Sigma Cat.# S-7920); 10mM Sodium Molybdate (Sigma Cat.# S-6646); Sodium orthovanadate (Sigma Cat.# S-6508); TEMED (N;N;N';N'-Tetramethylethylenediamine; USB Corporation Cat.# 76320); Tris base (Fisher Cat.# BPE152); Tris hydrochloride (Fisher Cat.# BPE153); Triton (Sigma Cat.# T-9284); Tween 20 (Polyethylenesorbitan monolaurate; Sigma Cat.# P5927); Urea (Fisher Cat.# U/0500/53); Xylene Cyanol FF (Fisher Cat.# BP565).

Agarose gel (1%):

Agarose (1%) and 0.001% Ethidium bromide in TBE buffer. The agarose in TBE buffer was melted before adding ethidium bromide then leave to set.

Agarose gel (2%):

Agarose (2%) and 0.001% Ethidium bromide in TAE buffer. Agarose in TAE buffer was heated before adding Ethidium bromide then leave to set.

DEPC-treated water:

0.1% DEPC in double-distilled water and was left for 12 hours before autoclaving.

EDTA solution:

0.5M EDTA in DEPC-treated water was adjusted to pH 8.0.

Hybridisation buffer:

1M Tris hydrochloride, 0.5M EDTA, 10% SDS, 1M Sodium chloride in DEPC-treated water was then filtered with a 0.2μm filter and autoclaved.

Lysis buffer:

50mM Tris base, 5mM EGTA, 150mM Sodium chloride, 1% Triton in distilled water. Adjust to pH 7.5 and store at 4°C.

Lysis buffer with protease inhibitors:

2mM Sodium orthovanadate, 50mM Sodium fluoride, 1mM PMSF, 20μM Phenylarsine, 10mM Sodium molybdate, 10μg/mL Leupeptin, 8μg/mL Aprotinin in Lysis buffer.

Microarray stripping solution:

100mM sodium carbonate, sodium bicarbonate solution (pH 9.8-10), 0.01% SDS in DEPC-treated water.

MOPS buffer:

0.2M MOPS (pH 7), 50mM Sodium acetate, 5mM EDTA (pH 8) in nuclease-free water.

PCR loading buffer:

0.05g Bromophenol blue, 0.05g Xylene cyanol FF, 3mL Glycerol was then made up to 10mL in TBE buffer.

PCR loading buffer from Tenovus:

6g Sucrose, small amount Bromophenol blue was then made up to 10mL with nuclease-free water and filtered with a 0.2μm filter.

PCR reaction mixture buffer from Tenovus (x10):

10mM Tris hydrochloride (pH 8.3), 50mM Potassium chloride, 1.5mM Magnesium chloride, 0.001% w/v Gelatin in nuclease-free water.

PBS buffer: (x10)

80.1g Sodium chloride, 2.0g Potassium chloride, 11.5g Disodium hydrogen orthophosphate, 2.0g Potassium phosphate in distilled water and made up to 1000mL was adjusted to pH 7.4, then aliquoted and autoclaved.

Stability loading buffer:

0.05g Bromophenol blue, 0.05g Xylene cyanol FF, 0.5mL Glycerol was then made up to 10mL in TBE buffer.

Stability Polyacrylamide Gel (20%):

193.4g Acrylamide, 6.6g Bis-acrylamide in TBE buffer made up to 1000mL, the resulting solution was then filtered. For polymerisation: 300μL of a 10% ammonium persulfate solution in distilled water and 60μL TEMED was added to 30mL of acrylamide solution, left for 30 minutes to fully polymerise, the gel was then pre-run at 150 volts for a least one hour.

Polyacrylamide Gel with 8M Urea (5%):

24g 8M Urea, 10mL TBE, 9.3mL acrylamide solution, and was made up to 50mL with distilled water and polymerised by the addition of 400μL APS and 53.3μL TEMED.

RNase H buffer:

100mM Tris (pH 7.4), 500mM Potassium chloride, 50mM Magnesium chloride in DEPC-treated water.

RNA sample buffer:

10mL de-ionised Formamide, 3.5mL Formaldehyde 37% solution, 2mL MOPS buffer was aliquoted and stored at -20°C.

RNA loading buffer:

50% Glycerol, 1mM EDTA, 0.4% Bromophenol blue, 0.1% Ethidium bromide in DEPC-treated water was aliquoted and stored at -20°C.

SSC buffer (20x):

3M Sodium chloride, 0.3M Sodium citrate in DEPC-treated water.

TAE buffer (50x):

242g Tris, 57.1mL Glacial acetic acid, 100mL 0.5M EDTA was made up to 1000mL in nuclease-free water.

TBE buffer (5x):

0.45M Tris base, 0.45M Boric acid, 0.01M EDTA (pH 8.0) in double-distilled water.

TBS buffer for ExpressOn arrays (10x):

0.5M Tris hydrochloride (pH 7.5), 1.5M Sodium chloride in DEPC-treated water.

TBS buffer for Western blots (10x):

100mM Tris base, 1.5M Sodium chloride in double-distilled water was adjusted to pH 7.6.

TBS Tween buffer:

0.05% Tween 20 in TBS buffer for arrays or Western blots.

TE buffer:

10mM Tris hydrochloride (pH 8.0), 1mM EDTA in nuclease-free water.

Western blot running buffer (10x):

0.25M Tris base, 1.92M Glycine, 0.1% SDS in distilled water was adjusted to pH 8.3.

Western blot SDS polyacrylamide resolving gel (8%):

2.7mL 30% acrylamide solution, 2.5mL 1.5M Tris base (pH 8.8) in distilled water solution, 0.1mL 10% SDS solution, 2.5mL distilled water. For polymerisation 100μL 10% APS in distilled water solution and 20μL TEMED.

Western blot polyacrylamide solution (30%):

30% acrylamide, 0.8% bisacrylamide in distilled water then filter the resulting solution.

Western blot SDS polyacrylamide stacking gel (5%):

1.7mL 30% acrylamide solution, 2.5mL 0.5M Tris base (pH 6.6) in distilled water solution, 0.1mL 10% SDS solution, 5.8mL distilled water. For polymerisation 50μL 10% APS in distilled water solution and 10μL TEMED.

Western blot transfer buffer:

0.25M Tris base, 1.92M Glycine, 20% Methanol in distilled water.

Appendix 2: Primers

All purchased from Invitrogen

EGFR cDNA fragment primers:

Forward EGFR primer with T7 polymerase promoter: 5'-[TTC TAA TAC GAC TCA CTA TAG GGA GA] A TGC GAC CCT CCG GGA CGG C-3' [T7 promoter region]

Reverse 560 bp fragment primer: 5'-CAG CTG CCC AGG TGG TTC TGG-3'

Reverse 1000 bp fragment primer: 5'-GGC AAG GCC CTT CGC ACT TCT-3'

Reverse 3,600 bp fragment primer: 5'-TCA GCT GTG GAG CCC TTA AAG-3'

RNase H primer sequences:

A1: 5'-TTT CCT CTG ATG ATC TGC-3'

A2: 5'-CGG TTT TAT TTG CAT CAT-3'

A3: 5'-TGC TCT CCA CGT TGC ACA-3'

W1: 5'-GAC TGC TAA GGC ATA GGA-3'

W2: 5'-ATT TCT CAT GGG CAG CTC-3'

Z: 5'-CTG AGA AAG TCA CTG CTG-3'

H1: 5'-TAC TCG TGC CTT GGC AAA-3'

SF: 5'-GTT CTG GAA GTC CAT CGA-3'

Original RT-PCR Primers:

Forward EGFR PCR primer: 5'-CGG AAC TTT GGG CGA CTA T-3'

Reverse EGFR PCR primer: 5'-CAA CAT CTC CGA AAG CCA-3'

Forward actin primer: 5'-AGG AGT TGA AGG TCC CTT CA-3'

Reverse actin primer: 5'-CCT TCC TGG GCA TGG AGT CCT-3'

The size of amplicon produced each primer pair was: 637 bp for EGFR and 204 bp for actin

PCR primer sequences that produce shorter amplicons:

Forward EGFR primer: 5'-CCA ACC AAG CTC TCT TGA GG-3'

Reverse EGFR primer: 5'-GCT TTC GGA GAT GTT GCT TC-3'

Forward actin primer: 5'-CCC AGC CAT GTA CGT TGC TA-3'

Reverse actin primer: 5'-AGG GCA TAC CCC TCG TAG ATG-3'

The size of amplicon produced each primer pair was: 168 bp for EGFR and 125 bp for actin.

Appendix 3: Position of Scanning Arrays 1, 3 and 4 on the EGFR mRNA

LOCUS NM_005228 5512 bp mRNA linear PRI 07-SEP-2003 DEFINITION Homo sapiens epidermal growth factor receptor (erythroblastic leukemia viral (v-erb-b) oncogene homolog, avian) (EGFR), mRNA. ACCESSION NM_005228 VERSION NM_005228.2 GI:29725608 BASE COUNT 1470 a 1475 c 1330 g 1237 t ORIGIN

```
1    gagctagccc cggcggccgc cgccgcccag accggacgac aggccacctc gtcggcgtcc
61   gcccgagtcc ccgcctcgcc gccaacgcca caaccaccgc gcacggcccc ctgactccgt
121  ccagtattga tcgggagagc cggagcgagc tcttcgggga gcagcgatgc gaccctccgg
181  gacggccggg gcagcgctcc tggcgctgct ggctgcgctc tgcccggcga gtcgggctct
241  ggaggaaaag aaagtttgcc aaggcacgag taacaagctc acgcagttgg gcacttttga
301  agatcatttt ctcagcctcc agaggatgtt caataactgt gaggtggtcc ttgggaattt
361  ggaaattacc tatgtgcaga ggaattatga tctttccttc ttaaagacca tccaggaggt
421  ggctggttat gtcctcattg ccctcaacac agtggagcga attcctttgg aaacctgca
481  gatcatcaga ggaaatatgt actacgaaaa ttcctatgcc ttagcagtct tatctaacta
541  tgatgcaaat aaaaccggac tgaaggagct gcccatgaga aatttacagg aaatcctgca
601  tggcgccgtg cggttcagca acaaccctgc cctgtgcaac gtggagagca tccagtggcg
661  ggacatagtc agcagtgact ttctcagcaa catgtcgatg gacttccaga accacctggg
721  cagctgccaa aagtgtgatc caagctgtcc caatgggagc tgctggggtg caggagagga
781  gaactgccag aaactgacca aaatcatctg tgcccagcag tgctccgggc gctgccgtgg
841  caagtccccc agtgactgct gccacaacca gtgtgctgca ggctgcacag gccccggga
901  gagcgactgc ctggtctgcc gcaaattccg agacgaagcc acgtgcaagg acacctgccc
961  cccactcatg ctctacaacc ccaccacgta ccagatggat gtgaaccccg agggcaaata
1021 cagctttggt gccacctgcg tgaagaagtg tccccgtaat tatgtggtga cagatcacgg
1081 ctcgtgcgtc cgagcctgtg gggccgacag ctatgagatg gaggaagacg gcgtccgcaa
1141 gtgtaagaag tgcgaagggc cttgccgcaa agtgtgtaac ggaataggta ttggtgaatt
1201 taaagactca ctctccataa atgctacgaa tattaaacac ttcaaaaact gcacctccat
1261 cagtggcgat ctccacatcc tgccggtggc atttaggggt gactccttca cacatactcc
1321 tcctctggat ccacaggaac tggatattct gaaaaccgta aaggaaatca cagggttttt
1381 gctgattcag gcttggcctg aaaacaggac ggacctccat gcctttgaga acctagaaat
1441 catacgcggc aggaccaagc aacatggtca gttttctctt gcagtcgtca gcctgaacat
1501 aacatccttg ggattacgct ccctcaagga gataagtgat ggagatgtga taatttcagg
1561 aaacaaaaat ttgtgctatg caaatacaat aaactggaaa aaactgtttg ggacctccgg
1621 tcagaaaacc aaaattataa gcaacagagg tgaaaacagc tgcaaggcca caggccaggt
1681 ctgccatgcc ttgtgctccc ccgagggctg ctggggcccg gagcccaggg actgcgtctc
1741 ttgccggaat gtcagccgag gcagggaatg cgtggacaag tgcaaccttc tggagggtga
1801 gccaagggag tttgtggaga actctgagtg catacagtgc cacccagagt gcctgcctca
1861 ggccatgaac atcacctgca caggacgggg accagacaac tgtatccagt gtgcccacta
1921 cattgacggc ccccactgcg tcaagacctg cccggcagga gtcatgggag aaaacaacac
1981 cctggtctgg aagtacgcag acgccggcca tgtgtgccac ctgtgccatc caaactgcac
2041 ctacggatgc actgggccag gtcttgaagg ctgtccaacg aatgggccta agatcccgtc
2101 catcgccact gggatggtgg gggccctcct cttgctgctg gtggtggccc tggggatcgg
2161 cctcttcatg cgaaggcgcc acatcgttcg gaagcgcacg ctgcggaggc tgctgcagga
2221 gagggagctt gtggagcctc ttacacccag tggagaagct cccaaccaag ctctcttgag
2281 gatcttgaag gaaactgaat tcaaaaagat caaagtgctg ggctccggtg cgttcggcac
2341 ggtgtataag ggactctgga tcccagaagg tgagaaagtt aaaattcccg tcgctatcaa
2401 ggaattaaga gaagcaacat ctccgaaagc caacaaggaa atcctcgatg aagcctacgt
2461 gatggccagc gtggacaacc cccacgtgtg ccgcctgctg ggcatctgcc tcacctccac
2521 cgtgcagctc atcacgcagc tcatgccctt cggctgcctc ctggactatg tccgggaaca
2581 caaagacaat attggctccc agtacctgct caactggtgt gtgcagatcg caaagggcat
2641 gaactacttg gaggaccgtc gcttggtgca ccgcgacctg gcagccagga acgtactggt
2701 gaaaacaccg cagcatgtca agatcacaga ttttgggctg gccaaactgc tgggtgcgga
2761 agagaaagaa taccatgcag aaggaggcaa agtgcctatc aagtggatgg cattggaatc
2821 aattttacac agaatctata cccaccagag tgatgtctgg agctacgggg tgaccgtttg
2881 ggagttgatg acctttggat ccaagccata tgacggaatc cctgccagcg agatctcctc
2941 catcctggag aaaggagaac gcctccctca gccacccata tgtaccatcg atgtctacat
3001 gatcatggtc aagtgctgga tgatagacgc agatagtcgc ccaaagttcc gtgagttgat
3061 catcgaattc tccaaaatgg cccgagaccc ccagcgctac cttgtcattc aggggatga
3121 aagaatgcat ttgccaagtc ctacagactc caacttctac cgtgccctga tggatgaaga
3181 agacatggac gacgtggtgg atgccgacga gtacctcatc ccacagcagg gcttcttcag
3241 cagcccctcc acgtcacgga ctcccctcct gagctctctg agtgcaacca gcaacaattc
3301 caccgtggct tgcattgata gaaatgggct gcaaagctgt cccatcaagg aagacagctt
3361 cttgcagcga tacagctcag accccacagg cgccttgact gaggacagca tagacgacac
3421 cttcctccca gtgcctgaat acataaacca gtccgttccc aaaaggcccg ctggctctgt
3481 gcagaatcct gtctatcaca atcagcctct gaaccccgcg cccagcagag acccacacta
3541 ccaggacccc cacagcactg cagtgggcaa ccccgagtat ctcaacactg tccagcccac
```

Array 1 (0-120)

Array 3 (301-450)

Array 4 (431-580)

```
3601 ctgtgtcaac agcacattcg acagccctgc ccactgggcc cagaaaggca gccaccaaat
3661 tagcctggac aaccctgact accagcagga cttctttccc aaggaagcca agccaaatgg
3721 catctttaag ggctccacag ctgaaaatgc agaataccta agggtcgcgc cacaaagcag
3781 tgaatttatt ggagcatgac cacggaggat agtatgagcc ctaaaaatcc agactctttc
3841 gatacccagg accaagccac agcaggtcct ccatcccaac agccatgccc gcattagctc
3901 ttagacccac agactggttt tgcaacgttt acaccgacta gccaggaagt acttccacct
3961 cgggcacatt ttgggaagtt gcattccttt gtcttcaaac tgtgaagcat ttacagaaac
4021 gcatccagca agaatattgt ccctttgagc agaaatttat ctttcaaaga ggtatatttg
4081 aaaaaaaaaa aaaaagtata tgtgaggatt tttattgatt ggggatcttg gagtttttca
4141 ttgtcgctat tgatttttac ttcaatgggc tcttccaaca aggaagaagc ttgctggtag
4201 cacttgctac cctgagttca tccaggccca actgtgagca aggagcacaa gccacaagtc
4261 ttccagagga tgcttgattc cagtggttct gcttcaaggc ttccactgca aaacactaaa
4321 gatccaagaa ggccttcatg gccccagcag gccggatcgg tactgtatca agtcatggca
4381 ggtacagtag gataagccac tctgtccctt cctgggcaaa gaagaaacgg aggggatgaa
4441 ttcttcctta gacttacttt tgtaaaaatg tccccacggt acttactccc cactgatgga
4501 ccagtggttt ccagtcatga gcgttagact gacttgtttg tcttccattc cattgttttg
4561 aaactcagta tgccgcccct gtcttgctgt catgaaatca gcaagagagg atgacacatc
4621 aaataataac tcggattcca gcccacattg gattcatcag catttggacc aatagcccac
4681 agctgagaat gtggaatacc taaggataac accgcttttg ttctcgcaaa aacgtatctc
4741 ctaatttgag gctcagatga aatgcatcag gtcctttggg gcatagatca gaagactaca
4801 aaaatgaagc tgctctgaaa tctcctttag ccatcacccc aaccccccaa aattagtttg
4861 tgttacttat ggaagatagt tttctccttt tacttcactt caaaagcttt ttactcaaag
4921 agtatatgtt ccctccaggt cagctgcccc caaacccccc ccttacgctt tgtcacacaa
4981 aaagtgtctc tgccttgagt catctattca agcacttaca gctctggcca caacagggca
5041 ttttacaggt gcgaatgaca gtagcattat gagtagtgtg aattcaggta gtaaatatga
5101 aactagggtt tgaaattgat aatgctttca caacatttgc agatgtttta gaaggaaaaa
5161 agttccttcc taaaataatt tctctacaat tggaagattg gaagattcag ctagttagga
5221 gcccattttt tcctaatctg tgtgtgccct gtaacctgac tggttaacag cagtcctttg
5281 taaacagtgt tttaaactct cctagtcaat atccacccca tccaatttat caaggaagaa
5341 atggttcaga aaatattttc agcctacagt tatgttcagt cacacacaca tacaaaatgt
5401 tccttttgct tttaaagtaa tttttgactc ccagatcagt cagagcccct acagcattgt
5461 taagaaagta tttgattttt gtctcaatga aaataaaact atattcattt cc
//
```

Appendix 4: Publications

Articles

BEALE, G., HOLLINS, A. J., BENBOUBETRA, M., SOHAIL, M., FOX, S. P., BENTER, I. & AKHTAR, S. (2003) Gene silencing nucleic acids designed by scanning arrays: anti-EGFR activity of siRNA, ribozyme and DNA enzymes targeting a single hybridization-accessible region using the same delivery system. *J Drug Target,* 11, 449-56.

GILMORE, I. R., FOX, S. P., HOLLINS, A. J. & AKHTAR, S. (2006) Delivery Strategies for siRNA-mediated Gene Silencing. *Current Drug Delivery,* 3, 147.

GILMORE, I. R., FOX, S. P., HOLLINS, A. J., SOHAIL, M. & AKHTAR, S. (2004) The design and exogenous delivery of siRNA for post-transcriptional gene silencing. *J Drug Target,* 12, 315-40.

HOLLINS, A. J., OMIDI, Y., FOX, S. P., GRIFFITHS, S. & AKHTAR, S. (2004) Polyethylenimine-mediated delivery of small interfering RNA targeting the epidermal growth factor receptor: a comparison of linear and branched polymer architecture. *Journal of Pharmacy and Pharmacology,* 56, 53-53.

HOLLINS, A.J., FOX, S.P. AND AKHTAR, S. (2004) "Exogenous siRNA delivery: protocols for optimising delivery to cells" in 'Gene Silencing by RNA Interference: Technology and Application' M Sohail (Ed) CRC Press, Boca Raton, USA, 127-46.

KHAN, A., BENBOUBETRA, M., SAYYED, P. Z., WOOI NG, K., FOX, S., BECK, G., BENTER, I. F. & AKHTAR, S. (2004) Sustained Polymeric Delivery of Gene Silencing Antisense ODNs, siRNA, DNAzymes and Ribozymes: In Vitro and In Vivo Studies. *J Drug Target,* 12, 393-404.

Poster presentations

FOX, S. P., BENBOUBETRA, M. & AKHTAR, S. (2003) Gene silencing by RNA interference: the biological stability of siRNA containing two 3'-terminal phosphodiester linkages in both strands. *Journal of Pharmacy and Pharmacology,* 55, 123-123.

STEPHEN FOX, AJ HOLLINS, M SOHAIL, Y OMIDI, E SOUTHERN, M BENBOUBETRA AND S AKHTAR (2004) The evaluation of small interfering RNA (siRNA) as potential therapeutic agents for the down-regulation of the Epidermal Growth Factor Receptor (EGFR): The Design, Biological Stability and Activity. Prize winning Poster at Welsh School of Pharmacy Postgraduate Research Day also subsequently presented at the Speaking of Science Postgraduate Conference 2004

FOX SP, GILMORE IR, HOLLINS AJ AND AKHTAR S (2004) The delivery and activity of scanning array designed siRNA targeted against the Epidermal Growth Factor Receptor (EGFR) Poster presented at RNAi Europe, London 2004

Poster & Oral Presentation

FOX, S. P., HOLLINS, A. J., SOHAIL, M., OMIDI, Y., SOUTHERN, E., BENBOUBETRA, M. & AKHTAR, S. (2004) The design and activity of small interfering RNA (siRNA) as a potential therapeutic agent for the down-regulation of the epidermal growth factor receptor (EGFR). *Journal of Pharmacy and Pharmacology,* 56**,** 28-28.

Oral Presentation

STEPHEN FOX, AJ HOLLINS, M SOHAIL, E SOUTHERN, AND S AKHTAR (2005) siRNA design for gene-silencing: Oral presentation at Welsh School of Pharmacy Postgraduate Research Day

References

AGRAWAL, S. & ZHAO, Q. (1998a) Antisense therapeutics. *Curr Opin Chem Biol,* 2, 519-28.

AGRAWAL, S. & ZHAO, Q. (1998b) Mixed backbone oligonucleotides: improvement in oligonucleotide-induced toxicity in vivo. *Antisense Nucleic Acid Drug Dev,* 8, 135-9.

AKAGI, K., MURAI, K., HIRAO, N. & YAMANAKA, M. (1976) Purification and properties of alkaline ribonuclease from human serum. *Biochim Biophys Acta,* 442, 368-78.

AKHTAR, S., KOLE, R. & JULIANO, R. L. (1991) Stability of antisense DNA oligodeoxynucleotide analogs in cellular extracts and sera. *Life Sci,* 49, 1793-801.

AL-OBEIDI, F. A. & LAM, K. S. (2000) Development of inhibitors for protein tyrosine kinases. *Oncogene,* 19, 5690-701.

ALLERSON, C. R., SIOUFI, N., JARRES, R., PRAKASH, T. P., NAIK, N., BERDEJA, A., WANDERS, L., GRIFFEY, R. H., SWAYZE, E. E. & BHAT, B. (2005) Fully 2'-modified oligonucleotide duplexes with improved in vitro potency and stability compared to unmodified small interfering RNA. *J Med Chem,* 48, 901-4.

AMARZGUIOUI, M., HOLEN, T., BABAIE, E. & PRYDZ, H. (2003) Tolerance for mutations and chemical modifications in a siRNA. *Nucleic Acids Res,* 31, 589-95.

AMARZGUIOUI, M. & PRYDZ, H. (2004) An algorithm for selection of functional siRNA sequences. *Biochem Biophys Res Commun,* 316, 1050-8.

ARTEAGA, C. L. (2001) The epidermal growth factor receptor: from mutant oncogene in nonhuman cancers to therapeutic target in human neoplasia. *J Clin Oncol,* 19, 32S-40S.

BAGGA, S., BRACHT, J., HUNTER, S., MASSIRER, K., HOLTZ, J., EACHUS, R. & PASQUINELLI, A. E. (2005) Regulation by let-7 and lin-4 miRNAs results in target mRNA degradation. *Cell,* 122, 553-63.

BAI, X., ZHOU, D., BROWN, J. R., CRAWFORD, B. E., HENNET, T. & ESKO, J. D. (2001) Biosynthesis of the linkage region of glycosaminoglycans: cloning and activity of galactosyltransferase II, the sixth member of the beta 1,3-galactosyltransferase family (beta 3GalT6). *J Biol Chem,* 276, 48189-95.

BANDRES, E., AGIRRE, X., RAMIREZ, N., ZARATE, R. & GARCIA-FONCILLAS, J. (2007) MicroRNAs as Cancer Players: Potential Clinical and Biological Effects. *DNA Cell Biol,* 26, 273-82.

BASELGA, J. (2006) Epidermal growth factor receptor pathway inhibitors. *Update on Cancer Therapeutics,* 1, 299.

BASS, B. L. (2001) RNA interference. The short answer. *Nature,* 411, 428-9.

BATZER, A. G., ROTIN, D., URENA, J. M., SKOLNIK, E. Y. & SCHLESSINGER, J. (1994) Hierarchy of binding sites for Grb2 and Shc on the epidermal growth factor receptor. *Mol Cell Biol,* 14, 5192-201.

BEALE, G., HOLLINS, A. J., BENBOUBETRA, M., SOHAIL, M., FOX, S. P., BENTER, I. & AKHTAR, S. (2003) Gene silencing nucleic acids designed by scanning arrays: anti-EGFR activity of siRNA, ribozyme and DNA enzymes targeting a single hybridization-accessible region using the same delivery system. *J Drug Target,* 11, 449-56.

BEIGELMAN, L., MCSWIGGEN, J. A., DRAPER, K. G., GONZALEZ, C., JENSEN, K., KARPEISKY, A. M., MODAK, A. S., MATULIC-ADAMIC, J., DIRENZO, A. B., HAEBERLI, P. & ET AL. (1995) Chemical

modification of hammerhead ribozymes. Catalytic activity and nuclease resistance. *J Biol Chem,* 270, 25702-8.

BERNSTEIN, E., DENLI, A. M. & HANNON, G. J. (2001) The rest is silence. *Rna,* 7, 1509-21.

BERTRAND, J. R., POTTIER, M., VEKRIS, A., OPOLON, P., MAKSIMENKO, A. & MALVY, C. (2002) Comparison of antisense oligonucleotides and siRNAs in cell culture and in vivo. *Biochem Biophys Res Commun,* 296, 1000-4.

BEVERLY, M., HARTSOUGH, K., MACHEMER, L., PAVCO, P. & LOCKRIDGE, J. (2006) Liquid chromatography electrospray ionization mass spectrometry analysis of the ocular metabolites from a short interfering RNA duplex. *J Chromatogr B Analyt Technol Biomed Life Sci,* 835, 62-70.

BOHULA, E. A., SALISBURY, A. J., SOHAIL, M., PLAYFORD, M. P., RIEDEMANN, J., SOUTHERN, E. M. & MACAULAY, V. M. (2003) The efficacy of small interfering RNAs targeted to the type 1 insulin-like growth factor receptor (IGF1R) is influenced by secondary structure in the IGF1R transcript. *J Biol Chem,* 278, 15991-7.

BRAASCH, D. A., JENSEN, S., LIU, Y., KAUR, K., ARAR, K., WHITE, M. A. & COREY, D. R. (2003) RNA interference in mammalian cells by chemically-modified RNA. *Biochemistry,* 42, 7967-75.

BRAASCH, D. A., PAROO, Z., CONSTANTINESCU, A., REN, G., OZ, O. K., MASON, R. P. & COREY, D. R. (2004) Biodistribution of phosphodiester and phosphorothioate siRNA. *Bioorg Med Chem Lett,* 14, 1139-43.

BROWN, K. M., CHU, C. Y. & RANA, T. M. (2005) Target accessibility dictates the potency of human RISC. *Nat Struct Mol Biol,* 12, 469-70.

BUTLER, M. & LEACH, R. H. (1964) A Mycoplasma Which Induces Acidity And Cytopathic Effect In Tissue Culture. *J Gen Microbiol,* 34, 285-94.

CAO, L., YAO, Y., LEE, V., KIANI, C., SPANER, D., LIN, Z., ZHANG, Y., ADAMS, M. E. & YANG, B. B. (2000) Epidermal growth factor induces cell cycle arrest and apoptosis of squamous carcinoma cells through reduction of cell adhesion. *J Cell Biochem,* 77, 569-83.

CAPLEN, N. J. (2002) A new approach to the inhibition of gene expression. *Trends Biotechnol,* 20, 49-51.

CAPODICI, J., KARIKO, K. & WEISSMAN, D. (2002) Inhibition of HIV-1 infection by small interfering RNA-mediated RNA interference. *J Immunol,* 169, 5196-201.

CAUDY, A. A., MYERS, M., HANNON, G. J. & HAMMOND, S. M. (2002) Fragile X-related protein and VIG associate with the RNA interference machinery. *Genes Dev,* 16, 2491-6.

CHALK, A. M., WAHLESTEDT, C. & SONNHAMMER, E. L. (2004) Improved and automated prediction of effective siRNA. *Biochem Biophys Res Commun,* 319, 264-74.

CHEN, Z. & RUFFNER, D. E. (1996) Modified crush-and-soak method for recovering oligodeoxynucleotides from polyacrylamide gel. *Biotechniques,* 21, 820-2.

CHIU, Y. L. & RANA, T. M. (2002) RNAi in human cells: basic structural and functional features of small interfering RNA. *Mol Cell,* 10, 549-61.

CHIU, Y. L. & RANA, T. M. (2003) siRNA function in RNAi: a chemical modification analysis. *Rna,* 9, 1034-48.

CHU, C. Y. & RANA, T. M. (2006) Translation repression in human cells by microRNA-induced gene silencing requires RCK/p54. *PLoS Biol,* 4, e210.

CHUANG, J. C. & JONES, P. A. (2007) Epigenetics and microRNAs. *Pediatr Res,* 61, 24R-29R.

COHEN, S. (1962) Isolation of a mouse submaxillary gland protein accelerating incisor eruption and eyelid opening in the new-born animal. *J Biol Chem,* 237, 1555-62.

COREY, D. R. (2007) RNA learns from antisense. *Nat Chem Biol,* 3, 8-11.

COUZIN, J. (2002) Breakthrough of the year. Small RNAs make big splash. *Science,* 298, 2296-7.

CROOKE, R. M. (1998) Antisense Research and Application: Handbook of Experimental Pharmacology.

CROOKE, S. T. & LEBLEU, B. (1993) *Antisense Research and Applications*, CRC Press.

CUI, W., NING, J., NAIK, U. P. & DUNCAN, M. K. (2004) OptiRNAi, an RNAi design tool. *Comput Methods Programs Biomed,* 75, 67-73.

CZAUDERNA, F., FECHTNER, M., DAMES, S., AYGUN, H., KLIPPEL, A., PRONK, G. J., GIESE, K. & KAUFMANN, J. (2003) Structural variations and stabilising modifications of synthetic siRNAs in mammalian cells. *Nucleic Acids Res,* 31, 2705-16.

DANCEY, J. E. & FREIDLIN, B. (2003) Targeting epidermal growth factor receptor--are we missing the mark? *Lancet,* 362, 62-4.

DING, Y., CHAN, C. Y. & LAWRENCE, C. E. (2004) Sfold web server for statistical folding and rational design of nucleic acids. *Nucleic Acids Res,* 32, W135-41.

DIVGI, C. R., WELT, S., KRIS, M., REAL, F. X., YEH, S. D., GRALLA, R., MERCHANT, B., SCHWEIGHART, S., UNGER, M., LARSON, S. M. & ET AL. (1991) Phase I and imaging trial of indium 111-labeled anti-epidermal growth factor receptor monoclonal antibody 225 in patients with squamous cell lung carcinoma. *J Natl Cancer Inst,* 83, 97-104.

DOI, N., ZENNO, S., UEDA, R., OHKI-HAMAZAKI, H., UI-TEI, K. & SAIGO, K. (2003) Short-interfering-RNA-mediated gene silencing in mammalian cells requires Dicer and eIF2C translation initiation factors. *Curr Biol,* 13, 41-6.

DOWLATI, A., NETHERY, D. & KERN, J. A. (2004) Combined inhibition of epidermal growth factor receptor and JAK/STAT pathways results in greater growth inhibition in vitro than single agent therapy. *Mol Cancer Ther,* 3, 459-63.

DOWNWARD, J., YARDEN, Y., MAYES, E., SCRACE, G., TOTTY, N., STOCKWELL, P., ULLRICH, A., SCHLESSINGER, J. & WATERFIELD, M. D. (1984) Close similarity of epidermal growth factor receptor and v-erb-B oncogene protein sequences. *Nature,* 307, 521-7.

DUDEK, P. & PICARD, D. (2004) TROD: T7 RNAi Oligo Designer. *Nucleic Acids Res,* 32, W121-3.

DY, G. K. & ADJEI, A. A. (2002) Novel targets for lung cancer therapy: part I. *J Clin Oncol,* 20, 2881-94.

DYKXHOORN, D. M. & LIEBERMAN, J. (2006) Running interference: prospects and obstacles to using small interfering RNAs as small molecule drugs. *Annu Rev Biomed Eng,* 8, 377-402.

ELBASHIR, S. M., HARBORTH, J., LENDECKEL, W., YALCIN, A., WEBER, K. & TUSCHL, T. (2001a) Duplexes of 21-nucleotide RNAs mediate RNA interference in cultured mammalian cells. *Nature,* 411, 494-8.

ELBASHIR, S. M., HARBORTH, J., WEBER, K. & TUSCHL, T. (2002) Analysis of gene function in somatic mammalian cells using small interfering RNAs. *Methods,* 26, 199-213.

ELBASHIR, S. M., LENDECKEL, W. & TUSCHL, T. (2001b) RNA interference is mediated by 21- and 22-nucleotide RNAs. *Genes Dev,* 15, 188-200.

ELBASHIR, S. M., MARTINEZ, J., PATKANIOWSKA, A., LENDECKEL, W. & TUSCHL, T. (2001c) Functional anatomy of siRNAs for mediating efficient RNAi in Drosophila melanogaster embryo lysate. *Embo J,* 20, 6877-88.

ELDER, J. K., JOHNSON, M., MILNER, N., MIR, K. U., SOHAIL, M. & SOUTHERN, E. M. (1999) DNA Microarrays: A Practical Approach. Oxford Press, New York.

ELLINGTON, A. (1998) Purification of Oligonucleotides Using Denaturing Polyacrylamide Gel Electrophoresis. *Current Protocols in Molecular Biology,* 1–2.12.

ESAU, C. C. & MONIA, B. P. (2007) Therapeutic potential for microRNAs. *Adv Drug Deliv Rev,* 59, 101-114.

FAN, Z., MASUI, H., ALTAS, I. & MENDELSOHN, J. (1993) Blockade of epidermal growth factor receptor function by bivalent and monovalent fragments of 225 anti-epidermal growth factor receptor monoclonal antibodies. *Cancer Res,* 53, 4322-8.

FILIPOWICZ, W., JASKIEWICZ, L., KOLB, F. A. & PILLAI, R. S. (2005) Post-transcriptional gene silencing by siRNAs and miRNAs. *Curr Opin Struct Biol,* 15, 331-41.

FILMUS, J., POLLAK, M. N., CAILLEAU, R. & BUICK, R. N. (1985) MDA-468, a human breast cancer cell line with a high number of epidermal growth factor (EGF) receptors, has an amplified EGF receptor gene and is growth inhibited by EGF. *Biochem Biophys Res Commun,* 128, 898-905.

FIRE, A., XU, S., MONTGOMERY, M. K., KOSTAS, S. A., DRIVER, S. E. & MELLO, C. C. (1998) Potent and specific genetic interference by double-stranded RNA in Caenorhabditis elegans. *Nature,* 391, 806-11.

GARNER, C. M., HUBBOLD, L. M. & CHAKRABORTI, P. R. (2000) Mycoplasma detection in cell cultures: a comparison of four methods. *Br J Biomed Sci,* 57, 295-301.

GEARY, R. S., YU, R. Z. & LEVIN, A. A. (2001) Pharmacokinetics of phosphorothioate antisense oligodeoxynucleotides. *Curr Opin Investig Drugs,* 2, 562-73.

GIACCONE, G., HERBST, R. S., MANEGOLD, C., SCAGLIOTTI, G., ROSELL, R., MILLER, V., NATALE, R. B., SCHILLER, J. H., VON PAWEL, J., PLUZANSKA, A., GATZEMEIER, U., GROUS, J., OCHS, J. S., AVERBUCH, S. D., WOLF, M. K., RENNIE, P., FANDI, A. & JOHNSON, D. H. (2004) Gefitinib in combination with gemcitabine and cisplatin in advanced non-small-cell lung cancer: a phase III trial--INTACT 1. *J Clin Oncol,* 22, 777-84.

GIARD, D. J., AARONSON, S. A., TODARO, G. J., ARNSTEIN, P., KERSEY, J. H., DOSIK, H. & PARKS, W. P. (1973) In vitro cultivation of human tumors: establishment of cell lines derived from a series of solid tumors. *J Natl Cancer Inst,* 51, 1417-23.

GILMORE, I. R., FOX, S. P., HOLLINS, A. J., SOHAIL, M. & AKHTAR, S. (2004) The design and exogenous delivery of siRNA for post-transcriptional gene silencing. *J Drug Target,* 12, 315-40.

GLOVER, J. M., LEEDS, J. M., MANT, T. G., AMIN, D., KISNER, D. L., ZUCKERMAN, J. E., GEARY, R. S., LEVIN, A. A. & SHANAHAN, W. R., JR. (1997) Phase I safety and pharmacokinetic profile of an intercellular

adhesion molecule-1 antisense oligodeoxynucleotide (ISIS 2302). *J Pharmacol Exp Ther,* 282, 1173-80.

GOLDSTEIN, N. I., PREWETT, M., ZUKLYS, K., ROCKWELL, P. & MENDELSOHN, J. (1995) Biological efficacy of a chimeric antibody to the epidermal growth factor receptor in a human tumor xenograft model. *Clin Cancer Res,* 1, 1311-8.

GRAUS-PORTA, D., BEERLI, R. R., DALY, J. M. & HYNES, N. E. (1997) ErbB-2, the preferred heterodimerization partner of all ErbB receptors, is a mediator of lateral signaling. *Embo J,* 16, 1647-55.

GRUNWELLER, A., WYSZKO, E., BIEBER, B., JAHNEL, R., ERDMANN, V. A. & KURRECK, J. (2003) Comparison of different antisense strategies in mammalian cells using locked nucleic acids, 2'-O-methyl RNA, phosphorothioates and small interfering RNA. *Nucleic Acids Res,* 31, 3185-93.

HAMMOND, S. M., BOETTCHER, S., CAUDY, A. A., KOBAYASHI, R. & HANNON, G. J. (2001) Argonaute2, a link between genetic and biochemical analyses of RNAi. *Science,* 293, 1146-50.

HAN, Y., CADAY, C. G., NANDA, A., CAVENEE, W. K. & HUANG, H. J. (1996) Tyrphostin AG 1478 preferentially inhibits human glioma cells expressing truncated rather than wild-type epidermal growth factor receptors. *Cancer Res,* 56, 3859-61.

HARBORTH, J., ELBASHIR, S. M., VANDENBURGH, K., MANNINGA, H., SCARINGE, S. A., WEBER, K. & TUSCHL, T. (2003) Sequence, chemical, and structural variation of small interfering RNAs and short hairpin RNAs and the effect on mammalian gene silencing. *Antisense Nucleic Acid Drug Dev,* 13, 83-105.

HAUPENTHAL, J., BAEHR, C., KIERMAYER, S., ZEUZEM, S. & PIIPER, A. (2006) Inhibition of RNAse A family enzymes prevents degradation and loss of silencing activity of siRNAs in serum. *Biochem Pharmacol,* 71, 702-10.

HAUPENTHAL, J., BAEHR, C., ZEUZEM, S. & PIIPER, A. (2007) RNAse A-like enzymes in serum inhibit the anti-neoplastic activity of siRNA targeting polo-like kinase 1. *Int J Cancer,* 121, 206-10.

HENSCHEL, A., BUCHHOLZ, F. & HABERMANN, B. (2004) DEQOR: a web-based tool for the design and quality control of siRNAs. *Nucleic Acids Res,* 32, W113-20.

HERBST, R. S., GIACCONE, G., SCHILLER, J. H., NATALE, R. B., MILLER, V., MANEGOLD, C., SCAGLIOTTI, G., ROSELL, R., OLIFF, I., REEVES, J. A., WOLF, M. K., KREBS, A. D., AVERBUCH, S. D., OCHS, J. S., GROUS, J., FANDI, A. & JOHNSON, D. H. (2004) Gefitinib in combination with paclitaxel and carboplatin in advanced non-small-cell lung cancer: a phase III trial--INTACT 2. *J Clin Oncol,* 22, 785-94.

HO, S. P., BAO, Y., LESHER, T., MALHOTRA, R., MA, L. Y., FLUHARTY, S. J. & SAKAI, R. R. (1998) Mapping of RNA accessible sites for antisense experiments with oligonucleotide libraries. *Nat Biotechnol,* 16, 59-63.

HOKE, G. D., DRAPER, K., FREIER, S. M., GONZALEZ, C., DRIVER, V. B., ZOUNES, M. C. & ECKER, D. J. (1991) Effects of phosphorothioate capping on antisense oligonucleotide stability, hybridization and antiviral efficacy versus herpes simplex virus infection. *Nucleic Acids Res,* 19, 5743-8.

HOLEN, T., AMARZGUIOUI, M., WIIGER, M. T., BABAIE, E. & PRYDZ, H. (2002) Positional effects of short interfering RNAs targeting the human coagulation trigger Tissue Factor. *Nucleic Acids Res,* 30, 1757-66.

HUDSON, A. J., LEWIS, K. J., RAO, M. V. & AKHTAR, S. (1996) Biodegradable polymer matrices for the sustained exogenous delivery of a biologically active c-myc hammerhead ribozyme. *International Journal of Pharmaceutics,* 136, 23.

HUGHES, J., ASTRIAB, A., YOO, H., ALAHARI, S., LIANG, E., SERGUEEV, D., SHAW, B. R. & JULIANO, R. L. (2000) In vitro transport and delivery of antisense oligonucleotides. *Methods Enzymol,* 313, 342-58.

HUTVAGNER, G. & ZAMORE, P. D. (2002) A microRNA in a multiple-turnover RNAi enzyme complex. *Science,* 297, 2056-60.

KABANOV, A. V. (2006) Polymer genomics: an insight into pharmacology and toxicology of nanomedicines. *Adv Drug Deliv Rev,* 58, 1597-621.

KENNERDELL, J. R. & CARTHEW, R. W. (1998) Use of dsRNA-mediated genetic interference to demonstrate that frizzled and frizzled 2 act in the wingless pathway. *Cell,* 95, 1017-26.

KHVOROVA, A., REYNOLDS, A. & JAYASENA, S. D. (2003) Functional siRNAs and miRNAs exhibit strand bias. *Cell,* 115, 209-16.

KIM, D. H., BEHLKE, M. A., ROSE, S. D., CHANG, M. S., CHOI, S. & ROSSI, J. J. (2005) Synthetic dsRNA Dicer substrates enhance RNAi potency and efficacy. *Nat Biotechnol,* 23, 222-6.

KRETSCHMER-KAZEMI FAR, R. & SCZAKIEL, G. (2003) The activity of siRNA in mammalian cells is related to structural target accessibility: a comparison with antisense oligonucleotides. *Nucleic Acids Res,* 31, 4417-24.

KRUEGER, U., BERGAUER, T., KAUFMANN, B., WOLTER, I., PILK, S., HEIDER-FABIAN, M., KIRCH, S., ARTZ-OPPITZ, C., ISSELHORST, M. & KONRAD, J. (2007) Insights into Effective RNAi Gained from Large-Scale siRNA Validation Screening. *Oligonucleotides,* 17, 237-50.

KUNITZ, M. (1940) CRYSTALLINE RIBONUCLEASE. *The Journal of General Physiology,* 24, 15-32.

KURRECK, J. (2003) Antisense technologies. Improvement through novel chemical modifications. *Eur J Biochem,* 270, 1628-44.

KURRECK, J. (2006) siRNA Efficiency: Structure or Sequence-That Is the Question. *J Biomed Biotechnol,* 2006, 83757.

KURRECK, J., WYSZKO, E., GILLEN, C. & ERDMANN, V. A. (2002) Design of antisense oligonucleotides stabilized by locked nucleic acids. *Nucleic Acids Res,* 30, 1911-8.

LASKOWSKI SR, M. (1985) Nucleases: historical perspectives. *Nucleases (Linn SM and Roberts, RJ, Eds.), pp1–21. Cold Spring Harbor Laboratory Press, Cold Spring Harbor, NY.*

LAVIGNE, C. & THIERRY, A. R. (2007) Specific subcellular localization of siRNAs delivered by lipoplex in MCF-7 breast cancer cells. *Biochimie.*

LAYZER, J. M., MCCAFFREY, A. P., TANNER, A. K., HUANG, Z., KAY, M. A. & SULLENGER, B. A. (2004) In vivo activity of nuclease-resistant siRNAs. *Rna,* 10, 766-71.

LEVENKOVA, N., GU, Q. & RUX, J. J. (2004) Gene specific siRNA selector. *Bioinformatics,* 20, 430-2.

LEVIN, A. A. (1999) A review of the issues in the pharmacokinetics and toxicology of phosphorothioate antisense oligonucleotides. *Biochim Biophys Acta,* 1489, 69-84.

LEVITZKI, A. & GAZIT, A. (1995) Tyrosine kinase inhibition: an approach to drug development. *Science,* 267, 1782-8.

LEWIS, D. L., HAGSTROM, J. E., LOOMIS, A. G., WOLFF, J. A. & HERWEIJER, H. (2002) Efficient delivery of siRNA for inhibition of gene expression in postnatal mice. *Nat Genet,* 32, 107-8.

LIBONATI, M. & GOTTE, G. (2004) Oligomerization of bovine ribonuclease A: structural and functional features of its multimers. *Biochem J,* 380, 311-27.

LIPPMAN, Z. & MARTIENSSEN, R. (2004) The role of RNA interference in heterochromatic silencing. *Nature,* 431, 364-70.

LIU, J., CARMELL, M. A., RIVAS, F. V., MARSDEN, C. G., THOMSON, J. M., SONG, J. J., HAMMOND, S. M., JOSHUA-TOR, L. & HANNON, G. J. (2004) Argonaute2 is the catalytic engine of mammalian RNAi. *Science,* 305, 1437-41.

LOWRY, O. H., ROSEBROUGH, N. J., FARR, A. L. & RANDALL, R. J. (1951) Protein measurement with the Folin phenol reagent. *J Biol Chem,* 193, 265-75.

MACRAE, I. J., ZHOU, K., LI, F., REPIC, A., BROOKS, A. N., CANDE, W. Z., ADAMS, P. D. & DOUDNA, J. A. (2006) Structural basis for double-stranded RNA processing by Dicer. *Science,* 311, 195-8.

MARTINEZ, J. & TUSCHL, T. (2004) RISC is a 5' phosphomonoester-producing RNA endonuclease. *Genes Dev,* 18, 975-80.

MATSON, R. S., RAMPAL, J. B. & COASSIN, P. J. (1994) Biopolymer synthesis on polypropylene supports. I. Oligonucleotides. *Anal Biochem,* 217, 306-10.

MATZKE, M. A. & MATZKE, A. J. (1995) Homology-dependent gene silencing in transgenic plants: what does it really tell us? *Trends Genet,* 11, 1-3.

MEISTER, G., LANDTHALER, M., PATKANIOWSKA, A., DORSETT, Y., TENG, G. & TUSCHL, T. (2004) Human Argonaute2 mediates RNA cleavage targeted by miRNAs and siRNAs. *Mol Cell,* 15, 185-97.

MERLINO, G. T., XU, Y. H., ISHII, S., CLARK, A. J., SEMBA, K., TOYOSHIMA, K., YAMAMOTO, T. & PASTAN, I. (1984) Amplification and enhanced expression of the epidermal growth factor receptor gene in A431 human carcinoma cells. *Science,* 224, 417-9.

MILLER, M., KENNEWELL, A. & SYMONDS, G. (1992) Transformation of murine pre-B-lymphocytes by v-erb-B: progression to growth factor independence and tumorigenicity. *Leukemia,* 6, 18-28.

MILNER, N., MIR, K. U. & SOUTHERN, E. M. (1997) Selecting effective antisense reagents on combinatorial oligonucleotide arrays. *Nat Biotechnol,* 15, 537-41.

MISHRA, N. C. (2002) *Nucleases: Molecular Biology and Applications,* Wiley-Interscience.

MONIA, B. P., JOHNSTON, J. F., SASMOR, H. & CUMMINS, L. L. (1996) Nuclease resistance and antisense activity of modified oligonucleotides targeted to Ha-ras. *J Biol Chem,* 271, 14533-40.

MOSCATELLO, D. K., HOLGADO-MADRUGA, M., GODWIN, A. K., RAMIREZ, G., GUNN, G., ZOLTICK, P. W., BIEGEL, J. A., HAYES, R. L. & WONG, A. J. (1995) Frequent expression of a mutant epidermal growth factor receptor in multiple human tumors. *Cancer Res,* 55, 5536-9.

NAGANE, M., LIN, H., CAVENEE, W. K. & HUANG, H. J. (2001) Aberrant receptor signaling in human malignant gliomas: mechanisms and therapeutic implications. *Cancer Lett,* 162 Suppl, S17-S21.

NAGY, P., ARNDT-JOVIN, D. J. & JOVIN, T. M. (2003) Small interfering RNAs suppress the expression of endogenous and GFP-fused epidermal growth factor receptor (erbB1) and induce apoptosis in erbB1-overexpressing cells. *Exp Cell Res,* 285, 39-49.

NAITO, Y., YAMADA, T., MATSUMIYA, T., UI-TEI, K., SAIGO, K. & MORISHITA, S. (2005) dsCheck: highly sensitive off-target search software

for double-stranded RNA-mediated RNA interference. *Nucleic Acids Res,* 33, W589-91.

NARZ, F., HUBNER, S., MAGYAR, S., BIELKE, W., WEBER, M. & DENNIG, J. (2007) Enrichment strategies for siRNA-transfected cells in an untransfected background. *J Biotechnol,* 130, 209-12.

NEGRINI, M., FERRACIN, M., SABBIONI, S. & CROCE, C. M. (2007) MicroRNAs in human cancer: from research to therapy. *J Cell Sci,* 120, 1833-40.

NORMANNO, N., DE LUCA, A., BIANCO, C., STRIZZI, L., MANCINO, M., MAIELLO, M. R., CAROTENUTO, A., DE FEO, G., CAPONIGRO, F. & SALOMON, D. S. (2006) Epidermal growth factor receptor (EGFR) signaling in cancer. *Gene,* 366, 2-16.

NYKANEN, A., HALEY, B. & ZAMORE, P. D. (2001) ATP requirements and small interfering RNA structure in the RNA interference pathway. *Cell,* 107, 309-21.

O'BRYAN, J. P., FRYE, R. A., COGSWELL, P. C., NEUBAUER, A., KITCH, B., PROKOP, C., ESPINOSA, R., 3RD, LE BEAU, M. M., EARP, H. S. & LIU, E. T. (1991) axl, a transforming gene isolated from primary human myeloid leukemia cells, encodes a novel receptor tyrosine kinase. *Mol Cell Biol,* 11, 5016-31.

OELGESCHLAGER, M., LARRAIN, J., GEISSERT, D. & DE ROBERTIS, E. M. (2000) The evolutionarily conserved BMP-binding protein Twisted gastrulation promotes BMP signalling. *Nature,* 405, 757-63.

OKAMURA, K., ISHIZUKA, A., SIOMI, H. & SIOMI, M. C. (2004) Distinct roles for Argonaute proteins in small RNA-directed RNA cleavage pathways. *Genes Dev,* 18, 1655-66.

OMIDI, Y., HOLLINS, A. J., BENBOUBETRA, M., DRAYTON, R., BENTER, I. F. & AKHTAR, S. (2003) Toxicogenomics of non-viral vectors for gene therapy: a microarray study of lipofectin- and oligofectamine-induced gene expression changes in human epithelial cells. *J Drug Target,* 11, 311-23.

PARKER, R. & SONG, H. (2004) The enzymes and control of eukaryotic mRNA turnover. *Nat Struct Mol Biol,* 11, 121-7.

PATZEL, V., RUTZ, S., DIETRICH, I., KOBERLE, C., SCHEFFOLD, A. & KAUFMANN, S. H. (2005) Design of siRNAs producing unstructured guide-RNAs results in improved RNA interference efficiency. *Nat Biotechnol,* 23, 1440-4.

PETCH, A. K., SOHAIL, M., HUGHES, M. D., BENTER, I., DARLING, J., SOUTHERN, E. M. & AKHTAR, S. (2003) Messenger RNA expression profiling of genes involved in epidermal growth factor receptor signalling in human cancer cells treated with scanning array-designed antisense oligonucleotides. *Biochem Pharmacol,* 66, 819-30.

PRUCH, J. M. & LASKOWSKI M, S. (1980) Covalently bound ribonucleotides in crab d (AT) polymer. *Journal of Biological Chemistry,* 255, 9409-9412.

RAEMDONCK, K., REMAUT, K., LUCAS, B., SANDERS, N. N., DEMEESTER, J. & DE SMEDT, S. C. (2006) In situ analysis of single-stranded and duplex siRNA integrity in living cells. *Biochemistry,* 45, 10614-23.

RANA, T. M. (2007) Illuminating the silence: understanding the structure and function of small RNAs. *Nat Rev Mol Cell Biol,* 8, 23-36.

REDEMANN, N., HOLZMANN, B., VON RUDEN, T., WAGNER, E. F., SCHLESSINGER, J. & ULLRICH, A. (1992) Anti-oncogenic activity of

signalling-defective epidermal growth factor receptor mutants. *Mol Cell Biol,* 12, 491-8.

REYNOLDS, A., LEAKE, D., BOESE, Q., SCARINGE, S., MARSHALL, W. S. & KHVOROVA, A. (2004) Rational siRNA design for RNA interference. *Nat Biotechnol,* 22, 326-30.

RIVAS, F. V., TOLIA, N. H., SONG, J. J., ARAGON, J. P., LIU, J., HANNON, G. J. & JOSHUA-TOR, L. (2005) Purified Argonaute2 and an siRNA form recombinant human RISC. *Nat Struct Mol Biol,* 12, 340-9.

ROBERTS, R. J. & LINN, S. M. (1982) *Nucleases,* Cold Spring Harbor Laboratory Cold Spring Harbor, NY.

ROSE, S. D., KIM, D. H., AMARZGUIOUI, M., HEIDEL, J. D., COLLINGWOOD, M. A., DAVIS, M. E., ROSSI, J. J. & BEHLKE, M. A. (2005) Functional polarity is introduced by Dicer processing of short substrate RNAs. *Nucleic Acids Res,* 33, 4140-56.

ROTTEM, S. & BARILE, M. F. (1993) Beware of mycoplasmas. *Trends Biotechnol,* 11, 143-51.

SAETROM, P. (2004) Predicting the efficacy of short oligonucleotides in antisense and RNAi experiments with boosted genetic programming. *Bioinformatics,* 20, 3055-63.

SAMBROOK, J., FRITSCH, E. F. & MANIATIS, T. (2001) *Molecular cloning,* Cold Spring Harbor Laboratory Press Cold Spring Harbor, NY.

SANTOYO, J., VAQUERIZAS, J. M. & DOPAZO, J. (2005) Highly specific and accurate selection of siRNAs for high-throughput functional assays. *Bioinformatics,* 21, 1376-82.

SCHLESSINGER, J. (2000) Cell signaling by receptor tyrosine kinases. *Cell,* 103, 211-25.

SCHUBERT, S., GRUNWELLER, A., ERDMANN, V. A. & KURRECK, J. (2005) Local RNA target structure influences siRNA efficacy: systematic analysis of intentionally designed binding regions. *J Mol Biol,* 348, 883-93.

SCHWARZ, D. S., HUTVAGNER, G., DU, T., XU, Z., ARONIN, N. & ZAMORE, P. D. (2003) Asymmetry in the assembly of the RNAi enzyme complex. *Cell,* 115, 199-208.

SEBASTIAN, S., SETTLEMAN, J., RESHKIN, S. J., AZZARITI, A., BELLIZZI, A. & PARADISO, A. (2006) The complexity of targeting EGFR signalling in cancer: from expression to turnover. *Biochim Biophys Acta,* 1766, 120-39.

SHARMA, S. V., BELL, D. W., SETTLEMAN, J. & HABER, D. A. (2007) Epidermal growth factor receptor mutations in lung cancer. *Nat Rev Cancer,* 7, 169-81.

SHARP, P. A. (2001) RNA interference--2001. *Genes Dev,* 15, 485-90.

SHAW, J. P., KENT, K., BIRD, J., FISHBACK, J. & FROEHLER, B. (1991) Modified deoxyoligonucleotides stable to exonuclease degradation in serum. *Nucleic Acids Res,* 19, 747-50.

SHEPARD, A. R., JACOBSON, N. & CLARK, A. F. (2005) Importance of quantitative PCR primer location for short interfering RNA efficacy determination. *Anal Biochem,* 344, 287-8.

SIERAKOWSKA, H. & SHUGAR, D. (1977) Mammalian nucleolytic enzymes. *Prog Nucleic Acid Res Mol Biol,* 20, 59-130.

SMITH, C. (2006) Sharpening the tools of RNA interference. *Nat Meth,* 3, 475.

SMITH, L., ANDERSEN, K. B., HOVGAARD, L. & JAROSZEWSKI, J. W. (2000) Rational selection of antisense oligonucleotide sequences. *Eur J Pharm Sci,* 11, 191-8.

SMYTH, D. G., STEIN, W. H. & MOORE, S. (1963) The sequence of amino acid residues in bovine pancreatic ribonuclease: revisions and confirmations. *J Biol Chem,* 238, 227-34.

SOHAIL, M. (2005) *Gene Silencing by RNA Interference: Technology and Application*, CRC Press.

SOHAIL, M., AKHTAR, S. & SOUTHERN, E. M. (1999) The folding of large RNAs studied by hybridization to arrays of complementary oligonucleotides. *Rna,* 5, 646-55.

SOHAIL, M., DORAN, G., KANG, S., AKHTAR, S. & SOUTHERN, E. M. (2005) Structural rearrangements in RNA on the binding of an antisense oligonucleotide: implications for the study of intra-molecular RNA interactions and the design of cooperatively acting antisense reagents with enhanced efficacy. *J Drug Target,* 13, 61-70.

SOHAIL, M. & SOUTHERN, E. M. (2000) Selecting optimal antisense reagents. *Adv Drug Deliv Rev,* 44, 23-34.

SOHAIL, M. & SOUTHERN, E. M. (2001) Using oligonucleotide scanning arrays to find effective antisense reagents. *Methods Mol Biol,* 170, 181-99.

SONG, E., LEE, S. K., WANG, J., INCE, N., OUYANG, N., MIN, J., CHEN, J., SHANKAR, P. & LIEBERMAN, J. (2003) RNA interference targeting Fas protects mice from fulminant hepatitis. *Nat Med,* 9, 347-51.

SONG, J. J., SMITH, S. K., HANNON, G. J. & JOSHUA-TOR, L. (2004) Crystal structure of Argonaute and its implications for RISC slicer activity. *Science,* 305, 1434-7.

SORDELLA, R., BELL, D. W., HABER, D. A. & SETTLEMAN, J. (2004) Gefitinib-sensitizing EGFR mutations in lung cancer activate anti-apoptotic pathways. *Science,* 305, 1163-7.

SORRENTINO, S. & LIBONATI, M. (1997) Structure-function relationships in human ribonucleases: main distinctive features of the major RNase types. *FEBS Lett,* 404, 1-5.

SOUTSCHEK, J., AKINC, A., BRAMLAGE, B., CHARISSE, K., CONSTIEN, R., DONOGHUE, M., ELBASHIR, S., GEICK, A., HADWIGER, P., HARBORTH, J., JOHN, M., KESAVAN, V., LAVINE, G., PANDEY, R. K., RACIE, T., RAJEEV, K. G., ROHL, I., TOUDJARSKA, I., WANG, G., WUSCHKO, S., BUMCROT, D., KOTELIANSKY, V., LIMMER, S., MANOHARAN, M. & VORNLOCHER, H. P. (2004) Therapeutic silencing of an endogenous gene by systemic administration of modified siRNAs. *Nature,* 432, 173-8.

SPEAKE, G., HOLLOWAY, B. & COSTELLO, G. (2005) Recent developments related to the EGFR as a target for cancer chemotherapy. *Curr Opin Pharmacol,* 5, 343-9.

STARK, G. R., KERR, I. M., WILLIAMS, B. R., SILVERMAN, R. H. & SCHREIBER, R. D. (1998) How cells respond to interferons. *Annu Rev Biochem,* 67, 227-64.

STEIN, C. A. (2001) Antisense that comes naturally. *Nat Biotechnol,* 19, 737-8.

TAKLE, G. B., THIERRY, A. R., FLYNN, S. M., PENG, B., WHITE, L., DEVONISH, W., GALBRAITH, R. A., GOLDBERG, A. R. & GEORGE, S. T. (1997) Delivery of oligoribonucleotides to human hepatoma cells using cationic lipid particles conjugated to ferric protoporphyrin IX (heme). *Antisense Nucleic Acid Drug Dev,* 7, 177-85.

TANG, G. (2005) siRNA and miRNA: an insight into RISCs. *Trends Biochem Sci,* 30, 106-14.

THOMAS, N. P. B. (2004) The involvement of caveolin within endocrine-sensitive and -resistant breast cancer. Cardiff University.

TIDD, D. M. & WARENIUS, H. M. (1989) Partial protection of oncogene, anti-sense oligodeoxynucleotides against serum nuclease degradation using terminal methylphosphonate groups. *Br J Cancer,* 60, 343-50.

TSCHAHARGANEH, D., EHEMANN, V., NUSSBAUM, T., SCHIRMACHER, P. & BREUHAHN, K. (2007) Non-specific Effects of siRNAs on Tumor Cells with Implications on Therapeutic Applicability Using RNA Interference. *Pathol Oncol Res,* 13, 84-90.TURNER, J. J., JONES, S. W., MOSCHOS, S. A., LINDSAY, M. A. & GAIT, M. J. (2007) MALDI-TOF mass spectral analysis of siRNA degradation in serum confirms an RNAse A-like activity. *Mol Biosyst,* 3, 43-50.

UI-TEI, K., NAITO, Y. & SAIGO, K. (2006) Essential Notes Regarding the Design of Functional siRNAs for Efficient Mammalian RNAi. *J Biomed Biotechnol,* 2006, 65052.

UI-TEI, K., NAITO, Y., TAKAHASHI, F., HARAGUCHI, T., OHKI-HAMAZAKI, H., JUNI, A., UEDA, R. & SAIGO, K. (2004) Guidelines for the selection of highly effective siRNA sequences for mammalian and chick RNA interference. *Nucleic Acids Res,* 32, 936-48.

UPHOFF, C. C. & DREXLER, H. G. (2002) Comparative PCR analysis for detection of mycoplasma infections in continuous cell lines. *In Vitro Cell Dev Biol Anim,* 38, 79-85.

VALENCIA-SANCHEZ, M. A., LIU, J., HANNON, G. J. & PARKER, R. (2006) Control of translation and mRNA degradation by miRNAs and siRNAs. *Genes Dev,* 20, 515-24.

VICKERS, T. A., KOO, S., BENNETT, C. F., CROOKE, S. T., DEAN, N. M. & BAKER, B. F. (2003) Efficient reduction of target RNAs by small interfering RNA and RNase H-dependent antisense agents. A comparative analysis. *J Biol Chem,* 278, 7108-18.

WALDMAN, S. A. & TERZIC, A. (2007) Translating MicroRNA discovery into clinical biomarkers in cancer. *Jama,* 297, 1923-5.

WANG, L. & MU, F. Y. (2004) A Web-based design center for vector-based siRNA and siRNA cassette. *Bioinformatics,* 20, 1818-20.

WARD, C. W., LAWRENCE, M. C., STRELTSOV, V. A., ADAMS, T. E. & MCKERN, N. M. (2007) The insulin and EGF receptor structures: new insights into ligand-induced receptor activation. *Trends Biochem Sci,* 32, 129-37.

WEICKMANN, J. L. & GLITZ, D. G. (1982) Human ribonucleases. Quantitation of pancreatic-like enzymes in serum, urine, and organ preparations. *J Biol Chem,* 257, 8705-10.

WEIL, D., GARCON, L., HARPER, M., DUMENIL, D., DAUTRY, F. & KRESS, M. (2002) Targeting the kinesin Eg5 to monitor siRNA transfection in mammalian cells. *Biotechniques,* 33, 1244-8.

WESTERHOUT, E. M. & BERKHOUT, B. (2007) A systematic analysis of the effect of target RNA structure on RNA interference. *Nucleic Acids Res,* 35, 4322-30.

WICKSTROM, E. (1986) Oligodeoxynucleotide stability in subcellular extracts and culture media. *J Biochem Biophys Methods,* 13, 97-102.

WIEMER, E. A. (2007) The role of microRNAs in cancer: No small matter. *Eur J Cancer.*

WIKSTRAND, C. J., REIST, C. J., ARCHER, G. E., ZALUTSKY, M. R. & BIGNER, D. D. (1998) The class III variant of the epidermal growth factor

receptor (EGFRvIII): characterization and utilization as an immunotherapeutic target. *J Neurovirol,* 4, 148-58.

WILLINGHAM, A. T., DEVERAUX, Q. L., HAMPTON, G. M. & AZA-BLANC, P. (2004) RNAi and HTS: exploring cancer by systematic loss-of-function. *Oncogene,* 23, 8392-400.

XIA, H., FITZGERALD, J., BREDT, D. S. & FORSAYETH, J. R. (1997) Detection of mycoplasma infection of mammalian cells. *Biotechniques,* 22, 934-6.

XU, Y., ZHANG, H. Y., THORMEYER, D., LARSSON, O., DU, Q., ELMEN, J., WAHLESTEDT, C. & LIANG, Z. (2003) Effective small interfering RNAs and phosphorothioate antisense DNAs have different preferences for target sites in the luciferase mRNAs. *Biochem Biophys Res Commun,* 306, 712-7.

YAMADA, T. & MORISHITA, S. (2005) Accelerated off-target search algorithm for siRNA. *Bioinformatics,* 21, 1316-24.

YIU, S. M., WONG, P. W., LAM, T. W., MUI, Y. C., KUNG, H. F., LIN, M. & CHEUNG, Y. T. (2005) Filtering of ineffective siRNAs and improved siRNA design tool. *Bioinformatics,* 21, 144-51.

YUAN, B., LATEK, R., HOSSBACH, M., TUSCHL, T. & LEWITTER, F. (2004) siRNA Selection Server: an automated siRNA oligonucleotide prediction server. *Nucleic Acids Res,* 32, W130-4.

ZAMECNIK, P. C. & STEPHENSON, M. L. (1978) Inhibition of Rous sarcoma virus replication and cell transformation by a specific oligodeoxynucleotide. *Proc Natl Acad Sci U S A,* 75, 280-4.